

**The far field migration of radionuclides in groundwater through
geologic media**

Thesis (Doctorate) - Univ. California

Daniel Kao Sun Ting

The Far Field Migration of Radionuclides In **Groundwater**"
through Geologic Media

By

Daniel Kao Sun Ting

Engineer (University of Sao Paulo, Brazil) 1973

M.Sc. (University of Sao Paulo, Brazil) 1976

DISSERTATION

Submitted in partial satisfaction of the requirements for the degree of

DOCTOR OF PHILOSOPHY

in

Engineering

in the

GRADUATE DIVISION

OF THE

UNIVERSITY OF CALIFORNIA, BERKELEY

Approved: *Paul H. Chamberlain* *November 17, 1981*
Chairman Date
..... *Thomas R. Goff* *Nov. 20, 1981*
..... *Geov. H. ...* *Oct 1981*

HO**

To my wife Selma, for her love and support.

To my parents, for the way they brought me

Acknowledgements

I would like to express my gratitude to Professor Paul L. Chambre, my thesis supervisor for his guidance during this research.

My gratitude also goes to Professor Thomas H. Pigford for many discussions and suggestions.

This research is part of the project: "Migration of Radionuclides through Sorbing Media - Analytical Solutions" which senior researchers are P. L. Chambre and T. H. Pigford and which is supported by the Office of Waste Isolation of the U. S. Department of Energy.

In my country, Brazil, I would like to thank the Instituto de Pesquisas Energéticas e Nucleares and the Comissão Nacional de Energia Nuclear, which support made my graduate study possible.

Daniel K. S. Ting

November, 19, 1981

University of California, Berkeley

CONTENTS

Introduction	1
Migration of Radionuclides in One-dimensional Groundwater Flows through Geologic Media	
2.1 Introduction	8
2.2 The radionuclide transport equation and side conditions	10
2.3 The general non-recursive analytical solution	12
2.4 Sample calculation with the program UCBNE25	15
Maxima of Release Bands	
3.1 Introduction	24
3.2 The governing equations and the approximate solution	27
3.3 Extremum of the solution for the first member	33
3.4 Extremum of the solution for the second member	36
3.5 Extremum of the solution for the third member	54
3.6 Example of the utilization of the method and comparison with the exact solution results	68
3.7 Analysis of the effect of variation in parameters values on the maxima concentrations	81
Migration of Radionuclides in Two-dimensional Groundwater Flows through Geologic Media	
4.1 Introduction	119

- 4.2 Theoretical background
- 4.3** Two-dimensional groundwater flows represented by analytical expression
- 4.4** Aquifer potentiometric surfaces represented by interpolation of field measured piezometric data
- 4.5 Description of the computer code UCBNE21
- 4.6 Modelling of the far-field radionuclide migration at the reference site of the Waste Isolation Pilot Plant (WIPP) in Eddy County, New Mexico
- 4.7** Modelling of the far-field radionuclide migration at the site of the Basalt Waste Isolation Project (BWIP) in Hanford, Washington

5. Literature References

Appendix A. Source listing and data input description for the computer program UCBNE25

Appendix B. Source listing and data input description for the computer program UCBNE20

Appendix C. Source listing and data input description for the computer program UCBNE21

Appendix D. Derivation of the contaminated region and contamination time

THE FAR-FIELD MIGRATION OF RADIONUCLIDES IN GROUNDWATER
THROUGH GEOLOGIC MEDIA

Daniel Kao Sun Ting

Ph.D.

Nuclear Engineering Department
University of California, Berkeley

Paul L. Chambre
Chairman of Committee

Abstract

This work models the radionuclide migration by groundwater flow in geologic media after nuclide release from a high level waste repository. Predictive analytical methods are presented that can be used to assess the performance of a repository site, and which estimate the potential hazard at the biosphere to the general public. The results of the analysis are presented by analytical formulas and a set of computer codes which evaluate these solutions has been developed.

The exact analytical non-recursive solution to the one-

1. Introduction

The viable disposal of high level nuclear waste in repositories located deep in a geologic media will depend among other factors, on the speed of the far field migration of radionuclides in the groundwater through the geologic media. This work intends to model the radionuclide migration in groundwater after their release from the waste package until their discharge into the biosphere.

This modelling produces a predictive method that can be used to assess the performance of a particular combination of waste package and repository site, and estimates the potential hazard to the general public. A set of computer codes based on these methods has been developed. An important aspect throughout this study is the analytical character of the solutions used. When contrasted against numerical schemes used to solve the equivalent problem (Si), the advantages of analytical methods are clearly evidenced. These consist of minimal computing time, the absence of convergence and precision criterias needed and the fact that the dependence on physical parameters of the solution are easier to recognize.

The overall waste disposal problem can be divided into three main parts: the near-field problem, the far-field problem and the pathways to ingestion. In the near-field problem, the design of the package containing the waste form and its

dimensional nuclide transport equation with sorption equilibrium and without solubility limitations is studied. A parametric study showing the influence of the water travel time, the leach time, the time for beginning of leaching and the retardation coefficients on the maximum concentration of every nuclide present in the high level waste is presented by an approximation method. The results indicate that for most of the parameter range considered, I-129 and Ra-226 are the potentially most hazardous nuclides. The hazard due to the leaching of high level waste packages is compared to that of the leaching of an equivalent amount of natural uranium ore.

The analytical non-recursive solution for the migration of radionuclides in two-dimensional groundwater flow is studied next. With neglect of dispersion, the solution to the one-dimensional transport equation is applicable along a streamline of the two-dimensional groundwater flow described by Darcy's law. The potential function driving this flow can be represented either by analytical expressions or by field piezometric measurements. The analysis yields the contaminated region for any member of a chain of arbitrary length and evaluates its concentration in that region. One can also evaluate the discharge rate as well as the cumulative discharge at the biosphere.

The far field migration of radionuclides in groundwater in two candidate repository sites has been studied. These are the

surrounding engineered barriers as well as the definition of the repositories parameters are addressed. The modelling of how the groundwater might reach the waste package, corroding it and releasing radionuclides into surrounding aquifers is studied. The result of the near-field problem should describe how the radionuclides are released into nearby aquifers.

The far-field problem uses the result of the near-field problem as the boundary condition and studies the migration of these radionuclides in groundwater through aquifers until they discharge into the biosphere. This is the problem analyzed in this work.

After these radionuclides are released into the biosphere, which can be a river, a well or any other possible source of fresh water, the actual pathways that the nuclides follow until they are ingested must be determined and the resultant health effects evaluated. The number of health effects caused by the accidental release of radionuclides from the repository will ultimately be the measure of the adequacy of the proposed combination of the waste package and the repository site.

Different investigations are being presently carried to describe the near-field problem (Chambre, Zavoshy in P.3) . Simplified models have in the past been proposed to describe the near-field problem (B4,H1) and the so called "decaying band release mode" is adopted as the boundary condition describing the

release of radionuclides from the repository. To avoid the detailed evaluation of the pathways to ingestion and to determine the health effects to the public due to the failure of a repository, the Maximum Permissible Concentration (MPC,10CFR20) was used as a potential hazard index. The radionuclide concentrations at the biosphere are compared to their MPC values.

By using these simplifications for the near-field problem and for the pathways to the ingestion, the entire effort of this work can be concentrated in the modelling of the far-field migration of radionuclides in groundwater through geologic media. The groundwater flow field is described by the Darcy's law in conjunction with the groundwater mass conservation equation and it is considered to be in steady state. Soil porosity and water density are assumed to be constant. Sorption reactions between nuclides in the groundwater with the solid phase are assumed to be governed by a linear isotherm. In this present study, the effects of hydrodynamic dispersion are assumed to be negligible. This is a conservative assumption since dispersion tends to broaden the migration bands reducing the magnitude of the concentrations. Reduction in the arrival time of the band is negligible (H3). Furthermore, any nuclide is allowed to dissolve without solubility limitations, which is also a conservative assumption.

Lester et al (L1) , Burkholder et al (B4) solved analytically the radionuclide transport equation for a one-dimensional constant groundwater flow. The solution is

sites of the Waste Isolation Pilot Plant (WIPP) in New Mexico and the Basalt Waste Isolation Project (BWIP) in Hanford, Washington. If an accident occurs after 1000 years, the contamination of nearby rivers due to the discharge of I-129 and Ra-226 leached out from the waste during a period of 10000 years does not exceed the maximum permissible concentrations.

restricted to actinide chains with three members only. Higashi (H2) solved the same problem using a corrected boundary condition and showed the resultant differences in the solution. Foglia et al (F3) use the superposition principle in the solution to the transport equation with the dispersion term included. Hadermann (H4), Foglia (Hi) propose solutions to the one-dimensional transport equation in a heterogeneous media consisting of several different layers. Chambre (Hi) derived the analytical non-recursive solution to the one dimensional transport equation without dispersion which evaluates the concentration of any member of a chain of arbitrary length. Later on, Chambre (Pi) extends the one-dimensional non recursive solution to describe the migration of radionuclides in two and three dimensional flow fields.

In chapter 2, a review of Chambre*s solution (HI) to the one-dimensional flow is presented and also a computer program (UCBNE25) that has been developed based on this solution is described (T1). Sample calculations are shown. In chapter 3, an approximate solution to the one-dimensional transport problem is presented. This simplified form of the solution allows one to obtain analytically the extremum of the solution: the time when the maximum concentration occurs at a fixed field position as well as the field position where the maximum concentration occurs at a fixed time. The results are presented in simple tabular form for easy use and they are applicable for chains with up to three members. This analytical method to determine the extremum

avoids time consuming evaluation of complete concentration histories to determine the maximum. A computer program, UCBNE20, based on this method has been developed.

Using this program, a parametric study showing the influence of each parameter (i.e. the water travel time, the leach time, the time for beginning of leaching and the retardation coefficients) on the maximum concentration of every nuclide present in the high level waste has been done. The result indicates that for most of the parameter ranges considered, I-129 and Ra-226 are the potentially most hazardous nuclides. The hazard due to the leaching of high level waste packages is compared to that of the leaching of an equivalent amount of natural uranium ore and also to the mill tailings resulted from processing the ore. Assuming that they have comparable leach rates, we show that the potential hazard due to the leaching of natural uranium ore is always larger than that of an equivalent amount of reprocessed high level waste.

In chapter 4, the analytical non-recursive solution for the two-dimensional transport equation (Chambre, Pi) is first reviewed. The most important result derived in the solution is that when dispersion is neglected, the solution to the one-dimensional transport equation is applicable along a streamline of the two-dimensional groundwater flow. In this study, the potential function driving the two-dimensional groundwater flow can be represented either by analytical expressions or by field

piezometric measurements.

Analytical representation of groundwater flows is carried out by superimposing an arbitrary number of point sinks and point sources. This superimposition can represent flow fields of arbitrary complexity. On the other hand, a given number of scattered potentiometric field data can be used to represent the potential level curves by fitting the data with a minimal total curvature spline function (Briggs, Bl). This later method allows the aquifer to have inhomogeneous hydraulic conductivity although isotropic.

Based on the above described methods, a computer program UCBNE21 has been developed and is described in this chapter. This program determines the two-dimensional contaminated region, at any time after the release started, for any member of a chain of arbitrary length and evaluates its concentration in the contaminated region. In addition, if the location of the intersection of the biosphere with the contaminated region is known, UCBNE21 evaluates the discharge rate as well as the cumulative discharge at the biosphere. The program has the capability of using the graphic software to automatically generate graphs of desired output functions.

The far-field migration of radionuclides in groundwater in two candidate repository sites has been studied. These are the sites of the Waste Isolation Pilot Plant (WIPP) in Eddy County,

New Mexico and the Basalt Waste Isolation Project (BWIP) in Hanford, Washington. In both cases, it is shown that contamination of nearby rivers due to the discharge of radionuclides from the aquifers surrounding the assumed locations for the repository sites does not exceed the Maximum Permissible Concentration for any nuclide, in the event of an accident.

Finally, source listings for the programs UCBNE25, UCBNE20 and UCBNE21 as well as their data input descriptions are given in Appendix A, B and C respectively.

2. Migration of Radionuclides in One-Dimensional Groundwater Flows Through Geologic Media

2.1 Introduction

In this section, the modelling of the far field migration of radionuclides in one-dimensional groundwater flow through geologic media is studied. There are two groups of radionuclides in high level wastes that present potential hazard to the biosphere: the long lived fission products (e.g. ^{129}Tc , ^{99}Tc , etc.) and the long actinide chains (e.g. ^{246}Cm , ^{242}Pu , ^{238}U , ^{234}U , ^{230}Th , ^{226}Ra).

To accurately predict the transport of an actinide, it is necessary to consider its linkage to all its precursors through the decay chain. Previous analytical solutions to the radionuclide transport equation were recursive in nature (L1). Due to the method of solution employed, the solution could be explicitly expressed for chains of up to three members only. Therefore, actual numerical evaluations were limited to three members chains only. However, in either spent fuel or in high level reprocessed waste there exist longer actinide chains and their analysis had to be treated by simplifying assumptions which allowed one to reduce these longer chains into three member chains.

In a previous report, Chambré (H1,section 4.4) presented the analytical non recursive solution to the radionuclide transport equation for one dimensional flows. This solution allows one to evaluate the concentration history of any member of a chain of arbitrary length without having to solve for its precursors. Evaluation of this solution requires little computing time.

The solution has been programmed into the computer program UCBNE25 and a typical calculation is done and graphical results are presented. The UCBNE25 program uses the graphic display software available at the LBL computer center to automatically generate graphical outputs.

2.2 The radionuclide transport equation and side conditions

The system considered is an one-dimensional single region geologic media where the groundwater velocity is constant. Dispersion effects are assumed to be negligible. The sorption-desorption reactions between radionuclides in the liquid with the solid phase are assumed to be in equilibrium. No solubility limit of any nuclide in the groundwater is considered. Media properties characterizing soil, water and radio-chemistry are treated as isotropic and constant.

Subject to the above assumptions, the conservation equation for the i -th member of a radionuclide chain in the groundwater can be written as follows (Hi, section 2.3).

$$K_i \frac{\partial N_i}{\partial t} + v \frac{\partial N_i}{\partial z} + X_i K_i N_i = X_{i-1} K_{i-1} N_{i-1} - \lambda_i N_i, \quad i = 1, 2, \dots, \quad X_0 = 0 \quad (2.2.1)$$

Here, $N_i(z, t)$ is the concentration of the i -th species in the water, K_j , are the retardation coefficients, λ_i the decay constants (1/yr), z the distance from the repository, v the constant groundwater velocity and t the time after the release starts. The initial condition, at any point $z > 0$, is expressed by

$$N_i(z, 0) = 0 \quad ; \quad z > 0 \quad (2.2.2)$$

The boundary condition can be represented by an arbitrary

release function

$$N_i(0, t) = N_i G_i(t) \quad t > 0 \quad (z \bullet 2 \ll 3)$$

where

$$N_i^T = M_i V Q T \quad (2.2.4)$$

Here N_i is the initial concentration of the i -th member nuclide when the leaching starts (HI, section 3.2), M_i is the corresponding initial number of atoms at the repository, Q is the total volumetric flow rate across the waste (m³/yr), T is the duration of the release (yr) and $G_i(t)$ is an arbitrary prescribed release function.

The solid waste form is assumed to be leached in such a way that the boundary condition can be represented by the so called decaying band release model (HI). In this model, every nuclide is assumed to be released during a time period T called the leach time. It can be shown that this model will produce a release function which is expressed by the following relationship (Hi, section 3.2)

$$G_i(0, t) = \sum_{j=1}^i B_j \exp(-\lambda_j t) [h(t) - h(t-T)] \quad (2.2.5)$$

where $h(t)$ is the step function and B_j are the Bateman coefficients

$$B_{i,i} = \sum_{m=1}^j \left\{ \prod_{r=m}^{i-1} \frac{\lambda_r - \lambda_m}{\lambda_r - \lambda_{r+1}} \right\} \frac{\lambda_m}{\lambda_m - \lambda_{m+1}} \quad (2.2.6)$$

1*3

2.3 The general non-recursive analytical solution

The solution to Eq. (2.2.1) subject to the side conditions Eq. (2.2.2) and Eq. (2.2.3) has been obtained analytically (Chambre, H1) and it can be written as

$$N_i(0, t) \ll N_i^0 e^{-\lambda_i x} G_i(t - K_i) + \sum_{r=j}^{i-1} A_r K_r a_l^{-r} D^{(j)} [g(t) \otimes G \bullet (tj)] \quad (2.3.1)$$

Here, a is defined as the water travel time

$$a = z/v \quad (2.3.2)$$

and the coefficients are defined as follows

$$A_r^{(j)} = \sum_{r=j}^{i-1} A_r K_r \quad (2.3.3)$$

$$n_m = (K - K) \quad (2.3.4)$$

$$D_{rm}^{(j)} = \sum_{q=j}^n (A_{qm} - A_{rm}) \quad (2.3.5)$$

$$I_j = \frac{A.K. - A.K.}{K_i - K_3} \quad (2.3.6)$$

and where

$$g_{rm}(t) = e^{-\lambda_m(t-K_0)} h(t-K_0) \quad (2.3.7)$$

the convolution integral is expressed as

$$c_{rm}(t) = \int_0^t V^{(0)}(t-\tau) g_{rm}(\tau) d\tau \quad (2.3.8)$$

One should note the non-recursive character of the above solution, which allows one to evaluate the concentration of an arbitrary member of a chain of any length directly, without having to solve for its precursors. Due to the analytical form of the solution, which does not require recursive calculation, this solution presents clear advantages when compared to numerical schemes utilized to solve the partial differential equation system, Eq.(2.2.1).

When the decaying band release boundary condition is used (Eq. (2.2.5)) to express the release function $h(t)$ in the convolution integral Eq. (2.3.8) the solution is rewritten as

$$N_i(c, t) = N_0 \exp(-X_i K_1 \sigma) \left[\int_0^t B_1(\tau) \exp[-\lambda_1(t-K_1 \sigma)] d\tau \right] \{ h(t-K_1 \sigma) - h(t-T-K_1 \sigma) \} \\ + \sum_{j=1}^{i-1} \sum_{k=1}^j Q^{(j)}_{im} B_{jk} \{ \exp[-\Delta_{im}(t-K_m \sigma) - \lambda_m K_m \sigma] [h(t-K_m \sigma) - \exp(-T(\ddot{A}_k - i_m)) h(t-K_m \sigma) - \exp[-A_k t - (X^i - X^{i+1} \sigma)] [h(t-K_m \sigma) - h(t-T-K_m \sigma)] \} \quad (2.3.9)$$

$$M1 \quad (K - K') \quad \sum_{q=j}^{i-1} A_{rj} X_{rj} K \quad (2.3.10)$$

$$q=j$$

$$q \cdot r \cdot m$$

The solution when written in the form of Eq. (2.3.9) has the advantage that when two nuclides in the same chain have the same value of the retardation coefficient, Eq. (2.3.9) shows that the concentration $N.(z.t)$ is finite. This is because $Q = 0$ when $K_r = K_m$ and the exponential terms containing A_{rj} tend to zero when K_r tends to K_m . Therefore, with the above manipulations to transform Eq. (2.3.1) into Eq. (2.3.10), the singularity which existed for $K_r = K_m$ is removed.

2.4 Sample calculations with the program UCBNE25

The general non-recursive analytical solution to the nuclide transport equation subject to the decaying band release boundary condition, Eq.(2.3.9) has been programmed into the computer with the label UCBNE25. A complete listing of the program as well as the description of the input requirements are given in Appendix A.

Here, a sample run of the program is presented. Two important long actinide chains are considered. The chains and their members parameters are shown in Table 2.1. The results in the printouts or in the graphs are given in terms of the

3

concentrations and/or water dilution rates $w^{\wedge}(z, t)$, (m /yr), which is defined by the following expressions

$$w_i(z, t) = Q_{x_i} N_i(z, t) / (MPC)_i \quad t > 0 \quad (2.4.1)$$

where MPC stands for Maximum Permissible Concentration (Ci/m) and it is given in 10CFR20. Physically, the water dilution rate represents the volumetric flow rate needed to dilute the activity discharge rate to drinking water standards (PI). Therefore it is an index of the potential harm to the public health and one can directly compare water dilution rates for different nuclides. Furthermore, if the water dilution rates of all nuclides are added one would obtain the total water dilution rate for all nuclides.

For the sample calculation, the leach time was assumed to be 10^4 years and the time delay for the beginning of leaching is 10^3 years. The time for beginning of leaching represents the durability of the canister and the engineered barriers surrounding the waste form. Figure 2.1 and Figure 2.2 show the concentration history for the chain which ends in Ra-226 ($4n+2$ chain, the second even actinide chain, see Table 3.11) for several different water travel times z/V (years). Because of the large retardation coefficients and relatively short half-lives, Cm-246 and Pu-242 cannot migrate as far as and U-238 can, decaying much earlier. Since U-238 migrates farther they carry their daughters Th-230 and Ra-226. This long migration capability allied to its high toxicity makes Ra-226 one of the most hazardous nuclides. Furthermore, one can notice that because Cm-246 and Pu-242 half lives are so much smaller than U-238 half life, their decay does not affect the U-238 concentration significantly. For practical purposes, for the assumed set of parameters, the $4n+2$ chain can be subdivided into two chains. This simplification is extensively used in Chapter 3. The behaviour of the migration bands of the actinide chains are discussed in detail in Chapter 3.

Figure 2.3, Figure 2.4 and Figure 2.5 show how the concentration of the "Np-237" chain ($4n+1$ chain, the first odd actinide chain, see Table 3.11) changes with time for several different water travel times z/V . For the same reasons stated as for the previous chain, Cm-245 and Am-241 cannot migrate very

far. Np-237 which has a low retardation coefficient can carry its short lived daughter relatively far.

Since dispersion effects are neglected in this work, the migration bands have well defined time intervals where the concentration is non trivial. This fact can be seen in any of above figures. These time intervals are the contamination times for that particular nuclide at that particular position characterized by z/V . Although the figures showing the results of the sample calculation expressed the concentrations in terms of the water dilution rates, the program UCBNE25 has the option of plotting the concentration curves of the individual nuclides of the chain instead. (See description of the program UCBNE25 in Appendix A).

Table 2.1 Nuclide Parameters for the Sample Calculation

Chain	Cm-246	Pu-242	U-238	U-234	Th-230	Ra-226
T* (yr)	5.5E+3	3.8E+5	4.5E+9	2.5E+5	8.0E+4	1.6E+3
K. ** x	3.0E+3	1.0E+4	1.4E+4	1.4E+4	5.0E+4	5.0E+2
MPC ***	4.0E-6	5.0E-6	4.0E-5	3.0E-5	2.0E-6	3.0E-8
**** i	1.9E+0	2.0E-1	4.3E-2	0.0	0.0	0.0
Chain	Cm-245	Am-241	Np-237	U-233	Th-229	
T* (yr)	9.3E+3	4.6E+2	2.1E+6	1.6E+5	7.3E+3	
v ** 1	3.0E+3	1.0E+4	1.0E+2	1.4E+4	5.0E+4	
MPC ***	4.0E-6	4.0E-6	3.0E-6	3.0E-5	5.0E-7	
Jw^ **** i	9.8E+0	4.5E+3	1.6E+0	0.0	0.0	

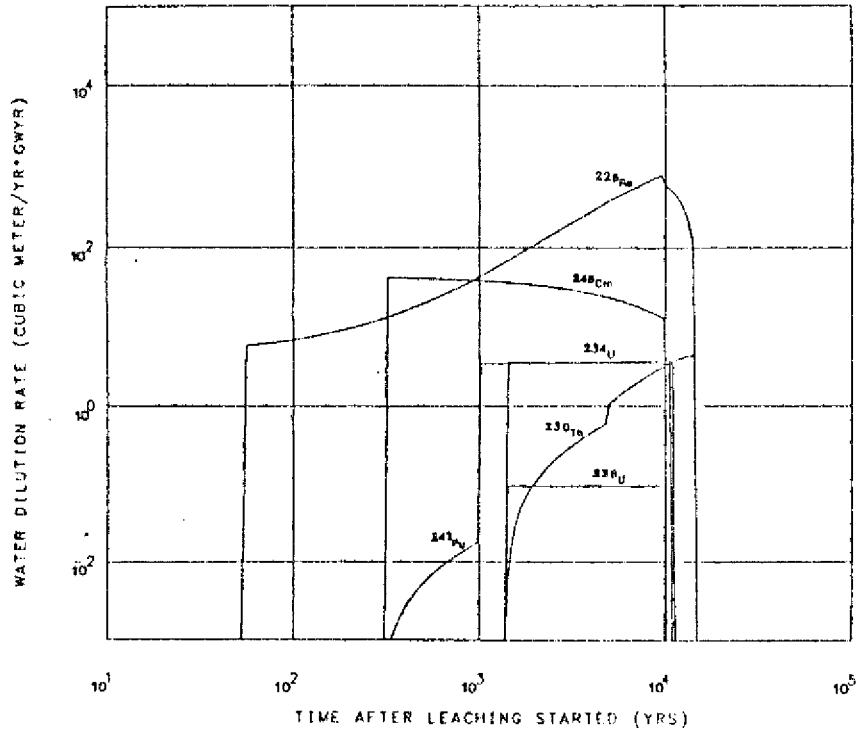
* T is the leach time, representing the duration of release

** From (LI)

*** From 10 CFR20, (Ci/m³)

**** From (B2), (Ci/Gwe.yr)

WATER TRAVEL TIME =1.00E-01 (YRS),LEACH TIME =1.00E+04 (YRS),TIME FOR BEGINNING OF LEACHING =1.00E+03 (YRS)



WATER TRAVEL TIME =1.00E+00 (YRS),LEACH TIME =1.00E+04 (YRS),TIME FOR BEGINNING OF LEACHING =1.00E+03 (YRS)

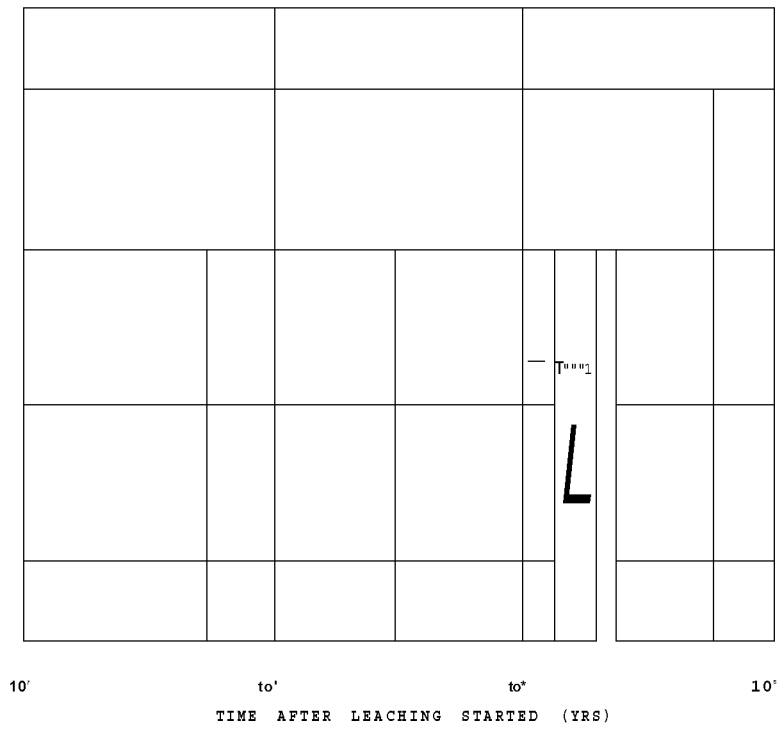
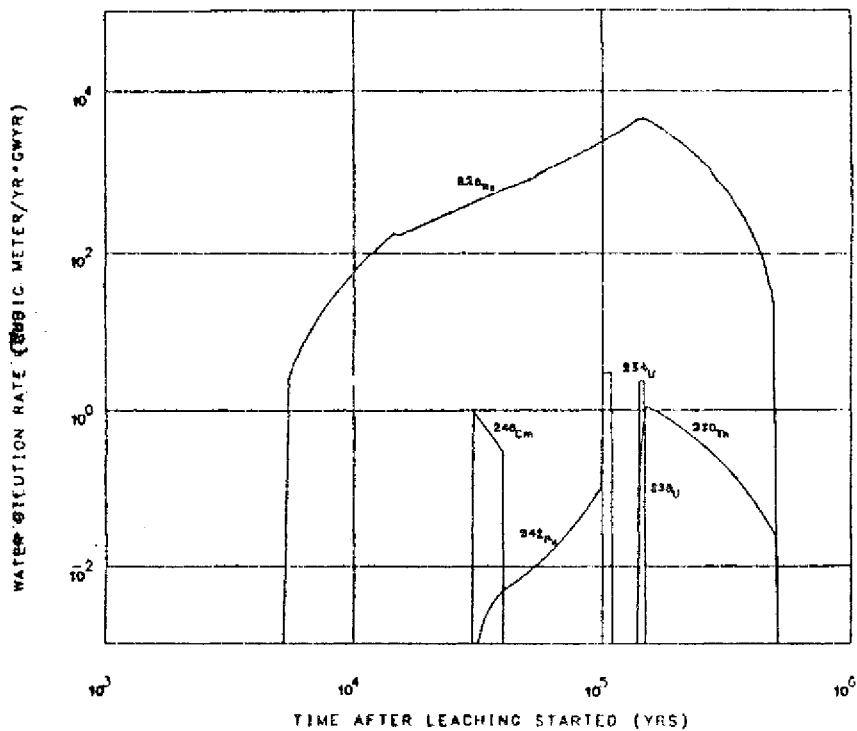


Figure 2.1 Concentration history at water travel times of $z/v=0.1$ and $z/v=1.0$ years for the $4n+2$ actinide chain.

WATER TRAVEL TIME =1.00E+01 (YRS), LEACH TIME =1.00E+04 (YRS), TIME FOR BEGINNING OF LEACHING =1.00E+03 (YRS)



WATER TRAVEL TIME =1.00E+02 (YRS), LEACH TIME =1.00E+04 (YRS), TIME FOR BEGINNING OF LEACHING =1.00E+03 (YRS)

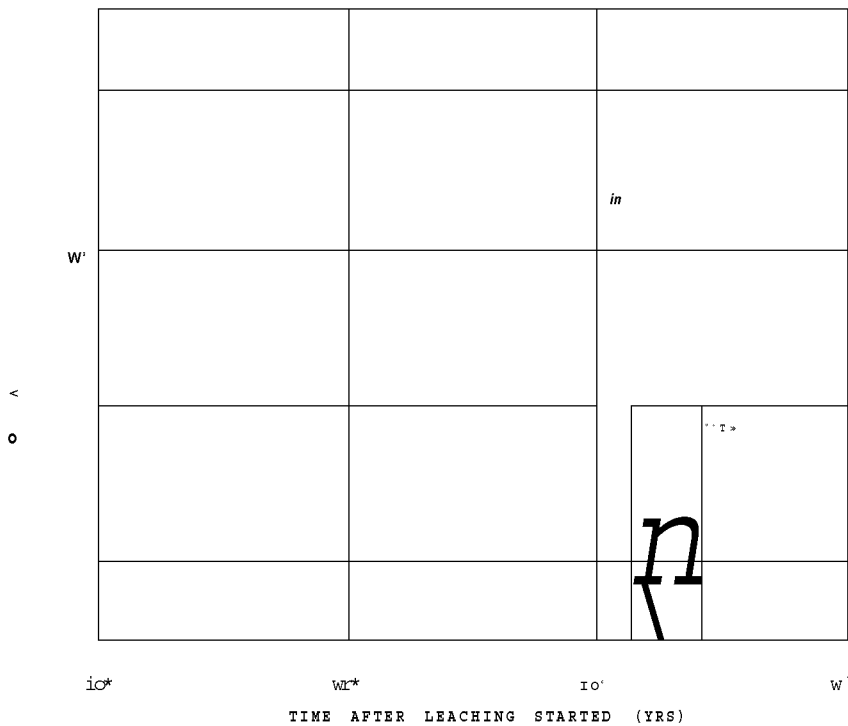
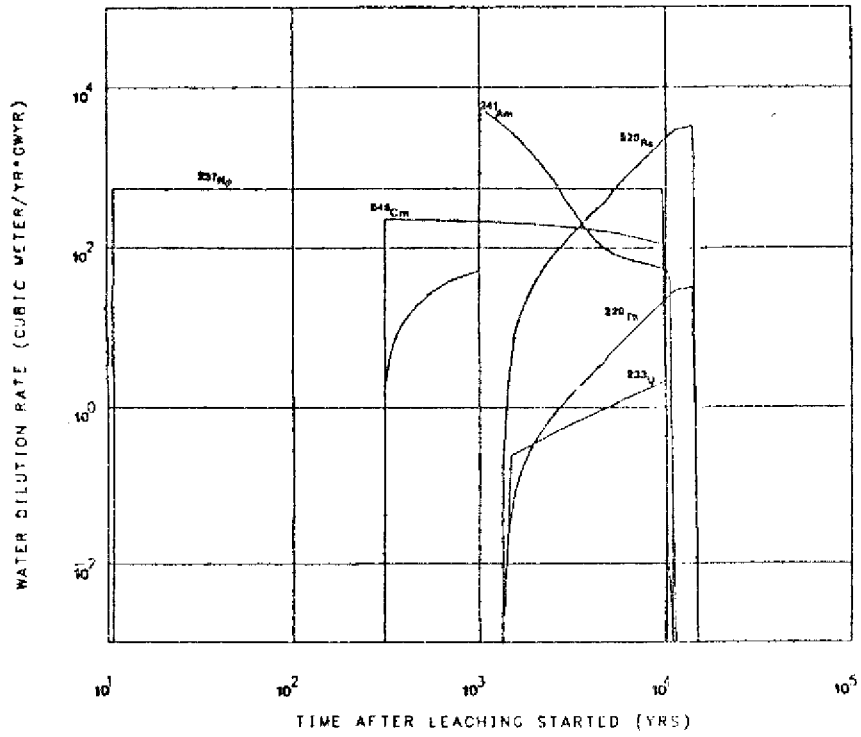


Figure 2.2 Concentration history at water travel times of $z/v=10$ and $z/v=100$ years for the $4n+2$ actinide chain.

WATER TRAVEL TIME >1.00E+01 (YRS), LEACH TIME = 1.00E-104 (YRS), TIME FOR BEGINNING OF LEACHING = 1.00E+01 (YRS)



WATER TRAVEL TIME = 1.00E+00 (YRS), LEACH TIME = 1.00E+04 (YRS), TIME FOR BEGINNING OF LEACHING = 1.00E+03 (YRS)

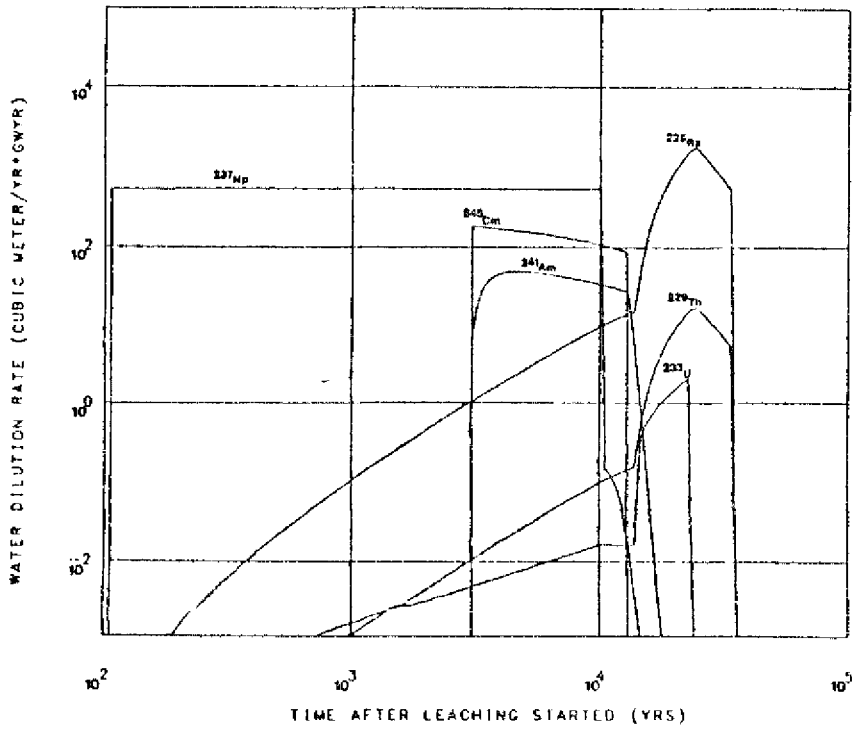
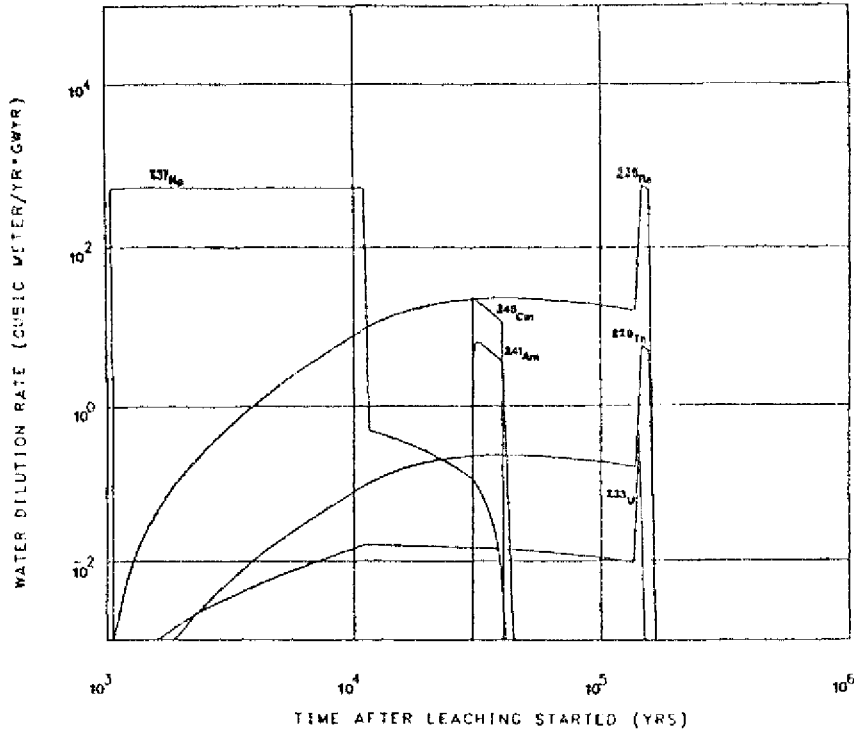


Figure 2.3 Concentration history at water travel times of $z/v=0.1$ year and $z/v=1.0$ year for the $4n+1$ actinide chain.

WATER TRAVEL TIME = 1.00E+01 (YRS), LEACH TIME = 1.00E+04 (YRS), TIME FOR BEGINNING OF LEACHING = 1.00E+03 (YRS)



WATER TRAVEL TIME = 1.00E+02 (YRS), LEACH TIME = 1.00E+04 (YRS), TIME FOR BEGINNING OF LEACHING = 1.00E+03 (YRS)

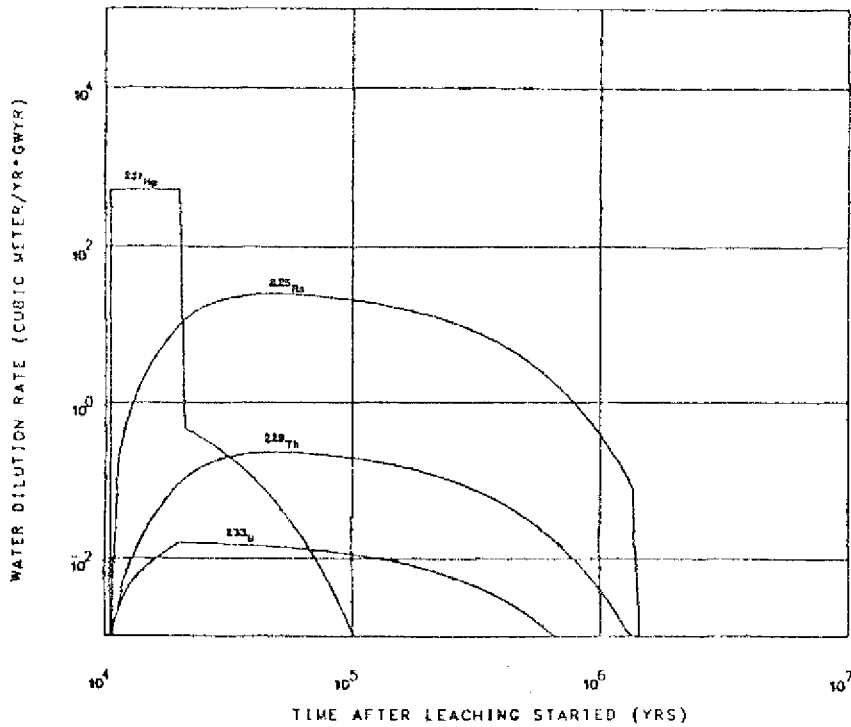
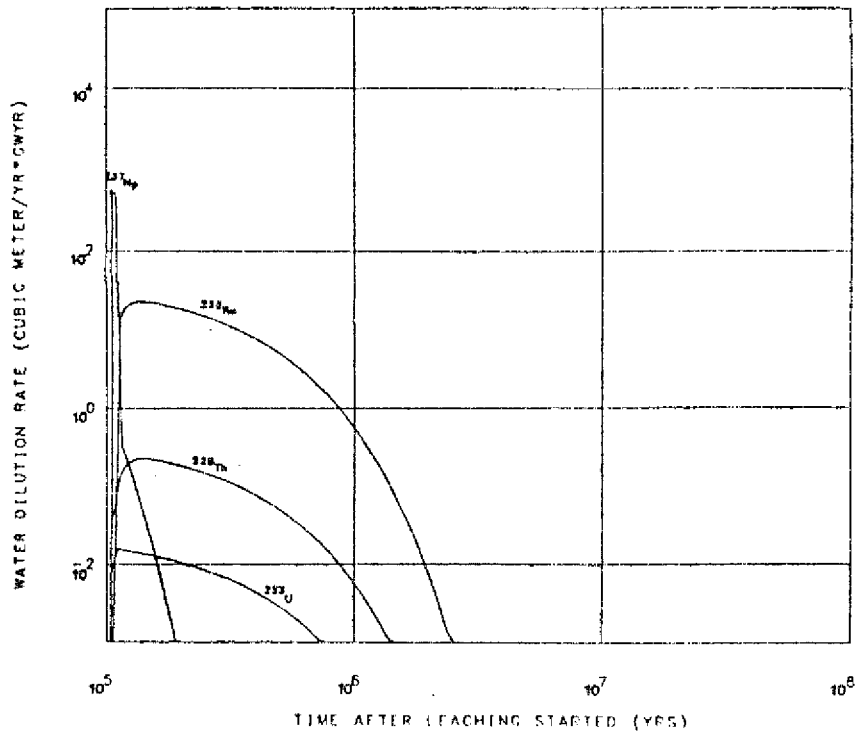


Figure 2.4 Concentration history at water travel times of $z/v=10$ years and $z/v=100$ years for the $4n+1$ actinide chain.

WATER TRAVEL TIME =1.00E+03 (YRS).LEACH TIME =1.00E+04 (YRS).TIME FOR BEGINNING OF LEACHING =1.00E+03 (YRS)



WATER TRAVEL TIME =1.00E+04 (YRS).LEACH TIME =1.00E+04 (YRS).TIME FOR BEGINNING OF LEACHING =1.00E+03 (YRS)

TIME AFTER LEACHING STARTED (YRS)

Figure 2.5 Concentration history at water travel times of $z/v=1000$ years and $z/v=10000$ years for the $4n+1$ actinide chain.

3. Maxima of Release Bands

3.1 Introduction

This research is concerned with the determination of the maxima values of nuclide concentrations which occur during the migration of nuclide chains in geologic media. One is interested in the determination of the position of the maximum concentration of a given nuclide at a fixed time as well as the time at which the maximum is observed at a fixed position in the field. The analysis should be applicable to actinide chains present in high level reprocessed waste and in unprocessed spent fuels.

Normally, the most direct method for the determination of the maxima concentrations would be to solve the appropriate system of transport equations and then search for the extrema of the solutions. Instead of doing this we present an approximation method which allows us to determine the extrema in concentrations without having to calculate the entire concentration history. The method concentrates entirely on the determination of the extrema: their positions in space at a fixed time and their occurrence at a fixed position.

In this study we are neglecting dispersion effects. The results obtained by using this assumption are more conservative

than those which take dispersion into account. One-dimensional water transport and equilibrium sorption for the nuclides in the water and on the soil is assumed. The soil and water properties as well as the water velocity are considered constants.

The basic idea in the approximation method is that when the leach time is small compared with a radionuclide half-life, the exact solution to a band release boundary condition can be approximated by solutions which have forms similar to those when an impulse release boundary condition is used. The extrema are then easily and directly determined from these approximate solutions and the results have a simple and compact form. The approximation method has been extensively tested for all nuclides which are present in high level unreprocessed wastes by comparing it with available results obtained from the exact solution. The range of values for the leach time for which the approximation is accurate has been determined.

Use of this method avoids time consuming evaluation of the complicated exact solution formulas and it provides a quick insight into the effects of the physical parameters on the extrema. As an additional result, the time interval during which a given position is contaminated (contamination time) and the spatial region that is contaminated at a given time (extent of the contamination region) can be also readily obtained. The method will evaluate with good accuracy the extremum of the exact solutions to a decaying band release (without dispersion) and it

is shown to work provided the leach time is smaller than the half-lives of the nuclides involved. Most of the waste forms considered have predicted lifetimes which satisfy such a condition.

The effects on the maxima concentration (expressed in terms of peak water dilution rates) due to the variation of a number of parameters values were studied. The parameters were: the water travel time, the leach time, the time for beginning of leaching and the sorption coefficients. Results are presented in tables and graphs.

Finally, to obtain a qualitative comparison of the potential harm to the biosphere caused by the groundwater leaching of the solid waste we evaluated water dilution rates of the leaching of an equivalent amount of natural uranium ore mill tailings generated in producing the fuel needed to generate 1 Gw(e)yr of electricity in a PWR which produced such a solid waste. In addition the water dilution rates of the leaching of an equivalent amount of the ore was also studied.

3.2 The governing equations and the approximate solution

The system considered is a one-dimensional single region where the flowing groundwater velocity and the soil and water properties are constant. The sorption-desorption process is in equilibrium and dispersion effects are negligible. The governing equation for the concentration $N^i(z,t)$ of the i -th member of a radioactive chain is written as (Hi, Eq.4.102)

$$\frac{\partial N_i}{\partial t} + v \frac{\partial N_i}{\partial z} - D \frac{\partial^2 N_i}{\partial z^2} = \lambda_{i-1} N_{i-1} - \lambda_i N_i \quad i = 1, 2, 3 \quad (3.2.1)$$

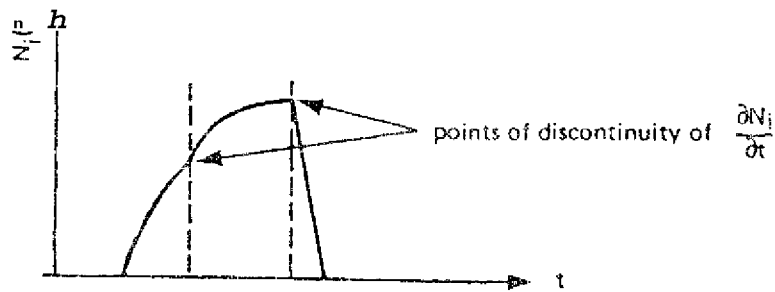
The initial and boundary conditions are expressed as (Hi, Section 3)

$$N_i(z, 0) = 0, \text{ for all } z > 0 \quad (3.2.2)$$

$$N_i(0, t) = N_i^0 \theta(t) [h(t) - h(t-T)] \quad (3.2.3)$$

When a decaying band release occurs at the repository, the general release function $S^i(t)$ is the Bateman's function, $h(t)$ is the unit step function and T is the leach time (yr), (see Section 2.2). The general solution to the governing equation Eq. (3.2.1) subject to the initial condition Eq. (3.2.2) and the boundary condition Eq.(3.2.3) was developed in the previous report (Chambre, H1), and it is rewritten in Section 2.3, Eq. (2.3.1) through Eq.(2.3.8).

The task of finding the extremum of the general solution Eq. (2.3.1) for an arbitrary i -th member is too complex to be performed analytically. This is caused by the presence of step functions which can result in a discontinuous first order derivative inside the domain where the concentration is non zero. The maximum could eventually be located at that point where the discontinuity occurs but the analytical methods provided by differential calculus would fail to detect it. Such a situation is depicted in the following sketch



The general solution Eq. (2.3.1) can be seen to be a function of the leach time T as well as z and t , i.e.: $N^{\wedge}(z, t, T)$. Furthermore, one can notice that the solution Eq. (2.3.1) can be rewritten in the following form

$$N_i = \frac{N_i^0}{v - 2}$$

$$N_i(z, t, T) = N_i^0 e^{-\left[\frac{v}{2} (t - f) + \frac{h}{v} (t - T) \right]} G_i(z, t, T) \quad (3, 2 - 4)$$

where the function $G_i(z, t, T)$ is readily identified from Eq. (2.3.1). Since most difficulties in evaluating analytically the extremum resulted from the terms represented by $G^{\wedge}(z, t, T)$, we

will approximate these functions by simpler forms in order to enable us to obtain the solution extremum in compact and closed form. Let us rewrite the function $G.(z,t,T)$

$$G(z,t,T) = \sum_{j=1}^n \frac{g_j(z)}{A_j} e^{-A_j t} \quad (3.2.5)$$

For small values of the leach time T , $T \ll 1/A_j$, $j=1, 2, \dots, n$, an approximation to the function $G(z,t,T)$ is obtained by using an approximation to the law of the mean for continuous functions

$$G(z,t,T) \approx G(z,t,T=c) + T \left\{ \frac{dG(z,t,T)}{dT} \right\}_{T=c}, \quad 0 < c < T \quad (3.2.6)$$

By setting $T=0$ in Eq.(3.2.5) one can readily see that $G(z,t,T=0) = 0$ and Eq. (3.2.6) is approximated by setting $c=0$

$$(3.2.7)$$

$$G(z,t,T) \approx T \sum_{j=1}^n g_j(z) A_j$$

Eq. (3.2.7) is next used to simplify Eq. (3.2.5). First note that

$$\frac{d}{dt} e^{-A_j t} = -A_j e^{-A_j t} \quad (3.2.8)$$

where $\delta(t)$ is the Dirac's delta function. By using Eq. (3.2.7) in Eq. (3.2.5) one has the following result

$$G(z,t,T) \approx \sum_{j=1}^n \frac{g_j(z)}{A_j} \left[1 - e^{-A_j t} \right] \quad (3.2.9)$$

$$\approx \sum_{j=1}^n g_j(z) \int_0^t \delta(\tau) (h(\tau) - h(\tau - T)) d\tau \quad T=0$$

The bracketed term is expanded below

$$\int_{aT}^a g_{r,n}(T) \ll S_j(t-\tau) [h(t-\tau) - h(t-T-\tau)] d\tau \quad (3.2.10)$$

by using Eq. (3.2.8) there results

$$\int g_{r,n}(\tau) \delta(t-T-\tau) \delta(t-T-\tau) d\tau = \quad (3.2.10a)$$

by using the integration property of the delta functions, it yields

$$= g_{r,n}(t) \delta(0) = g_{r,n}(t) \quad , \quad \text{since } \delta(0) = 1 \quad (3.2.11)$$

with the help of Eq.(3.2.11) one can rewrite Eq.(3.2.9)

$$G_i(z,t,T) = \sum_{j=1}^i \frac{A_j}{N^0} \int_0^t \frac{e^{-\lambda_j m / \nu m} \tau^{j-1}}{m} K_j T g_{r,n}(\tau) d\tau \quad (3.2.12)$$

The above expression for the function $G^i(z,t,T)$ has the same form as if we had solved Eq.(3.2.1) using the impulse release boundary condition instead of a decaying band release boundary condition. The solution to Eq. (3.2.1), Eq. (3.2.2) and an impulse release boundary condition which can be mathematically represented by $\delta(t) = T \delta(t)$, has been obtained in the previous report Hi, Eq.(5.10), (5.20), (5.21) and (5.22), where they are explicitly written for $i=1,2,3$. Those equations can be used here to explicitly express the approximate form of the function $G^i(z,t,T)$ for $i=1,2,3$. Therefore, the concentration of a i -th

member nuclide, Eq.(2.3.1) can be rewritten in its approximate form with the help of Eq. (3.2.12) as

$$N_i(z,t,T) = N_i^0 e^{-\lambda_i t} \left[L_i(t-f_i) [h_i(t-f_i) - h_i(t-f_i-T)] + \sum_{j=1}^{i-1} \frac{A_j^{(j)} N_j^0}{\lambda_j - \lambda_i} e^{-\lambda_j (t-f_j)} \left(\frac{\lambda_j - \lambda_i}{\lambda_j} \right) e^{-\lambda_i (t-f_i)} + \frac{M_j}{D_j} T_j \right] \quad (3.2.13)$$

The above general approximate solution for the concentration of an i-th member is specifically rewritten for the first three members of a radionuclide chain. With the help of Eq. (5.20) from reference Hi the solution for the first member is

$$N_1(z,t) = N_1^0 \exp(-\lambda_1 t) S[\lambda_1 t; \lambda_1 (t-T)] \quad (3.2.14)$$

by using Eq. (5.21) from reference Hi, the concentration of the second member is

$$N_2(z,t) = N_2^0 \exp\{-\lambda_2 z\} S[\lambda_2 t; \lambda_2 (t-T)] + (N_1^0 T) B_{1,2} \exp(-\lambda_2 t - \lambda_1 t) S(\lambda_1 t; \lambda_2 t) \quad (3.2.15)$$

Finally, with the help of Eq. (5.22) from HI, one writes the solution for the third member

$$N_3(z, t) = N^0_0(t) \exp(-\hat{z}) \mathbf{S}[v_3, t; v_3, (t-T)] +$$

$$(N^0T) B_{2,3} \exp(-\hat{z}) S(v_3, t; v_3, t) + \tag{3.2.16}$$

$$(NJT) A \exp(-A_{3,1}t - a_{3,1}z) S(v_1, t; v_3, t) + \exp(-A_{3,2}t - a_{3,2}z) S(v_2, t; v_3, t) +$$

$$+ \exp(-A_{2,1}t - a_{2,1}z) S^t \hat{t}$$

The constants in above equations are defined below

$$x \cdot v \cdot \tag{3.2.17}$$

$$v_{1J}^{TV}$$

$$\begin{matrix} x_i & x_j \\ v_i & v_j \\ i & r \\ v_1 & v_j \end{matrix} \quad \begin{matrix} x \cdot v \cdot \\ 1 J & J 1 \\ v_i \end{matrix} \tag{3.2.18}$$

$$a_{ij} = a_{ji} = \frac{x \cdot - x \cdot}{v_i - v_j} \tag{3.2.19}$$

$$A = x_1 x_2 v_3 / [v_1 (A_2 - X_3) + v_2 (x_3 - x_1) + v_3 (x_1 x_2)] \tag{3.2.20}$$

The function $S(a(t); b(t))$ which is actually a short hand notation for a difference of step functions is defined as follows

$$S[a(t); b(t)] = h[a(t) - z] - h[b(t) - z] \tag{3.2.21}$$

We have therefore obtained an approximate solution which represents the decaying band release problem for small leach times but which has a simpler form than the exact solution. In the next Sections analytical formulas for the **extremum** of this solution are derived.

3.3 Extremum of the solution for the first member

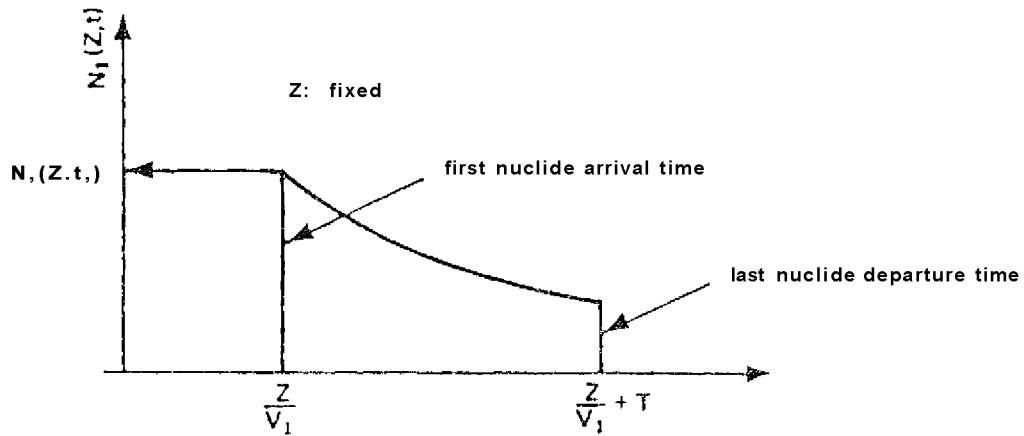
Let us denote the time of the maximum concentration of a given i -th member at a fixed position by t^{\wedge} and the corresponding concentration by $N^{\wedge}(z, t^{\wedge})$. Conversely, the position of maximum concentration at a given fixed time t will be denoted by $z..$ The corresponding concentration will be $(z^{\wedge}t)$. The solution for the first member is the simplest and reads

$$N_1(z, t) = N^{\circ} \exp(-\lambda t) \{h(v_1 t - z) - h(v_1 (t - T) - z)\} \quad (3.3.1)$$

One should note that for the first member the approximate solution is equal to the exact solution. The problem can be divided into two parts: the determination of the time of maximum concentration at a given fixed position and the determination of the position of the maximum concentration at a given fixed time.

3.3.1 Determination of the maximum concentration at a given fixed position.

At a fixed position, the solution Eq. (3.3.1) can be visualized by the following sketch



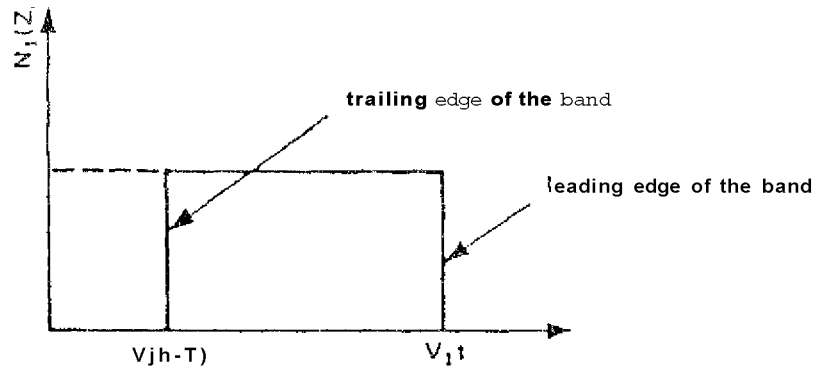
It is apparent that the maximum at a fixed position z occurs at the arrival time of the first nuclide: $t^{\wedge}=z/v^{\wedge}$ and the corresponding concentration is

$$N_1(z, t^{\wedge}) = N_1 \exp(-\lambda z/v^{\wedge}) \quad (3.3.2)$$

3.3.2 Determination of the position of the maximum concentration at a given fixed time

At a fixed time the concentration is constant with respect to position and the position of maximum could be any value of z

between $v^{\wedge}t$ and $v^{\wedge}(t-T)$. The following sketch illustrates this case



The maximum concentration is given by the following

$$N_i(z_i, t) = N^{\wedge} \exp(-A_i t) \quad (3.3.3)$$

but the position of extremum is not unique. It is located at

$$v_i(t-T) < z_i < v_i t \quad (3.3.4)$$

3.4 Extremum of the solution for the second member

The determination of t_2 and z_2 can be divided into stages:

1-The second member is not present at the repository

initially ($N_2=0$).

2-The initial amount of the second member at the repository

is significant ($N_2 \neq 0$).

3.4.1 The second member is not present initially at the repository

By setting $N_2=0$ in Eq.(3.2.15) one has, since $A_{21} = A_{12}$ (this property of interchangeability of the A_{ij} and a_{ij} coefficients subscripts shown in Eq.(3.2.18) and Eq.(3.2.19) will be extensively used throughout this work)

$$N_2(z, t) = N_1^0 T^{-S(v_1 t; v_2 t, \exp(-A_1 t - a_2 z))} \quad (3.4.1)$$

Note that the coefficient of the exponential term i.e. the bracketed term is always positive. This is because when

$$V_1 > V_2 \quad S(v_1 t; v_2 t) = h(v_1 t - z) - h(v_2 t - z) - 1 \quad (3.4.2)$$

$$V_1 < V_2 \quad S(v_1 t; v_2 t) = h(V_1 t - z) - h(v_2 t - z) = -1$$

The exponential term is a monotonically decreasing or

increasing function of either z or t , depending on the sign of either $A_{1,2}$ or λ_2 respectively. The determination of the time $t \rightarrow$ of the maximum concentration at a given fixed position z is first studied. At a fixed position z , the concentration of the second member is an exponential function of time. It will be a monotonically increasing or decreasing function of time depending if $A_{1,2}$ is negative or positive, respectively.

When λ_2 is positive the concentration $N_2(z, t)$ will decrease monotonically as t increases. Therefore, the maximum will always occur on the "arrival time of the first nuclide" at a fixed position z . When $v_2 < v_1$ the first nuclide arrives at z in a time $t_2 = z/v_2$, and when $v_2 > v_1$ the first nuclide arrives at $t_2 = z/v_1$. Figure 3.1.a and Figure 3.1.b represent schematically such situations.

Conversely, when $A_{1,2}$ is negative the concentration $N_2(z, t)$ will increase monotonically as t increases. Therefore, the maximum in this case will occur on the "departure time of the last nuclide" from the position z . When $v_2 > v_1$ the last nuclide departs from z at a time $t_2 = z/v_2$, and when $v_2 < v_1$ the last nuclide departs at a time $t_2 = z/v_1$. Figure 3.1.c and Figure 3.1.d represent schematically these cases. The above four possibilities are summarized in Table 3.1. In this case the maximum at a fixed position z always occurs at a time determined by the velocity of the nuclide which has the smaller product $A.K.$ according to Table 3.1. One can therefore reduce Table 3.1

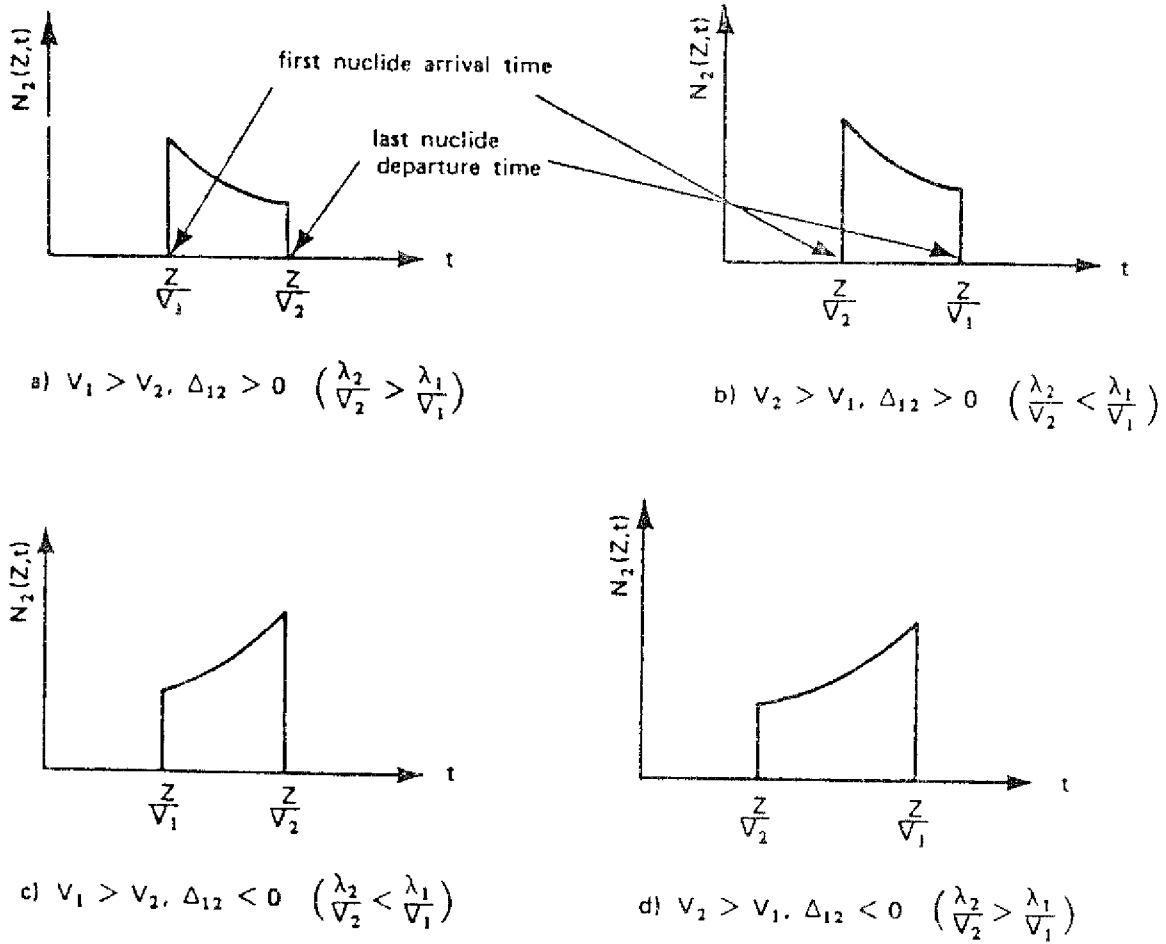


Figure 3.1- Different possibilities for the maximum of a 2nd member at a fixed position when $N^0 = 0$.

into the following more compact form shown in Table 3.2. The corresponding concentrations can then be evaluated using t^{\wedge} from Table 3.2 in Eq.(3.4.1)

Case:	$x_i r^{x_2} K_j - K_2 > v$	$x K_1 \rightarrow K_2$ $K_1 K_2 < v$
	$t_2 = \wedge (x_2 K_2 > X_j K_j)$	$*2 = (x_1^{x_1} > x_2^{x_2})$
$K_2 < K_j$	$i_2 \sim \sim_2 (hh > i_2^{x_2})$	$t_2 = v_j \wedge x_2^{x_2} > x_1^{x_1}$

Table 3.1-Different possibilities of the time to attain maximum concentration for second member at a fixed position
0

$x_j K_j y x$	$x_1^{x_1} x_2^{x_2}$
$i_2 = 7^{x_2}$	$t_2 = \frac{-K_1}{v} 1$

Table 3.2- Time of maximum concentration for the second member when $N_2 = 0$. at a fixed position.

Next, the determination of the position of the maximum concentration at a given fixed time is studied. One sees from Eq. (3.4.1) with a fixed time t , that when a^{\wedge} is positive the concentration $N_2(z, t)$ will decrease monotonically as z increases. Therefore, the maximum will always occur at the "trailing edge" of the migration band. When $v^{\wedge} > v_2 t$ the trailing edge is determined by $z_2 = v^{\wedge} t$ when $v_2 > v^{\wedge}$, the trailing edge is at $z_2 = v_2 t$. These situations are represented schematically by Figure 3.2.a and Figure 3.2.b.

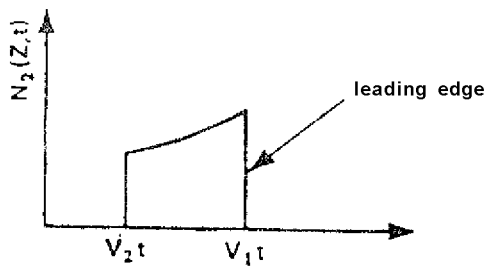
Conversely, when a^{\wedge} is negative the concentration $N_2(z, t)$ will increase monotonically as z increases. Thus, the maximum will always occur on the leading edge of the band. In this case, when $v_1 > v_2$ the leading edge is $z_2 = v_1 t$ and when $v_1 < v_2$, it is $z_2 = v_2 t$. Thus, the maximum will always occur on the leading edge of the migration band. Figure 3.2.c and Figure 3.2.d represent schematically these cases. The four possibilities for the location of the maxima, z_2 at a fixed time t are summarized in Table 3.3 below.

	$a^{\wedge} = \frac{v_1 - v_2}{v_1 + v_2} > 0$	$v_1 > v_2$
$v_1 > v_2$	$z_2 = v^{\wedge} t \quad (x_j > x_i)$	$z_2 = v_1 t \quad (x_i > x_j)$
$v_1 < v_2$	$z_2 = v_2 t \quad (x_i > x_j)$	$z_2 = v_2 t \quad (x_j > x_i)$

Table 3.3 Different possibilities of the position to attain a maximum concentration for a second member ($N^{\wedge} = 0$).

V_{1t}
 a) $V_1 > V_2, a_{12} > 0 \quad (X_1 > X_2)$

Z
 V_1t
 b) $V_1 > V_2, a_{12} > 0 \quad (A_1 > A_2)$



c) $V_1 > V_2, a_{12} < 0 \quad (A_1 > A_2)$

2
 V_1t V_2t
 d) $V_1 > V_2, a_{12} < 0 \quad (X_1 < X_2)$

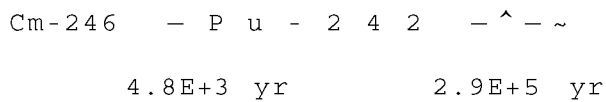
Figure 3.2 Different possibilities for the maximum of a 2nd member at a fixed time when $N^0 = 0$.

In this case one notices that the maxima always occurs at the location determined by the velocity of the nuclide with the smaller decay constant, regardless of which nuclide travels faster. Therefore, one can conclude that at a fixed time, the position of the maximum is determined by the decay constant of the nuclides. Hence, one can further simplify Table 3.3 into Table 3.4. The corresponding concentration can then be evaluated using Eq. (3.4.1)

$x_2 > x_x$	$x_2 < X_j$
$z_2 = V_j t$	$z_2 = v$

Table 3.4 Position of the maximum concentration for the second member at a fixed time when $N_2=0$.

The determination of the extremum for the second member is now illustrated with a numerical example. Consider for instance the following chain



For the purpose of illustration let us adopt the following values: $\lambda_1=3000$ and $K_2=10000$. The time of maximum concentration at a fixed z can be readily read from Table 3.2 by using the condition $\lambda_1 > \lambda_2$, and it is $t_2 = z/v_2$. The corresponding concentration is

$$N_2(z, t) = (N_1 T) B_{1,2} \exp(-\gamma v_2) z \quad (3.4.2a)$$

Similarly, the position of maximum concentration at a fixed time t can be obtained from Table 3.4 by using the condition $X > A$, X'

and it is $Z_2 = v_2 t$. *** , the maximum concentration at a fixed time t is

$$N_2(z, t) = (N^T) B \exp(-X_2 t) \quad (3.4.2b)$$

Consider a position $z=1000$ meters away from the repository, a time $t=1000$ years after the leaching started, a water velocity of $v=10$ m/yr and a leach time $T=103$ years. Then, at the position $z=1000$ meters the maximum concentration occurs at a time $t = 10^4$ years and it has a magnitude of $N_2(z, t)/N^T = 0.01$. Conversely, after $t=1000$ years, the maximum concentration occurs at a position $z = 1$ meter from the repository with a concentration $N_2(z, t)/N^T = 0.01$.

Besides the determination of the extremum of the solution, another features of the approximate solution can be deduced, namely: the contamination region at a fixed time and the contamination time interval at a fixed position. Let us denote by R_i the region which is contaminated by the i -th nuclide at a given time. For the second member, from Eq. (3.4.1) one notices that the solution is non trivial in the region defined by

$$z = v_2 t - v_2 t \quad (3.4.6)$$

Here v_{pt} is the front edge of the band and v is the fastest nuclide velocity, v^*t is the trailing edge of the band and v_s is the slowest nuclide velocity.

On the other hand, the contamination time interval which is the time interval in which there are i -th member nuclides present at a given position z , it is denoted by Δt_i . For the second member, from Eq.(3.4.1) one concludes that

$$\Delta t_2 = \frac{z}{v_1} - \frac{z}{v_s} \quad (3.4.7)$$

where z/v_1 is the first nuclide arrival time at a given position z and z/v_s is the last nuclide departure time. The effect of a large difference in nuclides velocities is a large contamination time interval and contaminated region (see Eq.(3.4.6) and Eq.(3.4.7)), but the corresponding maxima concentrations are reduced since they are inversely proportional (see Eq.(3.4.1)).

With the data from the previous example, the contaminated region at a given time t would be

$$R_c = (v^* - v_s)t \approx 2.33 \times 10^{-4} vt \quad (\text{meters})$$

while the contamination time at a given position z would be

3

$$\Delta t_2 = \frac{z}{v} - \frac{z}{v^*} = 7.00 \times 10^{-4} \left(\frac{z}{v}\right) \quad (\text{years})$$

where v is the groundwater speed

Suppose we are interested again in a time $t=1000$ years, $z=1000$ meters and $v=10$ m/yr, the contamination time interval $t_0=7.0E+5$ years while the contaminated region is $R^*=2.3$ meters. Therefore, at a position 1000 meters away from the repository, Pu-242 will be present during $7 \gg 0E+5$ years and after 1000 years of the beginning of leaching, the Pu-242 migration band has only spread to an extension of 2.3 meters.

3.4.2 The second member has non zero initial concentration at the repository

In this case, $N \neq 0$ and Eq. (3.2.15) contains both terms

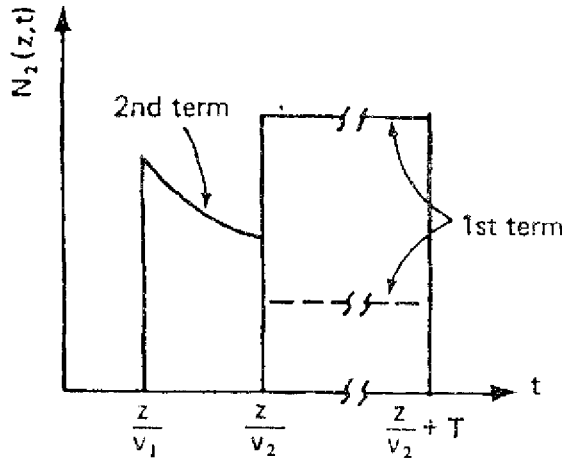
$$N_2(z, t) = N_2^0 \exp\left(-\frac{\lambda_2 z}{v_2}\right) S[v_2 t; v_2(t-T)] \phi_2(t) + N_1^0 \frac{T \lambda_1 v_2}{v_1 - v_2} \exp(-\Delta_{21} t - \alpha_{21} z) S(v_1 t, v_2 t) \quad (3.4.8)$$

The added term represents those second member nuclides initially emitted at the repository and it has the same form as the first member solution Eq. (3.2.14). The second term represents the decay of the first member nuclides which were emitted at the repository generating daughter nuclides. Evaluation of the extremum of each of these individual terms has been done in past sections.

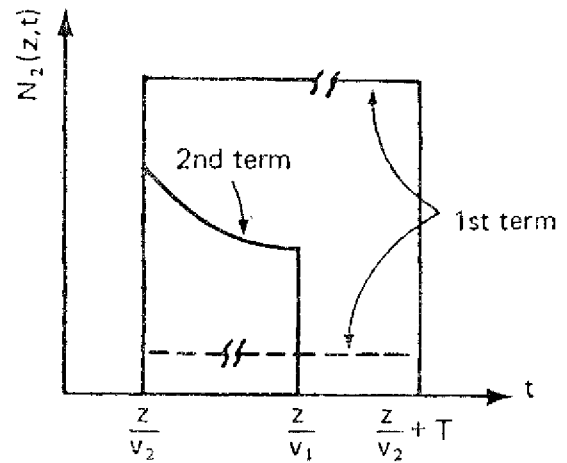
Eq. (3.4.8) can be seen as a superposition of two functions represented by each one of the terms described above. Let us consider a fixed position z , the first term is non trivial in the time interval $z/v_2, z/v_2+T$ and $\phi_2(t)$ is an exponential function of A_2, A_1 . But since we have assumed $T \ll 1/A_j$ $j=1,2$, the exponential decay during this time interval T is negligible and we can assume this term as being a band of constant magnitude. Hence, one can set $\phi_2(t)=1$ in Eq. (3.4.8).

The different configurations that Eq. (3.4.8) can take, depending on the relative magnitude of the nuclide velocities, are illustrated in Figure 3.3. When no daughters are present initially at the repository ($N_2=0$), the extremum is always located at one of the boundaries of either the contaminated time interval in the case of a fixed position or the contaminated region in the case of a fixed time. However, when N^0 , one can see in Figure 3.3 that one might have a interior maximum, i.e. when the time of maximum t_2 occurs inside the contamination time interval. In this case, the extremum cannot be determined based solely on the monotonic character of the functions involved.

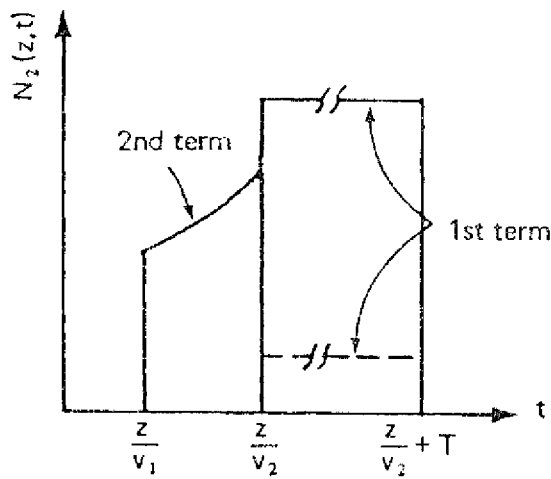
The dotted lines in Figure 3.3 represent the case when the first term contribution is smaller than the second term contribution. For the cases "b" and "c" the time of maxima is clearly $t_0=z/v_2$. However, in the cases "a" and "d", one must evaluate $N(z, t=z/v_1)$ and $N_2(z, t=z/v_2)$ using Eq. (3.4.8) to decide whether the extremum occurs at z/v_1 , or z/v_2 . Taking the ratio of



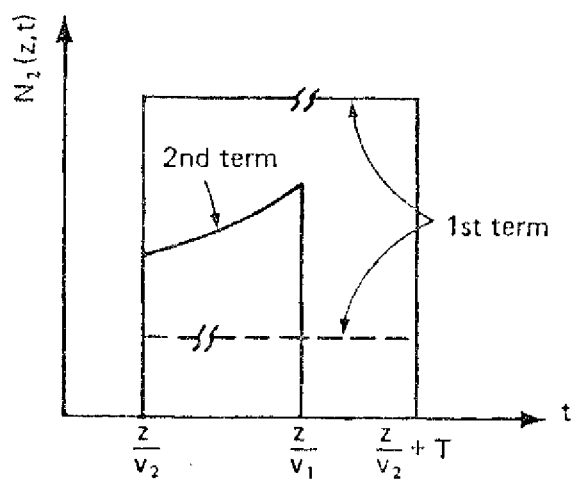
a) $v_1 > v_2, \lambda_2 k_2 > \lambda_1 k_1, z$ fixed



b) $v_2 > v_1, \lambda_2 k_2 < \lambda_1 k_1, z$ fixed



c) $v_1 > v_2, X_2 k_2 < X_1 k_1, z$ fixed



d) $v_2 > v_1, X_2 k_2 > X_1 k_1, z$ fixed

Figure 3.3 Possible configurations for the concentration $N_2(z, t)$ at a fixed position z ($N_2 \neq 0$).

above concentrations calculated by using Eq. (3.4.8) and denoting it by R one has

$$R = \frac{N_2(z, t = z/v)}{N_2(z, t = J)} \frac{\sqrt{2} \cdot \sqrt{1 + 12t}}{(NJT) \cdot b_{1,2}} \exp \quad (3.4.9)$$

therefore, when $R > 1$ the concentration $N_2(z, t = z/v)$ is the largest and $t = z/v$ but when $R < 1$ the concentration $N_2(z, t = z/v)$ is the largest and in this case $t = z/v$. The coefficient B is inside a modulus sign because the product B times the function $S(vjt; v_2t)$ is always positive as it is shown in Eq. (3.4.2).

Consider first the case when $R > 1$. For the cases "a" and "d" $\sqrt{2} \cdot \sqrt{1 + 12t}$ and if \dots Eq. (3.4.9) results

$$\ln \frac{N_2(z, t = z/v)}{(NJT) \cdot b_{1,2}} \sqrt{2} \cdot \sqrt{1 + 12t} \quad \text{yields: } t_0 = \dots \quad (3.4.10)$$

Similarly, for the case when $R < 1$, when Eq. (3.4.9) is solved for z one obtains

$$\ln \frac{\sqrt{2} \cdot \sqrt{1 + 12t}}{(NJT) \cdot b_{1,2}} \quad \text{yields: } t_0 = \dots \quad (3.4.11)$$

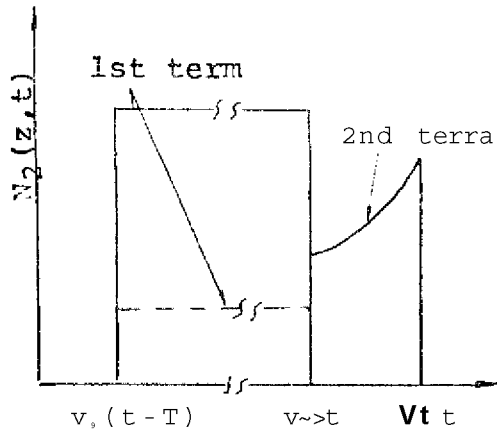
Denoting the quantity on the right hand side of Eq. (3.4.10) and Eq. (3.4.11) by W

The following Table 3.5 summarizes the time for the maxima concentration of the second member at a fixed position when its initial concentration is non zero.

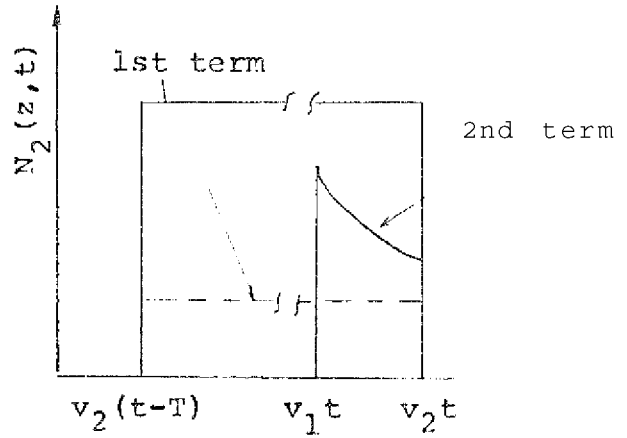
	$2 < W$	$2 > W$
	$2 v_2$	$t - \frac{2}{v_2}$
$x_1^{(1)} \quad x_2^{(2)}$	$2 v_2$	$2 v_1$

Table 3.5 The time when the maximum concentration of the second member occurs at a fixed position when the initial daughter concentration is non zero (N^0).

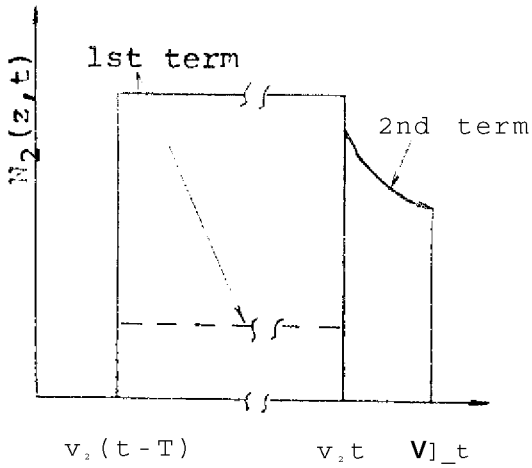
Next, the case of the extremum for the second member at a fixed time is studied. Figure 3.4 shows the different configurations that the second member concentration Eq. (3.4.8) can take, depending on the relative magnitude of the nuclide velocities. For a given fixed time, the cases "b" and "d" show clearly that the extremum occurs at $z = v_2 t$. This is because when the two terms are added, the largest value of the concentration will always occur at $z = v_2 t$.



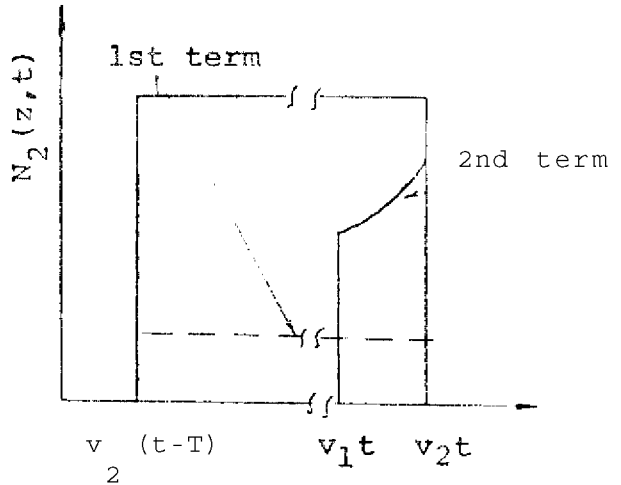
a) $v > v_2, x_2 > X-j, t$ fixed



b) $v_1 > v_1, a_2 < >_{11}, t$ fixed



c) $v_1 > v_2, A_2 < \hat{^}_1, t$ fixed



d) $v_2 > v_1, > . > x_1, t$ fixed

Figure 3.4 Possible configurations for the concentration of the second member $N_2(z, t)$ at a fixed time ($N_2 \neq 0$)

For the cases "a" and "c" one must compute the concentrations at the points $z=v^+t$ and $z=v^-t$ where the extremum may occur and compare them to decide which one is actually the maximum. By using Eq. (3.4.8) one evaluates the concentrations at $z=v^-t$ and $z=v^+t$ and denoting their ratio by R' results

$$R' = \frac{N_2(z=v^+,t)}{N_2(z=v^-,t)} = \frac{N_2 + TNj B_{1,2} \exp(X^+ - X_2) t}{t n_0 | b_{1,2}} \quad (3.4.13)$$

When $R' > 1$ the concentration at $z=v^+,t$ is the largest and the maximum occurs at $z \sim v^+t$. The time t is solved in Eq.(3.4.13) when the condition $R > 1$ is satisfied (i.e. the maximum occurs at $z=v^+,t$)

$$t < \sim \frac{\ln \left(\frac{N_2 + TNj B_{1,2} \exp(X^+ - X_2) t}{t n_0 | b_{1,2}} \right)}{X^+ - X_2} \quad (3.4.14)$$

Conversely, when $R < 1$, the concentration at $z=v^-t$ is the largest and the extremum occurs at $z=v^-t$. Solving Eq.(3.4.13) for the time t when the condition $R < 1$ is satisfied results

$$t > - \frac{\ln \left(\frac{N_2 + TNj B_{1,2} \exp(X^+ - X_2) t}{t n_0 | b_{1,2}} \right)}{X^+ - X_2} \quad (3.4.15)$$

The different possible cases for the extremum of the concentration of the second member when $N_2 \neq 0$ at a fixed time shown in Figure 3.4 and Eq. (3.4.14) and Eq. (3.4.15) are summarized in Table 3.6 below

	$t < W$	$t > w'$
$x_1 > x_2$	$x_2 = V$	
$x_1 < x_2$	$x_2 = v_2 t$	$t_2 = v_x t$

In (N?T; '12!
 where $w's - x_1 \sim x_2$

Table 3.6 The position of the maximum concentration for the second member at a fixed time when N^0 .

When the second member is initially present at the repository, the contamination time and the contaminated region can be determined according to Eq.(3.4.8). They are summarized in Table 3.7 below (see Appendix D for the derivations). One should notice that when the initial amount of the second member is negligible Tables 3.5 and 3.6 reduce to Tables 3.2 and 3.4 respectively. This is because W and $W \gg$ are null when $N_2^0 = 0$ and the conditions $z > W$ and $t > W'$ are always satisfied.

Cases	Contamination time	Contaminated region
$v_1 > v_2$	$\bullet^* - (V_{ii})^* T$	$R_2 = v_1 t \sim v_2 \wedge \sim T \wedge$
$v_1 < v_2$	$g_2 = \frac{v_1}{v_2} - \text{if } \frac{v_1}{v_2} > T$	$R_2 = (v_2 - v_1) t \text{ if } (v_2 - v_1) t > v_2 T$
	$e_2 = T \text{ if } \frac{v_1}{v_2} < T$	$R_2 = v_2 t \wedge \wedge v_2 \sim v_1 \wedge \wedge v_2 t$

Table 3.7 Contamination time and contamination region for the 2 member when $N^0 + 0$.

3.5 Extremum of the solution for the third member

This problem is again subdivided into two stages:

1-The initial amount of the third member present at the repository is zero ($N_3^0 = 0$).

2-The initial amount of the third member is significant at the repository, ($N_3^0 \neq 0$),

3.5.1 The initial amount of the third member at the repository is zero

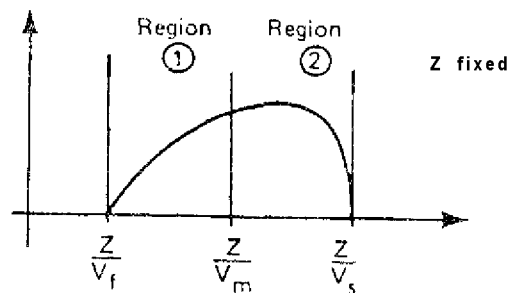
By setting $N_3^0 = 0$ in Eq.(3.2.16) the solution for this case reads

$$N_3(z,t) = T(B_{33}N_3^0 - AN_3^0) \exp(-A^*t - a_{13}z) S(v_3t; v_3t) + N_3^0 TA \exp(-A_{13}t - a_{13}z) S(v_1t; v_1t) - N_3^0 TA \exp(-A_{12}t - a_{12}z) S(v_2t; v_2t) \quad (3.5.1)$$

Depending on the relative magnitudes of the nuclide velocities, the functions $S(v^*t; v^*t)$ can assume the values of -1, 0 or +1. Therefore, for each one of the six possible different combinations of the three nuclide velocities, different signed terms in Eq. (3.5.1) will arise. The task of determining the extremum of the Eq. (3.5.1) is indeed expanded to the task of

determining the extremum of six different functions, depending on the relative magnitude of the nuclide velocities.

In order to determine the time of the maximum concentration at a fixed position, the following procedure is adopted. For a particular set of nuclide velocities, v_s, v_m, v_f , where subscript s stand for slowest, m for medium and f for fastest, the solution can be sketched as follows



The form of the solution for the concentration of a third member Eq.(3.5.1) does not permit two nuclides in the same chain to have the same velocity. The terms represented by B_i (see Eq. (3.2.17)) have a singularity when $v_i = v_j$. Since the three nuclides have necessarily different velocities, at a fixed position z , the migration band boundaries z/v_f , z/v_m and z/v_s have different values. Two different regions are thus defined: region 1 where $z/v_s < t < z/v_m$ and region 2 where $z/v_m < t < z/v_f$.

Consider for instance the case where $v_f > v_m > v_s$ ($f=1, m=2, s=3$). Therefore, in region 1 $z/v_f < t < z/v_2 < z/v_3$ and in region 2 $z/v_f < z/v_2 < t < z/v_3$. Recalling the definition of the functions $S(v_i, t; v_j) = h(v_i t - z) - h(v_j t - z)$ one can evaluate the value

of these functions in Eq.(3.5.1) in each region.

In region 1

$$S(v_2t; v_3t) = h(v_2t - z) - h(v^{\wedge}t - z) = 0 - 0 = 0$$

$$S(v_3t; v_3t) = h(v_x t - z) - h(v_3t - z) = 1 - 0 = 1$$

$$S(v_1t; v_2t) = h(v - ^{\wedge} - z) - h(v_2t - z) = 1 - 0 = 1$$

In region 2

$$S(v_2t; v_3t) = h(v_2t - z) - h(Vgt - z) = 1 - 0 = 1$$

$$S(v_1t; v_3t) = h(Vjt - z) - h(v_3t - z) = 1 - 0 = 1$$

$$S(v^{\wedge}t; v_2t) = h(v_1t - z) - h(v_2t - z) = 1 - 1 = 0$$

The solution Eq.(3.5.1) takes different form in each of these regions, because the functions $S(v^{\wedge}t; \mathbf{v}j t)$ assumes different values in each region for the same set of nuclide velocities. Let us summarize in Table 3.8 the values of the functions $S(v-t; v_j t)$ in each region and for the six possible combinations of the nuclide velocities, (see Eq. (3.2.21)).

In the case of the solution for the second member concentration discussed in last section, the functions were always monotonically decreasing or increasing inside the domain of definition and the extremum was located at the boundaries of the domain of definition. However, for the third member solution, the first partial derivative of the concentration with respect to time may vanish inside one of the two regions defined above. In this case, one might have a interior maximum and this possibility must be investigated,

Case	\mathbf{W}^v_s	Region 1			Region 2		
		$S(v_1, t; v_1, t)$	$S(v_1, t; v_2, t)$	$S(v_2, t; v_2, t)$	$S(v_2, t; v_1, t)$	$S(v_2, t; v_2, 0)$	$S(v_1, t; v_2, t)$
1	\mathbf{W}^v_3	0	1	1	1	1	0
2	\mathbf{W}^v_i	-1	-1	0	0	-1	-1
3	\mathbf{W}^v_2	0	1	1	-1	0	1
4	$2 \ 3 \ I$	1	0	-1	0	-1	-1
5	$\mathbf{V}_{, >v_1, >v_2}$	-1	-1	0	-1	0	1
6	$v_2 \cdot v_1 \cdot v_3$	1	0	-1	1	1	0

Table 3.8: Values for the functions $S(v_1, t; v_2, t) = h(v_1, t - z) - h(v_2, t - z)$

The procedure adopted to evaluate the time of maximum for each of the six cases will be to evaluate the individual maximum of the concentration for each region and then to compare them in order to decide which one is actually the true extremum of the solution in both regions. The first of the six cases listed in Table 3.8 will be studied in detailed. For the case 1, where $v^>$ region is studied individually. In region 1, from Eq.(3.2.16) and Table 3.8 the concentration distribution in this region is given by

$$N_1(z,t) = TA \exp(-A_{13}t - a_{13}z) - TA \exp(-A^t - a_1z) \quad (3.5.2)$$

and it is non trivial for a given $z>0$ in the time interval: $z/v^<$ $t<z/v_1$ which is the domain of definition of Eq. (3.5.2). The partial derivative with respect to time of Eq.(3.5.2) is

$$\frac{\partial N_1}{\partial t} = -A_{13}TA \exp(-A_{13}t - a_{13}z) + TA \exp(-A^t - a_1z) \quad (3.5.3)$$

The function described by Eq. (3.5.2) can have, if any, only one extremum in its domain of definition because Eq.(3.5.3) can have only one zero, if any, in its domain of definition (region 1). The zero of Eq. (3.5.3), if it exists, occurs at

$$t_3 = \frac{1}{A_{21} - A_{31}} \quad (3.5.4)$$

By evaluating Eq.(3.5.3) at the beginning of its domain of

definition $t = z/v^{\wedge}$ one has

$$1 \quad 3 \quad z \quad *] \quad (3.5.5)$$

furthermore, one can show that

$$A(A_{,1} - A_{,1}) = -V P_v \longrightarrow 0 \quad (3.5.6a)$$

hence,

$$3N \quad -r^{\wedge}(z, t = -) > 0 \text{ for any } 2 > 0.$$

Therefore, Eq.(3.5.2) is initially increasing and if the zero of Eq. (3.5.3) lies inside the domain of definition the extremum will be a maximum, i.e., if $z/v^{\wedge} < t_3$ (Eq. (3.5.4)) $< z/v_2$, t_3 will be a point of maximum. On the other hand, if t^{\wedge} given by Eq. (3.5.4) does not exist or it lies outside the domain of definition, the function Eq.(3.5.2) is monotonically increasing in its domain of definition and the maximum will occur at the end of the region 1, i.e. $t_3 = z/v_2$. The inequality resulting from t_3 lying inside the domain of definition can be expressed in terms of the position z by using Eq. (3.5.4)

$$1 \quad 21 \sim 31 \quad \ln \quad (a 21^{\circ} 31)^2 \quad (3.5.6)$$

The same derivation is repeated for the second region. From Eq. (3.2.6) and using Table 3.8 the concentration

distribution in this region is given by

$$U, t) = T \left(\frac{2^2 \lambda}{N} - A \right) \exp(-A_{23} t - a_{23} z) + T A \exp(-i^2 t - a^2 z) \quad (3.5.7)$$

and it is non trivial for a given $z > 0$ in the interval $z/v_2 < t < z/v_3$, which is the domain of definition of Eq. (3.5.7). The partial derivative with respect to time of Eq.(3.5.7) is

$$\frac{\partial}{\partial t} U(z, t) = T \left(\frac{2^2 \lambda}{N} - A \right) A_{23} \exp(-A_{23} t - a_{23} z) - T A a_{23} \exp(-i^2 t - a^2 z) \quad (3.5.8)$$

Again, the function described by Eq.(3.5.7) can have, if any, only one extremum in its domain of definition. This is because Eq.(3.5.8) can have, if any, only one zero in its domain of definition. The zero of Eq. (3.5.8) , if any, occurs at

$$\ln \frac{A - B_{23} t / N}{A_{23}} = (a_{23} - a_{13}) z \quad (3.5.9)$$

Let us evaluate Eq.(3.5.8) at the end of the domain, $t = z/v_3$

$$\frac{\partial}{\partial t} U(z, t) = T \left(\frac{2^2 \lambda}{N} - A \right) A_{23} \exp(-A_{23} z/v_3 - a_{23} z) - T A a_{23} \exp(-i^2 z/v_3 - a^2 z) \quad (3.5.10)$$

Two possibilities results from Eq. (3.5.10)

$$jATip^{\wedge} \hat{f} < 1 \text{ yields } \wedge (z, t, f - X O) \quad (3.5.12)$$

Suppose given by Eq. (3.5.9) exists and it is interior, i.e.,

$$z/v_2 < L t_3 (Eq. 3.5.9) < z/v_1 \quad (3.5.13)$$

Then, when Eq. (3.5.11) is true, if the partial derivative Eq. (3.5.10) is positive t^{\wedge} is necessarily a point of minimum, while if the inverse occurs t^{\wedge} given by Eq. (3.5.9) is a point of maximum. On the other hand, if t_3 given by Eq. (3.5.9) does not exist or it is outside the domain of definition, the function Eq. (3.5.7) is monotonically increasing if the derivative evaluated in Eq. (3.5.10) is positive and the extremum occurs at $t_3 = z/v_3$. Conversely, $N_3(z, t)$ is monotonically decreasing if the derivative in Eq. (3.5.10) is negative and there results the extremum on $t_3 = z/v_2$. The inequality Eq. (3.5.13) can be rewritten by using Eq. (3.5.9) to express this condition in terms of the position z

$$\frac{2}{v_2} < \frac{1}{v_1} < \frac{z}{v_3} \quad (3.5.14)$$

After having determined the time of the maximum in each region, one substitute these values of time back into the corresponding Eq. (3.5.2) and Eq. (3.5.7) to evaluate the maxima concentrations in each region. By comparing these concentrations one can finally decide about the actual maximum for both regions.

Above procedure will yield the extremum for the third member concentration for the first case of the Table 3.8 at a fixed position. This derivation is repeated for the other five cases listed in Table 3.8 and a general form of the extremum can be obtained and it is summarized in Table 3.9. As before, a given case is denoted by: $v_f v_m v_s$ where the subscripts indicate

f =fastest nuclide velocity, $f=1, 2, 3$.

m =intermediate nuclide velocity, $m=1, 2, 3$.

s =slowest nuclide velocity, $s=1, 2, 3$.

(For example, the case 1 in Table 3.8 would be $f=1, m=2, s=3$).

3.5.2 Extremum of the solution for the third member when its initial amount at the repository is non zero

In this case, the complete solution Eq. (3.5.1) is required

$$N_3(t) = N_3^0 \exp(-\lambda_3 t) S[v_3 t; v_3(t-T)] + \dots \quad (3.5.15)$$

$$N^0(TB_{23} - N^0 TA) \exp(-\lambda_3 t) S[v_3 t; v_3(t-T)] + N^0 TA \exp(-A_3 t - a_3 j_2) S(v_3 t; v_3 t) + N^0 TA \exp(-A^* t - a^* z) S(v^* t, v^* t)$$

The second term which is inside the bracket was analyzed in the previous section and its extremum can be determined by using Table 3.9. When $N^0 \neq 0$, a new term (first term on the right

Region 1

Region 2

Condition: $\frac{Ma_{11}}{77} \frac{t - \langle \rangle mf - fs}{mf - fs} z - 17$

Satisfied Not Satisfied

Condition: $\frac{fs}{ms fs} < \frac{2}{s}$

Satisfied Not Satisfied

$\ln(\frac{mf}{mf fs}) - (0_{+1} - a_{11})^2$

Cases 1,3: t^A

$\frac{Ma_{11}}{fs} \frac{t - \langle \rangle fs}{Vs - fs}$

Cases 2,4: t^A

Note: Cases 1, 3: $M > 1$

$W_1 > 1: t_3 < -\frac{1}{v}$

Note: Cases 2, 4: $M < 1$

$W_1 > 1: t_3 > -\frac{1}{v}$

Cases 2,4: $M = 1 - N_j A$

$W_1 < 1: t_3 = -\frac{1}{v}$

Cases 1, 3: $H = 1$

$W_2 < 1: \frac{2}{3} < \frac{1}{v_m}$

Cases 5, 6: M

Cases 5, 6; if: $W_1 < -1: t_3 = -\frac{1}{v}$

Cases 5, 6: H

Cases 5, 6; if: $W_2 < -1: t_3 = L$

$W_1 > -1: t_3 = v$

$W_2 > -1: t_3 = -$

Table 3.9 Summary of the determination of the extremum for the 3 member ($N^A = 0$)

hand side) is superimposed. Recalling the assumption of small leach time, i.e., $T \ll 1/X_j$, $j=1,2,3$, and by realizing that this added term is non trivial in the interval $(z/v_3, z/v_3+T)$ of duration T , one can neglect changes in the Bateman's functions and take $\phi(t)=1$. Therefore, the first term can be seen as a band of duration T and constant magnitude.

Depending on the relative magnitude of the nuclide velocities, different configurations result from the superimposition of the two terms. Consider for example Figure 3.4. In case "a" of Figure 3.4 the two terms are non trivial in independent time domains and one can evaluate the extremum of the second term (using Table 3.9) and the extremum of the first term (using Eq.(3.3.2)5 separately. The largest concentration will define the true maximum for both terms.

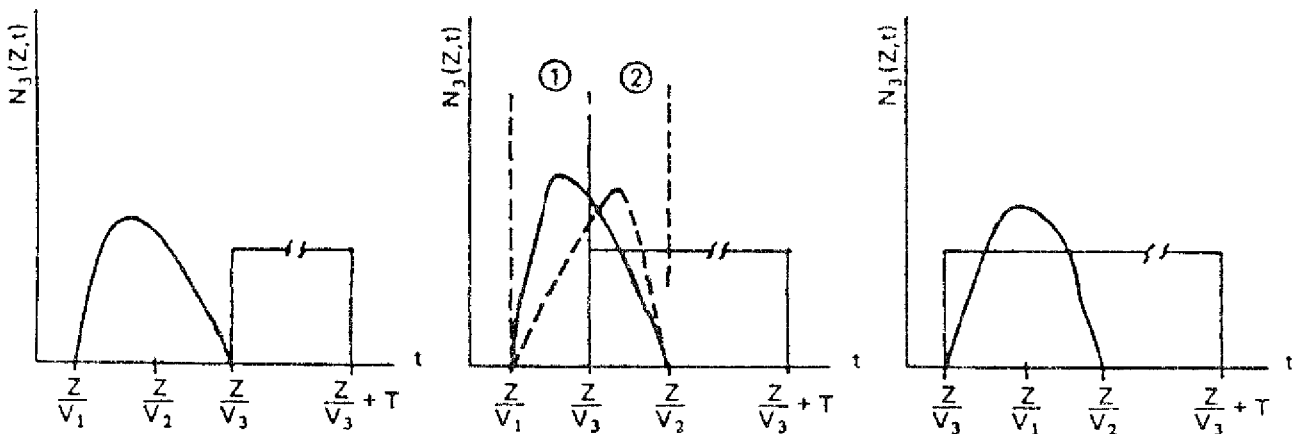


Figure 3.4 Possible configurations of the solution for the 3rd member when $N^0 \neq 0$.

In case "b" of Figure 3.4 we have two possibilities: when the extremum of the second term occurs in region 1 and when it occurs in region 2 (dotted line). In either case, one can decide about the true maximum by evaluating the concentration Eq. (3.5.15) at $t=z/v$, which is the point of extrema for the first term and comparing to the concentration Eq. (3.5.1) at the point of extrema for the second term alone obtained by using Table 3.9 and taking $N^0=0$ in Eq. (3.5.15). Again, the larger of them will define the true maximum.

In case "c" of Figure 3.4 the extremum occurs clearly at the point of extremum of the second term but the magnitude is larger by the addition of the first term. Above examples does not exhaust all possibilities, since we might have a sufficiently large z so that z/v^*+T lies inside the domain of the second term. But in any case, it can be shown that the following steps will yield the time of maximum t^* at a fixed position z

- 1-Evaluate $(z, t=z/v)$ using Eq. (3.5.15) with both terms.
- 2-Use Table 3.9 to obtain t_3 for the second term alone.
- 3-Evaluate $N_3(z, t_3)$ with t_3 obtained in step 2 above.
- 4-Compare $(z, t=z/v)$ from step 1 and $N^*(z, t_3)$ from step 3.
- 5-If concentration from step 1 is larger than that from step 3 then $t^*=z/v$
- 6-If the opposite is true then t_3 is obtained from step 2.

Two cases can be distinguished in the determination of the

contamination time and in the contaminated region for the third member,

a-When the third member is not present at the repository initially the contamination time $\frac{6}{3}$ as well as the contaminated region can be readily obtained from Eq.(3.5.1) and Table 3.8. They can be expressed by

$$0_3 = z/v_s - z/v_r \quad (3.5.18)$$

$$R_3 = (v_r - v_s) t \quad (3.5.13)$$

b-When the third member has non zero initial concentration at the repository, using Eq.(3.5.15) and Table 3.8 one can construct the following Table 3.10. The derivations are shown in Appendix D.

	v_3		v_3	
Case:	$\frac{v_3}{v_3} + T > -$	$\frac{v_3}{v_3} J < \sim$	$v_3(t-T) > v_s t$	$v_3(t-T) < v_s t$
$v_3 < v_2 < v_x$ $v_3 < v_1 < v_2$	$(v_3 - v_s) T$		$v_s t - v_3(t-T)$	$v_s t - v_3(t-T)$
$v_2 < v_3 < v_1$ $v_1 < v_3 < v_2$	$\frac{v_3 - v_s}{v_3} T$		$(v_s - v_3) t$	$v_s t - v_3(t-T)$
$v_3 > v_2 > v_1$ $v_3 > v_1 > v_2$	T	1 «)	$(v_3 - v_s) t$	

Table 3.10: Contamination time and contaminated region for the 3 member (N^0).

3.6 Example of the utilization of the method and comparison with the exact solution results

To verify the validity of the approximation and to determine the range in leach time for which this approximate solution is accurate in representing the exact solution to a decaying band release the results of the approximate solution with those of the exact solutions are compared. These comparisons are done for different leach times. Comparisons for the first member solutions are not necessary since the exact and approximate solutions have the same form. We studied the U-234 and the Np-237 chains. First consider the following three member chain

	U-234	Th-230	Ra-226	
K_1	1.4E+4	5.0E+4	5.0E+2	
X_1	2.8E-6	9.0E-6	4.3E-4	(1/yr)

Let us consider the water velocity as being $v=110$ m/yr. The case of no initial daughters at the repository is first studied. In this case, $v^1 > v^2 > v^3$. The extremum for the second member Th-230 can be readily obtained from Table 3.2 with the condition $A_2 K_2 > A^1 \lambda^1$. The time when the maximum occurs at a fixed position is $t_2 = z/v^1$ and corresponding concentration will be, by using Eq.(3.4.1)

$$(z, t_2) = (N^1 T)^{\lambda^1} \exp(-) z \quad (3.6.1)$$

$$(v_1 v_2)$$

consequently, the contamination time is

$$t = z / v_2 - z / v_1 \tag{3.6.2}$$

The time of maxima for the third member at a fixed position can be obtained from Table 3.9. In this present chain $f=3$, $m=1$ and $s=2$. Thus, according to Table 3.8 we are in case 5. The coefficients a_{ij} and c_{u_j} are first evaluated.

	$i=3, j=2$	$i=1, j=3$	$i=1, j=2$	
a_{ij}	4.75E-6	-1.29E-5	1.14E-5	(1/yr)
	1.92E-3	2.01E-3	-1.11E-3	(1/m)

In the column titled region 1 in Table 3.9 we first check the condition for the existence of interior maximum. Since $N_2=0$ and $B_{23}=0$; hence $M=1$ and $W_J=0$. Therefore, $\ln(M A_{rar} / A_{fs}) = \ln(A_{rar} / A_{fs})$. But since $A_{rar} / A_{fs} < 0$, the condition for interior maximum cannot be satisfied. Under the column "not satisfied", for the case 5 and with $W_j=0$, the time of maximum is read out: $t_{J \rightarrow} = z/v_m = z/v_1$ for the region 1.

Similarly, the condition for existence of interior maximum in region 2 is first checked: $\ln(M A_{rar} / A_{fs}) = \ln(A_{rar} / A_{fs})$. And again the condition for interior maximum is not satisfied, for case 5 and with $W_2=0$ the time of maximum is read from Table 3.9 and it is $t_{J \rightarrow} = z/v_m = z/v_1$. Since the time of maximum in both region is the same one concludes that $t_3 = z/v_1$. The corresponding maximum concentration is

$$\frac{(z, t) J}{v_1} = TA \exp\left(\frac{A_{3,2}}{v_1} a_{3,2}\right) z - TA \exp(-X_1/v_1) z \quad (3.6.3)$$

and the contaminated time will be given by

$$e_3 = d/v_2 - 1/v_3) z \quad (3.6.4)$$

The above results agree well with the exact solution presented by Higashi (H2) for leach time values up to 3.0E+4 years. (see Figure 3.5a and Figure 3.5b). A more detailed study has been conducted to determine upper bounds for the error as one increases the leach time for larger values at the end of this section.

In Figure 3.5a the maximum dimensionless Ra-226 concentration ($N_3(z, t_3)/N^*$) is plotted for each fixed position z . There are no initial daughters present at the repository and the leach time is 3500 years. For this value of leach time the agreement was complete.

Figure 3.5b is a similar plot but for a leach time value of 35000 years. Although this value of leach time is larger than the Ra-226 half life, the approximate solution deviation from the exact solution is smaller than 10%. This is because the Ra-226 concentration is controlled by the decay of U-234 whose half life is much larger than the leach time used.

In Figure 3.6a the calculation was the same as in Figure 3.5a but this time the daughters were initially in transient equilibrium. For this leach time (3500 years) the agreement was complete. In Figure 3.6b a leach time of 35000 years was used which is about an order of magnitude larger than the Ra-226 half-life. Although this fact violates the basic assumption the comparison with exact solution shows that the error is larger only for distances smaller than 10 meters where the decay of the initial Ra-226 nuclides is important. For distances larger than 10 meters where the concentration of Ra-226 is controlled by the decay of U-234 the error is smaller than 10%.

A second important three member decay chain starts with Np-237

	Np-237	U-233	Th-229	
T_H	2.1E+6	1.6E+5	7.3E+3	(years)
K_1	1.0E+4	1.4E+4	5.0E+4	

The retardation coefficients used were taken arbitrarily for the purpose of this illustration. The same calculation done for the U-234 chain are repeated here. Let us first determine the extremum of the solution for the second member. From Table 3.2 and with the condition $\lambda_2 \ll \lambda_1$ the time of maximum at a fixed $z: t_2 = z/v_1$ and the corresponding maximum concentration will be

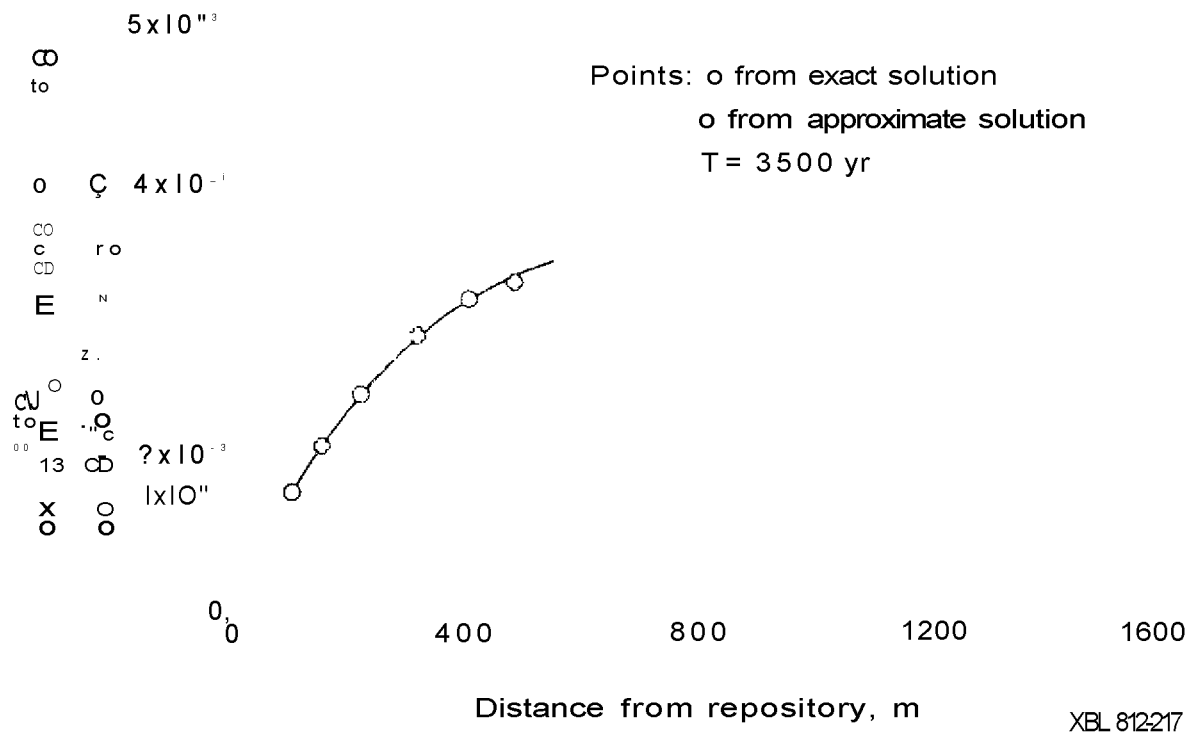


Figure 3.5a Maxima concentrations of ^{226}Ra at different fixed positions
 No initial daughters ($N^0 = N^0 = 0$). No dispersion. T = 3500 years.

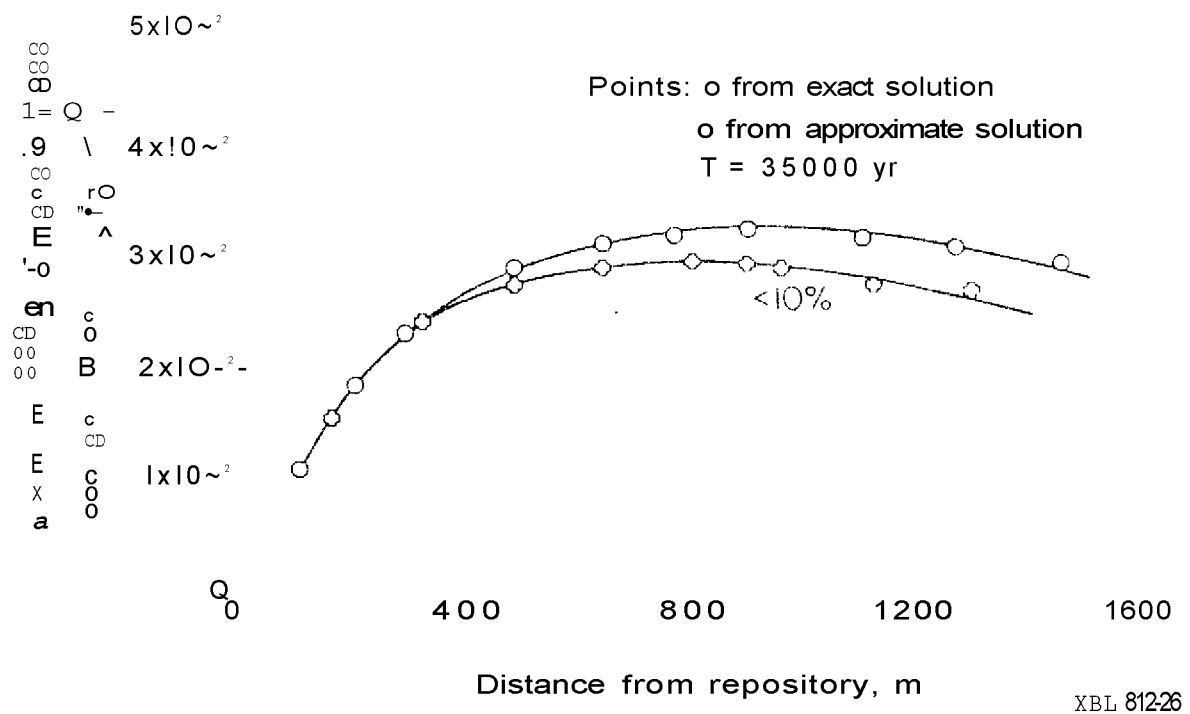


Figure 3.5b Maxima concentrations of ^{226}Ra at different fixed positions
 No initial daughters ($N^0 = 0$). No dispersion. T = 35000 years.

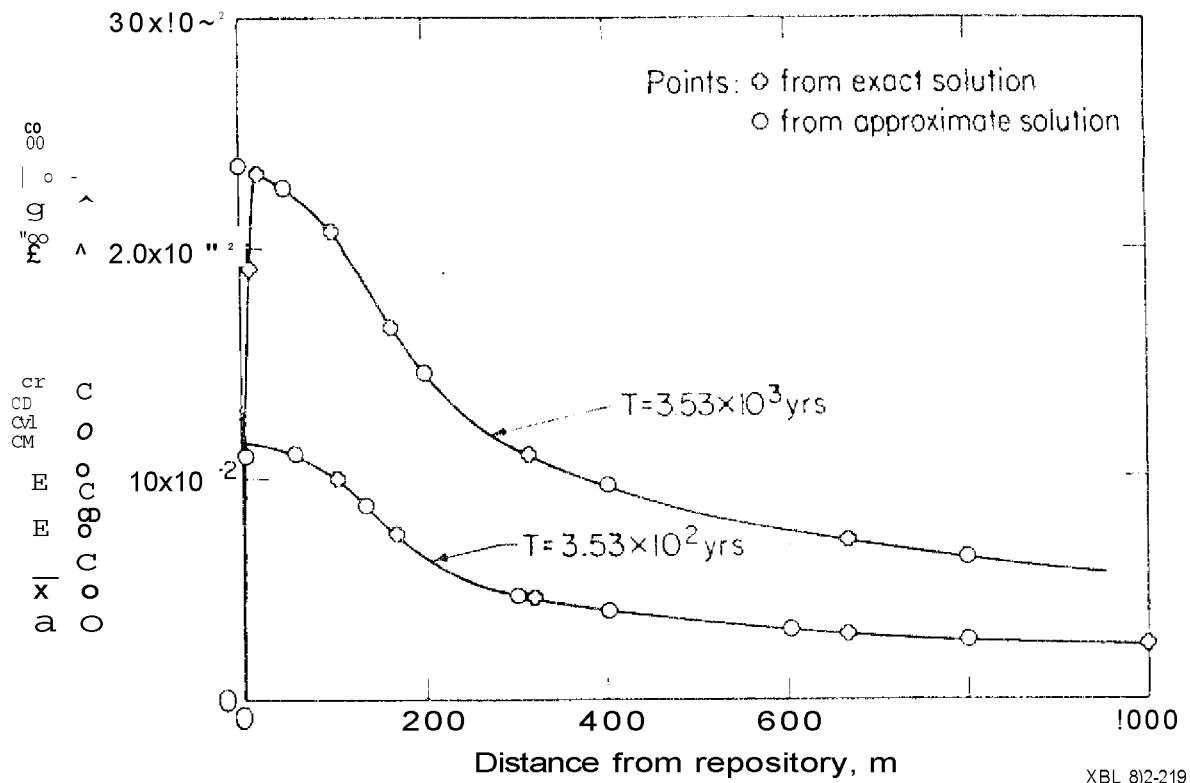


Figure 3 .6a Maxima concentrations of ^{226}Ra at different fixed positions Initial transient equilibrium. No dispersion. $T = 3500$ years.

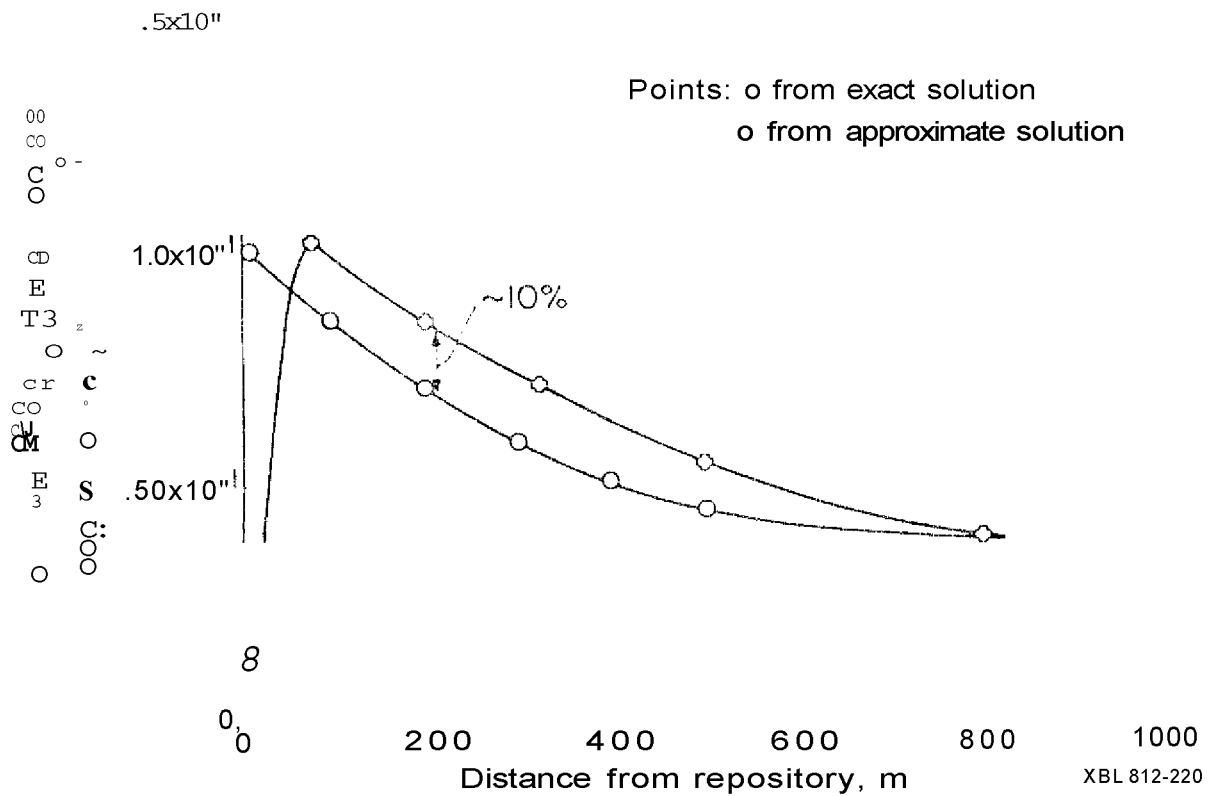


Figure 3 -6b Maxima concentrations of ^{226}Ra at different fixed positions. Initial transient equilibrium. No dispersion. $T = 35000$ years.

$$N_2(z, t_2) \approx \sum_{i=1}^3 \sum_{j=1}^2 A_{ij} e^{-\lambda_j t_2} e^{-\lambda_i z/v_j} \quad (3.6.5)$$

The time of maximum for the third member at a fixed position can be determined from Table 3.9. The nuclide velocities are ordered in such a way that we have a case 5. The coefficients A_{ij} and a_{ij} are first evaluated

	$i=3, j=2$	$i=3, j=1$	$i=1, j=2$	
A_{ij}	$-4.56E-5$	$-9.38E-5$	$1.45E-5$	(1/yr)
a_{ij}	$6.37E-3$	$8.55E-3$	$-1.20E-3$	(1/m)

Consider first the case of no initial daughters. Under the column titled "Region 1" in Table 3.9 the condition for the existence of interior maximum is first checked. Since N^0 and $B_{23} = 0$ hence $M=1$ and $W_1 = 0$, thus: $\ln(M A_{mf} A_{fs}) = \ln(A_{13} A_{32}) = 0.721$. The condition for interior maximum cannot be satisfied for positive z . Under the column not satisfied, for a case 5, one reads the time for the maximum: $t_{max} = z/v = z/v_1$

Similarly, for region 2 the condition for interior maximum cannot be satisfied and from Table 3.9 the time of maximum is obtained: $t^* = z/v^*$. Since the maximum concentration in either region occurs at the common boundary $t^* = z/v^*$, the maximum concentration for both region is the same and can be expressed by

$$N^*(z, t^*) = \frac{TA}{H} \left[\exp\left(-\frac{\lambda_{23} z}{v^*} - \lambda_{23} t^*\right) - \exp\left(-\lambda_{13} t^* - \lambda_{13} z/v_1\right) \right] \quad (3.6.6)$$

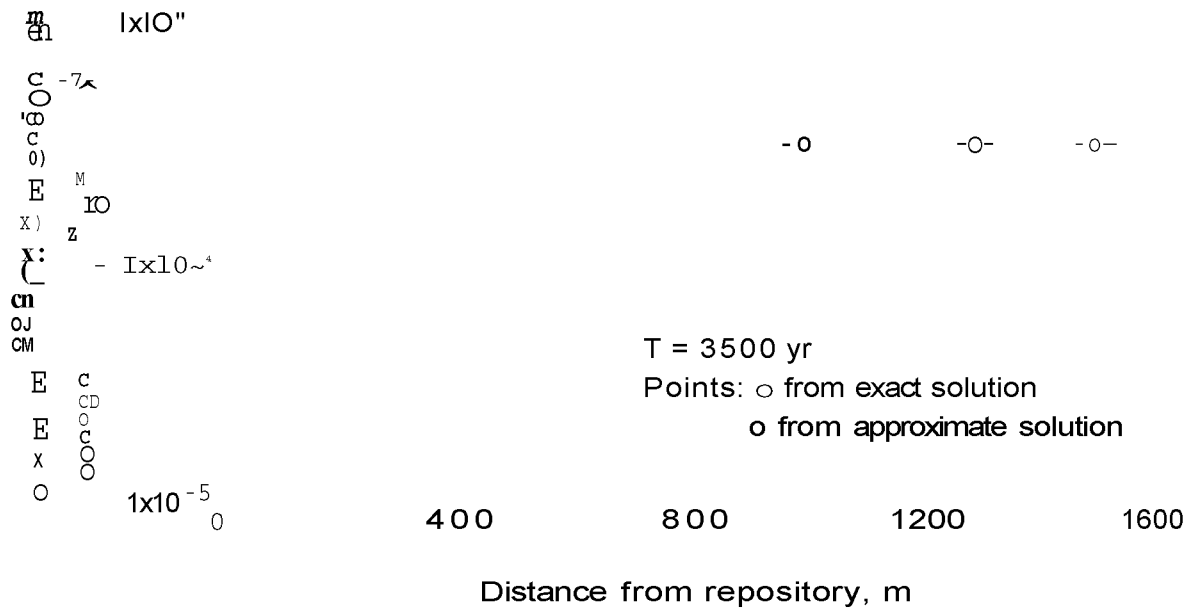
Figure 3.7a and Figure 3.7b show the case of zero initial daughters concentration for leach times of 3500 and 35000 years respectively. Also for this chain, the agreement between the exact and approximate solution is quite good for leach times smaller than 35000 years. Finally, in Figure 3.8a and Figure 3.8b the comparisons are made for the case when the initial daughter concentrations are in transient equilibrium. The curves for the case of a leach time of 3500 years still show good agreement but the curves for the case of a leach time of 35000 years show a small deviation.

Additional comparisons between maxima concentrations obtained by evaluating the exact solutions formulas (reference Hi) and by using the approximate method developed in this work are summarized next. Deviations of the values obtained by the approximate method from those of the exact solution are expressed in terms of percent error which is defined as:

$$e (\%) = ((\text{exact} - \text{approximate}) / \text{exact}) * 100 \quad (3.6.7)$$

Here, the two chains analyzed previously in this section are studied again but using instead the initial concentrations and retardation coefficients listed in Table 3.14a.

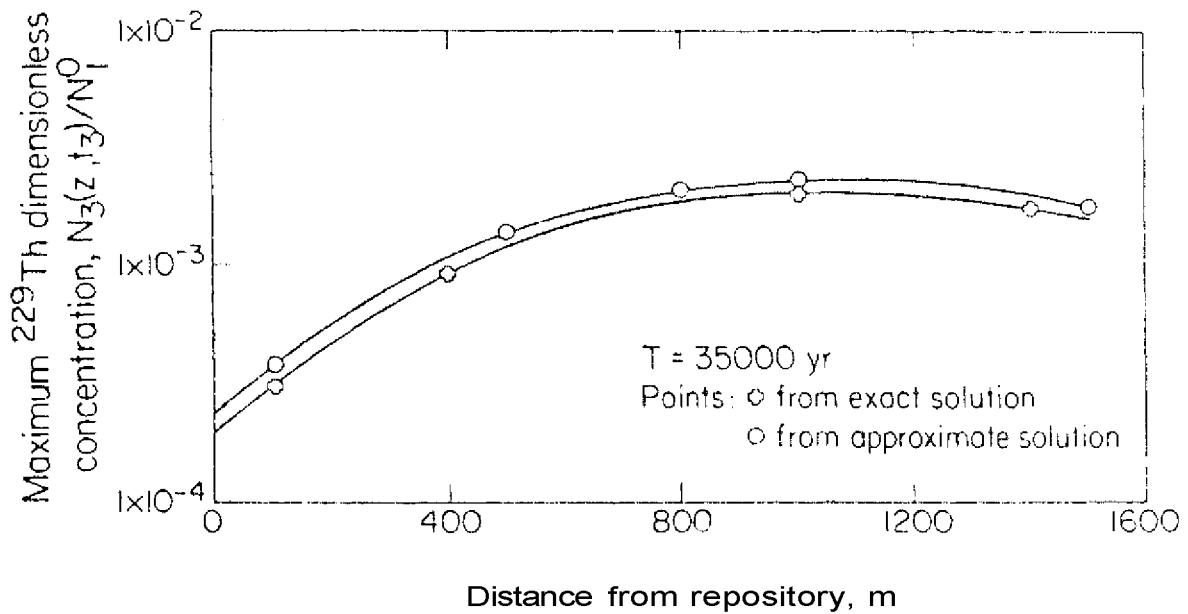
Tables 3.10a through Table 3.10d show the percent error in the maxima concentrations calculations of Ra-226, Th-229, Th-230 and U-233 respectively, at different values of the ratio



X6L 812-221

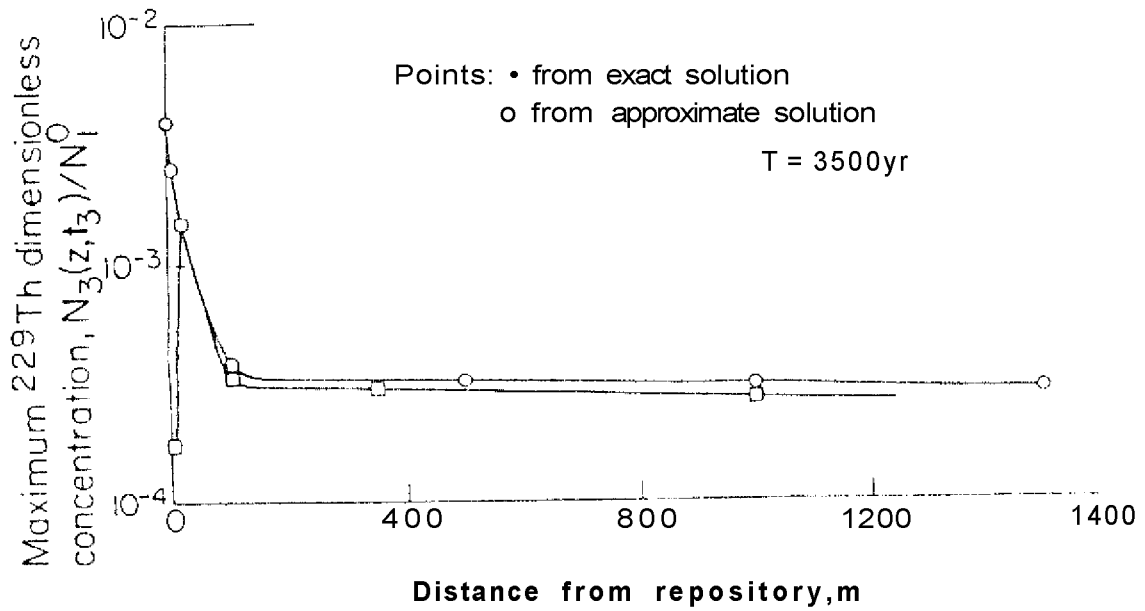
229

Figure 3.7a Maxima concentrations of ^{235}U at different fixed positions. No initial daughters ($N^0 = N^0 = 0$). No dispersion. $T = 3500$ years.



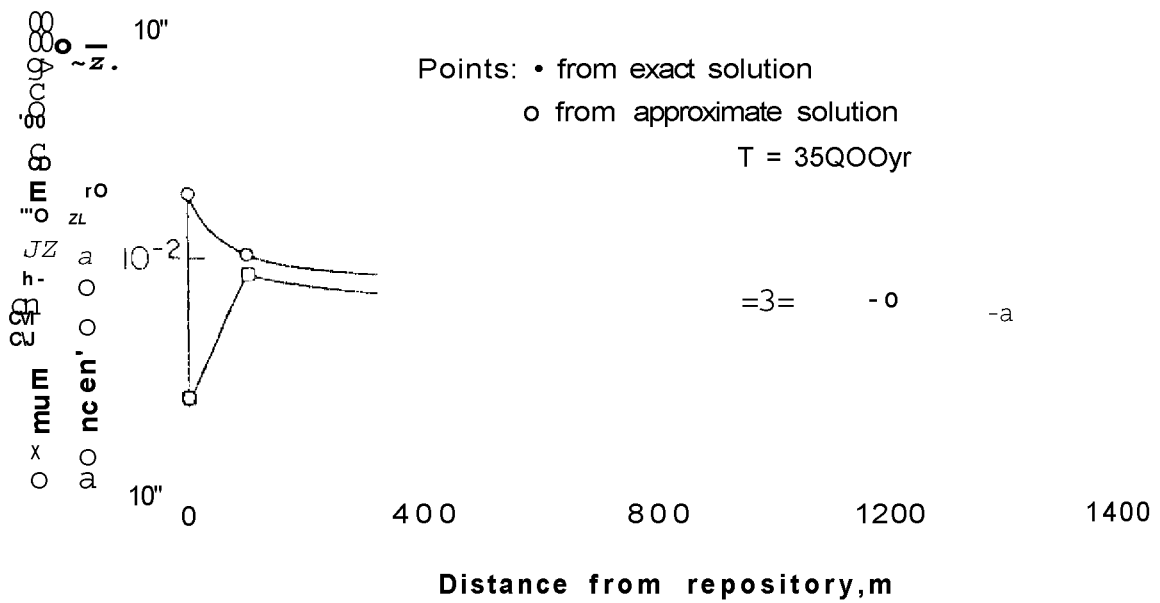
XBL 812-222

Figure 3.7b Maxima concentrations of ^{229}Th at different fixed positions. No initial daughters ($N^0 = N^0 = 0$). No dispersion. $T = 35000$ years.



XBL 812-223

Figure 3.8a Maxima concentrations of ^{229}Th at different fixed positions Initial transient equilibrium. No dispersion. $T = 3500$ years.



XBL812-224

Figure 3.8b Maxima concentrations of ^{229}Th at different fixed positions. Initial transient equilibrium. No dispersion. $T = 35000$ years.

distance/water velocity (z/V , water travel time) and for different leach times.

All four tables show that for leach times smaller than **1000** years where the condition $T \ll T^*$ is satisfied, the error is negligible for all values of z/V . For leach times between 1000 and 10000 years the error is greater than 10% only for water travel times smaller than 1 year. Since groundwater velocities are expected to be smaller than 10 m/yr, for leach times of the order of 10000 years the approximate method is applicable for path lengths z greater than 10 meters which in general is the range of interest for far field migration studies.

5

Finally, for leach times of the order of 10 years or larger, the error becomes unacceptable for any value of water travel time. In view of above results, the condition $T \ll T^*$, can be relaxed and the validity of the method can be extended to leach time of the order of 10000 years provided the water travel time is larger than one year.

z/v (yr)	T(yr):	10	10^2	10^3	10^4	10^5
10^{-1}		0	8.0	10.0	49.0	24.0
10^0		0	1.0	3.0	38.0	98.0
10^1		0	0	0.2	11.0	42.0
10^2		0	0	0	3.0	39.0
10^3		0	0	0	3.0	43.0
10^4		0	0	0	3.0	40.0
		-	-	-	-	50.0

Table 3.10a: Percent error of the approximate method in the evaluation of the maxima concentrations of ^{226}Ra

z/v (yr)	T(yr)	10	10^1	10^2	10^3	10^4
10^{-2}		0	7.0	55.0	85.0	95.0
10^{-1}		0	7.0	42.0	75.0	93.0
10^0		0	5.0	18.0	50.0	82.0
10^1		0	4.0	9.0	19.0	82.0
10^2		0	0	0	1	14.0
10^3		0	0	0	1	10.0
10^4		0		0	1	10.0

Table 3.10b: Percent error of the approximate method in the evaluation of the maxima concentrations of ^{229}Th

z/v (yr)	T (yr)	10	10 ¹	10 ²	10 ³	5
10 ⁻²		0	7.0	19.0	52.0	33.0
10 ⁻¹		0	5.0	9.0	41.0	30.0
10 ⁰		0	0	5.2	22.0	2.0
10 ¹		0	0	1.0	8.0	94.0
10 ²		0	0	1.0	6.0	96.0
10 ³		0	0	1.0	6.0	124.0
10 ⁴		-	-	-	-	-

Table 3.10c: Percent error of the approximate method in the evaluation of the maxima concentrations of Th

z/v (yr)	T (yr)	10	10 ¹	10 ²	10 ³	10 ⁴
10 ⁻²		0	7.0	30.0	81.0	99.0
10 ⁻¹		0	6.0	22.0	72.0	99.0
10 ⁰		0	0	9.0	55.0	99.0
10 ¹		0	0	5.0	23.0	98.0
10 ²		0	0	1.0	2.0	27.0
10 ³		0	0	1.0	2.0	33.0
10 ⁴		0	0	1.0	2.0	23.0

Table 3.10d: Percent error of the approximate method in the evaluation of the maxima concentrations of ²³⁵U

3.7 Analysis of the effects of variation in parameters values on the maxima concentrations

In this section we apply the method developed in previous sections to analyse the effects on the maximum concentration caused by variations in the values of the parameters. The main advantage of this present method is that it avoids the need of detailed evaluation of the complete solution and the subsequent search for the extremum. One can use this method to analytically evaluate directly the extremum, saving therefore considerably computing time.

Although this can be done with the help of a pocket calculator, when a large number of cases is to be evaluated as in the case of a parametric analysis, it is very useful to program this method into the computer so that one can evaluate the extremum of any number of nuclides and for any number of sets of parameters all at once. A computer program called UCBNE20 was developed which uses this method in evaluating the potential hazard at the biosphere resultant from the release of radionuclides present in the waste packages. A complete listing and description of data input requirements are given in Appendix B.

According to the assumptions made in the development of the method, UCBNE20 will be restricted to the following:

1. One dimensional systems.

2. Constant water velocities, soil and water properties.
3. Negligible dispersion effects.
4. Leach times smaller than nuclide half lives.
5. Maximum chain size is three members.

If above conditions are met, UCBNE20 will evaluate the following quantities for a given i-th member of a chain:

1. Time of maximum at a fixed position, t^{\wedge}
2. The coreespondent maximum concentration.
3. The correspondent maximum water dilution rate.
4. The contamination time for that position.

In order to apply this method for any nuclide, it is necessary first to reduce the long actinide chains into three members or less chains by suitable simplifications.

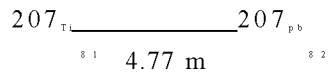
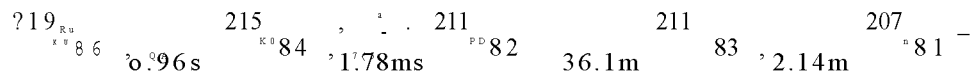
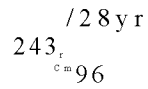
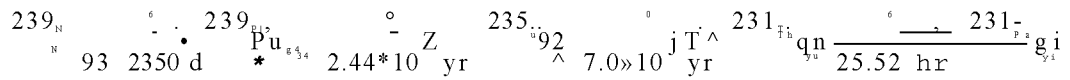
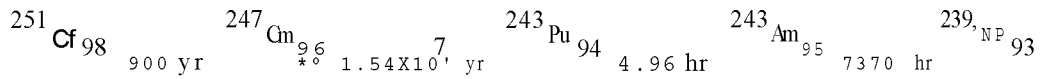
3.7.1 Reduction of actinide chains

The actinide chains present in high level wastes have more than three members and cannot be treated by the method above. But because some elements have very short half lives while some others have very long half lives, these chains can be broken into shorter chains.

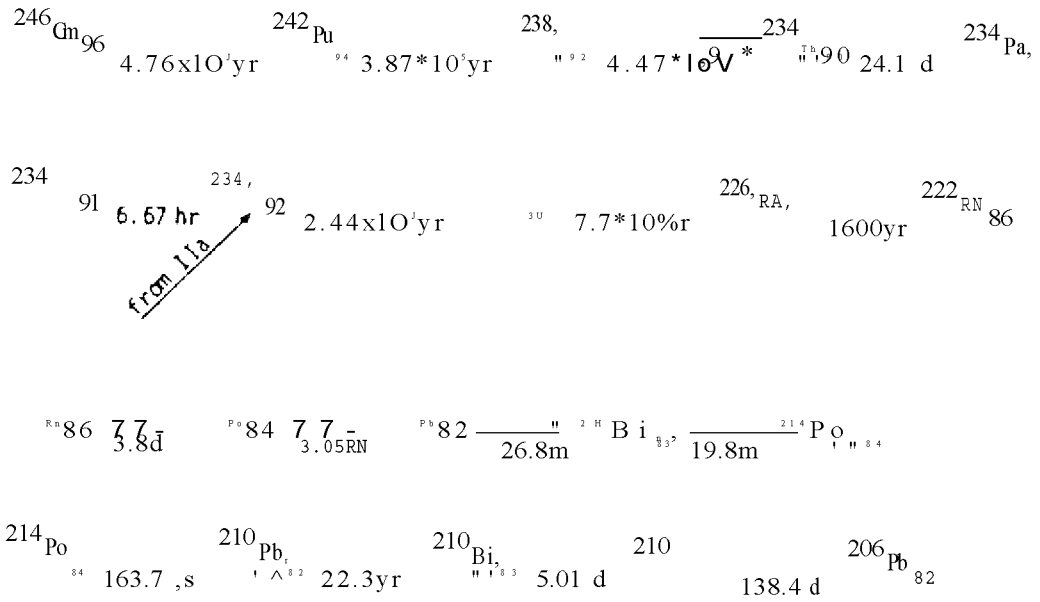
There are four distinct complete actinide chains present in high level wastes. They are shown in Table 3.11 below. In order to reduce these chains into smaller chains, the following factors

Table 3.11: Actinides Chains Present in PWR Spent Fuel and Reprocessed Waste.

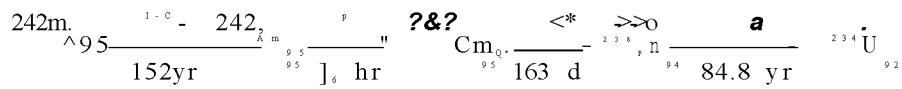
I) The 4n+3 chain:



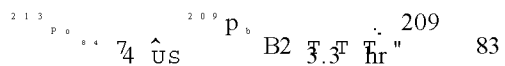
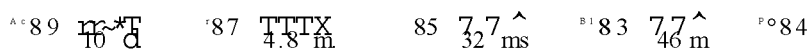
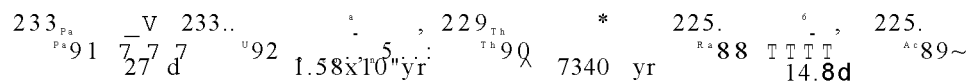
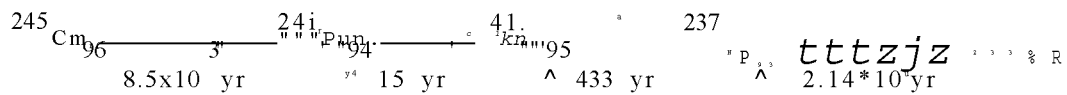
11) The 4n+2 chain:



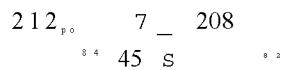
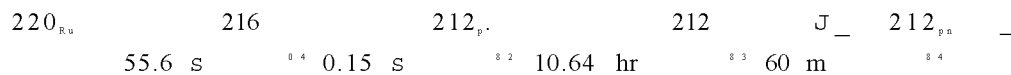
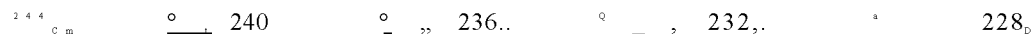
Ha) : Branch of 4n+2 chain



III) The 4n+1 chain:



IV) The 4n chain:



must be taken into account:

a) Whether the waste is unprocessed or reprocessed; which type of reactor has generated it; when the leaching starts after the burial. These factors determine basically the initial amount of a given nuclide.

b) The relative magnitude of the retardation coefficients and the half lives of a precursor and its daughters. (See discussion about secular equilibrium for migrating chains in HI, section 4.5).

For this present study, we will consider the initial amount of actinides in the waste as being that of the reprocessed HLW from spent fuels of a PWR and the range of time for beginning of leaching is below 10 years. With these assumptions we have defined the nuclides activities that are initially present in the repository.

In addition, we assume that the sorption equilibrium constants of the actinides do not differ more than four orders of magnitude from each other. With above assumptions the following simplifications can be made:

1. A very short-lived nuclide can be considered as being in secular equilibrium with its long-lived precursor, i.e. $X_i^{K_i} = X_{i-1}^{K_{i-1}}$

According to reference (Hi), the necessary condition to have secular equilibrium is that $X_i^{K_i} \gg X_{i-1}^{K_{i-1}}$. Since we have assumed

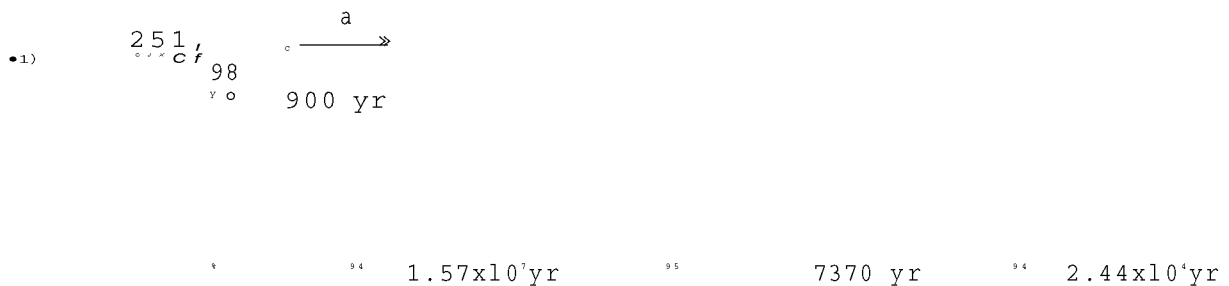
that the retardation coefficients do not differ more than four orders of magnitude from each other, the half life of the

daughter must be at least four orders of magnitude smaller.

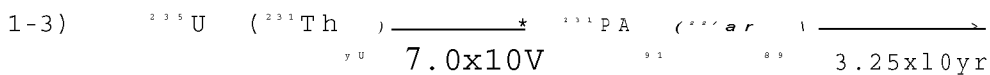
2. On the other hand, if a nuclide has a much shorter half life than its precursors one can assume that every short lived precursor initially present in the waste has decayed by the time that the waste dissolution begins. The initial concentration of this long-lived nuclide should include those nuclides of the precursors which have already decayed.

With these two assumptions, each one of the four chains can be broken into the following smaller chains: (The nuclide in parentheses are in secular equilibrium with its precursor).

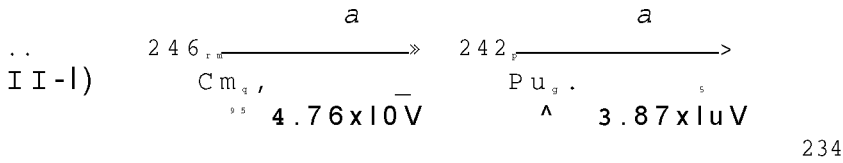
The first chain 1, (4n+3 chain) can be subdivided into the following chains



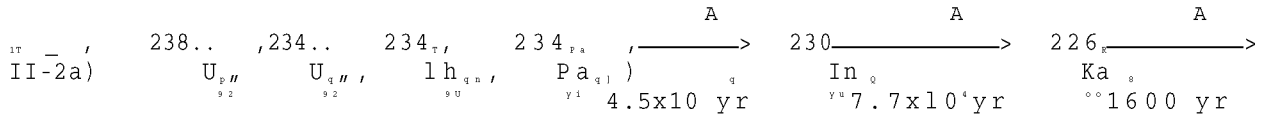
(assume that all ${}^{243}\text{Cm}$ has decayed to ${}^{239}\text{Pu}$)



Subsequent elements are in secular equilibrium with Pa-231. The next chain II, (4n+2 chain) can be subdivided into the following chains

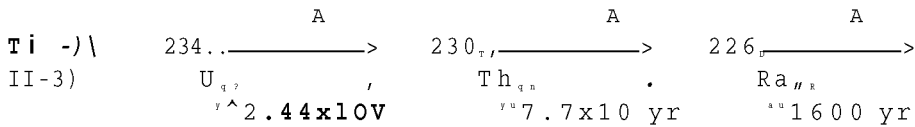
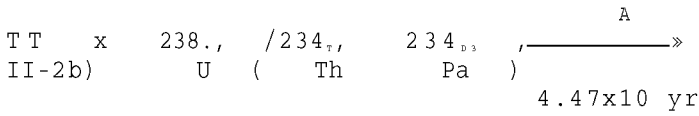


If the times of interest are of the order of the ^{238}U half-life or longer one should consider the following chain:



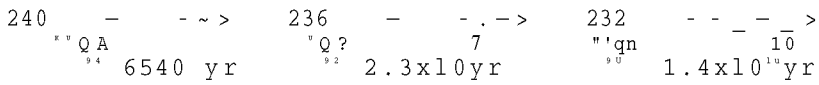
234

On the other hand, if the time scale is smaller than ^{238}U half-life the following chains should be considered instead of (II-2a):



In this later case, if the dissolution begins after hundreds of years or more one can assume that every nuclide in the branch Ila of the 4n+2 chain has decayed to form U-234 nuclides. But sometimes we are interested in the effects of fuel dissolution beginning at the time the waste is emplaced, and at other times we are interested in what happens if dissolution does not begin for hundreds of years or more. The decay of the initial Pu-238, Am-242m and Cm-242 in the waste to form U-234 is important. In waste from fuel reprocessed a few months after discharge, Cm-242 is the most important source of U-234 (B2).

equilibrium with Th-229. Finally, chain IV (4n chain) can be reduced to the following chain



U-232 can be neglected, and all other subsequent nuclides are in secular equilibrium with Th-232).

3.7.2 Evaluation of peak water dilution rate

To estimate the potential hazard to the biosphere we use the Maximum Permissible Concentration (MPC) according to 10CFR part 20, Appendix B. These are the nuclide concentrations in water which will result in the maximum allowable dose for an average individual who has all his daily water intake from such a source. The water dilution rate is the volumetric flow rate of a aquifer or surface water into which the migrating radionuclides discharge such that the concentration of any nuclide will not be above the MPC concentrations. Therefore, the peak water dilution rate is calculated as follows

$$w_1 = Q \times \frac{N_1(z, t_1)}{X_1} / (\text{MPC})_1 \tag{3.7.1}$$

Where Q is the volumetric groundwater flowrate (m³/yr) across the waste and $(\text{MPC})_i$ has units of (Ci/m³) and they are listed in Table 3.14a).

3,7.3 The reference case and the range of variation of the parameters

The reference case is defined by the following set of parameters:

1. The time lapsed between the emplacement and the beginning of the waste dissolution is denoted by t_0 and is taken to be 1000 years. This parameter represents the expected lifetime of the protective barriers. t_0 does not show up directly in the solutions but its variation leads to changes in the initial inventories of each nuclide present in the waste when the leaching starts. The nuclide inventories present in the waste at $t_0=1000$ years are listed in Table 3.14a and they were obtained from reference (B2). These inventories are from the reprocessed waste of spent fuels of a PWR after generating 1 Gw(e)yr of electricity with a load factor of 80%, a thermal efficiency of 34% and a burnup of 30.4 Mwd/kg. These spent fuels are reprocessed after 150 days cooling period and 0.5% of the Pu and U are lost to the waste. The time elapsed between discharge and emplacement in the repository is assumed to be negligible.

2. The duration of the release (leach time) is denoted by T
4
and is taken to be 10 years. This number represents the expected lifetime of a proposed waste form. It is assumed that the waste matrix dissolves at a constant rate over time T and all

contained radionuclides dissolve when the matrix dissolves.

3. The position downstream where the contaminated water streamline meets the aquifer is called the path length. It is denoted by z and for the reference case it will be 1000 meters.

4. The reference velocity of the water flowing past the repository will be $v=10$ m/yr. The reference water travel time will therefore be $z/V=100$ years.

5. The sorption retardation coefficient is denoted by K^{\wedge} . The reference set of values is given in Table 3.14a, obtained from (B2).

The procedure adopted here to analyse the effects of the variation of the parameters values on the peak water dilution rate is to keep all parameters fixed at the reference values with the exception of one of them which is varied. This is done in turn for each one of the relevant parameters. Each parameter is varied in the range given by Table 3.12 below. The analysis of the variation of the retardation coefficient for nuclides which are first members of a chain can be studied by the results of the variation in water velocity. This is because they are both related to the same parameter $V^{\wedge}=V/K^{\wedge}$. For three member chains the following cases shown in Table 3.13 were calculated.

In each one of the six cases described in Table 3.13 one of

		Minimum	Maximum
Time of beginning of leaching		1 yr	10^5 yr
Leach time	T	10 yr	50,000 yr
Water travel time	z/v	10^{-3} yr	10^8 yr
Equilibrium constant		10^2	10^4

Table 3.12 Range of variation of the parameters

	Cases :	K_1	K_2	K_3
1	$K_2 > K_1 > K_3$	10^2	Varied	10^4
2	$K_1 > K_2 > K_3$	10^4	Varied	10^2
3	$K_2 > K_1 > K_3$	10^2	10^4	Varied
4	$K_1 > K_3 > K_2$	10^4	10^2	Varied
5	$K_2 > K_3 > K_1$	Varied	10^4	10^2
6	$K_3 > K_1 > K_2$	Varied	2	10^4

Table 3.13 Variation of equilibrium constants values for three-member chain analysis.

the retardation coefficient is kept fixed at the lower limit

4

(100), the other at the upper limit (10), while the third is varied inside the range (100-10000). The calculations are done for every one of the six possible combinations described in Table 3.13. With these six cases we cover the possible different combinations of retardation coefficient for three member chains. Consider for instance case 1. When K_2 approaches $K^*=100$, case 1 tends to case 6 and if K_3 approaches $K^*=10000$, case 1 in this case tends to case 3. By analyzing these six cases one can predict qualitatively the behaviour of the solution for a three member chain for any different combination of sorption coefficients.

3.7.4 Results of the calculations

Table 3.14a and Table 3.14b show the results of the calculations for the reference case. In Table 3.14a the nuclide parameters are listed. The column titled "member" indicates whether the element is considered a first, second or third member in a chain. A number 4 indicates that the nuclide is in secular equilibrium with the nearest long lived precursor.

The last column which is titled "Attenuation factor" is the product $X^*K^*, (1/yr)$. Table 3.14b actually shows the results of the calculation. The number under the column "1-st" is the identification number of the first precursor of that nuclide (if

any) in the chain, and the number under column "2-nd" is the identification number of the second precursor. Let us identify the results in each column with the nomenclature used in past sections

"TIME OF PEAK (YR)" = t_i

"MAXIMUM N/N" = $N.(z, t.) / N?$

"WAT.DIL. ($m^3/yr.Gw(e)yr$)" = w_i

"CONTAM.TIME (YR)" =

For the reference case, the largest peak water dilution rate is that of 1-129 which is a volatile fission product. Although it has been recovered separately it is assumed to be also present in the dissolving waste material. In addition, it is also assumed that 1-129 has a dissolution leach time equal to that of the reprocessing high level waste. Similar assumptions are made about H-3 and C-14.

Because of its unit retardation coefficient, 1-129 peak is the first to arrive at the reference water travel time. Following 1-129, the next important contributor is the actinide Np-237 which has high toxicity and initial activity. Ra-226 produced by the decay of the U-234 originally present at the repository presents also significant peak water dilution rate at this reference water travel time because of its low MPC value. Ra-226 has the smallest MPC value followed by 1-129. In addition to 1-129, the fission products Tc-99, Sn-126, Se-79 and Zr-93 also present significant peak water dilution rates.

Table 3.14a Sample Output - Nuclide Parameters for the Reference Case. (The Nuclide Parameters are Listed Below) Time for Beginning of Leaching is 1.00E+03(YR)

NUMBER	NUCLIDE	MEMBER	HALF-LIFE (YR)	SORPTION CONST.	MPC (CI/M**3)	INITIAL ACTIVITY(CI)	ATTENUATION FACTOR (1/YR)
1	H-3	1	1.20E+01	1.00E+00	3.00E-03	1.58E-21	5.78E-02
2	C-14	1	5.60E+03	1.00E+01	8.00E-04	1.15E+01	1.24E-03
3	SE-79	1	6.50E+04	1.00E+02	3.00E-04	1.09E+01	1.07E-03
4	SR-90	1	2.80E+01	1.00E+02	3.00E-07	3.74E-05	2.48E+00
5	ZR-93	1	9.50E+05	1.00E+04	8.00E-04	5.20E+01	7.29E-03
6	NB-93M	1	1.40E+01	1.00E+04	4.00E-04	1.59E-21	4.95E+02
7	TC-99	1	2.10E+05	1.00E+00	2.00E-04	3.89E+02	3.30E-06
8	RU-106	1	1.00E+00	1.00E+01	1.00E-05	1.00-200	6.93E+00
9	CO-113	1	1.40E+01	1.00E+04	3.00E-05	4.13E-19	4.95E+02
10	SM-126	1	1.00E+05	1.00E+03	2.00E-05	1.49E+01	6.93E-03
11	SB-125	1	2.70E+00	1.00E+02	1.00E-04	7.13-107	2.57E+01
12	1-129	1	1.70E+07	1.00E+00	6.00E-08	1.00E+00	4.08E-08
13	CS-134	1	2.00E+00	1.00E+03	2.00E-05	1.91-144	3.47E+02
14	CS-135	1	3.00E+06	1.00E+03	1.00E-04	7.80E+00	2.31E-04
15	CS-137	1	3.00E+01	1.00E+03	2.00E-05	2.69E-04	2.31E+01
16	CE-144	1	7.80E-01	2.20E+03	1.00E-05	1.00-200	1.95E+03
17	PM-147	1	4.40E+00	2.50E+03	2.00E-04	1.07E-62	3.94E+02
18	SM-151	1	8.70E+01	2.50E+03	4.00E-04	1.18E+01	1.99E+01
19	EU-152	1	1.30E+01	2.50E+03	6.00E-05	2.33E-21	1.33E+02
20	EU-154	1	1.60E+01	2.50E+03	2.00E-05	2.94E-14	1.08E+02
21	EU-155	1	1.80E+00	2.50E+03	2.00E-04	1.06-162	9.62E+02
22	RA-225	4	4.10E-02	5.00E+02	5.00E-07	2.86E-03	8.45E+03
23	RA-226	3	1.60E+03	5.00E+02	3.00E-08	3.25E-03	2.17E-01
24	TH-228	4	1.90E+00	5.00E+04	7.00E-06	2.45E-02	1.82E+04
25	TH-229	3	7.30E+03	5.00E+04	5.00E-07	2.86E-03	4.75E+00
26	TH-230	2	8.00E+04	5.00E+04	2.00E-06	1.72E-02	4.33E-01
27	U-233	2	1.60E+05	1.40E+04	3.00E-05	6.22E-02	6.06E-02
28	U-234	1	2.50E+05	1.40E+04	3.00E-05	1.99E+00	3.88E-02
29	U-235	1	7.10E+08	1.40E+04	3.00E-05	7.60E-03	1.37E-05
30	U-238	1	4.50E+09	1.40E+04	4.00E-05	4.50E-02	2.16E-06
31	NP-237	1	2.10E+06	1.00E+02	3.00E-06	1.44E+01	3.30E-05
32	PU-238	2	8.60E+01	1.00E+04	5.00E-06	2.84E+00	8.06E+01
33	PU-239	2	2.40E+04	1.00E+04	5.00E-06	5.58E+01	2.59E-01

Table 3.14a (Continued)

NUMBER	NUCLIDE	MEMBER	HALF-LIFE (YR)	SORPTION CONST.	MPC (CI/M**3)	INITIAL ACTIVITY(CI)	ATTENUATION FACTOR (1/YR)
34	PU-240	2	6.60E+03	1.00E+04	5.00E-06	2.45E+02	1.05E+00
35	PU-241	4	10.3E+01	1.00E+04	2.00E-04	9.10E+00	5.33E+02
36	PU-242	2	3.80E+05	1.00E+04	5.00E-06	1.93E-01	1.82E-02
37	AM-241	2	4.60E+02	1.10E+04	4.00E-06	1.91E+04	1.66E+01
38	AM-42M	1	1.50E+02	1.10E+04	4.00E-06	1.18E+00	5.08E+01
39	AM-243	1	7.90E+03	1.10E+04	4.00E-06	4.40E+02	9.65E-01
40	CM-242	4	4.50E-01	3.00E+03	2.00E-05	1.18E+00	4.62E+03
41	CM-243	1	3.20E+01	3.00E+03	5.00E-06	3.54E-08	6.50E+01
42	CM-244	1	1.80E+01	3.00E+03	7.00E-06	1.41E-12	1.16E+02
43	CM-245	1	9.30E+03	3.00E+03	4.00E-06	9.10E+00	2.24E-01
44	CM-246	1	5.50E+03	3.00E+03	4.00E-06	1.63E+00	3.78E-01

- a) 1,2,3; indicate first, second or third member of a chain respectively; 4 indicates secular equilibrium with the nearest long lived precursor
- b) Sorption constants are the overall equilibrium constant, i.e., the ratio of the amount in water and solid to the amount in water (see B3)
- c) MPC are the maximum permissible concentrations in water (see B2)
- d) Nuclide activities in waste, 10³ yrs after emplacement. High level reprocessing waste from 7Gwe produced in a LWR (see B2)
- e) Attenuation factors are the products of decay constants and sorption constants.

Table 3.14b Sample output, results for the reference case using UCBNE20

LEACH TIME (YR) 1.0000E+04			PATH LENGTH (M) 1.0000E+02		WATER VELOCITY (M/YR) 1.0000E+00				
No.	NUCLIDE	MEMBER	1ST	2ND	TIME OF PEAK (YR)	MAXIMUM N/NO	WAT. OIL. (M**3/ GW*YR**2)	CONTAM. TIME (YR)	PERCENTAGE
1	H-3	1	0	0	1.00E+02	3.10E-03	1.63E-25	1.00E+04	.000
2	C-14	1	0	0	1.00E+03	8.84E-01	1.27E+00	1.00E+04	.047
3	SE-79	1	0	0	1.00E+04	8.99E-01	3.26E+00	1.00E+04	.121
4	RB-90	1	0	0	1.00E+04	3.25-108	4.06-110	1.00E+04	.000
5	ZR-93	1	0	0	1.00E+06	4.82E-01	3.13E+00	1.00E+04	.116
6	NB-93M	1	0	0	1.00E+06	0.	0.	1.00E+04	0.
7	TC-99	'	0	0	1.00E+02	1.00E+00	1.94E+02	1.00E+04	7.195
8	RU-106	1	0	0	1.00E+03	0.	0.	1.00E+04	0.
9	CD-113	1	0	0	1.00E+06	0.	0.	1.00E+04	0.
10	SM-126	1	0	0	1.00E+05	5.00E-01	3.72E+01	1.00E+04	1.379
11	SB-125	1	0	0	1.00E+04	0.	0.	1.00E+04	0.
12	1-129	1	0	0	1.00E+02	1.00E+00	1.67E+03	1.00E+04	61.715
13	CS-134	1	0	0	1.00E+05	0.	0.	1.00E+04	0.
14	CS-135	1	0	0	1.00E+05	9.77E-01	7.62E+00	1.00E+04	.282
15	CS-137	1	0	0	1.00E+05	0.	0.	1.00E+04	0.
16	CF-144	1	0	0	2.20E+05	0.	0.	1.00E+04	0.
17	PM-147	1	0	0	2.50E+05	0.	0.	1.00E+04	0.
18	SM-151	'	0	0	2.50E+05	0.	0.	1.00E+04	0.
19	EU-152	1	0	0	2.50E+05	0.	0.	1.00E+04	0.
20	EU-154	1	0	0	2.50E+05	0.	0.	1.00E+04	0.
21	EU-155	1	0	0	2.50E+05	0.	0.	1.00E+04	0.
22	RA-225	4	25	0	4.40E+04	3.77E-01	2.16E+01	4.99E+06	.008
23	RA-226	3	26	28	1.40E+06	2.96E-04	3.07E+02	4.95E+06	11.381
24	TH-228	4	34	0	1.00E+06	2.51E-467	8.78E-43	1.00E+06	.000
25	TH-229	3	27	31	4.40E+04	2.61E-07	2.16E-01	4.99E+06	.008
26	TH-230	2	28	0	1.40E+06	2.22E-04	6.93E-02	5.00E+06	.003
27	U-233	2	31	0	1.00E+04	2.44E-05	1.54E-02	1.40E+06	.001
28	U-234	1	0	0	1.40E+06	2.06E-02	1.37E-01	1.00E+04	.005
29	U-235	1	0	0	1.40E+06	9.99E-01	2.53E-02	1.00E+04	.001
30	U-238	1	0	0	1.40E+06	1.00E+00	1.12E-01	1.00E+04	.004
31	NP-237	1	0	0	1.00E+04	9.97E-01	4.78E+02	1.00E+04	17.710

Table 3.14b (continued)

LEACH TIME (YR)			PATH LENGTH(M)		WATER VELOCITY (M/YR)				
1.0000E+04			1.0000E+02		1.0000E+00				
No.	NUCLIDE	MEMBER	1ST	2ND	TIME OF PEAK (YR)	MAXIMUM N/NO	WAT. DIL. (M**3/GW*YR**2)	CONTAM. TIME (YR)	PERCENTAC
32	PU-238	2	38	0	1.10E+06	0.	0.	1.00E+06	0.
33	PU-239	2	39	0	1.00E+06	2.89E-12	8.37E-09	1.00E+06	.000
34	PU-240	2	42	0	1.00E+06	1.60E-29	1.23E-42	1.00E+06	.000
35	PU-241	4	43	0	3.00E+05	1.96E-10	8.90E-10	1.00E+04	.000
36	PU-242	2	44	0	1.00E+06	1.37E+00	6.65E-01	1.00E+06	.025
37	AM-241	2	43	0	3.00E+05	5.47E-11	2.51E-07	1.10E+06	.000
38	AM-42M	1	0	0	1.10E+06	0.	0.	1.00E+04	0.
39	AM-243	1	0	0	1.10E+06	1.24E-42	1.36E-38	1.00E+04	.000
40	CM-242	4	38	0	1.10E+06	0.	0.	1.00E+04	0.
41	CM-243	1	0	0	3.00E+05	0.	0.	1.00E+04	0.
42	CM-244	1	0	0	3.00E+05	0.	0.	1.00E+04	0.
43	CM-245	1	0	0	3.00E+05	1.96E-10	4.45E-08	1.00E+04	.000
44	CM-246	1	0	0	3.00E+05	3.83E-17	1.15E-15	1.00E+04	.000

Identification number (first column) of the first precursor;

Identification number of the 2nd precursor

Time of maximum concentration at the given path length

Maximum dimensionless concentration:; $N_j(z, t_j)/N_j$

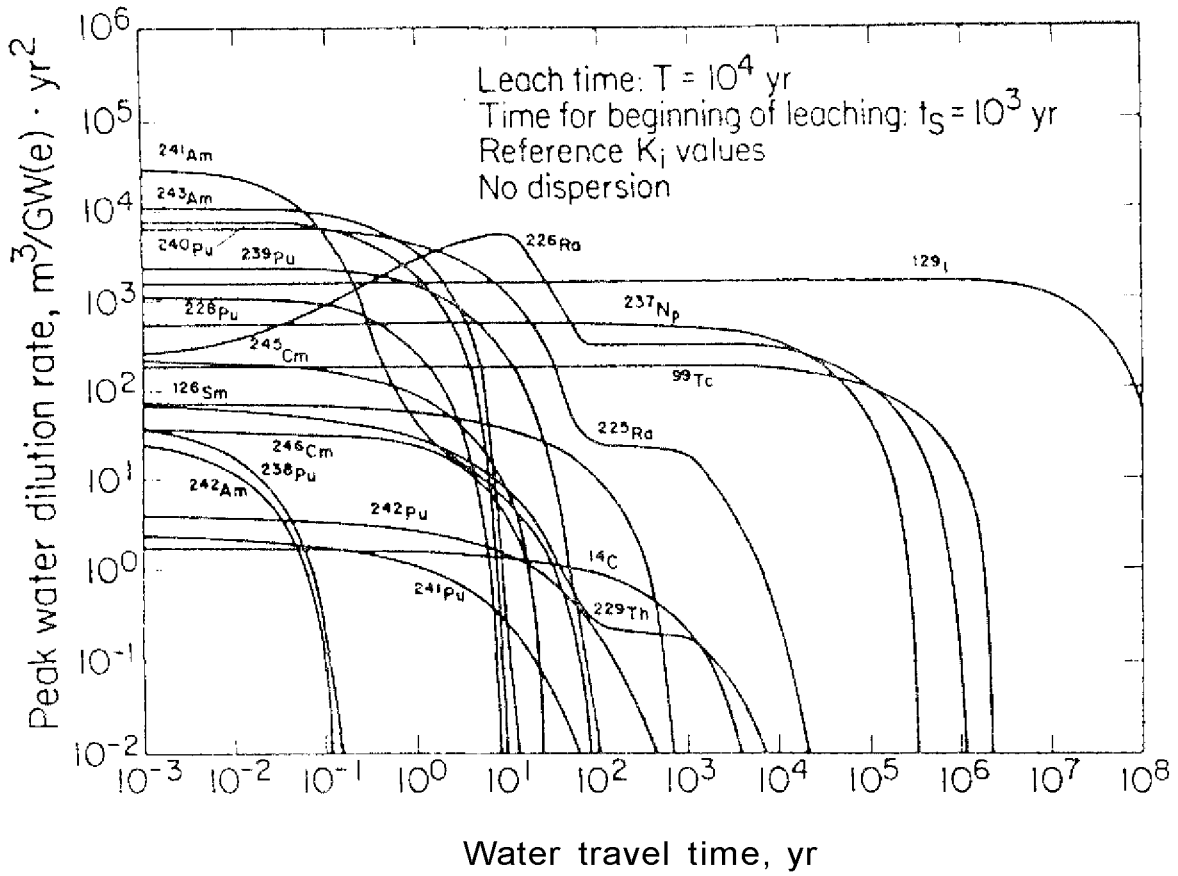
Correspondent maximum water dilution rate (see Eq. (2.7.68))

Time interval that this nuclide is present at the given path length

Percentage of the sum of all peak water dilution rates (in Column 8) for all nuclides.

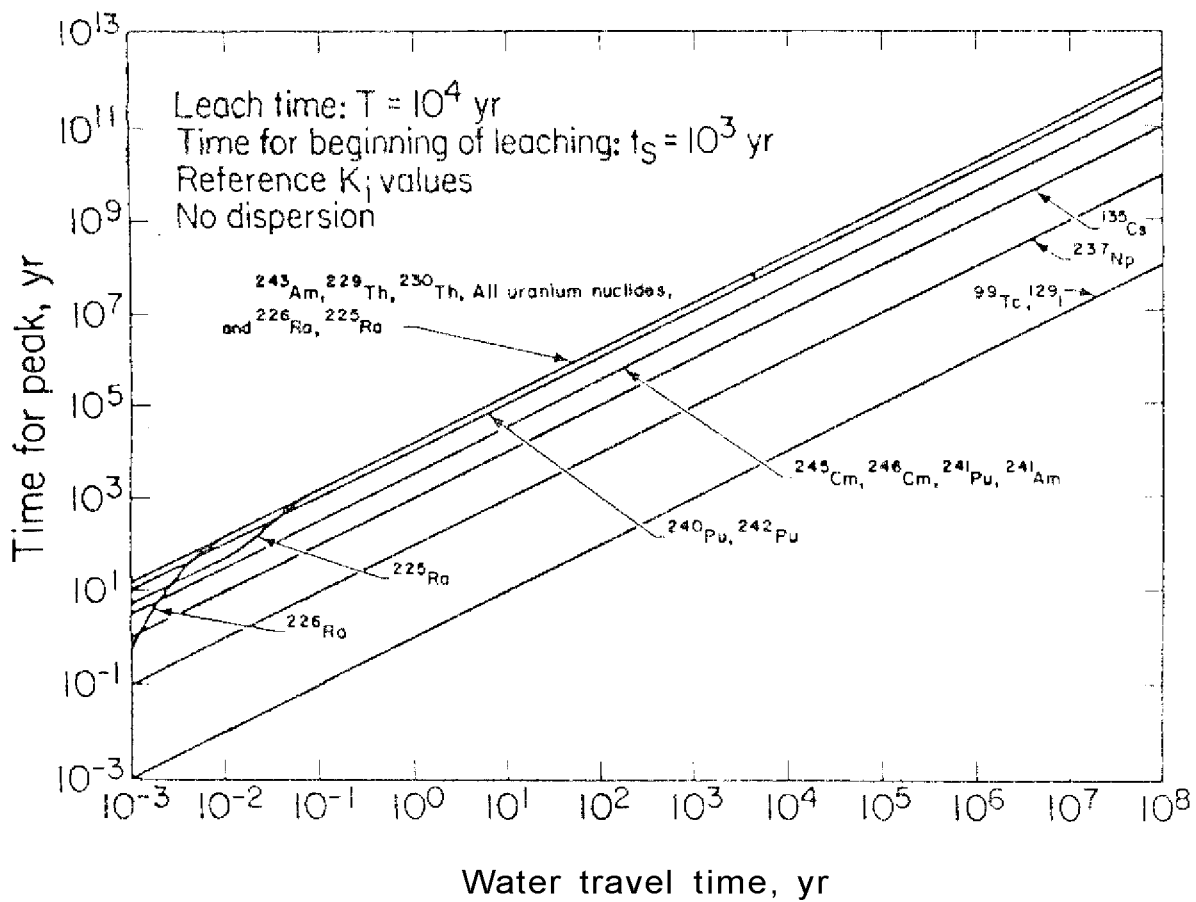
The variation of peak water dilution rate w^{\wedge} with water travel time is shown in Figure 3.9. For water travel times smaller than 10 years, Am-241 and Pu-239 produce the largest peak water dilution rates. Their peaks die out quickly for larger water travel times. Ra-226 water dilution rate builds up from the decay of U-234 and reaches the largest value at a water travel time of about 100 years. Between 10 and 1000 years, Ra-226 is the largest contributor. For water travel times larger than 1000 years only those nuclides with small attenuation factor will be present. This is the case of I-129 which has the smallest attenuation factor of them all being the last to die out at about 10^8 years. Allied to its high toxicity, I-129 is one of the most important nuclides to be contained. Besides I-129, at large water travel times, Np-237 and Tc-99 also present significant water dilution rates. They roll off at about 10^4 years. With the exception of I-129, Np-237 and Tc-99 all other significant radionuclides have peak water dilution rate curves which roll-off quickly before water travel time of 1000 years.

The variation of the time for peak t^{\wedge} with water travel time is shown in Figure 3.10. The linear variation is expected for the first and second members of chains according to the results of the method developed in preceding sections. For third member nuclides Ra-225 (Th-229) and Ra-226 we see that their times for peak are interior to the time domain only for very short water travel times (less than 0.1 year). For larger times



XBL 812-225

Figure 3.9 Variation of peak water dilution rate with water travel time for reprocessed PWR high level waste.



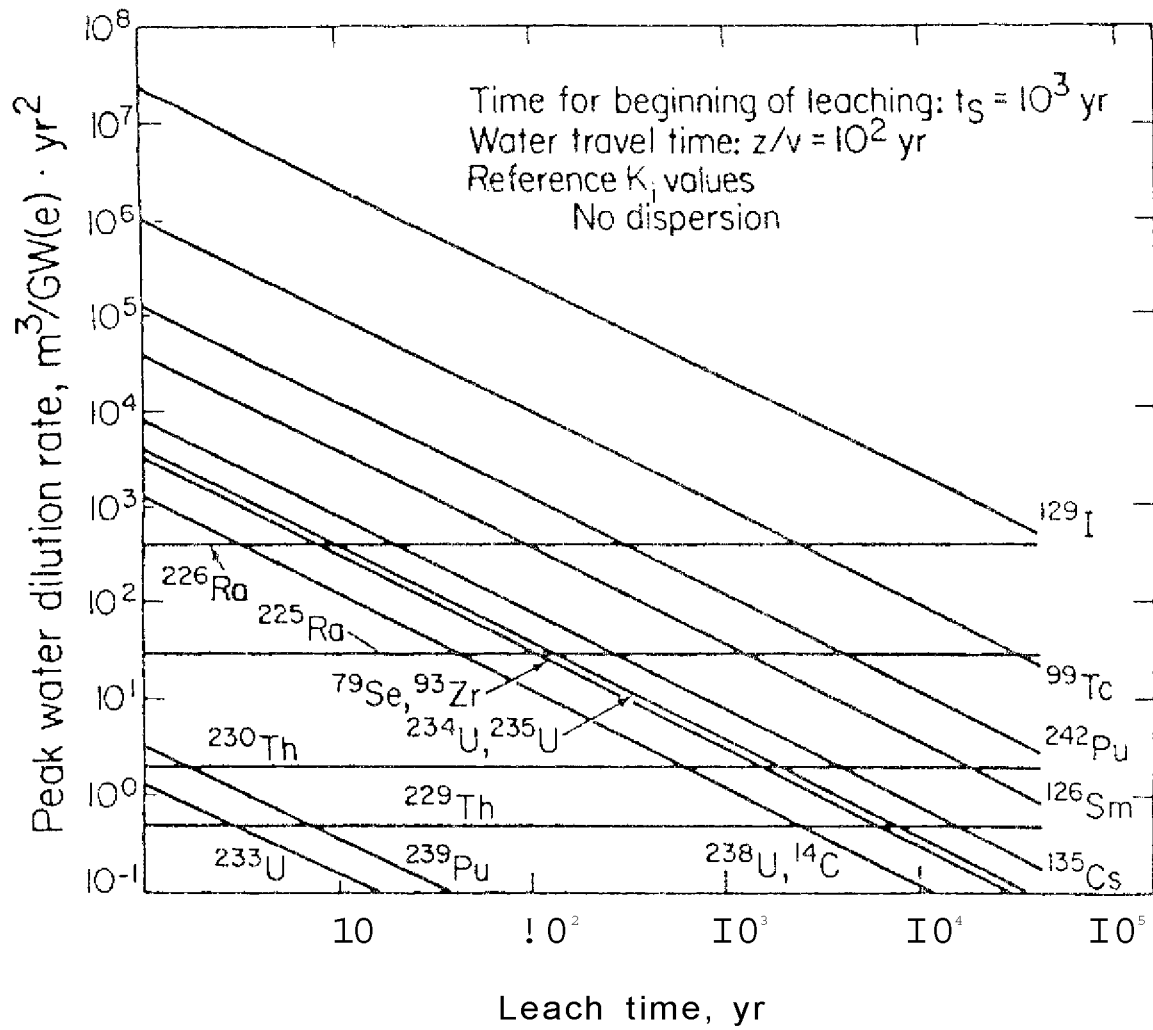
XBL812-226

Figure 3.10 Variation of time for peak with water travel time for reprocessed PWR high level waste.

their peaks travel on the U-234 and U-233 characteristics respectively.

At a fixed water travel time the first peaks to arrive are those of I-129 and Tc-99 which travel with the water front velocity because of their assumed unit retardation coefficient. One hundred years later the Np-237 peak reaches that position⁴ followed by Cs-135 peak 10 years later. Only after about 10 years later all other nuclides peaks start to arrive. The nuclides Ra-226, Pu-240, Pu-239, Am-241 and Am-243 take a much longer time (10^4 years) to reach a given position than do I-129 and Tc-99. If these nuclides (I-129, Tc-99, Ra-226 (U-238) and Np-237) could be contained, the range of water travel time of concern would be reduced to 1000 years, because all other nuclides with significant peak water dilution rates have already decayed to negligible values of water dilution rates before water travel times of 1000 years.

Figure 3.11 shows the variation of peak water dilution rate with leach time T for a fixed water travel time. For all first member nuclides for each order of magnitude increase in leach time we have an order of magnitude decrease in its peak water dilution rate. However, for the third members Th-229 (Ra-225) and Ra-226 changes in leach time have no effect on their peak water dilution rates. Therefore, changes in waste forms will not affect the magnitude of the peak water dilution rates of Ra-226 and Ra-225 (Th-229). Another important result which is not shown



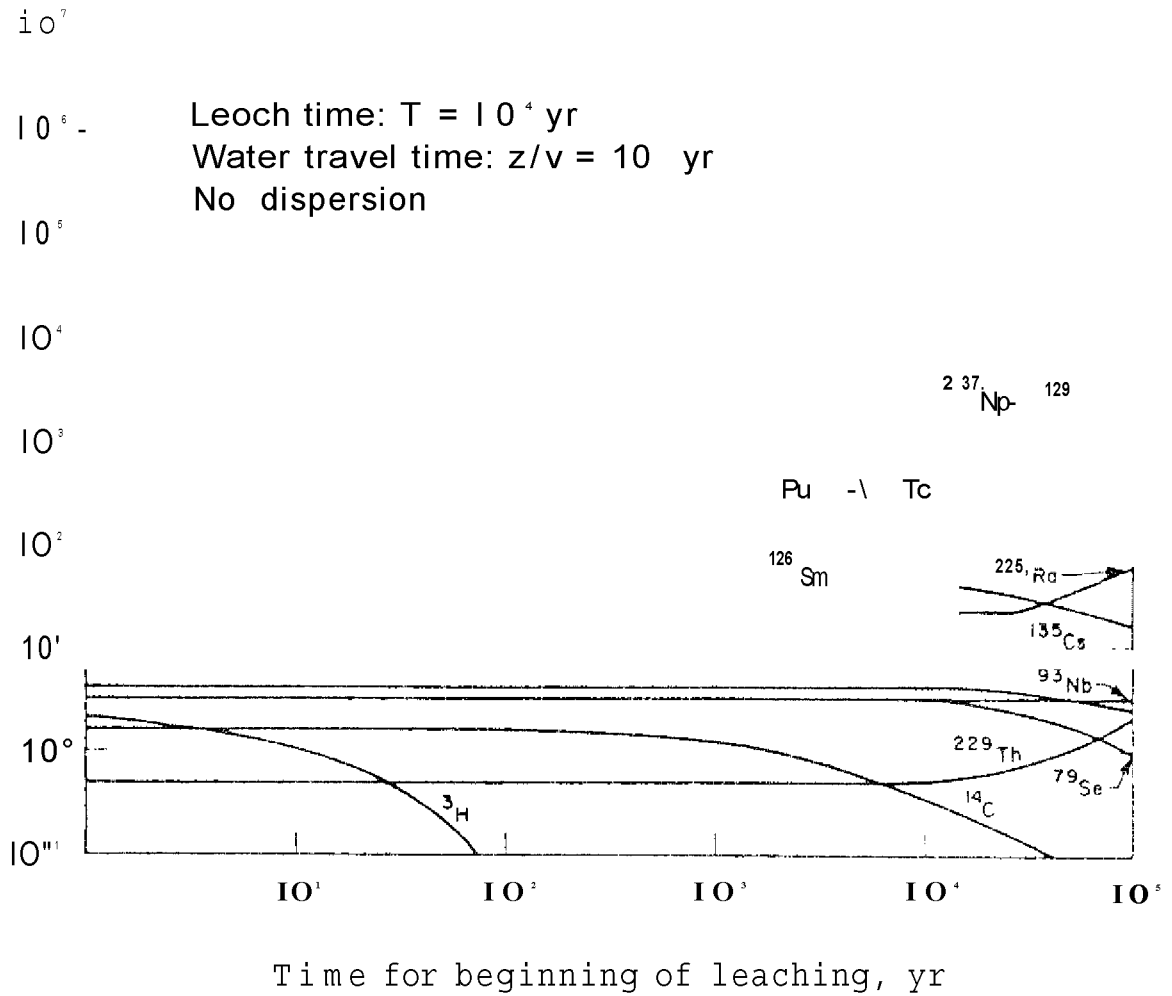
XBL 812-227

Figure 3 .11 Variation of peak water dilution rate with leach time for reprocessed PWR high level waste.

graphically but it is implicit in the method is that the time for peak of any nuclide is independent of the leach time.

The effect of variation of the time for beginning of leaching on the peak water dilution rate is minimal as one can see in Figure 3.12. A delay in starting the dissolution can eliminate the shorter lived fission product like H-3, C-14, Sr-90 and Cs-137. When leaching begins as early as one year after emplacement the actinides Pu-241, Pu-238 and Cm-242 have not decayed to their long lived daughters yet and they will be present in the groundwater. But at the assumed reference water travel time of Figure 3.12, they have already decayed before they can migrate such a distance. All other important nuclides have half lives larger than 10^5 years. The initial inventory will not be changed significantly by the presence of engineered barriers. Although these barriers will not affect the magnitude of the peak water dilution rates they will delay the time when these peaks occur.

The variation of peak water dilution rate of the third members Ra-225 and Ra-226 with the value of the retardation coefficient are shown in Figure 3.13 through Figure 3.18. Each figure shows each one of the six cases described in Table 3.13. The half lives of the radionuclides in the U-234 chain are ordered in the same way as the half lives of the nuclides in the Np-237 chain are ordered. When the equilibrium coefficient of correspondent nuclides in each chain are equal, the behaviour of



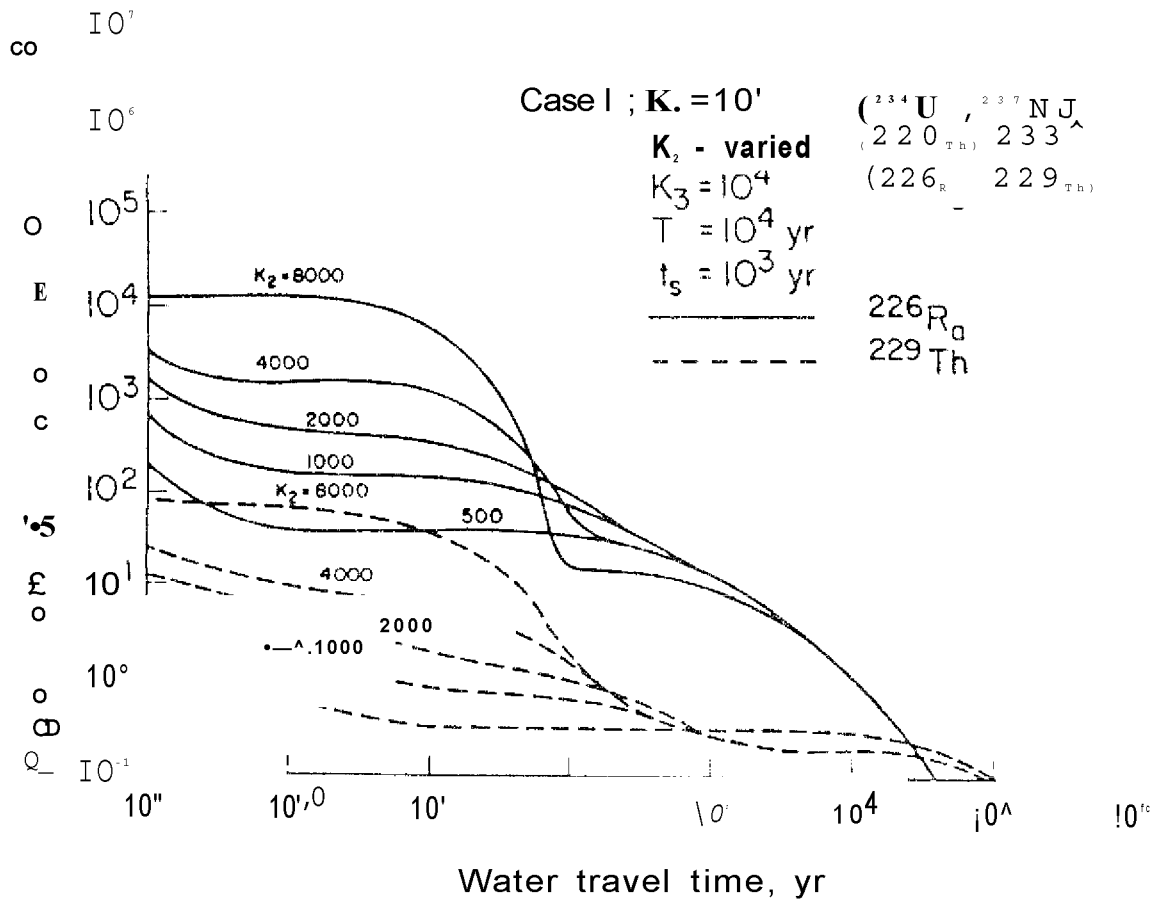
XBL 812-228

Figure 3.12 Variation of peak water dilution rate with the time for beginning of leaching for reprocessed PWR high level waste.

the solutions is expected to be also the same. In the figures for each one of the six cases, the above mentioned fact is confirmed. The variation of the peak water dilution rates with water travel time for each case shows its own characteristic behaviour differing from case to case in each of the six cases.

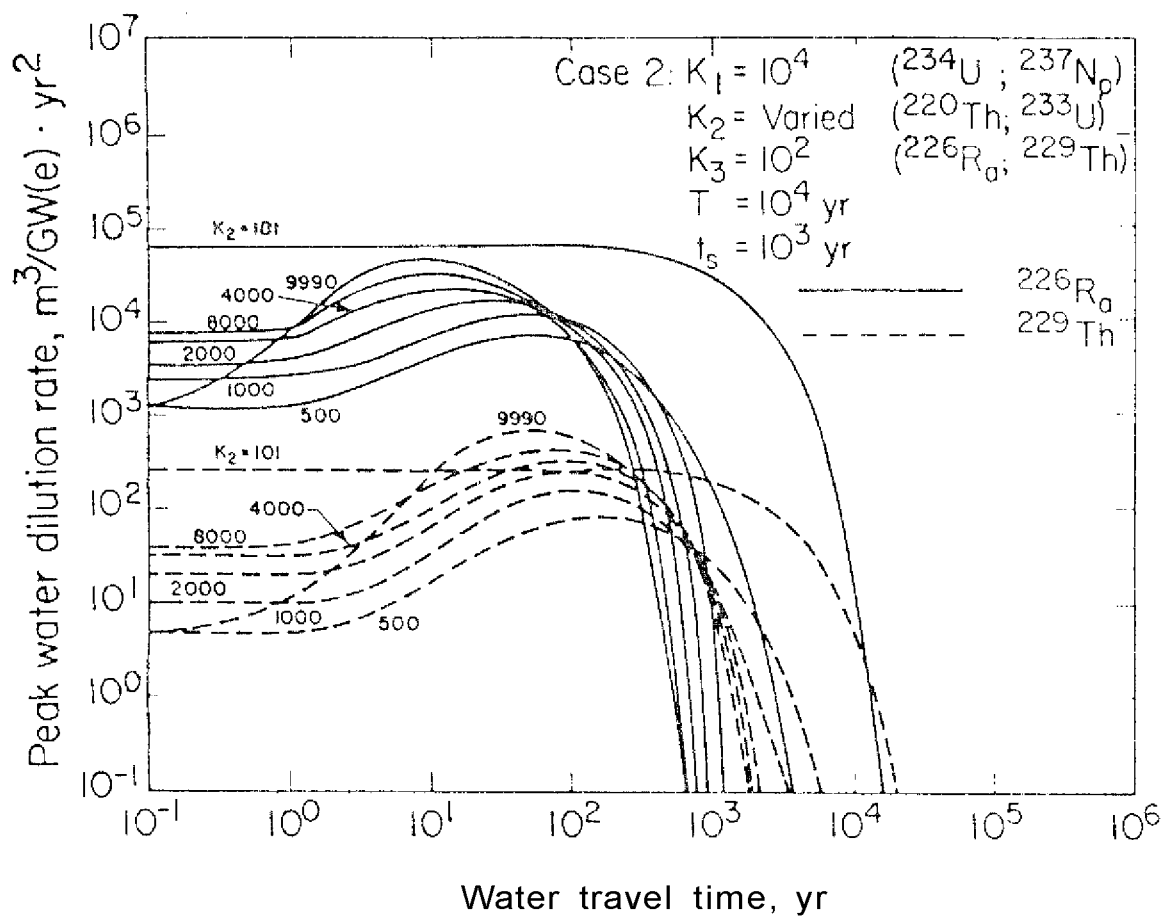
Figure 3.13 shows the case 1 where $K^4 > K^2 > K_2$. The curves for Ra-226 show same behaviour as the curves for Th-229 differing only in the magnitude of the peak water dilution rates. In case 1 the value of K^4 and K^2 were fixed at 10 and 10, respectively and K_2 was varied between those extremes. For all values of K_2 taken, the peak water dilution rate is approximately constant for water travel times of up to 100 and decaying monotonically thereafter. When K_2 value tends to 100, case 1 is approaching case 6. This fact can be confirmed by looking at the curves representing the case 6 (Figure 3.18) where $K^4 > K^2 > K_2$ and comparing to the curves in case 1 when K_2 is smallest. In case 1 as well as in case 6, no increase in peak water dilution rate with increased water travel time is observed.

Figure 3.14 shows case 2 where $K^4 > K^2 > K_2$. In this case, an increase in peak water dilution rate with water travel time is observed. As K_2 is reduced to values close to 100 we are departing from case 2 and entering the case 4 where no increase is observed for any value of K_2 which is being varied. On the other hand, when K_2 approaches 10, case 2 tends to case 5 whose curves also show an increase in peak water dilution rate with



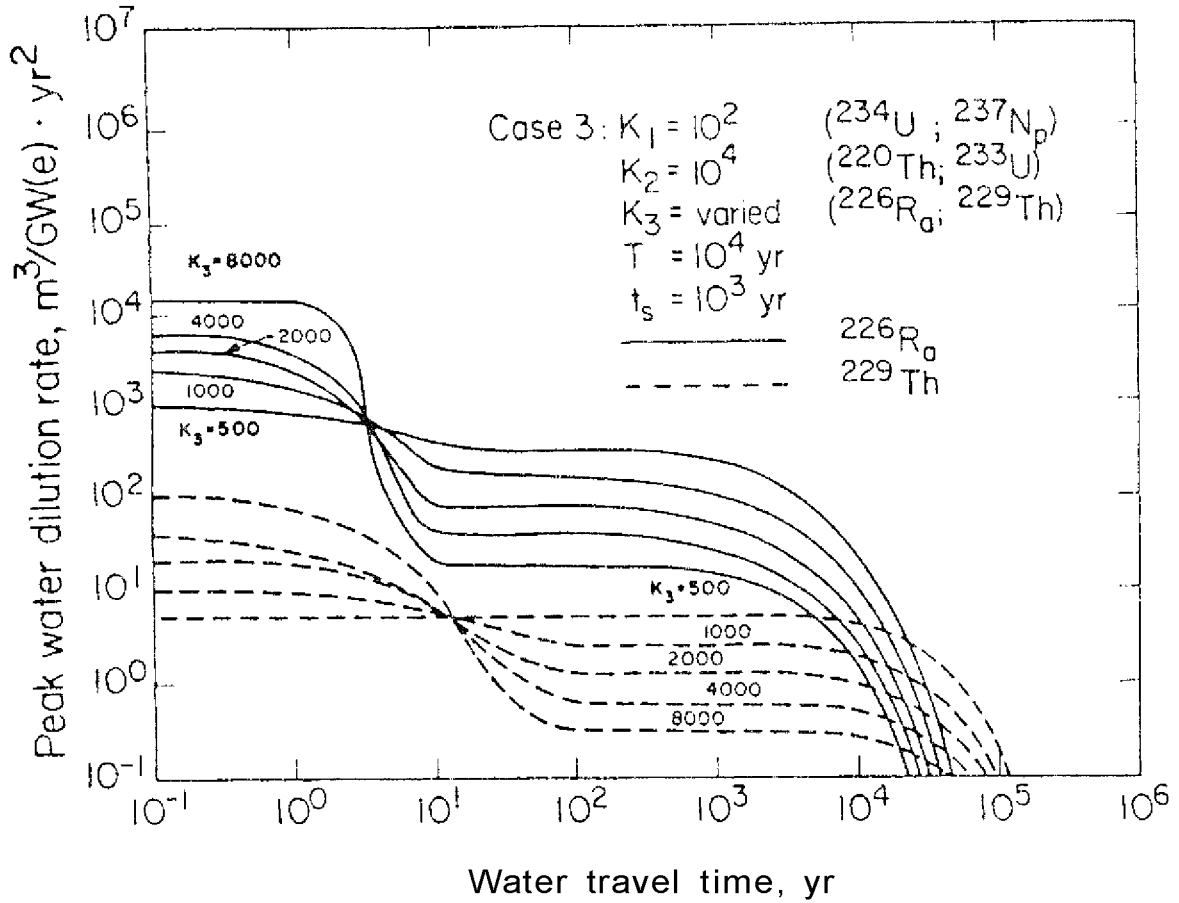
XBL 812-229

Figure 3-13 Variation of peak water dilution rate of third members ^{229}Th , ^{226}Ra , ... in, R_a with the sorption coefficient and with water travel time for reprocessed PWR high level waste.



XBL 812-230

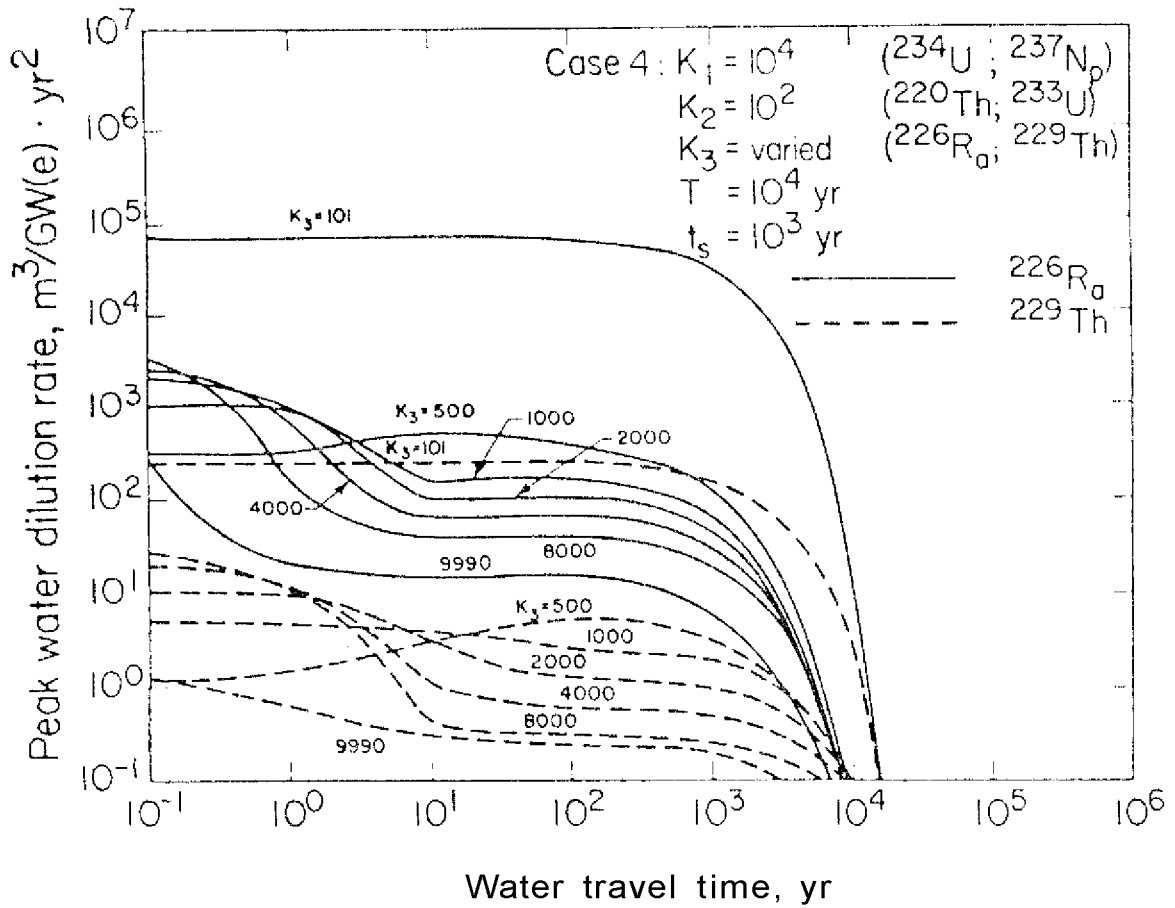
Figure 3.14 Variation of peak water dilution rate of third members ^{229}Th , ^{226}Ra with the sorption coefficient and with water travel time for reprocessed PWR high level waste.



XBL 812-231

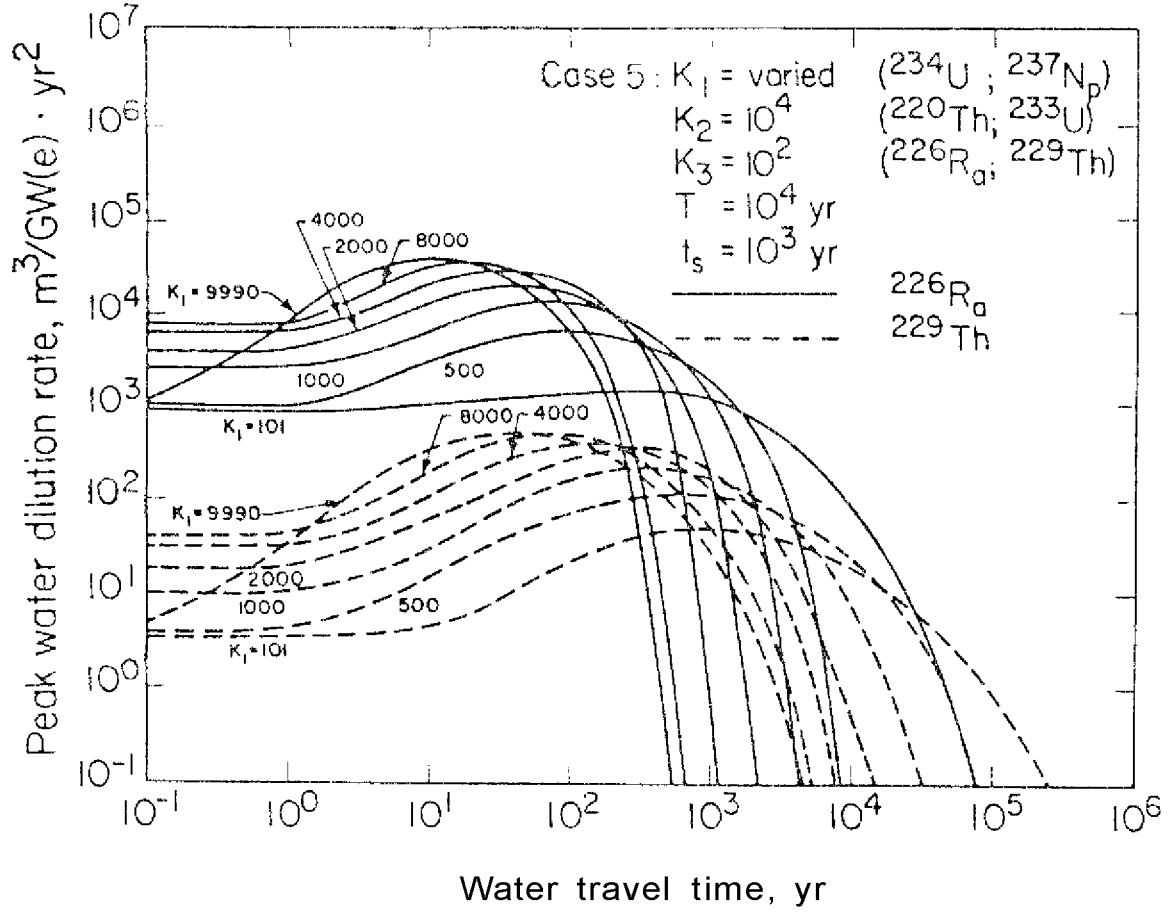
Figure 3 .15 Variation of peak water dilution rate of third members ^{229}Th ^{226}Ra

with the sorption coefficient and with water travel time for reprocessed PWR high level waste



XBL812-232

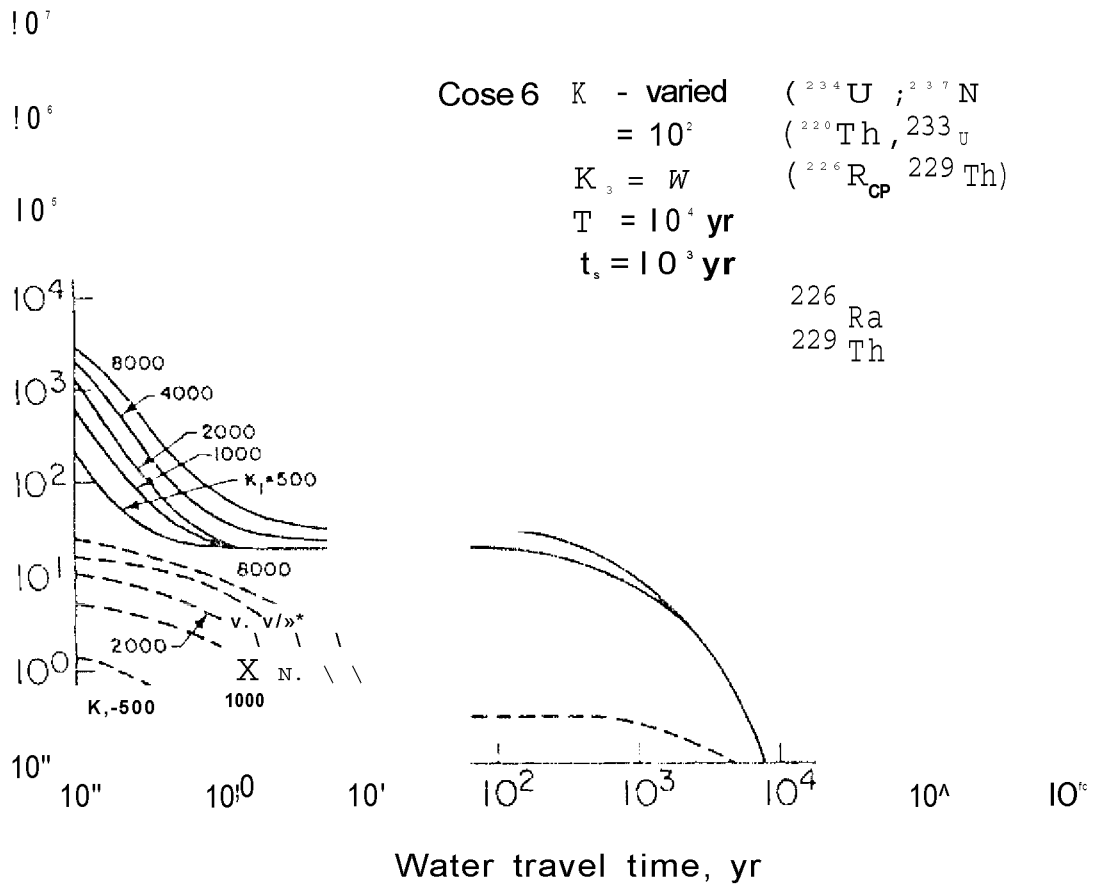
Figure 3.16 Variation of peak water dilution rate of third members ^{229}Th , ^{226}Ra with the sorption coefficient and with water travel time for reprocessed PWR high level waste.



XBL 612-233

Figure 3 .17 Variation of peak water dilution rate of third members
 229 226

Th, Ra with the sorption coefficient and with water travel time
 for reprocessed PWR high level waste



XBL812 -234

Figure 3.18 Variation of peak water dilution rate of third members
 ^{229}Th , ^{226}Ra

^{229}Th , ^{226}Ra with the sorption coefficient and with water travel time for reprocessed PWR high level waste.

time. Case 2 and case 5 are the only cases where these build up and subsequent roll off in peak water dilution rate occur. These two cases have the common fact that λ has a smaller value than K and K_2 . In all other cases, the peak water dilution rate decreases monotonically with water travel time.

3.7.5 Leaching of natural uranium ore and ore mill tailings

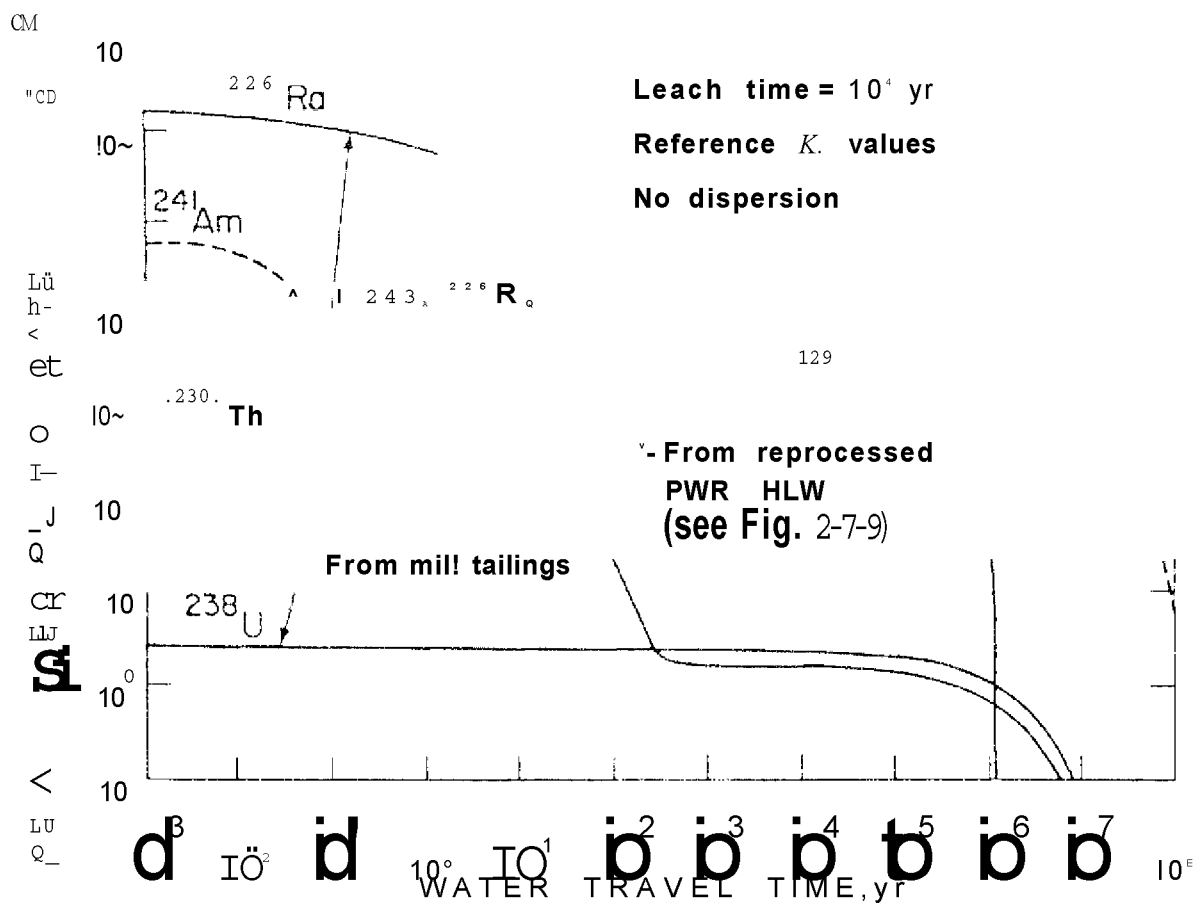
The nuclide inventories of the reprocessed high level waste used in the reference case is the result of the generation of 1 Gw(e)yr of electricity by a PWR. They operate at 33% thermal efficiency, 80% load factor and with a burnup of 30.4 MWD/kg. Such an electrical generation requires the total amount of 30.3 Mg of U_0 , fuel enriched to 3.3% U-235. To evaluate the amount of natural uranium ore required to produce this amount of fuel let us consider a gaseous diffusion enrichment plant with a depleted uranium stream with 0.0036 atom fraction of U-235. By a simple mass balance in both the total number of atoms and in U-235 atoms, one conclude that it is required 250 Mg of natural uranium ore. The eventual losses during fabrication are 1%, in conversion to hexafluoride is 0.5% and in milling and concentration is 5% (B2). The total activity of the uranium present in such ore will be 82 Ci of U-238 and 1.7 Ci of U-235.

When the uranium ore is processed, it is milled and

purified to remove the non-uranium rock. The non-uranium radioactive decay daughters, e.g. Th-230 and Ra-226 are also separated and are left with the piles of mill tailings. Suppose these piles of mill tailings are buried in such a way that a equivalent initiating event which started the leaching of the high level reprocessed waste canisters also happens for the piles of mill tailings. One can assume that the leach rate of the mill tailings is the same as the reference value adopted for HLW, i.e. 10000 years.

Since the ore body is expected to be where it has been for periods longer than 10^5 years, the initial activities of all daughters are in transient equilibrium with U-238. Also, for the purpose of this illustration, one can assume that U-238 and U-234 are in solution with the same chemical form (thus, with the same retardation coefficient) which allows us to consider U-234 as in secular equilibrium with U-238 because the intermediates Th-234 and Pa-234 have very short half-lives.

The peak water dilution rates resulting from the leaching of such piles of mill tailings are calculated and shown in Figure 3.19. The peak water dilution rate for Ra-226 from the mill tailings as well as the envelope of the peak water dilution rates of all nuclides present in a reprocessed HLW (Figure 3.9) are plotted against water travel time. Ra-226 peak water dilution rate due to the dissolution of the mill tailings is larger than the envelope of the peaks due to the leaching of the high level

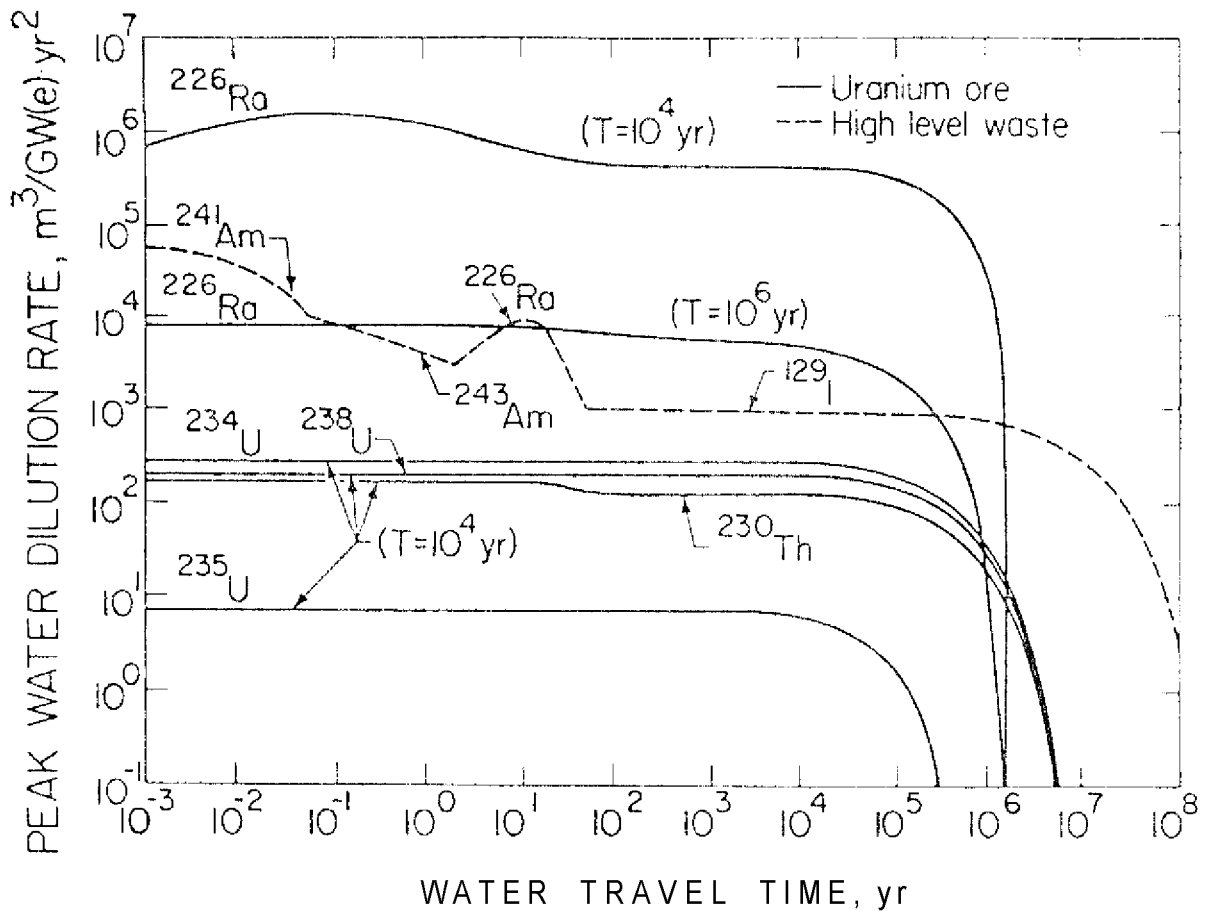


XBL 812-235

Figure 3.19 Variation of peak water dilution rate from natural uranium ore mill tailings with water travel time.

waste canisters. After water travel time of 10^6 years Ra-226 peak water dilution rate roll off rapidly because its precursor has already decayed. However, for water travel times larger than 10^9 , HLW curve still shows the contribution of I-129 although three orders of magnitude smaller than that of Ra-226 resulting from mill tailing leaching.

The same calculation done for the leaching of the mill tailings is repeated for the equivalent amount of natural uranium ore. In this case all the uranium will be present, not only 5% as in the case of mill tailings. One assume again that the same scenario adopted for the high level waste is valid for the uranium ore. Figure 3.20 shows the peak water dilution rate of Ra-226 due to the leaching of the uranium ore compared to the envelope of the peak water dilution rates of all nuclides present in the HLW. Again, the peak water dilution rate for Ra-226 in the ore is always larger than the envelope of the HLW nuclides indicating that for this set of retardation coefficients, the leaching of the equivalent amount of natural uranium ore used to produce the amount of waste considered is potentially more hazardous than the high level waste itself.



XBL 812-236

Figure 3.20 Variation of peak water dilution rate with water travel time, from leaching of natural uranium ore.

4. Migration of Radionuclides in Two-Dimensional Groundwater Flows Through Geologic Media

4.1 Introduction

This research is concerned with the prediction of radionuclide concentrations in aquifers in which a stationary two-dimensional groundwater flow is established. Repositories will be located in rock formations with no significant water content. However, abnormal events can occur which can cause radionuclide release from the waste package. These nuclides can eventually reach a nearby aquifer discharging into a fresh-water source.

Both migration of long actinide chains and long lived fission products in two-dimensional geological media as well as their discharges into the biosphere is modelled in this work. The theory on which this modelling is based upon was developed and presented in a previous report (Chambre, P1). This method provides a more realistic way than a one-dimensional model to assess the potential hazard to the biosphere posed by the accidental release of radionuclides from a high-level waste repository.

Analytical solutions to the radionuclide transport equation existent to date have been restricted to one-dimensional

groundwater flows. When two-dimensional flow fields needed to be considered, numerical schemes had to be invoked. Besides the capability of analyzing two-dimensional flow fields, the analytical non-recursive character of the present solution to the transport equation allows one to evaluate the concentration of an arbitrary member of a chain of any length without having to solve for its precursors. The evaluation of this solution requires little computing time.

In this present study, the two-dimensional groundwater flow is in steady state and dispersion effects are neglected. Adsorption reactions between nuclides in the water with the geologic media are assumed to be in equilibrium and there is no solubility limit of the nuclides in the groundwater.

The most important result derived in the theory is that when dispersion is negligible, the solution to the one-dimensional radionuclide transport equation is applicable along a streamline of the two-dimensional potential flow (Darcy's flow). The problem is then divided into two parts, namely: the determination of the hydrological flow net (i.e. the potential lines and the streamlines of the flow) and the evaluation of the radionuclide concentrations along the streamlines which passed by the source line in the aquifer being thereby contaminated. The discharge rate into the biosphere is also obtained.

The groundwater flow field can be represented either by

analytical expressions or by (scattered) field measurements of the groundwater potentials. The analytical representation is affected by superimposing an arbitrary number of point sinks and point sources. This superimposition can represent flow fields of arbitrary complexity. On the other hand, a given number of scattered potentiometric field data can be used to represent the flow net by fitting the data with a minimal total curvature spline function (B1). The above two methods can be combined to analyze the effects of injection and pumping wells in existing aquifers.

Once the potentiometric surface is determined and values for the hydraulic conductivity at the site obtained, the streamlines and the water travel time function (see Eq.(4.2.10)) can be obtained by the method of characteristics. The next step is to apply the solution of the one dimensional nuclide transport equation along a streamline. Finally, if the location of the intersection of the biosphere with the contaminated streamlines is known one can evaluate the discharge rate into the biosphere.

The above described steps are performed by the computer program (UCBNE21). Due to the semi-analytical character of this program, the computing time is much smaller than finite-difference schemes used to solve the equivalent problem. A complete listing of the program is given in Appendix C. The program has the capability of using the LBL Computer Center plotting software to automatically generate graphs.

As an application of the utilization of this computer program we studied the far field migration of radionuclides for two candidate repository sites. These are the Waste Isolation Pilot Plant (**WIPP**) in Eddy County, **New** Mexico and the Basalt Waste Isolation Project (BWIP) in Hanford, Washington. Hydrological data available for both sites are reviewed and the contaminated regions for the most important nuclides as well as the nuclide discharge rates, are estimated by applying this two dimensional analytical theory for radionuclide transport.

4.2 Theoretical Background

The theoretical developments leading to the solution of the radionuclide transport equation in a two-dimensional geological media are presented in a previous report (Chambré, PI.). In this section we summarize the important steps shown in that work and we also emphasize the important results needed in the present work.

4.2.1 The governing equations

The two-dimensional hydrological groundwater flow is time independent, incompressible and it is a Darcy-type flow. Dispersion effects are neglected and sorption reactions are assumed to be in equilibrium. No solubility limits are considered, but by suitably defining the boundary condition one should be able to apply the present solution with solubility limit of the first member. Water density and soil porosity are considered constants.

Subject to above assumptions, the conservation equation for the nuclide concentration in water (x, y, t) for the i -th member of a chain is given by (PI, Eq.(5.1.1))

$$K_i \frac{\partial N_i}{\partial t} + \nabla \cdot (v N_i) = K_{i-1} X_{i-1} - K_{i-1} N_i \quad , \quad i=1, 2, \dots \quad (4.2.1)$$

Here K_i are the retardation coefficients, v is the groundwater velocity (m/yr), λ_i are the decay constants (1/yr). In view of the incompressibility assumption the groundwater velocity satisfies the following conservation of mass relation

$$\nabla \cdot v = 0 \quad (4.2.2)$$

where the groundwater velocity is given by Darcy's law

$$v = -K \nabla \phi \quad ; \quad k = k'/e \quad (4.2.3)$$

Here k' is the hydraulic conductivity of the soil (m/yr), e is the porosity and ϕ is the hydraulic head (m). Although k is the hydraulic conductivity divided by the porosity, we will refer to k as being the hydraulic conductivity. Substituting Eq. (4.2.3) into Eq. (4.2.1) and using Eq. (4.2.2) the transport equation is rewritten as

$$\frac{\partial N_i}{\partial t} + \nabla \cdot \left(\frac{K_i}{e} \nabla \phi \right) N_i + \lambda_i N_i = \sum_{j=1}^A \frac{K_j}{e} \nabla \cdot \left(\nabla \phi \right) N_j \quad (4.2.4)$$

$$i = 1, 2, \dots, A \quad \phi = 0$$

Let us denote by R the region of interest and by P any point inside R (see Figure 4.1). The radionuclides are assumed to be released along a line source S in R and a point on S will be called Q . With the above notation, the initial condition (Pi, Eq. (5.1.4)) and the boundary condition (Pi, Eq. (5.1.5)) can be expressed by the following relationships

$$N_i(P, 0) = 0 \quad ; \quad P \neq Q \quad ; \quad P \in R \quad (4.2.5)$$

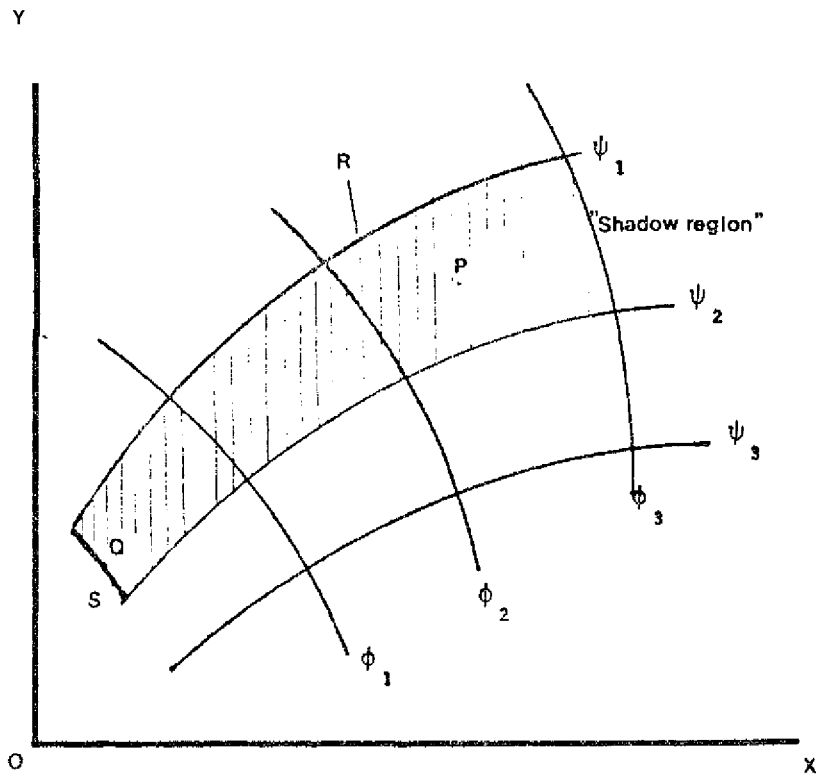


Figure 4.1 Pictorial view of the system being studied: R is the region of interest, P is any point inside R, S is the source line, Q is a point on the source line, ψ_j are the streamlines and ϕ_j are potential lines.

$$N_i(0,t) = N_i^0 G_i(Q,t) \quad ; \quad Q \leq t, \quad t > 0 \quad (4.2.6)$$

$$G_i(P,t) = 0 \quad ; \quad t < 0, \quad \text{PeRUS} \quad (4.2.7)$$

where $G^{\wedge}(Q,t)$ is an arbitrary release function which describes the time dependent dissolution and release of the waste into the aquifer. N_i^0 is the initial concentration of the i -th nuclide. Eq. (4.2.2) and Eq. (4.2.3) describe the groundwater flow field while Eq. (4.2.4), Eq. (4.2.6) and Eq. (4.2.7) govern the radionuclide transport through the geologic media.

4.2.2 Two-dimensional groundwater flow fields and the water travel time function

Two-dimensional groundwater flows are representable by potential flows and one can define the streamfunction of the flow $\psi(x,y)$ by the following (Pl, Eq. (5.2.2))

$$\frac{\partial \psi}{\partial x} = -k \frac{\partial \phi}{\partial y} \quad (4.2.8)$$

$$\frac{\partial \psi}{\partial y} = k \frac{\partial \phi}{\partial x} \quad (4.2.9)$$

The water travel time function $t_o(x,y)$, (yr), is defined along a fixed streamline by the following equation

(Pl, Eq. (5.2.7))

$$d_s = \frac{dx}{u} \quad \text{for } u(x,y) = \text{constant} \quad (4.2.10)$$

Physically, $\phi(x,y)$ represents the time an elementary volume of water, initially at a position (x_0, y_0) , takes to reach a given position (x,y) downstream travelling along the streamline which passes through these two points. By using the orthogonality condition between the streamfunction $\psi(x,y)$ and the potential function $\phi(x,y)$ in addition to the definition of the water travel time function $\phi(x,y)$, the conservation equation for the i -th member of a radioactive chain Eq.(4.2.4) can be reduced to the following greatly simplified form (Pl, Eq. (5.2.6))

$$\frac{dN_i}{dt} + \lambda_i N_i = \lambda_{i-1} N_{i-1}$$

Eq. (4.2.11) is valid along a streamline where $\psi(x,y) = c$. The concentration along this streamline is now a function of only two variables, i.e. $N_i = N_i(\phi(x,y), t)$. We will now change the notation $\phi(x,y)$ showing explicitly the dependence on (x,y) along a streamline by simply writing a . Therefore, the concentration of the i -th member will be denoted by $N_i(a, t)$.

Thus the two-dimensional problem of evaluating $N_i(x,y,t)$ can be reduced to a one-dimensional problem of evaluating $N_i(a,t)$ along a streamline provided one knows how the water travel time varies along that streamline. In the next section we will show how this problem can be solved by making use of the previously

derived analytical solution for the one-dimensional problem
(Chambre, Hi, section 4.4).

4.2.3 The solution of the two-dimensional transport
equation

From the definition of the water travel time function ϕ
Eq.(4.2.10) one can realize that lines of constant potential are
parallel to lines of constant water travel time along a
streamline (i.e. , when $d\phi=0$ implies $d\phi=0$ in Eq. (4.2.10) when $d|\phi| = 0$.

This parallelism is mathematically expressed as

$$(kv^{**}) \cdot (Vc) = -1 \quad ; \quad *M_{x,y} = c \quad (4.2.12)$$

The side conditions that $\phi(x,y)$ must satisfy are
(Pl, Eq. (5.3.3) and Eq. (5.3.4)), see Figure 4.1.

$$a(Q) = 0 \quad ; \quad QcS \quad (4.2.13)$$

$$a(P) > 0 \quad ; \quad P \text{ is a point in the shadow region} \quad (4.2.14)$$

(see Figure 4.1)

The initial and boundary conditions for the radionuclide
concentrations along a streamline can be restated as
(Pl, Eq. (5.3.8))

$$N_i(P, 0) = N_i(a, 0) = 0 \quad ; \quad \phi > 0 \quad (4.2.15)$$

$$N(Q,t) = 1^{\wedge}(0,0 = N_i G_i(0,t) ; t > 0, o=0 \quad (4.2.16)$$

Let us define $G_i(t) = G_i(0,t)$. Figure 4.1 illustrates the system being studied. Only those streamlines which cross the source line S will be contaminated. In the case of Figure 4.1 all the streamlines contained between the lines $\mathbf{1}$ and $\mathbf{2}$ form the region which can contain radionuclides since there is no dispersion. This region downstream from the repository will be called the "shadow region". Therefore, the shadow region is the specific region of interest where the calculations are going to be performed.

For a given streamline crossing the line source S at a point Q one must solve Eq. (4.2.11) subject to the initial condition Eq. (4.2.15) and the boundary condition Eq. (4.2.16). The radionuclide concentrations are now expressed as a function of the time t started after the beginning of the release and of the water travel time o counted from the time when the water leaves the source line S.

Mathematically, this problem can be made equivalent to its one-dimensional counterpart with a constant water velocity. Replacing (z/v) in the governing equation Eq. (2.2.1) for the equivalent one-dimensional problem by o, one obtains the governing equation for the two-dimensional problem valid along a streamline of the flow i.e. Eq.(4.2.11). Therefore, the solution for the one-dimensional case $N_j(z/v,t)$ can be used to express

the radionuclide concentration along a streamline $N_i(\mathbf{o}, t)$ once we replace z/V by cr . The solution to the one-dimensional radionuclide transport equation with constant water velocity was developed in a previous report (Chambre, H1). Here the solution is rewritten

$$N_i(Kt) = N^0 ; \sum_{i=1}^n A_i K_i^0 (t - K_{i,0}) f_i \quad (4.2.17)$$

$$f_i = \sum_{j=1}^m \sum_{r=j}^m \frac{A_j K_j^0}{r^{j-1}} \exp\left(-\frac{K_j}{r} t\right)$$

The coefficients are defined as follows

$$A_i = \frac{N_i^0}{K_i^0} \quad (4.2.18)$$

$$A_i = \sum_{r=j}^m \frac{A_j K_j^0}{r^j} \quad (4.2.19)$$

$$D_{rm}^{(Cj)} = \sum_{q=j}^m \frac{n_q}{q^m} (A_q - A_{rm}^j) \quad (4.2.20)$$

$$A_{il} = \frac{A_i K_i^0 - \hat{A}_i K_i}{K_i - K_i} \quad (4.2.21)$$

The function $g(t)$ is defined by the following expression

$$g_{rnr}(t) = e^{-A(t-K_a)} h(t-K_m\sigma) \quad (4.2.22)$$

The symbol * represents the convolution integral of the function in the bracketed term

$$g_{rm}(t) \otimes G_j(t) = \int_0^t g_{rm}(\zeta) G_j(t-\zeta) d\zeta \quad (4.2.23)$$

Repositories will be located in rock formations with no significant quantities of water, and release of radionuclides from the waste package and consequent contamination of surrounding aquifers will occur in case of an abnormal event. The proposed scenario (D1,R2) for the accidental release of radionuclides from the repository assumes that a fracture is formed which connects the repository to a surrounding aquifer. The water flowing through this fracture leaches out radionuclides from the waste package and carries them to the aquifer. Although the transport of radionuclides through this fracture takes actually some time, in this study we assume this time to be negligible. In other words, the repository is assumed to be placed directly in the aquifer being considered. This is a conservative assumption. Therefore, the source line S described in Figure 4.1 will indeed represent the repository.

A commonly used release mode of radionuclides from the repository is the so called decaying band release. This model states that every nuclide is released with the same constant

release rate during a period called leach time T (yr).

Mathematically this release mode is expressed by the following

(HI)

$$G_i(t) = \sum_{j=1}^i B_j \cdot \exp(-X_j \cdot t) [h(t) - h(t-T)] \quad (4.2.24)$$

where B^j are the Bateman coefficients. The initial concentration N_i^0 is given by the following expression

(Hi, section 3.2)

$$N_i^0 = \frac{M_i^0}{QT} \quad (4.2.24a)$$

here M^i is the total activity of the i-th nuclide when the leaching started, Q is the total groundwater flowrate in the

3

aquifer through the waste (m /yr) and T is the leach time (yr).

In this present work we adopted the above model and the solution

Eq. (4.2.17) is rewritten after substituting Eq. (4.2.24) and

evaluating the convolution integral

$$N_i(t) = N_i^0 \exp(-X_i \cdot K_1 \cdot t) \cdot \left[\sum_{j=1}^i B_{ji} \exp(-X_j \cdot (t - K_1 \cdot t)) \right] \cdot [h(t - K_1 \cdot t) - h(t - T - K_1 \cdot t)]$$

$$+ \sum_{j=1}^{i-1} \sum_{m=j}^i \sum_{r=j}^i \sum_{k=1}^j Q_{rm}^{(j)} B_{jk} \{ \exp[-\Delta_{rm} (t - K_m \cdot t) - \lambda_m K_m \cdot t] [h(t - K_m \cdot t) - \exp(-T - A) h(t - K_m \cdot 0) - \exp[-X_k t - (X_m - X_k) \cdot 0] [h(t - a) - h(t - T - K_1 \cdot 0)]] \} \quad (4.2.26)$$

- exp (-T - A)) h (t - K_m 0) - exp [-X_k t - (X_m - X_k) 0] [h (t - ^a) -

-h (t - T - K₁ 0)])

where the new coefficient is defined by

$$\begin{aligned}
 & i-1 \\
 & q^{\wedge} j \\
 & r^m \left(\sqrt{v} \sqrt{v} \frac{r^k}{r^k} r^k + w_H \frac{t}{v} \frac{q^3}{q} \frac{g}{q} \frac{q}{q} \frac{m^k}{q} r^k \frac{r^k}{r^k} \frac{r^k}{r^k} \frac{q^5}{q} J \right) \\
 & q=j \\
 & q^* r^{\#m}
 \end{aligned}
 \tag{4.2.27}$$

An important feature of this later form of the solution is that it allows the possibility of two or more nuclides in the same chain to have the same retardation coefficient value. The singularity caused by equal values that the previous solution contained is thus removed.

If the boundary condition along every point on the source line S has the same value, this will cause the concentration along a line of constant water travel time (isochronous lines) to be also constant (see Eq. (4.2.26)). Hence, the isochronous lines and the iso-concentration lines coincide with each other although each function has different values on these lines.

Therefore, to completely describe the concentration history one must obtain the groundwater flow net (i.e. the streamlines of the flow) and how $c(x,y)$ varies along each streamline. When $c(x,y)$ is substituted into Eq. (4.2.26), it will yield the concentration of the i -th member in the groundwater.

In the next Section 4.3 a superposition of an arbitrary number of point sinks and point sources is used to represent some

complex groundwater flows. An analytical expression for the Potentiometric surface is derived and we show how to determine the streamlines, the water travel time function and the radionuclide concentrations. In Section 4.4, a set of (scattered) Potentiometric field data for a groundwater aquifer is used to construct the Potentiometric surface. This is done by fitting the data with a minimal total curvature spline surface.

4.3 Two-Dimensional Groundwater Flows Represented by an Analytical Expression

Many groundwater flows can be adequately simulated by the superposition of an arbitrary number of point sinks and point sources in an uniform flow. In addition, when such an analytical potential function is superimposed onto the potentiometric surface of an actual aquifer (see next Section 4.4) one can analyze the effects of injection and/or pumping wells.

4.3.1 The analytical solution for a point sink-point source flow field

Before studying the general case of an arbitrary number of point sinks and sources, let us first consider an injection well and a pumping well located at a distance 2a apart in an infinite homogeneous isotropic medium. The hydraulic head is given by the expression (PI, Section 5.4)

$$h(x,y) = \frac{Q}{4kD_0} \ln \frac{\sqrt{(x-a)^2 + y^2}}{\sqrt{(x+a)^2 + y^2}} \quad (4.3.1)$$

3

Where Q is the volumetric flow rate (m³/yr) of either the source or the sink. D₀ is the aquifer thickness (m) and ϕ_0 is the porosity of the geologic media. Here the hydraulic conductivity k (m/yr) is taken as being constant. The corresponding stream function is given by the following relationship

$$f(x, y) = \frac{Q}{gDq2tt} \arctan\left(\frac{y}{x-a}\right) - \arctan\left(\frac{y}{x+a}\right) \quad (4.3.2)$$

To obtain the water travel time function for this flow field one substitutes Eq. (4.3.1) into Eq. (2.10). One then integrates the resultant expression along a streamline (i.e. holding ψ constant) starting from a curve of constant potential on which one assumes the source to be located, up to a line of constant potential * downstream. Along the initial constant potential line $\psi = 0$. In the previous report (Chambre, PI) this integration was performed and the resultant expression is

$$\phi(x, y) = \frac{a^2 D_0 2 \pi^2}{(1-c^2)} \left(-\frac{\sinh\langle J \rangle}{c + \cosh^*} - \frac{2c}{(1-c^2)^{1/2}} \tan^{-1} \left| \left(\frac{1-c}{1+c} \right) \tanh\left(\frac{x}{2}\right) \right| \right) \quad (4.3.3)$$

where $c = \cos(\theta) = \frac{eD_0 2 \pi r}{Q}$; $\langle t \rangle = \frac{4eD_0 2 \pi t}{Q}$

$$\text{if } c = \cos(\theta) = \pm 1 \text{ and} \quad (4.3.4)$$

$$\phi(x, y) = \frac{E a^2 D_0 2 \pi^2}{Q} \left\{ -\tanh\left(\frac{x}{2}\right) \frac{1}{6} \tanh\left(\frac{x}{2}\right) \right\} \quad (4.3.5)$$

if $c = \pm 1$

Let us first define the dimensionless hydraulic head * by the following

$$* = \frac{kD_0 e 2 \pi r}{Q} \quad (4.3.5a)$$

and the dimensionless stream function by

$$Y = \frac{D_e}{Q} \frac{\partial^2 \phi}{\partial x^2} \quad (4.3.5b)$$

and finally, the dimensionless water travel time function by

$$I = \frac{Q}{a^2 D_e} \frac{\partial \phi}{\partial x} \quad (4.3.5c)$$

Eq. (4.3.5a), Eq. (4.3.5b) and Eq. (4.3.5c) are plotted in Figure 4.2. The streamlines are circular segments centered along the dimensionless ordinate axis (y/a) and the potential lines are circles with centers on the dimensionless abscissas (x/a). The lines of constant water travel time are shown by the dotted curves.

To evaluate the concentration of a given member of a radioactive chain at a given time t after the leaching started one simply substitutes Eq. (4.3.3) or Eq. (4.3.5) into the general non-recursive solution Eq. (4.2.26). Clearly, the isochronous lines will also be the iso-concentration lines. This completely analytical solution will be used as a benchmark example for comparisons with the results from the semi-analytical methods used in next Section 4.3.2 where completely analytical solutions are difficult to obtain.

A point sink-point source configuration can be used in practice to experimentally determine aquifer parameters like the hydraulic conductivity k and radionuclide migration parameters

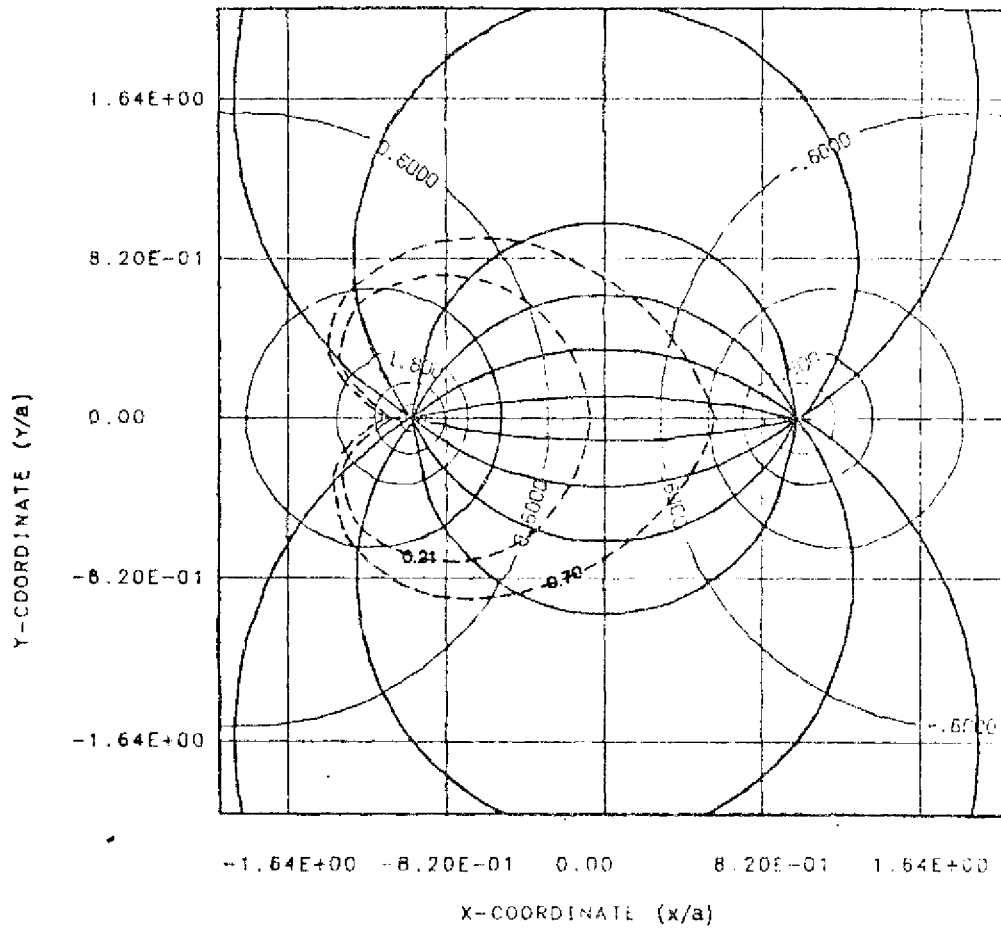


Figure 4.2 Potential lines and streamlines for the point source and point sink flow. Dotted lines indicate isochronous lines (which also are the iso-concentration lines).

like the retardation coefficient . For this illustration, let us assume that the hydrological parameters are known and one is interested in experimentally determine the retardation coefficient of a nuclide.

In order to use the solution to the two-dimensional nuclide concentration Eq. (4.2.26) one must simulate a decaying band release Eq. (4.2.24) at the injection well (the point source).

This is done by preparing an initial inventory (C_i) for each member of the chain. These nuclides are injected at a rate M^3/T

3

into the well, of volumetric flow rate Q (m³/yr), during a period of time T (yr). For a choosen medium, the transmissivity (i.e. the product kD^2 (m³/yr) is known. The retardation coefficients of the precursors are also assumed to be known. The parameters Q and T are selected to provide reasonable water travel times at the pumping well (point sink) so that the arrival time of the first nuclide is not too long. By monitoring the concentration history at the pumping well and comparing with the analytical solution one can determine the retardation coefficient for the i -th member of the chain.

For the purpose of this illustration, let us consider a geologic medium with the following parameters: $\theta^3=10$ meters and $k=5$ m/yr, the injection well flow rate is $Q=7000$ m³/yr and the duration of the release is $T=0.3$ years. Furthermore, one curie of pure Ra-226 is released at a constant rate of $1/0.3$ Ci/yr into the injected water. The injection well and the pumping well are

separated by a distance $2a=60$ meters.

The first nuclide arrives at the pumping well at a time given by

$$t_1 = \frac{a}{v} \left(1 + \frac{K_{min}}{v} \right) \quad (4.3.5d)$$

where K_{min} is the smallest retardation coefficient of all nuclides in the chain. if the nuclide has no precursors, K_{min} is its own retardation coefficient. t_1 is the smallest water travel time to the pumping well of all the contaminated streamlines.

The last nuclide arrives at the pumping well at a time given by

$$t_d = \frac{a}{v} \left(1 + \frac{K_{max}}{v} \right) \quad (4.3.5e)$$

where K_{max} is the largest retardation coefficient of all nuclides in the chain, if the nuclide has no precursors, K_{max} is its own retardation coefficient. t_d is the longest of all water travel time to the pumping well for any of the contaminated streamlines.

One can conclude that the duration of release will be given by

$$t_d - t_1 = \frac{a}{v} \left(\frac{K_{max}}{v} - \frac{K_{min}}{v} \right) + T \quad (4.3.5f)$$

Figure 4.2a and Figure 4.2b show the location of the Ra-226 contaminated region (dotted area) for two different times after the experiment started. For these figures, the assumed retardation coefficient is 10. Figure 4.2c shows the Ra-226 discharge rate history Eq. (4.4.20) at the pumping well for different values of the retardation coefficient. Figure 4.2d show the Ra-226 cumulative discharge history Eq. (4.4.21) at the pumping well for the same retardation coefficients of Figure 4.2c. By plotting the actual measured Ra-226 cumulative discharge and/or the discharge rate history on Figure 4.2c and/or Figure 4.2d one can extrapolate an experimental value for the Ra-226 retardation coefficient in that geologic media.

4.3.2 Superposition of an arbitrary number of point sinks and point sources on a uniform flow field

When Darcy's law Eq. (4.2.3) with constant hydraulic conductivity k is combined with the conservation of mass Eq. (4.2.2) there results

The linear character of the above governing equation for the groundwater potential allows one to superimpose different

RA-226 CONTAMINATED REGION-POINT SINK-SOURCE
AFTER 5.00E-01 YRS

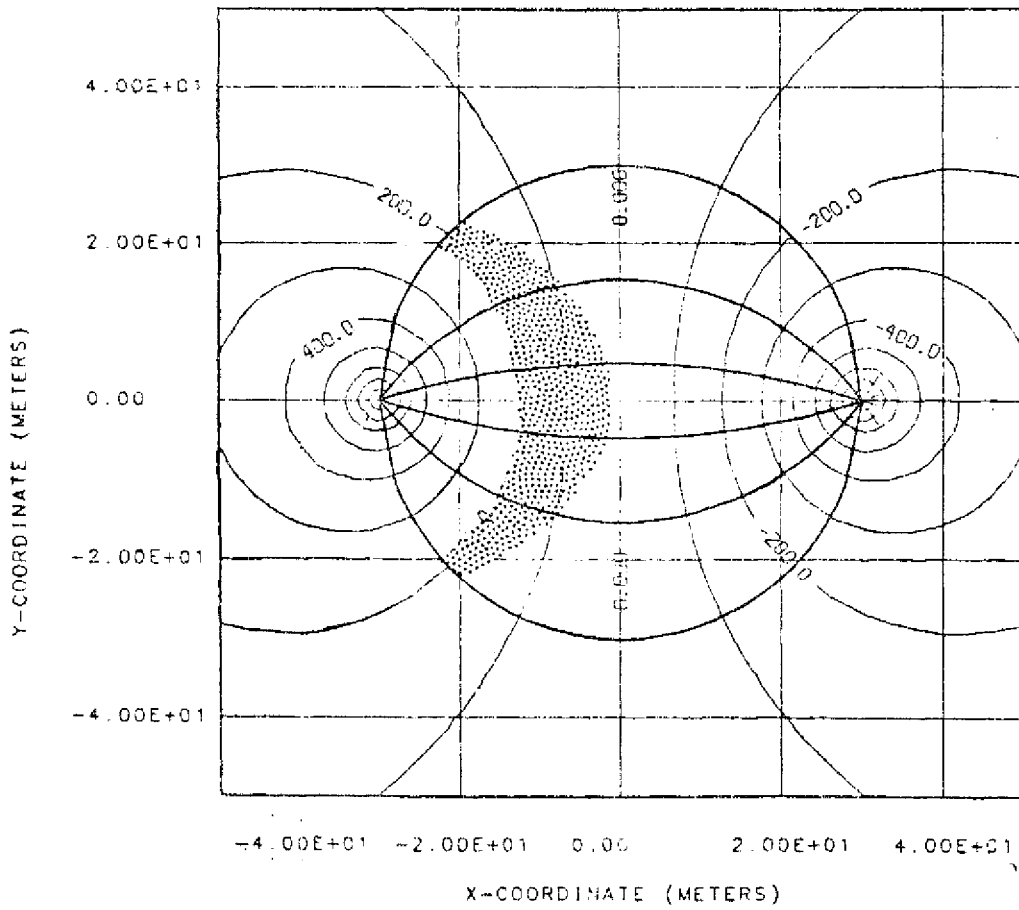


Figure 4.2a Ra-226 contaminated region after 0.5 years in the point sink and point source experiment with an injection angle of (- ν_2 to ν_2) at the injection pump. The flow rate is 7000 m ν yr. Potentials are in meters above MSL.

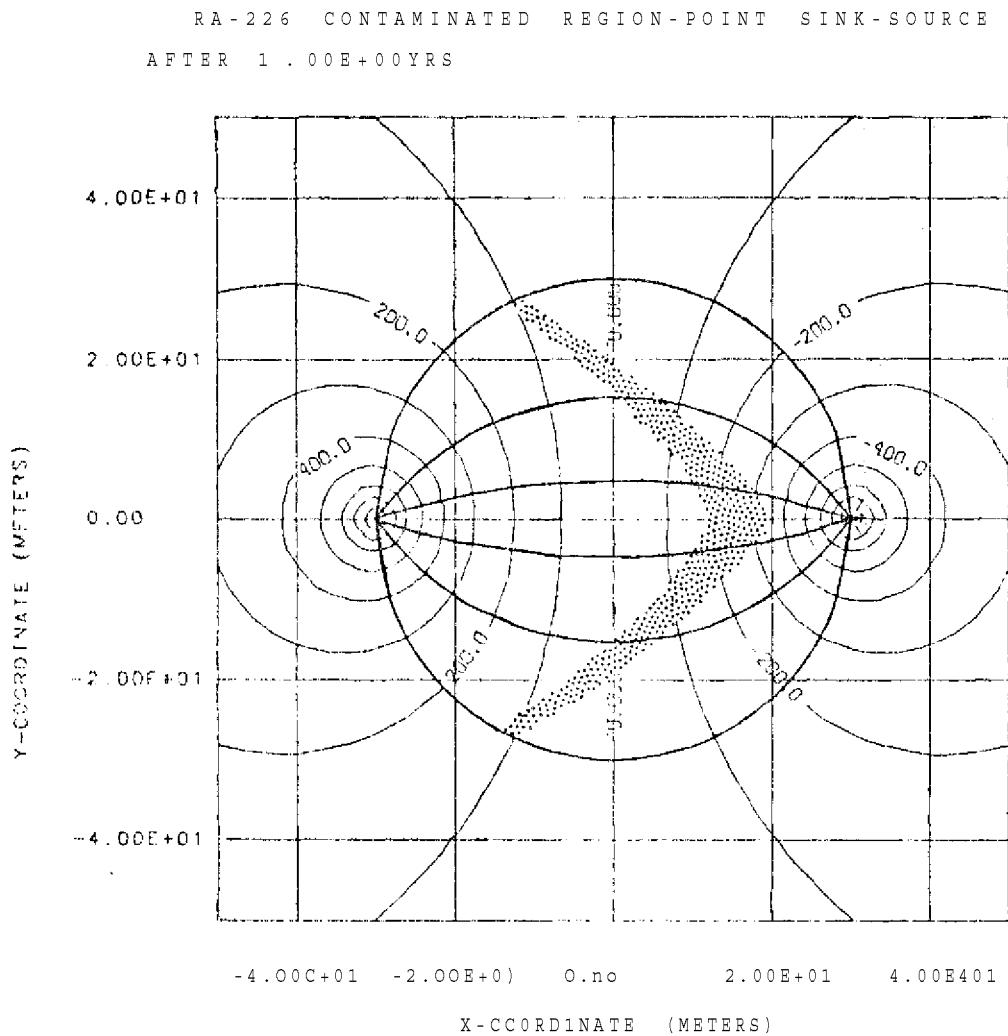
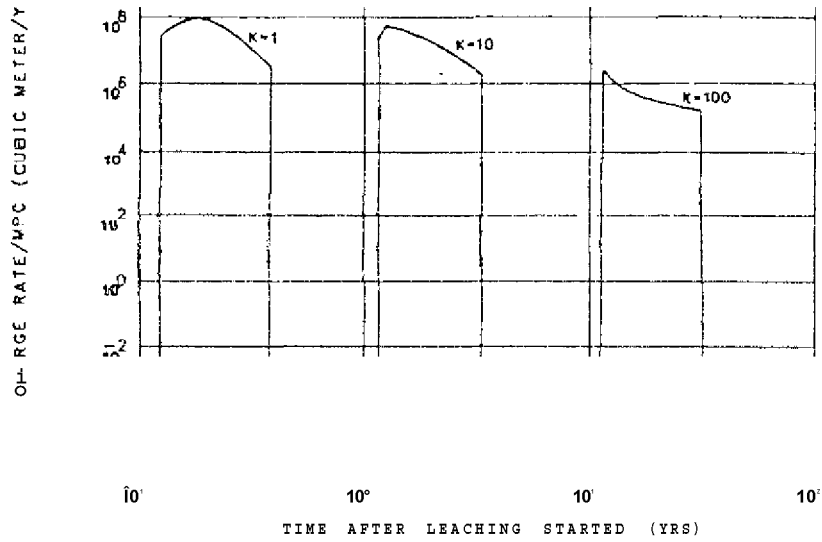


Figure 4,2b Ra-226 contaminated region after 1 year in the point sink and point source experiment with an injection angle of $(-\sqrt{2} \text{ to } T/2)$ at the injection well. The flow rate is 7000 m/yr. Potentials are in meters above MSL.

RA-226 DISCHARGE RATE HISTORY AT PUMPING WELL



RA-226 CUMULATIVE DISCHARGE HISTORY AT PUMPING WELL

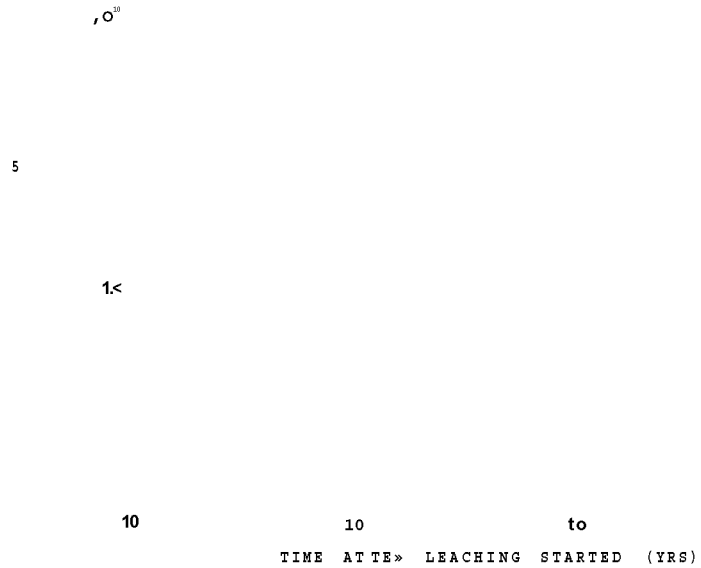


Figure 4.2c and 4.2d Ra-226 water dilution rate (discharge rate/MPC) and Ra-226 water dilution volume (cumulative discharge/MPC) at the pumping well for retardation coefficients of 1,10 and 100.

potential fields to obtain a composite configuration. A single point source or point sink located at a position (x^{\wedge}, y_{\cdot}) produces a potential field given by (L2)

$$\Phi(x, y) = \frac{-Q}{4\pi k D_0} \ln[(x-x_{\cdot})^2 + (y-y_{\cdot})^2] \quad (4.3.7)$$

3

where Q_{\cdot} is the volumetric flow rate (m³/yr) and when $Q_{\cdot} > 0$, Eq. (4.3.7) represents the hydraulic head of a point source, while when $Q_{\cdot} < 0$, it will represent the hydraulic head of a point sink. The uniform flow in the x-direction yields a hydraulic head given by

$$\Phi(x, y) = -v_{\cdot} x \quad (4.3.8)$$

Superimposing the hydraulic heads due to N distinct point sources or point sinks with an uniform flow will generate the following hydraulic head and stream functions

$$\Phi(x, y) = \frac{v_{\cdot} x}{k} - \frac{Q_{\cdot}}{4\pi k D_0} \sum_{j=1}^N \ln[(x-x_{\cdot j})^2 + (y-y_{\cdot j})^2] \quad (4.3.9)$$

$$\psi(x, y) = -v_{\cdot} y - \frac{Q_{\cdot}}{2\pi k D_0} \sum_{j=1}^N \left[\arctan\left(\frac{y-y_{\cdot j}}{x-x_{\cdot j}}\right) \right] \quad (4.3.10)$$

The velocities in the x and y directions will be respectively be given by

$$v_x = -k \frac{\partial \phi}{\partial x} = v_0 + \frac{E}{2} \sum_{j=1}^N \frac{Q_j}{eD} \frac{1}{\sqrt{(x-x_j)^2 + (y-y_j)^2}} \quad (4.3.11)$$

$$v_y = -k \frac{\partial \phi}{\partial y} = \frac{E}{2} \sum_{j=1}^N \frac{Q_j}{eD} \frac{y-y_j}{\sqrt{(x-x_j)^2 + (y-y_j)^2}} \quad (4.3.12)$$

Although in the last section it was possible to analytically obtain the water travel time function for the case of a single point sink and a single point source, the integration of Eq. (4.2.10), when Eq. (4.3.9) is used instead, becomes difficult to be performed analytically. We will resort to the use of the method of characteristics in conjunction with a Runge-Kutta numerical integration scheme to obtain the water travel time function. First recall the parallelism condition between the potential lines and the isochronous lines, Eq. (4.2.12)

$$\left(k \frac{\partial \phi}{\partial x} \right) \frac{\partial \phi}{\partial x} + \left(k \frac{\partial \phi}{\partial y} \right) \frac{\partial \phi}{\partial y} = -1 ; \quad d^2 \phi = 0 \quad (4.3.13)$$

which is a first order partial differential equation (hyperbolic equation) for the variable ϕ , since the partial derivatives of the hydraulic head multiplied by the constant hydraulic conductivity k are known (Eq. (4.3.11.) and (4.3.12)). The method of characteristics consists in determining a direction at each point of the (x,y) plane along which the integration of Eq. (4.3.13) transforms to an integration problem of an ordinary differential equation (ODE).

Consider first the definition of total derivative of the water travel time function

$$d_o = \frac{1}{3x} dx + \frac{1}{8y} dy \quad (4.3.13a)$$

Eliminating the partial derivative of d_o with respect to x from Eq. (4.3.13) and (4.3.13a) results

$$(v \frac{d_o}{dx} + \frac{1}{3x}) + (v \frac{d_o}{dy} - \frac{1}{8y}) \frac{8c}{3y} = 0 \quad (4.3.13b)$$

This equation is independent of z because c and v are functions of x, y only and do not depend on z , z . The

equation can also be made independent of z by choosing points on a curve C in such a way that the following relationship is satisfied

$$v \frac{d_o}{dy} - \frac{1}{8y} = 0 \quad (4.3.13c)$$

With this choice Eq. (4.3.13b) yields

$$v \frac{d_o}{dx} + \frac{1}{3x} = 0 \quad (4.3.13d)$$

Eq. (4.3.13c) is a differential equation for the curve C which is called the characteristic equation of the partial differential equation Eq. (4.3.13) and Eq. (4.3.13d) is an ordinary differential equation for the solution a along the curve C . The solution of the partial differential equation for o , Eq. (4.3.13)

can thus be obtained by the simultaneous solution of two ordinary differential equations. These equations can be restated as follows

$$\frac{dx}{v_x} = \frac{dy}{v_y} = \frac{dt}{-1} \quad (4.3.14)$$

The simultaneous integration of Eq. (4.3.13c) and Eq. (4.3.13d) starting from a point (x^*, y^*) on the initial source line S up to a point (x, y) downstream will yield the value of the water travel time at that point (x, y) . The partial derivatives of the potential function being given by Eq. (4.3.11) and Eq. (4.3.12), the above integration can be carried out by using the Runge-Kutta integration method.

Let us first demonstrate that the characteristics of the above differential equation Eq. (4.3.13) coincide with the streamlines of the flow. Along a streamline where $d\psi = 0$, and by using the definition of total derivatives one has

$$d\psi = \frac{\partial \psi}{\partial x} dx + \frac{\partial \psi}{\partial y} dy = 0 \quad (4.3.16)$$

By using the relationships Eq. (4.2.8) and Eq. (4.2.9) which define the streamlines one has

$$\frac{\partial \psi}{\partial x} dx + \frac{\partial \psi}{\partial y} dy = 0 \quad (4.3.17)$$

which yields

$$\frac{dx}{v_x} = \frac{dy}{v_y} \quad (4.3.17a)$$

Therefore, Eq. (4.3.17) defines a streamline and it has the same form as the characteristic equation for the water travel time function Eq. (4.3.13c). This result will be of practical importance for us since both the water travel time function and the radionuclide concentration being evaluated along the same curves facilitates the calculations.

One chooses along the source line S a given point (x^0, y^0) where $0 < x^0 / Y_g < 1$. After defining a new abscissa $x = x^0 + nAx$ one integrates Eq. (4.3.14) from x^0 to x to obtain the new ordinate y_n corresponding to the position (x_n, y_n) along the streamline which passes through (x^0, y^0) . Simultaneous integration of Eq. (4.3.15) will yield the value of $c(x_n, y_n)$. Substitution of this $c(x_n, y_n)$ into the solution for the radionuclide concentration Eq. (4.2.26) will yield $N_i(x_n, y_n, t)$ on that streamline. This can be repeated for any arbitrary number of points (y_n, Y_n) on that same streamline by choosing adequate values for Ax and n . Once that streamline has been analyzed one can start from another point (x^0, y^0) on the source line S and repeat this procedure for this new streamline. By starting from enough points along the source line one can cover the entire "shadow region".

To assess the accuracy of this method we use it to solve

the pair point source and point sink problem and we compared the solution to the exact solution presented in the last section Eq. (4.3.3). The difference between the exact solution for the water travel time and the approximate solution is expressed in terms of percent error defined as

$$e(\%) = \frac{\text{exact} - \text{approximate}}{\text{exact}} \quad (4.3.18)$$

Table 4.1a show the result of the calculations for the different streamlines shown in Figure 4.2, characterized by the angle of the initial point on the source line. Since the system is symmetric with respect to the x axis, only the results for half of the streamlines are reported. The first column is the dimensionless x coordinate (x/a) and the second column **is** the corresponding dimensionless y coordinate (y/a) for that streamline. The third column is the dimensionless hydraulic head as defined in Eq. (4.3.5a), the fourth column is the dimensionless streamfunction Eq. (4.3.5b) and as one expected it is constant along this streamline. The fifth and sixth column are the exact and approximate values of the dimensionless water travel time function as defined by Eq.(4.3.5c), respectively. Finally, the last column is the percent error Eq.(4.3.18) and one can see that the agreement is quite complete.

Streamlines coordinates for the point sink and point source flow with the corresponding values of the dimensionless potentials, streamfunctions, water travel times and the error percentage of the semi analytical water travel time calculations.

CHARACTERIS X-CCORDIN	IC NO. 1 RI Y-CUCRD IN	SITORY AN3L POTENTIAL	=-9. CCE+ 01 STREAMFUN.	EXACT TIME	APRQX TIME	ERROR PERCNT
-9.000E-01	-4.401E-01	1.463E+00	-1.575E+00	1.019E-01	1.019E-01	7.596E-05
-8.000E-01	-6.042E-31	1.393E+03	-1.575E+03	2.027E-01	2.327E-31	7.442E-05
-7.000E-01	~ -7.134E-01	8.632E-01	"-1.575E+00"	"3.033E-01"	3.033E-01	5.096E-05
-6.000E-01	-8.042E-01	6.900E-01	-1.575E+00	4.039E-01	4.039E-01	3.842E-05
-5.000E-01	-8.702E-01	5.469E-01	-1.575E+03	5.344E-01	5.044E-01	3.080E-05
-4.000E-01	-9.207E-01	4.218E-01	-1.575E+00	6.049E-01	6.049E-01	2.569E-05
-3.000E-01	-9.582E-01	3.822E-01	-1.575E+03	7.053E-01	7.053E-01	2.204E-05
-2.000E-01	-9.943E-01	2.019E-01	-1.575E+30	8.058E-01	8.053E-01	1.929E-05
-9.999E-01	-9.992E-01	9.990E-02	-1.575E+00	9.062E-01	9.062E-01	1.716E-05
7.963E-06	-1.000E+00	-7.930E-06	-1.575E+00	1.307E+30	1.000E+00	1.545E-05
1.000E-01	-9.992E-01	-9.992E-02	-1.575E+00	1.107E+00	1.000E+00	1.405E-05
2.000E-01	-9.042E-01	-2.019E-01	-1.575E+30	1.207E+00	1.207E+00	1.290E-05
3.000E-01	-9.582E-01	-3.082E-01	-1.575E+03	1.308E+00	1.308E+00	1.192E-05
CGOE-01	-9.207E-01	-4.218E-01	-1.575E+00	1.408E+00	1.408E+00	1.110E-05
5.000E-01	-8.702E-01	-5.469E-01	-1.575E+00	1.509E+00	1.509E+00	1.044E-05
b.000E-01	-8.042E-01	-6.900E-01	-1.575E+03	1.609E+00	1.539E+00	1.032E-05
7.000E-01	-7.134E-01	-6.632E-01	-1.575E+00	1.710E+00	1.710E+00	1.032E-05
8.000E-01	-6.042E-01	-1.093E+00	-1.575E+00	1.811E+00	1.811E+00	1.565E-05
9.000E-01	-4.401E-01	-1.464E+00	-1.575E+00	1.911E+03	1.911E+03	1.441E-04
1.000E+00	-5.019E-01	-5.878E+00	4.708E+00	2.013E+00	2.013E+00	9.102E-04

4.4 Aquifers Potentiometric Surfaces Represented by- Interpolation of Field-Measured Piezometric Data

4.4.1 Introduction

Hydrogeological studies of a proposed site for a high level waste repository usually provide an approximate description of the aquifer geometry with geologic maps and some distributed piezometric head observations collected during field tests accumulated over the past. In addition, limited data on hydraulic conductivities are also supplied.

The most common utilization of these data in the determination of the potentiometric surface of the aquifer as well as its parameters is the so called "model calibration" (L3,N3). This is done by solving the groundwater mass conservation equation Eq.(4.4.1) subject to suitable boundary conditions and some initial guesses for the aquifer parameters. The resultant solution $\phi(x,y)$ is then compared to the field data. By using assumed weighting functions new guesses for the aquifer parameters are obtained. This procedure is repeated until a satisfactory agreement is obtained between the calculated and measured potential function. The governing equation in the absence of sources and sinks is

$$-\left\{ \frac{\partial^2 \phi}{\partial x^2} \right\} + -\left\{ \frac{\partial^2 \phi}{\partial y^2} \right\} = 0 \quad (4.4.1)$$

The above method presents some disadvantage since uniqueness cannot be guaranteed because infinite number of combinations of hydraulic head and hydraulic conductivity can be solutions to Eq.(4.4.1) and local parameters values can be calculated by traditional methods only under the assumption of homogeneity {e.g. pumping tests based on the Theis equation (Fl)}. These measured parameters will only represent local behavior of the aquifer failing to represent the inhomogeneous character of the aquifer on a regional scale (S3).

4.4.2 Determination of the potentiometric surface

In our present study we use the measured piezometric data to fit a potential function. Once the potential function is determined one can solve Eq. (4.4.1) for the hydraulic conductivity k . This problem is known as the "inverse problem" (Fl).

The problem of interpolating a smooth two dimensional function to a finite number of data points was treated by Briggs (Bl). He optimizes a third order spline fit in two dimensions by minimizing the total curvature (also called the Gauss curvature) of the function. It is shown (Bl) that this condition requires the desired function to satisfy the following biharmonic equation

$$\nabla^4 \phi = \frac{q}{k} \quad (4.4.2)$$

Here ϕ are given piezometric data points at the discrete points $(x_n, y_n), n=1,2,\dots,M$. Eq. (4.4.2) is the equation which describes the displacement of a thin elastic sheet in two dimensions under the influence of point forces. The desired function must satisfy constraining values ϕ_n within the region of interest. Numerical solution to Eq. (4.4.2) when written as a set of algebraic equation by expressing the derivatives with finite differences yields the desired function $\phi(x,y)$. This method has been programmed into the Surface Gridding Library (SGL) and implemented at the LBL computer center (S2).

Therefore, by specifying a given number of values for the potential function at different points inside the region of interest one can construct the potentiometric surface by using the SGL computer program. Once the potential function is known, the next step is to solve the inverse problem, i.e. to determine the hydraulic conductivity k .

t

4.4.3 Solution to the inverse problem

Different solutions have been proposed to the inverse problem. Among those, Emsellem and Marsily (E1) propose a modified form of the Cauchy's problem, Frind and Pinder (F2) propose a Galerkin's scheme solution, Nelson (N2) makes use of the energy dissipation method while Sagar (S3) solves algebraically the finite difference form of the Eq. (4.4.1).

These solutions require either complex numerical schemes or assumptions which might bias the original data.

In this present, work the method of characteristics is used to solve the Cauchy's problem. Consider Eq. (4.4.1) where $\phi(x,y)$ is known. Eq.4.4.1 can be rewritten as a first order differential equation (hyperbolic equation) in the unknown variable $k(x,y)$

$$m(x,y) \frac{\partial k}{\partial x} + n(x,y) \frac{\partial k}{\partial y} = -k \quad (4.4.4)$$

where $m(x,y)$ and $n(x,y)$ are known functions given by the following

$$m(x,y) = \frac{3\phi/3x}{V_{cf}}; \quad n(x,y) = \frac{94/3y}{V_{cf}} \quad (4.4.5)$$

It can be shown (CI) that integration of Eq. (4.4.4) in the region of interest R is possible when boundary conditions for $k(x,y)$ are prescribed along a line S cutting every streamline of the flow in the region R i.e. when a value of k is known on every streamline of the region R . Since the potential function $\phi(x,y)$ has already been evaluated by SCI,, the streamline which are independent of the values of k (see Eq.(4.3.17a)) can be determined by using the method of characteristics as described in Section 4.3,2. So defined the problem of finding the hydraulic conductivity can be solved by the method of characteristics and possess an unique solution (CI). Since the governing equation

for the hydraulic conductivity has the same form (hyperbolic equation) as the governing equation for the water travel time function Eq. (4.3.13), the derivation of the characteristic equation Eq.(4.3.13a) through Eq.(4.3.14) for the water travel time is applicable for the hydraulic conductivity provided one changes v_x by $m(x,y)$ and v_y by $n(x,y)$. Therefore, from Eq. (4.3.14) one can obtain the characteristic equations of Eq. (4.4.4)

$$\frac{dx}{m(x,y)} = \frac{dy}{n(x,y)} = \frac{dk}{-k} \tag{4.4.6}$$

Rewriting separately the differential equations

$$\frac{dy}{dx} = \frac{n(x,y)}{m(x,y)} \tag{4.4.7}$$

$$\frac{dk}{dx} = \frac{-kV\langle f \rangle}{3\langle \rangle/3x} \tag{4.4.8}$$

Comparing Eq. (4.4.7) with Eq. (4.3.17a) one concludes that the characteristic curves of Eq. (4.4.4) are indeed the streamlines of the flow. The region R of interest is the "shadow region" of the repository. The "shadow region" is formed by the streamlines which pass through the source line represented by a curve S. In order to integrate Eq. (4.4.8) one needs therefore to specify values for the hydraulic conductivity k along the source line S.

To evaluate the water travel time function let us first recall Eq. (4.3.13)

$$v \frac{\partial \phi}{\partial x} + v \frac{\partial \phi}{\partial y} = -1 \quad ; \quad \text{dip} = 0 \quad (4.4.9)$$

The characteristic equations are rewritten from Eq. (4.3.13c) and Eq. (4.3.13d)

$$\frac{dy}{dx} = \frac{v}{v} \quad (4.4.10)$$

$$\frac{d\phi}{dx} = -1 \quad (4.4.11)$$

$$\frac{d\phi}{dx} = \frac{v}{x}$$

Utilization of this method presents an additional practical advantage since the solution to the transport equation Eq. (4.2.27) applies along a streamline of the flow and one must integrate Eq. (4.4.7) anyway. At the same time integration to obtain the water travel time and the hydraulic conductivity can also be carried out. Eq. (4.4.7), Eq. (4.4.8) and Eq. (4.4.11) are to be integrated simultaneously in this order.

One starts from a point (x_0, y_0) on the repository curve S where the initial value for the hydraulic conductivity $k(x_0, y_0)$ is assumed to be known and the water travel time is $t(x_0, y_0) = 0$. Defining a new abscissa $x = x_0 + n\Delta x, n=1, 2, \dots, N$ and Δx is arbitrarily chosen one integrates first Eq. (4.4.7) to obtain y corresponding to the abscissa x on the same streamline.

Simultaneous integration of Eq. (4.4.8) and Eq. (4.4.11) will yield

$$k(x_n, y_n) \text{ and } \phi(x_n, y_n) "$$

After repeating this integration for all abscissas $x_n, n=1, 2, \dots, N$ one will have defined that particular streamline of the shadow region. At the same time the values of the water travel time and hydraulic conductivity have also been determined at the same points along this streamline. Substitution of (x, y) into Eq. (4.2.27) will yield the value of the radionuclide concentration along this streamline.

By choosing different points (x_n, y_n) on the source line S and repeating the above described calculation one can cover the entire "shadow region". This method calculates therefore the two-dimensional distribution of the i -th member of a radionuclide chain of arbitrary length in a stationary two-dimensional groundwater flow through an inhomogeneous isotropic geologic medium.

The integrations are carried out numerically using a Runge-Kutta scheme. The partial derivatives of the potential function are expressed in finite central difference form

$$\frac{\partial^3 \phi}{\partial x^3} = \frac{\phi_{n+1} - \phi_{n-1}}{2\Delta x^3} \quad (4.4.12)$$

$$\frac{\partial^3 \phi}{\partial y^3} = \frac{\phi_{j+1} - \phi_{j-1}}{2\Delta y^3} \quad (4.4.13)$$

And the Laplacian operator is approximated by

$$\frac{(\phi_{n+1,j} - 2\phi_{n,j} + \phi_{n,j+1})}{\Delta x^2} + \frac{(\phi_{n,j+1} - 2\phi_{n,j} + \phi_{n,j-1})}{\Delta y^2} = H12_{-}(1.4.14)$$

One must keep in mind that this method assumes the measured piezometric data in the region of interest as well as the measured hydraulic conductivity along the repository curve as being reliable. By using this data this method provides a way of modelling actual groundwater flows through aquifers.

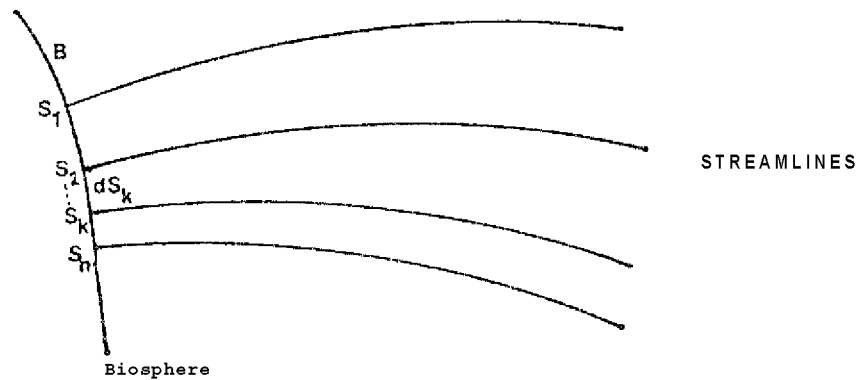
If hydraulic conductivity data are provided in the shadow region one can compare them with the calculated value. Assuming that these data are reliable, in case of disagreement between the calculated data and the field data one can justify these differences by considering them as the result of localized sinks or sources which were not considered in the governing equation Eq. (4.4.4).

4.4.4 Evaluation of radionuclide discharge rates into the biosphere and cumulative discharge in the biosphere

Having determined $N_i(x,y,t)$ provided us with a quantitative picture of the migration of that particular nuclide through the geologic media after being released from the repository. However, one measure of the potential hazard to the general public can be obtained by evaluating the cumulative amount of

curies of individual nuclides actually discharged into a potential source of fresh water, taking into account decay after discharge.

Let us denote by $q^{\wedge}(t)$ the discharge rate (Ci/yr) of the i -th member of a radionuclide chain into the biosphere at a time t after the chain was released from the source line. Consider the intersection of the "shadow region" streamlines with the biosphere which is represented by a curve B . This curve is subdivided into n subcurves of arc with length ds^{\wedge} as shown in the following sketch



Let the water velocity at a point s_k be $v(s_k)$, (m/yr), the aquifer thickness be $h(s_k)$, (m) and the nuclide concentration $N_i(s_k, t)$. The discharge rate through an element ds_k is given by

$$dq_i = v(s_k)h(s_k)N_i(s_k, t)ds_k \quad (4.4.15)$$

To obtain the discharge rate for all the contaminated streamlines that reach the biosphere one integrates Eq (4.4.15) along the entire curve B

$$q_i(t) = \int_{s_1} v(s_k) h(s_k) N \cdot \{ o(s_k, t) ds \} \quad (4.4.16)$$

The concentration $N \cdot (o(s), t)$ is readily evaluated by using Eq. (4.2.26). The water velocity is obtained by the following expression

$$v(s_k) = [v_x + v_M] \frac{h}{h} \quad (4.4.17)$$

However, the aquifer thickness at the biosphere $h(s^{\wedge})$ is generally not known. To avoid this problem we make use of the fact that the volumetric flow rate between two streamlines is constant throughout the field. Since the product $v(s) h(s) ds$ is the volumetric flow rate between the streamlines passing through two points along the curve B, this is equal to the volumetric flow rate at the source line between corresponding streamlines. Aquifer thickness at the repository is generally better known than in the far field because more extensive geological studies are carried near the repository site than in the far field. This allows one to evaluate the volumetric flow rate between those streamlines.

The integral in Eq.(4.4.16) is readily evaluated by a proper numerical scheme (Romberg method,D3) once the integrand is determined for a number of points along the curve B.

The cumulative discharge of a i -th member of a radionuclide

chain. $Q_i(t) \cdot (Ci)$ is obtained by integrating the discharge rate $q^{\wedge}(t)$ from the first nuclide arrival time up to a time t afterwards. The integral is multiplied by the Bateman function to account for the decay of the members of the chain after they are discharged. The radionuclides are assumed to remain stationary in a reservoir after their discharge.

$$Q_i(t) = \int_{t_a}^t \frac{q_j(t-x)}{\lambda_j} \prod_{j=1}^i B_j \cdot \exp(-\lambda_j(t-x)) dx \quad (4.4.18)$$

The first nuclide arrival time t_a (yr) is an important quantity in assessing the potential hazard of a particular radionuclide. It can be evaluated by the following formula

$$t_a = \frac{c}{\min_m K_m} \quad (4.4.19)$$

Here, $\frac{c}{\min_m}$ (yr) is the smallest value of the water travel time on the biosphere curve and K_{\min} is the smallest retardation coefficient of all the precursors in the chain. If the chain has only one member, K^{\wedge} will be its own retardation coefficient.

In order to be able to compare the potential hazard due to the discharge of different radionuclides into the biosphere one can use the water dilution rate $w_i(t)$, (m^3/yr) as defined in (Pi, Section 2.7). The water dilution rate is obtained by dividing the discharge rate by the Maximum Permissible Concentration, MPC given in (Ci/m^3) by 10CFR20. Thus

$$W_i(t) = q_i(t)/MPC_i \quad (4.4.20)$$

This ratio is the necessary water flow rate in the biosphere so that it will dilute the discharge rate of that nuclide to drinking water standards. This calculation provides an additional advantage since one can add these required flow rates for every nuclide to obtain an overall hazard index for all nuclides present in the repository.

Similarly, if one divides the cumulative discharge $Q_i(t)$ by the MPC of that i -th member one obtains the total amount of water that is needed at the biosphere to dilute the cumulative amount of that nuclide to drinking water standards. This quantity is called water dilution volume (PI, Section 2.7) and is expressed as follows

$$W_i(t) = Q_i(t)/MPC_i \quad (4.4.21)$$

Finally, the total water dilution rate is the sum of all water dilution rates of individual nuclides

$$w(t) = \sum_{i=1}^M w_i(t) \quad (4.4.22)$$

In the same way, the total water dilution volume is given

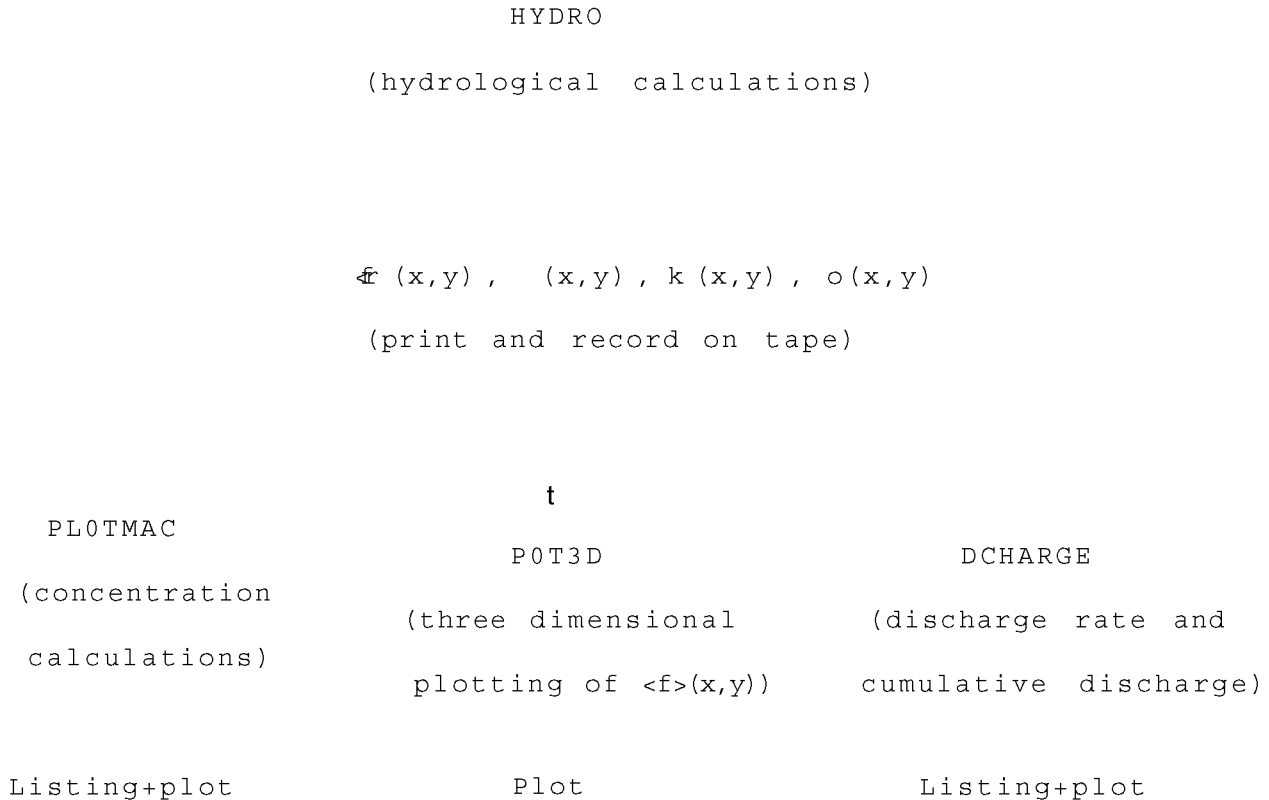
by

$$w(t) = \sum_{i=1}^M I_i^*(t) \quad (4.4.23)$$

where M is the total number of nuclides having been discharged into the biosphere at that time t .

4.5 Description of the Computer Code UCBNE21

A computer program labeled UCBNE21 has been developed to perform the calculations described in the previous sections. To give added flexibility the program was subdivided into four subprograms which can be run individually. This is a convenient feature since the concentrations and discharge rate calculations are independent from the hydrological calculations. Once the hydrological calculations for a particular aquifer is done there is no need to repeat it for every nuclide concentration calculation. A complete source listing of the programs is given in Appendix C. The following diagram shows the interrelationship between the four subprograms



The subprogram HYDRO evaluates the potential function on every grid point inside the region of interest. Then it determines a number of streamlines in the "shadow region" of the repository by specifying a number of coordinates for each streamline. On each of these coordinates, the hydraulic conductivity and the water travel time are calculated. Finally it prints out a listing of the coordinates of each streamline with the corresponding values of potential function, hydraulic conductivity and water travel time. These results are saved into tape for posterior use. Description of the data input requirements is given in Appendix C. The structure of the program HYDRO is shown in Figure 4.4. One should notice the possibility of merging the potentials resulting from the analytical representation with those from fitting field data.

The subprogram PLOTMAC reads in data on the radionuclide chain such as decay constants, retardation coefficient, activities at the time of burial, and maximum permissible concentration for each member of the chain. In addition one must specify the migration parameters such as the delay time for the beginning of leaching, the leach time and the time after the leaching started when the calculations are to be performed. Complete description of data input is given in Appendix C. PLOTMAC reads in the shadow region streamlines coordinates and the corresponding water travel times from the tape file produced by HYDRO. By evaluating Eq. (4.2.27) it determines the concentration of each member of the chain on each coordinate of

Figure 4.4 Structure of the program HYDRO

Define region of interest, repository
location, Cauchy data on hydraulic
conductivity and grid sizes.

Define the number of point Read in measured
sinks and point sources, piezometric data
their location, their strength
and if needed a uniform flow field

Evaluate analytical potential Evaluate measured potential
function Eq. (4.2.26) on every function using the Surface
grid point. Oridding Library

I

Superimpose the analytical potential
with the measured potential, if desired.

Evaluate V_x , V_y and V^2
using Eq. (4.4.12), Eq. (4.4.13) and Eq. (4.4.14)

Numerical integration of
Eq. (4.4.7), Eq. (4.4.8) and Eq. (4.4.11)

Print and store on tape
 $\langle Mx, y \rangle$, $\phi(x, y)$, $k(x, y)$, $c(x, y)$

each streamline in the shadow region. A printed output is produced and it also uses the graphic software available at the LBL computer center to produce plots. Each nuclide contaminated region is shown in a plot with the contour map of the potential function, the streamlines of the shadow region, the contaminated region and the biosphere curve B as described in Section 4.4.4 (see for example Figure 4.15).

The program POT3D reads the potential function calculated by HYDRO from the tape file and using the graphical software produces a three dimensional view of the potentiometric surface in the aquifer being studied.(see for example Figure 4.11).

The program DCHARGE evaluates the discharge rate and the cumulative discharge at the biosphere. The calculation is performed for the entire time span of interest (i.e. from the first nuclide arrival time until the last nuclide departure time). Both printed output as well as plots for the discharge rate (expressed as water dilution rate) and cumulative discharge (expressed as water dilution volume) are produced (see for example Figure 4.21). The structure of the subprogram DCHARGE is given in Figure C.1 in Appendix C.

4.6 Modelling of the Far Field Radionuclide Migration at the Reference Site of the Waste Isolation Pilot Plant (WIPP) in Eddy County, New Mexico

4.6.1 Review and interpretation of existent hydrological data

Hydrological data used in this work were obtained primarily from the Department of Energy report: Waste Isolation Pilot Plant (D1) which summarizes the data reviewed by several authors. Among these are Mercer and Orr (M1), Register (R1) and others. In this report we present a brief summary of the available information and the reader should refer to above references for more detailed descriptions of the hydrology in the region of the WIPP site.

A map of the modelled region is shown in Figure 4.5. A geologic cross section of the site area looking northwest is presented in Figure 4.6. As it is described in (D1): "The Santa Rosa Sandstone is a moderately permeable formation containing relatively fresh water. However, the low permeability of the Dewey Lake Red Beds prevents significant seepage of water from the Santa Rosa Sandstone to the Rustler Formation below. Two thin aquifers, the Magenta and the Culebra are contained in the Rustler Formation, which is predominantly composed of impervious anhydrite, polyhalites and gypsum. The WIPP reference repository

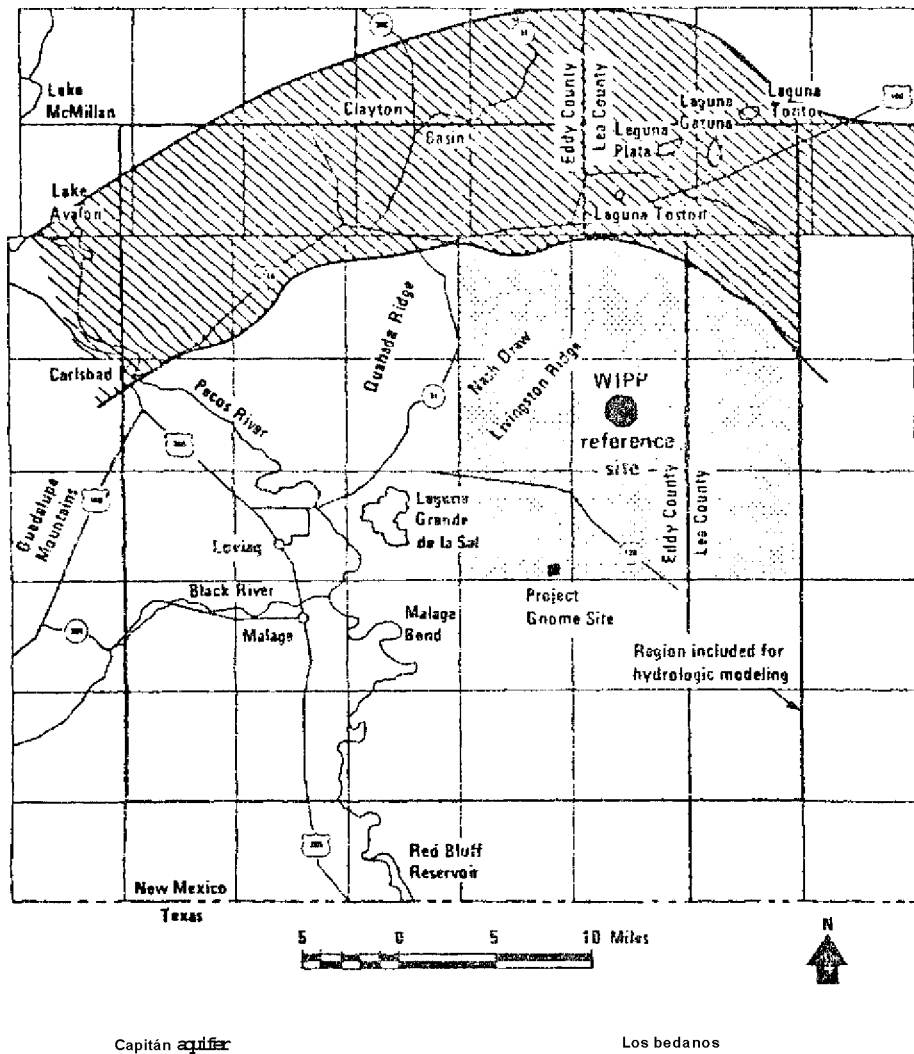


Figure 4.5 Hydrologic modelling region for the WIPP site (D1)

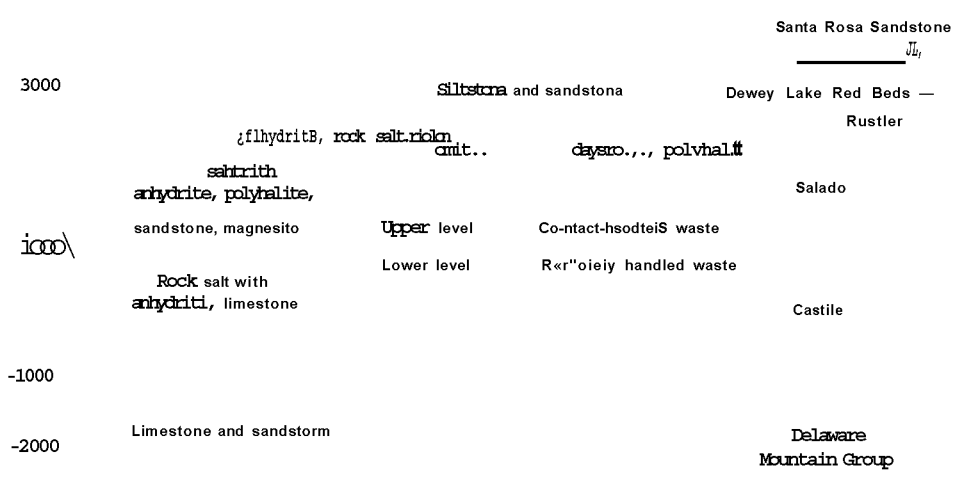


Figure 4.6 Geologic cross section of the WIPP site area (D1)

will be in the Salado Formation. The Castile Formation, composed of very pure halite and anhydrite, contains no water-bearing strata. Beneath it lies the Delaware Mountain Group, approximately 3000 ft thick which contains aquifers",

In addition, there is a brine aquifer which contains substantial quantity of water and it is found in the subsurface above the Salado formation in the region of the W1PP site. Register (R1) gives the following description: "The brine aquifer which occurs along the top of the Salado and the base of the Rustler and underlies Nash Draw extends to the Pecos River in the vicinity of Malaga Bend. The aquifer is apparently replenished from precipitation and brine discharge that penetrates the overlying units through fractures and solution zones, then moves southward along the top of the salt and increases in salt concentration until it discharges into the Pecos River at Malaga Bend. The calculated discharge from the brine aquifer is about 200 gal/min".

There are two potential pathways for the radionuclides to reach the biosphere after they are released from the repository. The aquifers contained in the Rustler formation overlying the Salado formation flow southwestward and discharge into Pecos River in the vicinity of Malaga Bend. On the other hand, underlying the repository site we have the Delaware Mountain Group aquifers which, contrary to Rustler aquifers, flow northward, discharging into the Capitan aquifer which is a source of fresh-water.

Two sets of hydraulic potentials representing the Rustler aquifer are given in (D1). In Figure 4.7 a contour map of the measured hydraulic potential for the Rustler aquifer is shown while in Figure 4.8 the calculated hydraulic potential (using model calibration) is shown. Calculations will be done using both set of hydraulic potentials and comparisons will be drawn.

In the same way, two sets of hydraulic potentials for the underlying Delaware Mountain Group aquifers are presented (D1). Figure 4.9 is the mapping of the raw data while Figure 4.10 is the calculated set of hydraulic potential. Data on measured aquifer parameters in the region are not extensively available and the reported values are distributed over a large range of values making the choice of a representative value difficult (C5,D1). However, hydraulic conductivity at the repository site can be estimated (R1). A summary of the hydrological data at the site used in this work is given in Table 4.1

Table 4.1 Summary of hydrological data at the repository site (D1,R1)

	Rustler aquifer	Delaware aquifer
Thickness (m)	65	900
Hydraulic conductivity (m/yr)	A range from 0.1 to 1400;used value=11.	0.3
Porosity	0.10	0.16

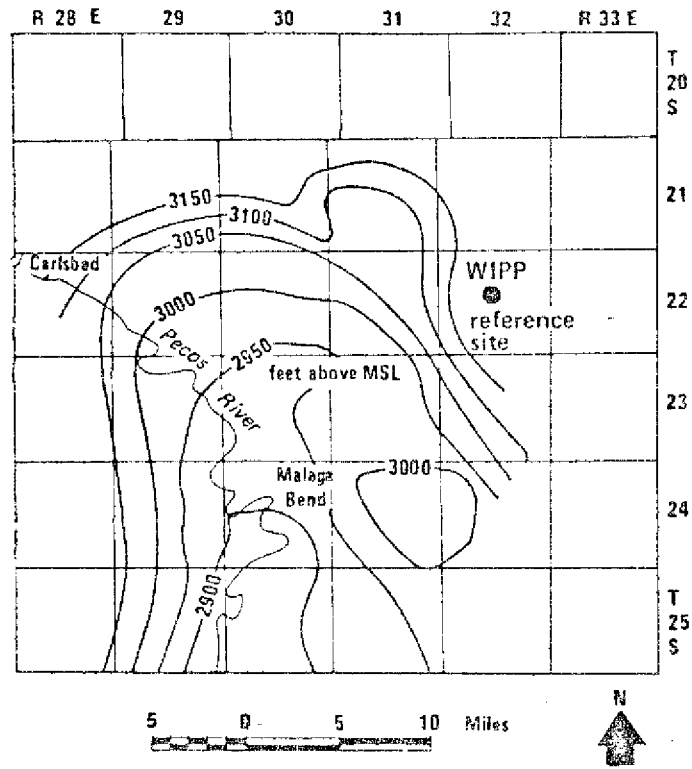


Figure 4.7 Measured hydraulic potential data for the Rustler aquifer (feet above MSL), from (D1)

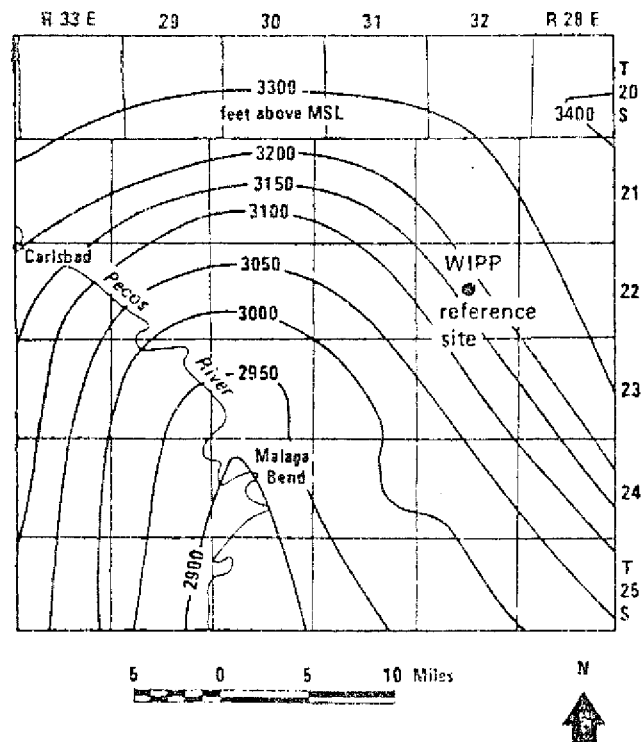


Figure 4.8 Calculated hydraulic potential data for the Rustler aquifer (feet above MSL), from (D1)

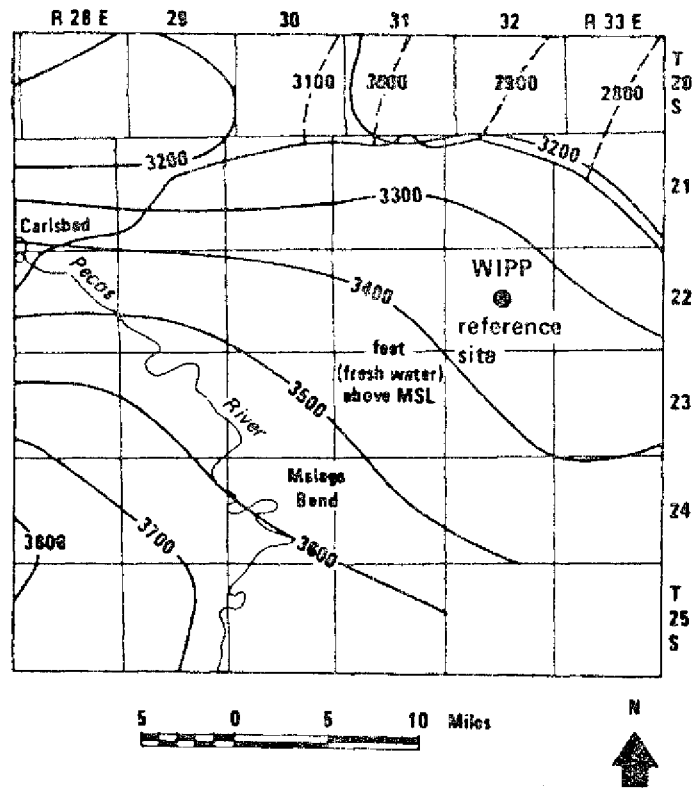


Figure 4.9 Measured hydraulic potential data for the Delaware aquifer (feet above MSL), from D1

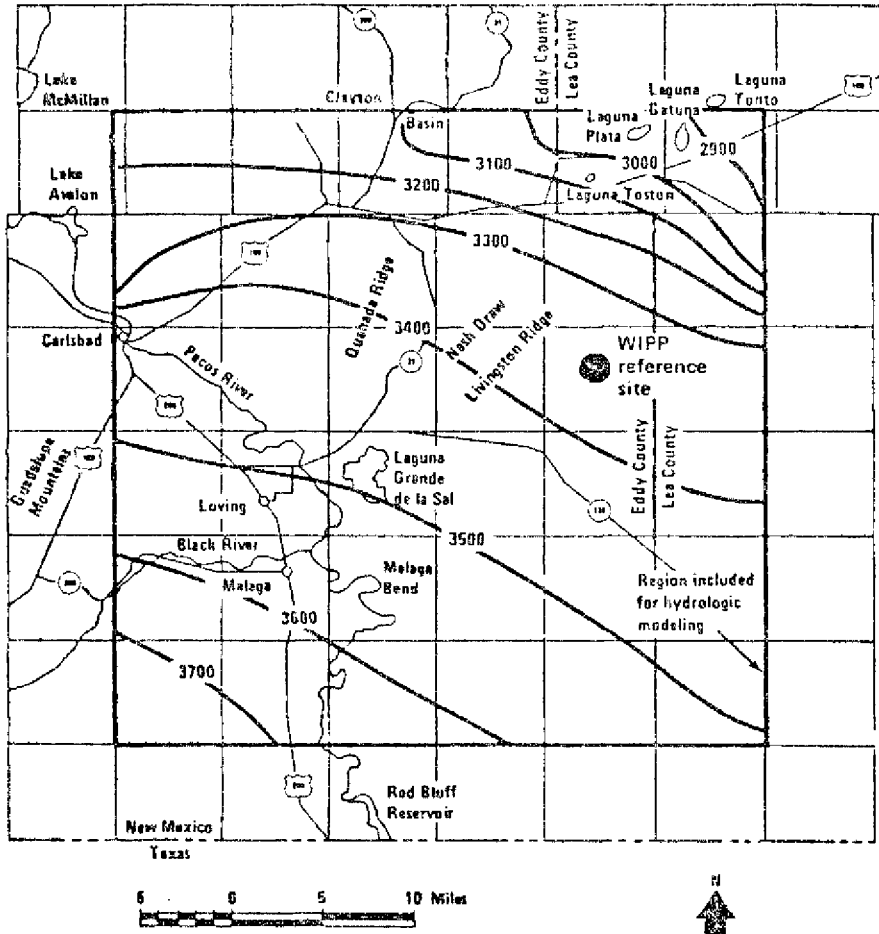


Figure 4.10 Calculated hydraulic potential data for the Delaware Mountain Group aquifer (feet above MSL), from (D1)

The Salado formation (see Figure 4.6) where the repository will be located and the underlying Castile formation are essentially impermeable and contain no water. In this present analysis we postulate that any radionuclide accidentally released from the waste package due to any abnormal event is transferred through an open fracture to either the overlying aquifers in the Rustler formation or to the underlying Delaware Mountain Group aquifers.

Although the transport of radionuclides in groundwater through these fractures might take some time, we assume this time to be negligible when compared to the transport time in the aquifer itself (typical values are ten years compared to 10000 years, E2). Therefore, conceptually, the model assumes the repository is located in the aquifer being studied. This is a conservative assumption because, if the travel time in the fracture was to be considered, the arrival time of the first nuclide would be larger and also, the concentrations would be smaller.

In assessing the safety characteristic of the site, the Rustler formation aquifers are of primary importance because the hydraulic head in the Delaware aquifer being larger than that of the Rustler aquifer produces an upward driving gradient. In addition, thermally induced convective flows makes the downward seepage of groundwater unlikely to occur. However, we calculated the migration of radionuclides in both aquifers for the sake of completeness.

4.6.2 Determination of the contaminated regions and radionuclide discharge rates for the WIPP site

The method described in the previous Section 4.4 to predict radionuclide concentrations in a two-dimensional groundwater flow, which is implemented into the computer code UCBNE21 described in Section 4.5, is used in this section. The contaminated regions of the most hazardous nuclides (e.g. I-129, Ra-226) for different times after the leaching started are determined.

The important result derived from these calculations are the time of contaminant arrival to the biosphere and the location of arrival. In addition, once the location and time of contaminant arrival are known, one can evaluate the discharge rate as well as the cumulative discharge into the biosphere. These quantities present a quantitative measure of the efficiency of the repository as well as of the geologic media as barriers for the radionuclide migration (N2).

All the long lived fission products and the four long actinide chains (Pi) are considered in this calculation, although only the results for the most hazardous ones will be reported. Several nuclides can be discarded as potentially hazardous because they either have a small half life (with no long lived precursors), a large retardation coefficient, small toxicity, small initial activity or a combination of these possibilities.

To rank the potential hazard of each nuclide due to its discharge into the biosphere let us consider the following group of parameters

$$10T_{5j} / K_{TTS1j1} \quad \text{and} \quad 0.001M^1 / (MPC)_i \quad (4.6.1)$$

Physically, the first group of parameters (see Eq. (4.4.19)) represents the water travel time if the nuclides were to arrive at the biosphere after 10 half lives. Therefore, if the calculated water travel time at the biosphere is equal to or larger than the first parameter in Eq. (4.6.1), the concentration of that nuclide has already decayed to a fraction $\exp(-X^t) = \exp(-(\ln 2) * 10) = .001$.

This leads us to the meaning of the second group of parameters. M^0 are the initial activities of each nuclide at the time of burial and therefore $M^1 / (MPC)_j$ represents the volume of water required to dilute that activity to drinking water standards. Hence, the second parameter in Eq.(4.6.1) is the water volume required to dilute the activity present after ten half lives, which was arbitrarily chosen to yield 0.1% of the original activity. For shorter lived actinides (e.g. Ra-226) we consider the parameters of its controlling precursor (e.g. U-234 for times scales of the order of 10 years or U-238 for longer time scales) and one assumes Ra-226 to be in secular equilibrium with either U-234 or U-238 because the time scale is large enough. Therefore, the potential hazard a nuclide poses to the

biosphere can be measured by the first group of parameters ($10T_i$, λ_{mi} represents the migration characteristic of that nuclide and by the second group of parameter ($0.001M_i/MPC$) which represents the toxicity and the total amount of that nuclide initially present. By considering the product of the two group of parameters one can obtain an overall hazard index which can be used to compare different radionuclides in order to rank them.

$$I_i = (10T_i / K_{sm}) \ln(0.001M_i / MPC) \quad (4.6.2)$$

The long lived fission products parameters are listed in Table 4.2 and the actinide chains parameters in Table 4.3. By comparing the product of the two parameters in Eq. (4.6.1) one can rank all nuclides as far as potential hazard to the public goes. This ranking is shown in Table 4.4. Ra-226 is ranked first because its controlling parent, U-238, requires a water travel time of about 10^9 years to decay ten half lives. The next ranked nuclide is I-129 which, due to its retardation coefficient of 8 unity, requires a water travel time of 10^8 years to decay ten half lives. As our calculation will show, the next ranked nuclides Tc-99, U-234, etc. contribute very little to the total discharge rate (expressed in terms of total water dilution rate, Eq. (4.4.22)).

Table 4.2 Long Lived Fission Products Parameters for WIPP site

Nuclide	K_i (yr)	a_j K_i	hf (MPC) (Ci/m ³)	$c/$ $M.$ (Ci/GwYr)	$10T_H/K_i$ (yr)	$.001M_i^-$ (m ³ /GwYr)
H-3	1.2E+1	1.0E+0	3.0E-3	1.9E+4	1.2E+2	6.3E+3
C-14	5.6E+3	1.0E+1	8.0E-4	1.3E+1	5.6E+3	1.6E+1
Se-79	6.5E+4	6.0E+2	3.0E-4	1.1E+1	1.1E+3	3.6E+1
Sr-90	2.8E+1	1.0E+0	3.0E-7	2.1E+6	2.8E+2	7.0E+8
Zr-93	9.5E+5	1.0E+4	8.0E-4	5.2E+1	9.5E+2	6.4E+1
Nb-93m	1.4E+1	1.0E+4	4.0E-4	5.0E+0	1.4E-2	1.2E+1
Tc-99	2*1E+5	1.0E+0	2.0E-4	3.9E+2	2.1E+6	1.9E+3
Ru-106	1.0E+0	1.0E+1	1.0E-5	1.1E+7	1.0E+0	1.1E+9
Cd-113m	1.4E+1	1.0E+4	3.0E-5	1.3E+3	1.4E-3	4.5E+4
Sn-126	1.0E+5	1.0E+3	2.0E-5	1.5E+1	1.0E+3	7.4E+2
Sb-125	2.7E+1	1.0E+2	1.0E-4	2.1E+5	2.7E+0	2.1E+6
I-129	1.7E+7	1.0E+0	6.0E-8	1.0E+0	1.7E+8	1.7E+4
Cs-137	3.0E+1	4.1E+2	2.0E-5	2.9E+6	7.3E-1	1.5E+8
Cs-135	3.0E+6	4.1E+2	1.0E-4	7.8E+0	7.3E+4	7.8E+1
Ce-144	7.8E-1	1.2E+4	1.0E-5	2.1E+7	6.5E-4	2.1E+9
Pm-147	4.4E+0	2.5E+3	2.0E-4	2.6E+6	1.8E-2	1.3E+7
Sm-151	8.7E+1	2.5E+3	4.0E-4	3.4E+4	3.5E-1	8.5E+4
Eu-152	1.3E+1	2.5E+3	6.0E-5	3.3E+2	5.1E-1	5.5E+3
Eu-154	1.6E+1	2.5E+3	2.0E-5	1.9E+5	6.4E-2	9.4E+6
Eu-155	1.8E+0	2.5E+3	2.0E-4	1.7E+5	7.2E-3	8.7E+5

_a/:From reference -(D1), (C2).

b/:From 10CFR20,Appendix B and (P2).

c/:For reprocessed high level waste, 10 years decay, 0.5% U and Pu loss into the waste, (B2).

Table 4.3 Actinide Chains Parameters for The WIPP site.

Nuclide	K. (yr)	(MPC) (Ci/m ³)	M (Ci/GwYr)	10 T ^a / K. (yr)	.001M ^b / MPC (m ³ / GwYr)
Ra-225	4.1E-2	6.8E+2	5.0E-7		1.1E+3
Ra-226***	1.6E+3	6.8E+2	3.0E-8		8.9E+4
Ra-226*** _a	1.6E+3	6.8E+2	3.0E-8		1.6E+9
Th-228	1.9E+0	5.9E+4	7.0E-6	-	1.1E+0
Th-229	7.3E+3	5.9E+4	5.0E-7		1.1E+3
Th-230***	8.0E+4	5.9E+4	2.0E-6		8.9E+4
Th-230*** _a	8.0E+4	5.9E+4	2.0E-6	-	1.6E+9
U-233	1.6E+5	2.8E+1	3.0E-5		1.1E+3
U-234	2.5E+5	2.8E+1	3.0E-5	1.2E+0*	8.9E+4
U-235	7.1E+8	2.8E+1	3.0E-5	2.3E-3	2.5E+8
U-238	4.5E+9	2.8E+1	4.0E-5	4.3E-2	1.6E+9
Np-237	2.1E+6	1.9E+4	3.0E-6	1.5E+1**	1.1E+3
Pu-238	8.6E+1	5.7E+4	1.0E-6	5.1E+2	1.5E-2
Pu-239	2.4E+4	5.7E+4	5.0E-6	4.4E+1	4.2E+0
Pu-240	6.6E-3	5.7E+4	5.0E-6	2.7E+2	1.1E-0
Pu-241	1.3E+1	5.7E+4	2.0E-4	1.4E+4	3.1E+1
Pu-242	3.8E+5	5.7E+4	5.0E-6	1.9E-1	6.6E+1
Am-241	4.6E+2	1.0E+4	4.0E-6	4.9E+3	4.6E-1
Am-242m	1.5E+2	1.0E+4	4.0E-6	1.2E+2	1.5E-1
Am-243	7.9E+3	1.0E+4	4.0E-6	4.8E+2	7.9E+0
Cm-242	4.5E-1	3.0E+3	2.0E-5	4.4E+5	1.5E-1
Cm-243	3.2E+1	3.0E+3	5.0E-6	9.0E+1	1.0E-1
Cm-244	1.8E+1	3.0E+3	7.0E-6	7.4E+4	5.9E-2
Cm-245	9.3E+3	3.0E+3	4.0E-6	9.8E+0	3.1E+1
Cm-246	5.5E+3	3.0E+3	4.0E-6	1.9E+0	1.8E+1

*Includes the decay of Pu-238, Am-242m and Cm-242.

**Includes the decay of Pu-241 and Am-241.

***Based on U-234 value

****Based on U-238 value

_a/:From reference (D1), (C2).

Jo/:From 10CFR20, Appendix B and (P2).

_c/:For reprocessed high level waste, LWR, 10 years decay, 0.5% U and Pu loss into the waste, (B2). Am-242m is in the metastable form.

Table 4.4 Potential Hazardous Nuclide Ranking for the WIPP site

Ranking	Nuclide	$10T^{\wedge}/Kj^{\wedge}$	$1\backslash$
1	Ra-226	1.6E+9*	6.5E+9
2	1-129	1.7E+8	1.7E+9
3	Tc-99	2.1E+6	1.6E+7
4	11-234	8.9E+4	3.2E+5
5	Cs-135	7.3E+4	3.2E+5
6	Se-179	1.1E+3	2.3E+4

*Ra-226 is assumed to be in secular equilibrium with U-238. Thus values of half-life and retardation coefficients for U-238 are used

The calculated (Dl, using model calibration as described in Section 4.4.1) Potentiometric data shown in Figure 4.8 is represented in a three dimensional plot in Figure 4.11. The projection of the Pecos River flow pattern onto the Potentiometric surface is also shown. The shape of the surface clearly indicates that the general direction of flow is southward. The presence of a "valley" in the Potentiometric surface will cause the streamlines to converge in that region. Such valleys are caused either by a strong sink, as in the case of a river, or by a region of high hydraulic conductivity, as in the case of fracture zones. In the case of the Rustler aquifer with the calculated Potentiometric data it seems that the valley in the Potentiometric surface near Malaga Bend is caused by the both the river and a large value of the hydraulic conductivity.

The three dimensional representation of the Potentiometric surface obtained from the raw data exhibited in Figure 4.8 is

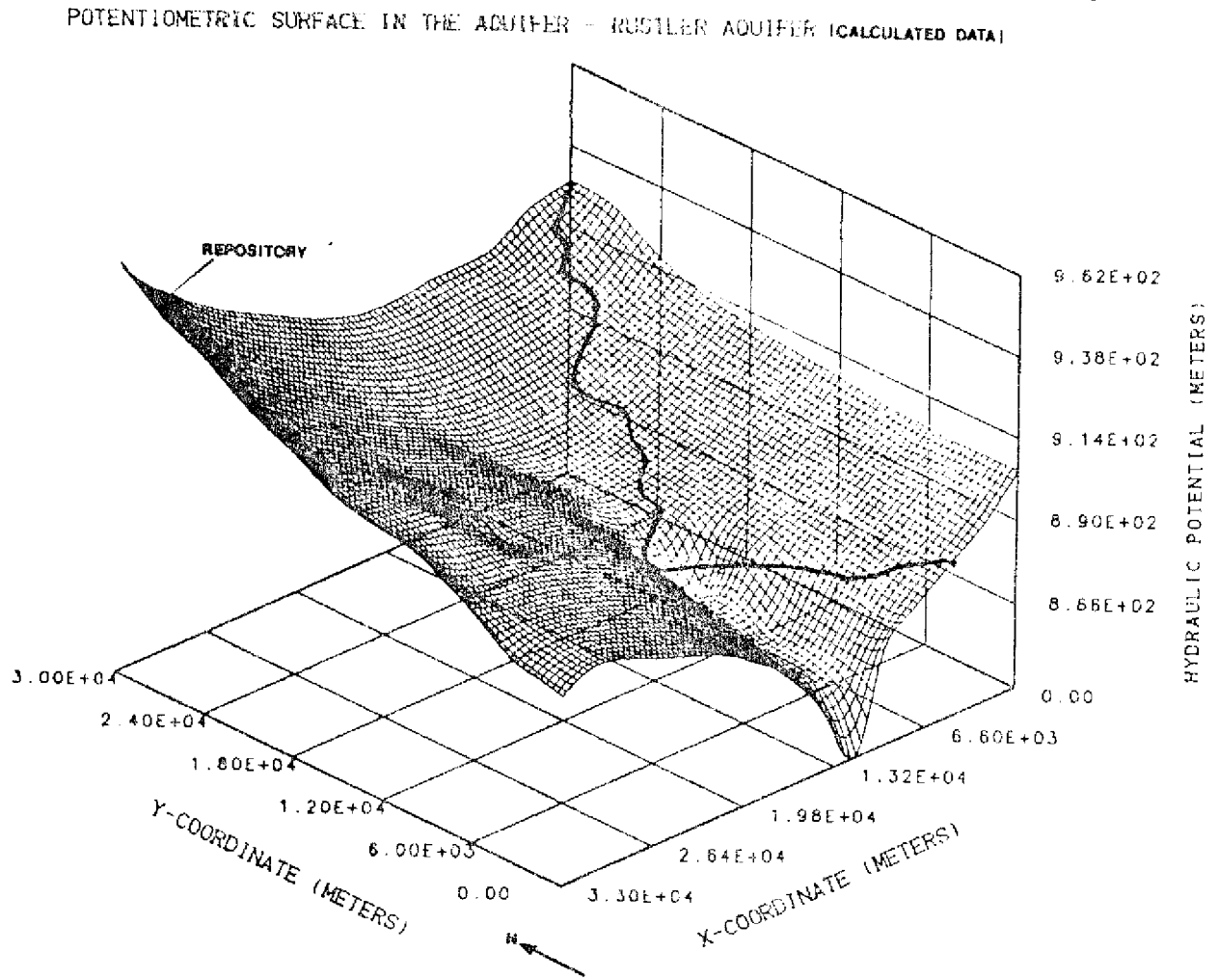


Figure 4.11 The Potentiometric surface (calculated data) in Rustler aquifer with the projection of Pecos River onto the surface

shown in Figure 4.11a. The same general trend observed in the calculated potential is seen here. However, the "valley" begins in a region located about 10 km to the north. The streamlines of the flow coming from the repository will tend to converge in the "valley" north of Malaga Bend, away from the river. After the streamlines are bunched they will move towards Pecos River.

Hydrological calculations for the determination of the contaminated streamlines, hydraulic conductivities and water travel times were performed by the computer program HYDRO for both sets of potentiometric data. The entire shadow region is covered by five streamlines in each case. The water travel time to reach the biosphere (Pecos River) for each streamline for each set of the potentiometric data is shown in Table 4.5.

Table 4.5 Water Arrival time at the Biosphere for the WIPP site

Streamline no. a/	Water arrival time (years)		
	Rustler Aquifer (calculated data)	Rustler Aquifer (raw data)	Delaware Aquifer (raw data)
1	2.23E+4	2.17E+4	1.68E+6
2	3.15E+4	9.73E+3	6.24E+6
3	4.65E+4	1.82E+4	1.80E+6
4	4.24E+4	3.33E+5	1.40E+6
5	4.11E+4	3.50E+5	3.46E+6

a/ See streamline number in Figure 4.12 and Figure 4.19

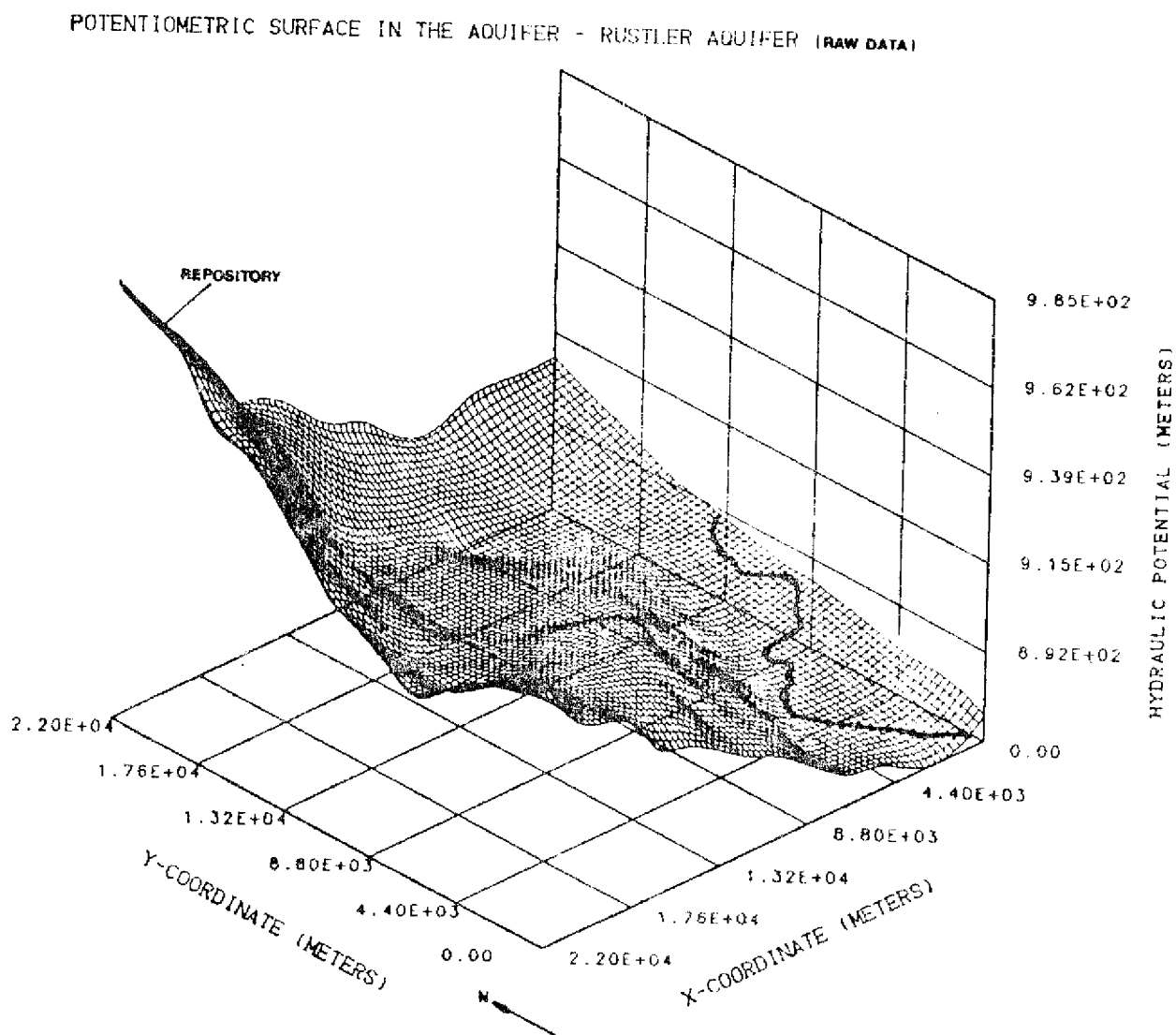


Figure 4.11a Potentiometric surface (raw data) in Rustler aquifer with the projection of Pecos River onto the surface.

For the calculated (D1) potentiometric data set the shortest water travel time to the biosphere is $2.23E+4$ years, while for the raw data set the shortest water travel time to the biosphere is $9.73E+3$ years. From these values one can conclude that only the first five ranked nuclides in Table 4.4 will reach the Pecos River after migrating through Rustier aquifer. All other nuclides will be retarded and they will have decayed before reaching the Pecos River.

Figure 4.12 and Figure 4.13 show the 1-129 contaminated region at 10^1 , 10^4 and 10^5 years after the leaching started indicated by the dotted areas. The lines of constant potential are labelled with their values expressed in meters above mean sea level. Only the streamlines of the repository shadow region are shown. For these figures the calculated potential data were used. As was expected, the 1-129 will discharge into Pecos River near Malaga Bend. According to Figure 4.13, after 10^5 years almost all 1-129 have already been discharged into Pecos River.

Figure 4.14 and Figure 4.15 show the Ra-226 contaminated region in the WIPP site region. After about 10^6 years Ra-226 starts discharging into the river while the trailing edge of its migration band is still near the repository site, because of the large retardation coefficient for Th-230.

Figure 4.16 shows the water dilution rate of 1-129 in the Pecos River for the calculated set of potentiometric data. Three

4 5 6

values of leach time were used for comparisons (10^4 , 10^5 and 10^6). Increasing the value of the leach time by an order of magnitude decreases the water dilution rate by approximately one order of magnitude for 1-129.» The first nuclide arrival time is about $2.0E+4$ years for 1-129.

Similarly, Figure 4.17 shows the water dilution rate and water dilution volume for Ra-226 discharging into Pecos River from Rustler aquifer with the calculated set of potentiometric data. The peak water dilution rate and the peak water dilution volume are three orders of magnitude smaller than for 1-129. And the first arrival time for Ra-226 is $8.0E+5$ years.

The calculations were repeated for the other nuclides ranked in Table 4.4 but their contribution to the total water dilution rate were negligible when compared to 1-129 and Ra-226 contributions. Therefore, the total water dilution rate before $8.0E+5$ years is due primarily to 1-129 and after that time Ra-226 becomes the major contributor but with a peak value three orders of magnitude smaller. In addition to these quantitative considerations one should notice that the location of discharge for the contaminated streamlines into the Pecos River is practically localized.

Comparable calculations were repeated for the Rustler aquifer, but in this case with the raw set of piezometric data. Figure 4.18 show the 1-129 contaminated region after 10^3 and 10^4

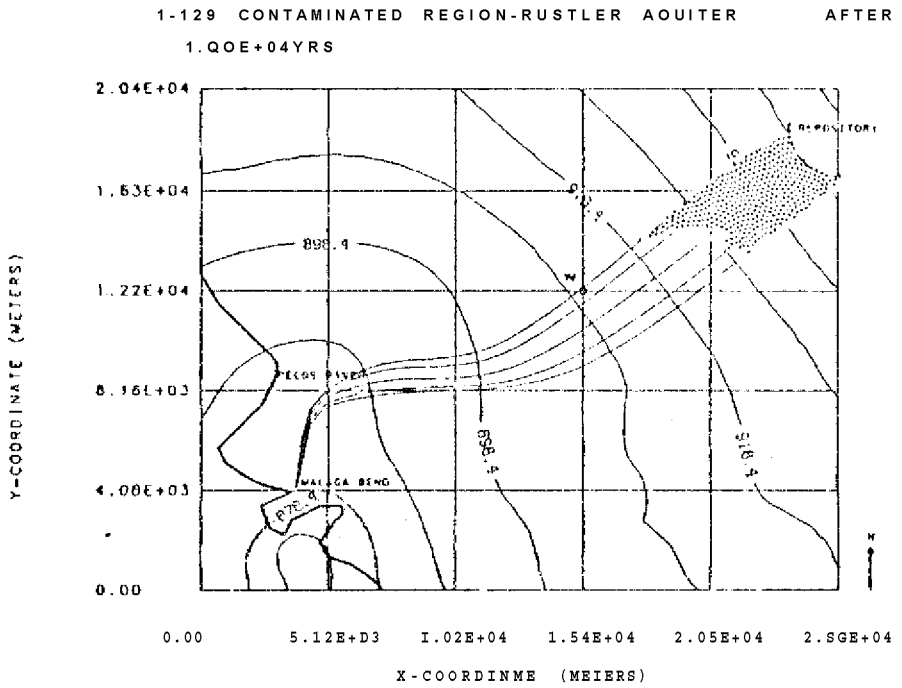
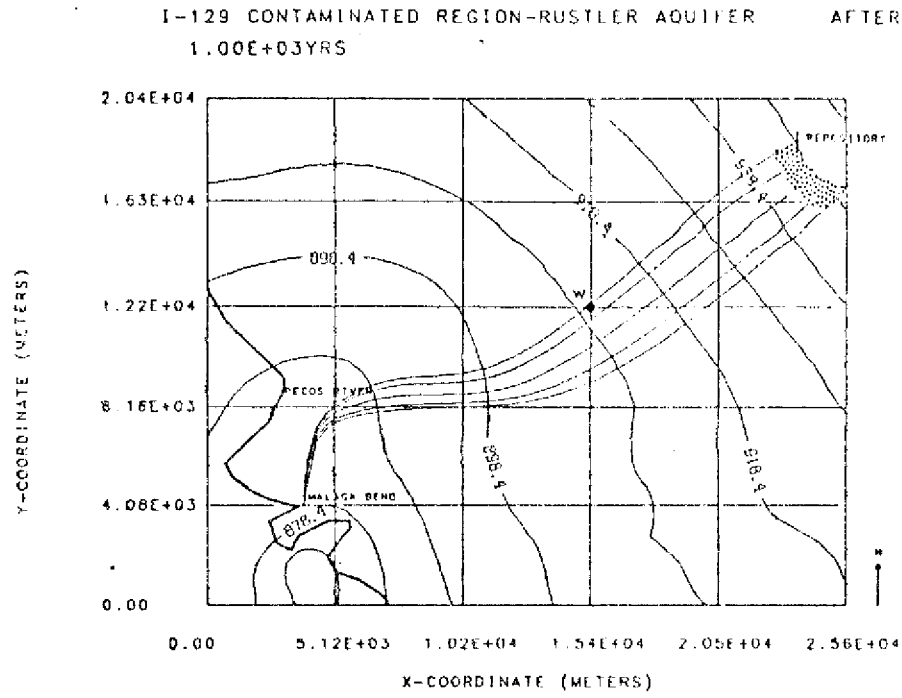


Figure 4.12 1-129 contaminated region in Rustler aquifer (calculated data) after 1,000 and 10,000 years. Potentials are in meters above MSL.

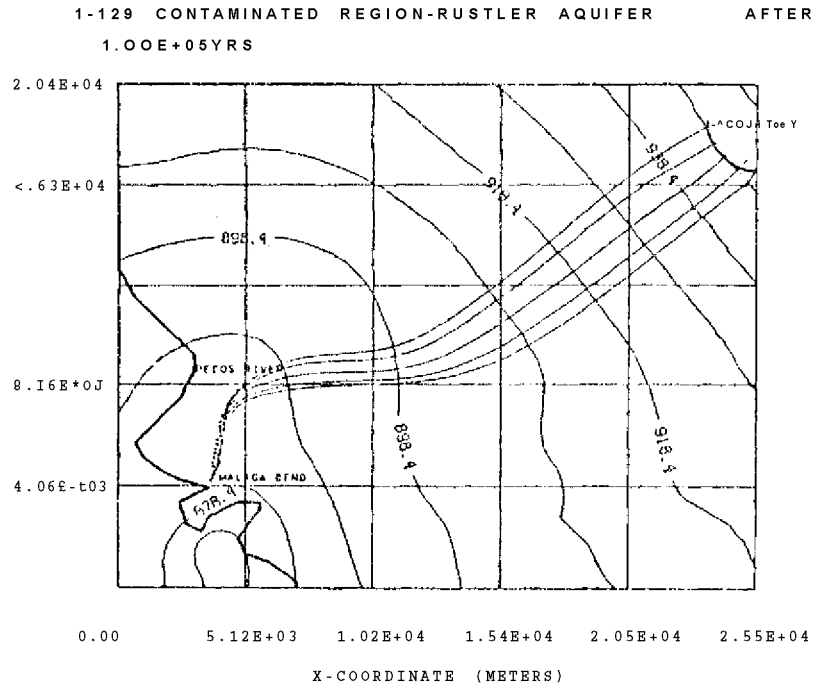
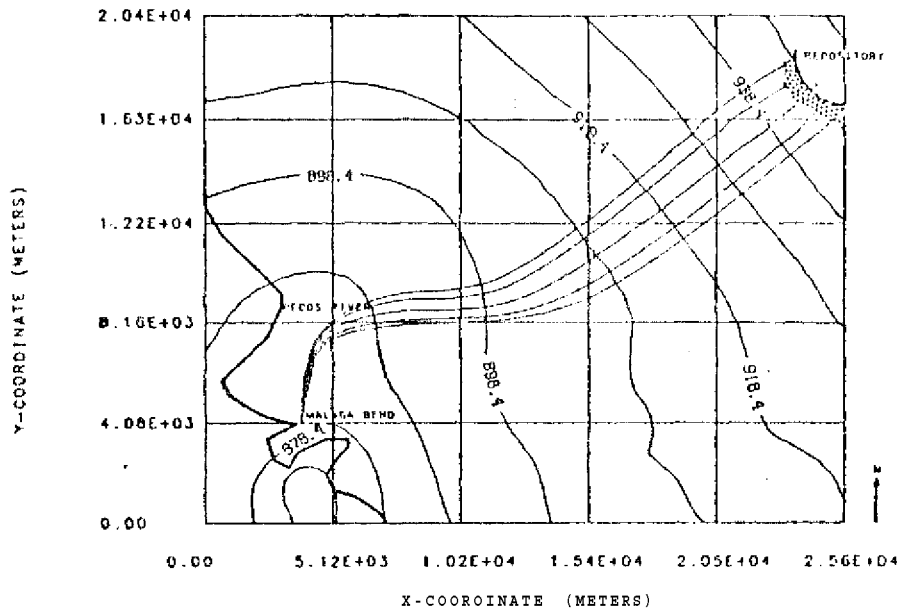


Figure 4.13 1-129 contaminated region in Rustler aquifer
 (calculated data) after 10⁵ years.
 Potentials are in meters above MSL.

RA-226 CONTAMINATED REGION-RUSTLER AQUIFER AFTER
1.00E+04 YRS



RA-226 CONTAMINATED REGION-RUSTLER AQUIFER AFTER
1.00E+05 YRS

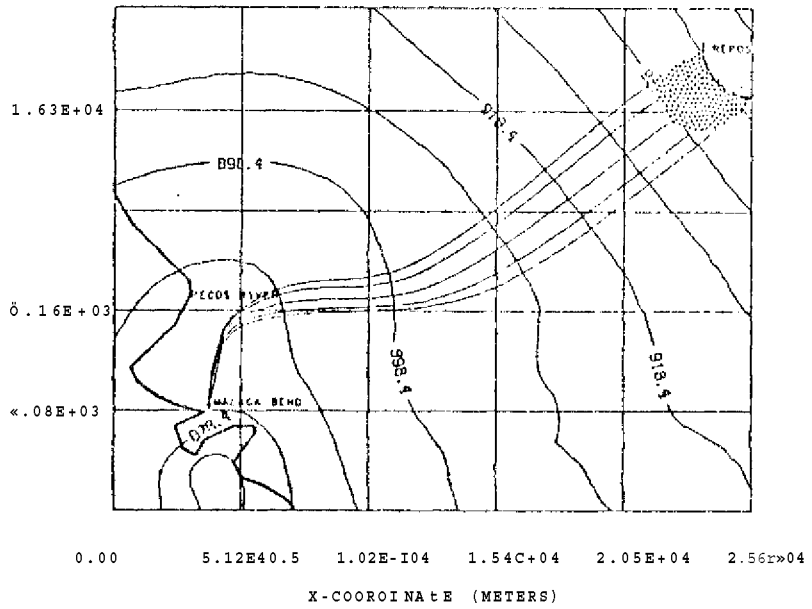


Figure 4.14 Ra-226 contaminated region in Rustler aquifer (calculated data) after 10^4 and 10^5 years. Potentials are in meters above MSL.

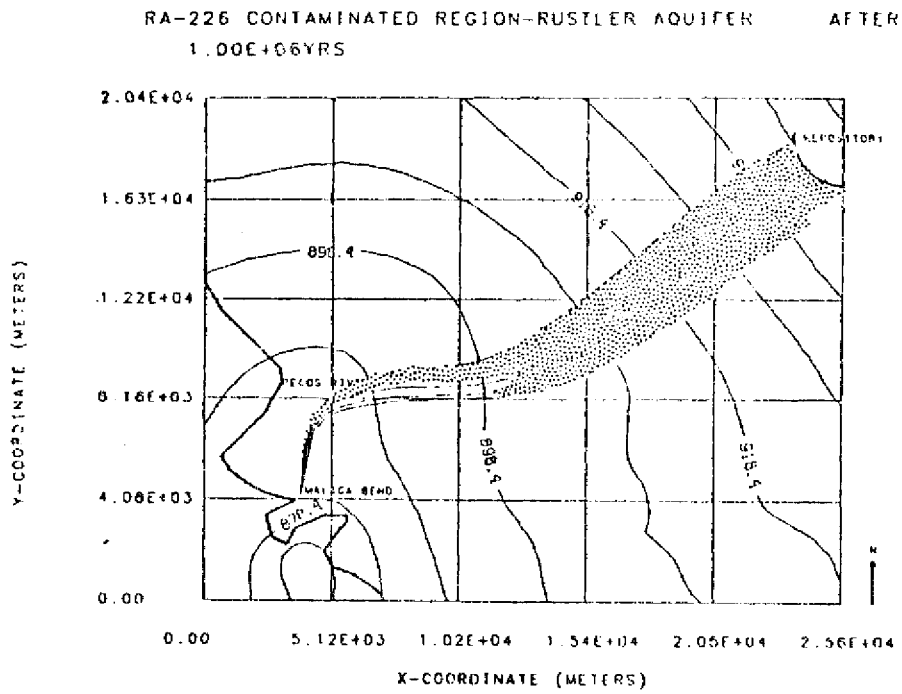


Figure 4.15 Ra-226 contaminated region in Rustler aquifer (calculated data) after 10* years. Potentials are in meters above MSL.

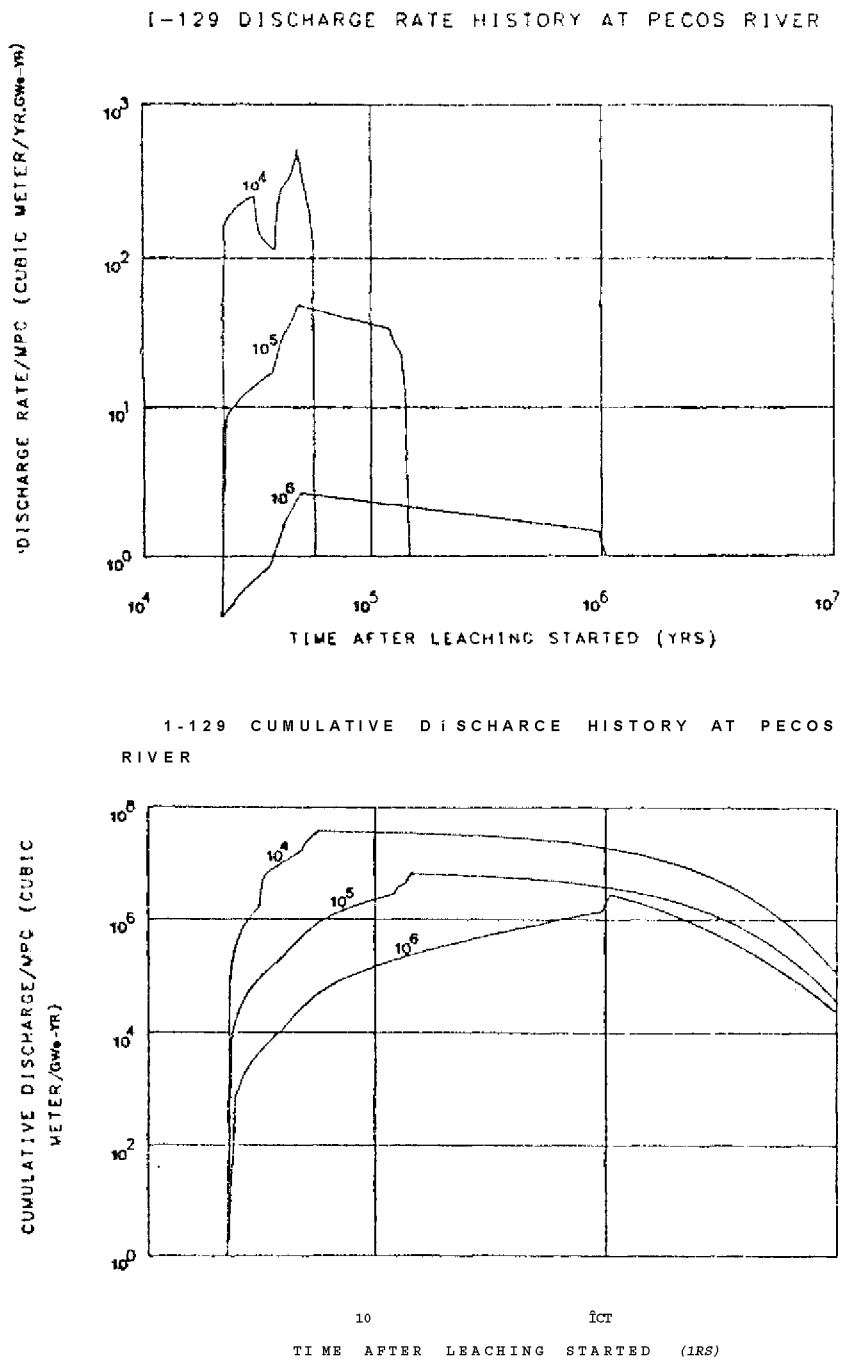


Figure 4.16 1-129 discharge rate/MPC (water dilution rate) and cumulative discharge (water dilution volume) at Pecos River discharging from Rustler aquifer (calculated data) for leach times of 10⁴, 10⁵ and 10⁶ years

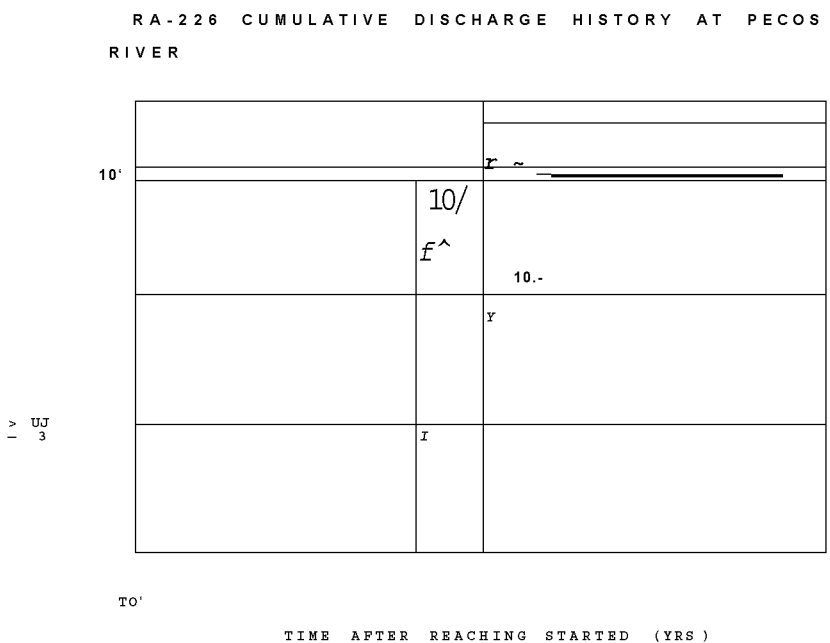
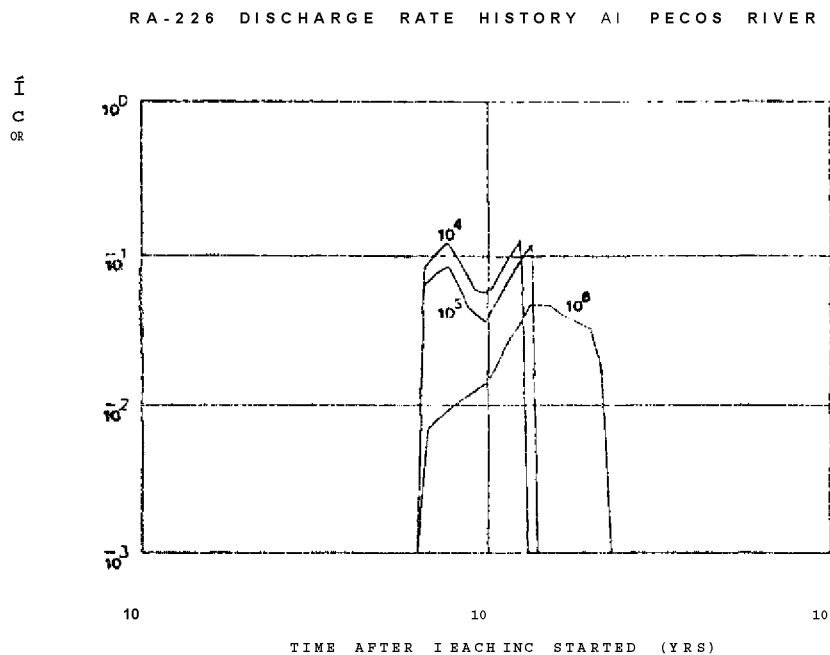


Figure 4.17 Ra-226 discharge rate/MPC (water dilution rate) and cumulative discharge/MPC (water dilution volume) at Pecos River discharging from Rustler aquifer (calculated data) for leach times of 10^4 , 10^5 and 10^6 years

years from the beginning of leaching. Compared to the figures for the calculated potential data case one notices that the confluence of streamlines occurs earlier and the discharge into Pecos River is farther north of the Malaga Bend. After 10 years 1-129 has been totally discharged from the Rustler aquifer.

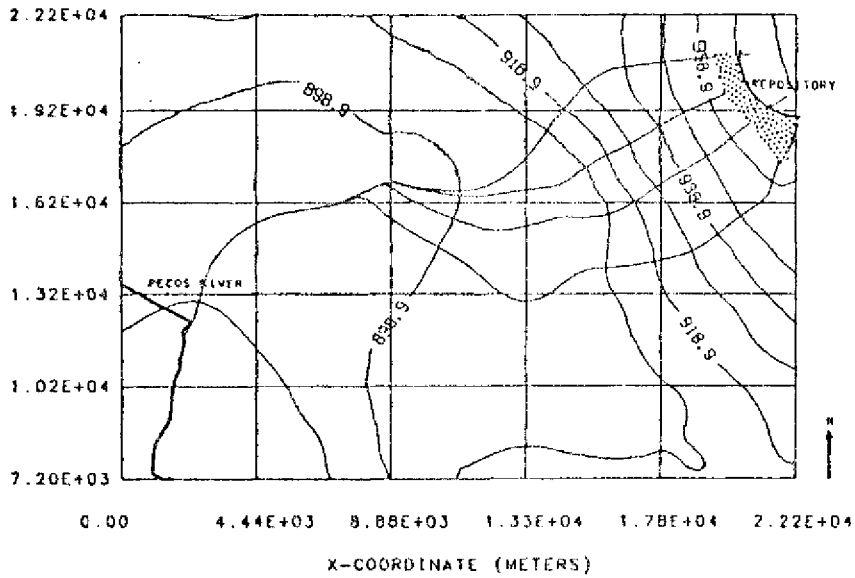
Figure 4.19 and Figure 4.20 show the contaminated region for Ra-226 in Rustler aquifer with the raw set of data for 10^7 thru 10 years. Figure 4.21 shows the 1-129 water dilution rate and water dilution volume, respectively, while Figure 4.22 show the water dilution rate and water dilution volume of Ra-226.

For this case, using the raw set of data, the first 1-129 reaches Pecos River after 10 years and Ra-226 after $4.0E+5$ years instead of $3.0E+4$ years and $9.0E+5$ years for the calculated set of potentials. The magnitude of the water dilution rate are comparable to those obtained in the calculated set. of data case.

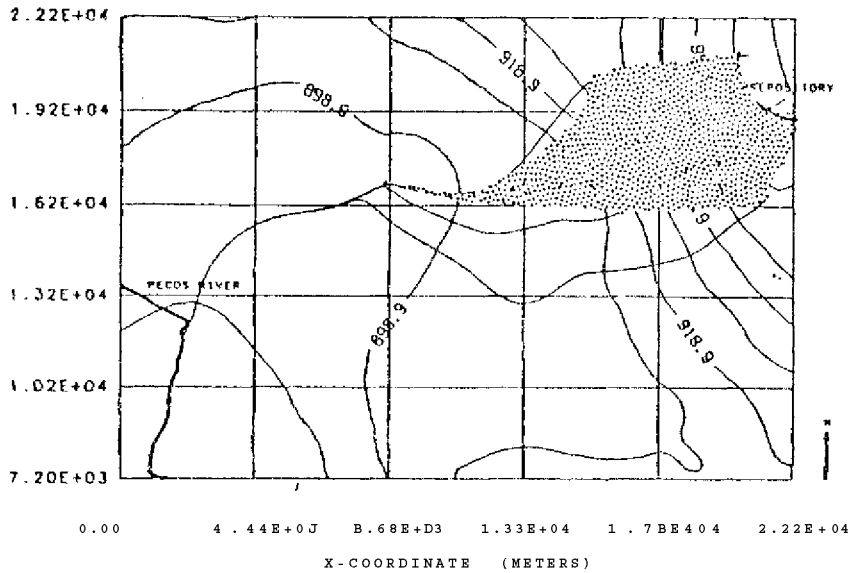
During the period between 1937 and 1975 the maximum recorded Pecos River flow rate at Malaga Bend was $1.1E+11$ m³/yr while the lowest was $4.5E+6$ m⁻¹/yr. In the same period the average river flow rate was $1.7E+8$ m³/yr.

These Pecos River flow rates at the Malaga Bend are compared to the maximum total water dilution rate of 500 m³/yr for radionuclides discharging into Pecos River at any time. This maximum occurs for 1-129, using the calculated potential and a

1-129 CONTAMINATED REGION-RUSTLER AQUIFER AFTER
1.00E+03VRS



1-129 CONTAMINATED REGION-RUSTLER AQUIFER AFTER
1.00E+04YRS



18 1-129 contaminated region in Rustler aquifer
(raw data) after 10³ and 10⁴ years.
Potentials are in meters above MSL.

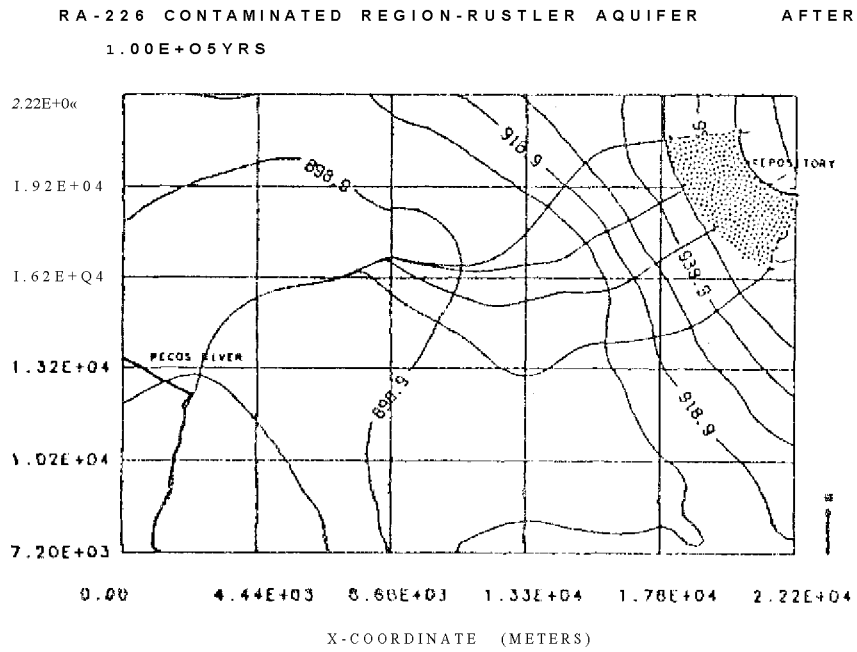
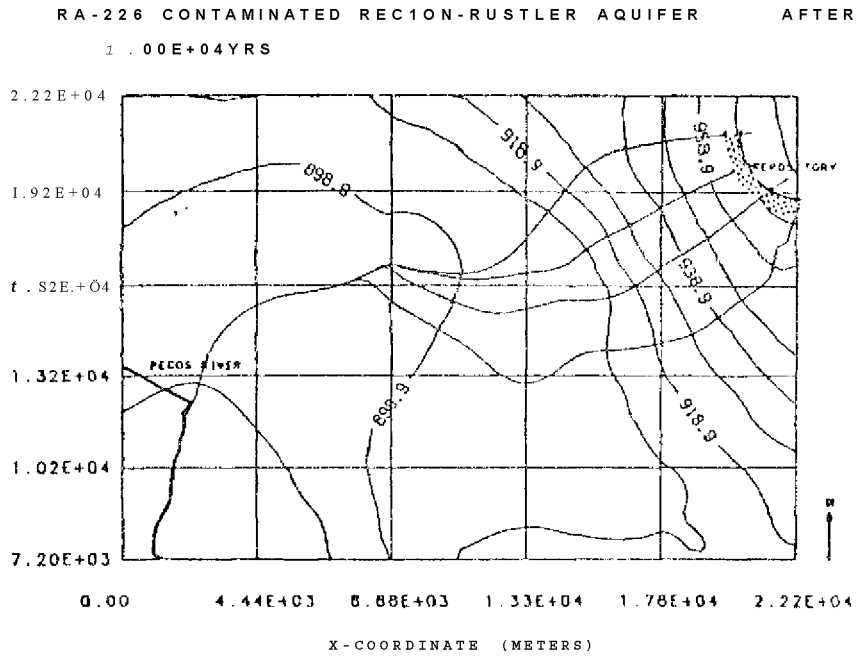


Figure 4.19 Ra-226 contaminated region in Rustler aquifer (raw data) after 10^4 and 10^5 years. Potentials are in meters above MSL.)

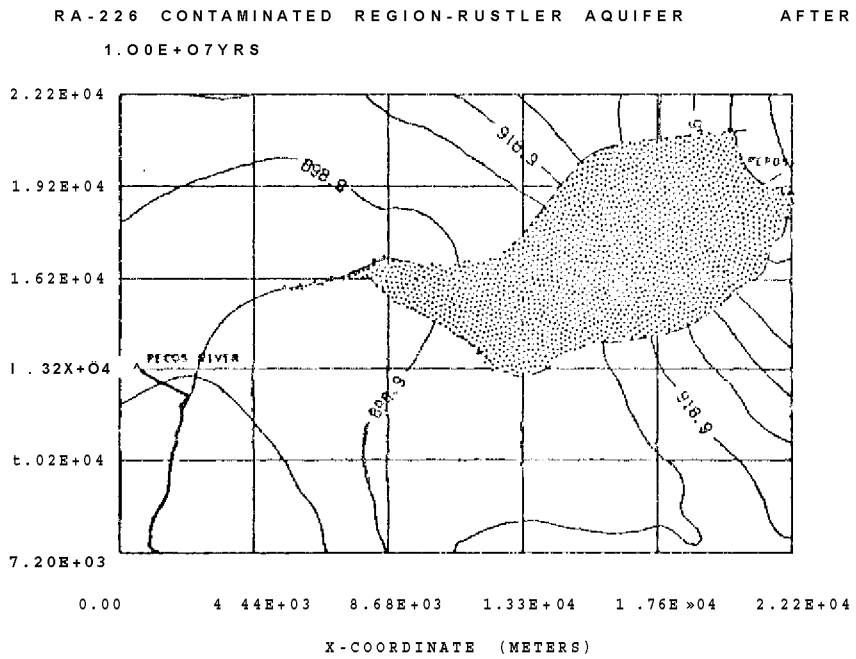
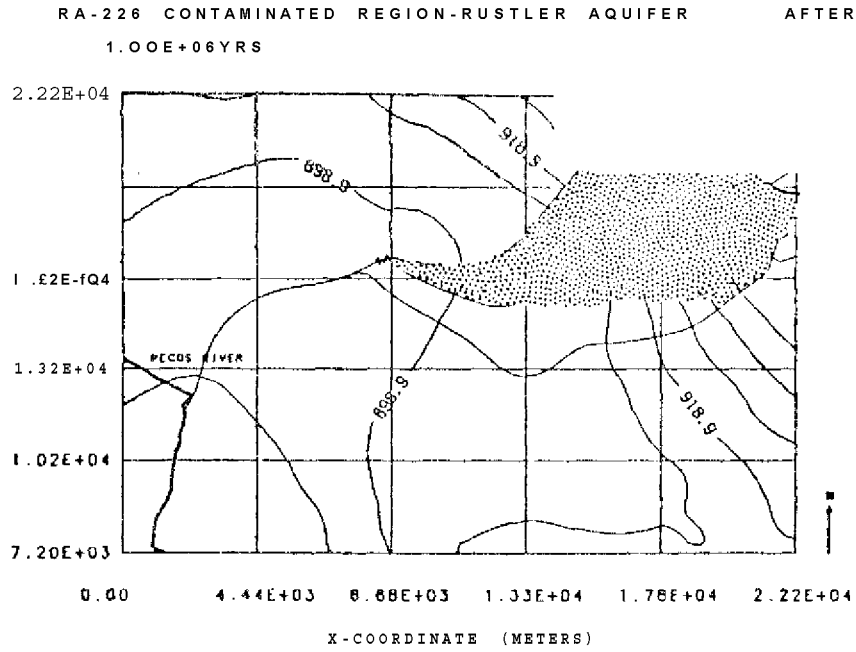
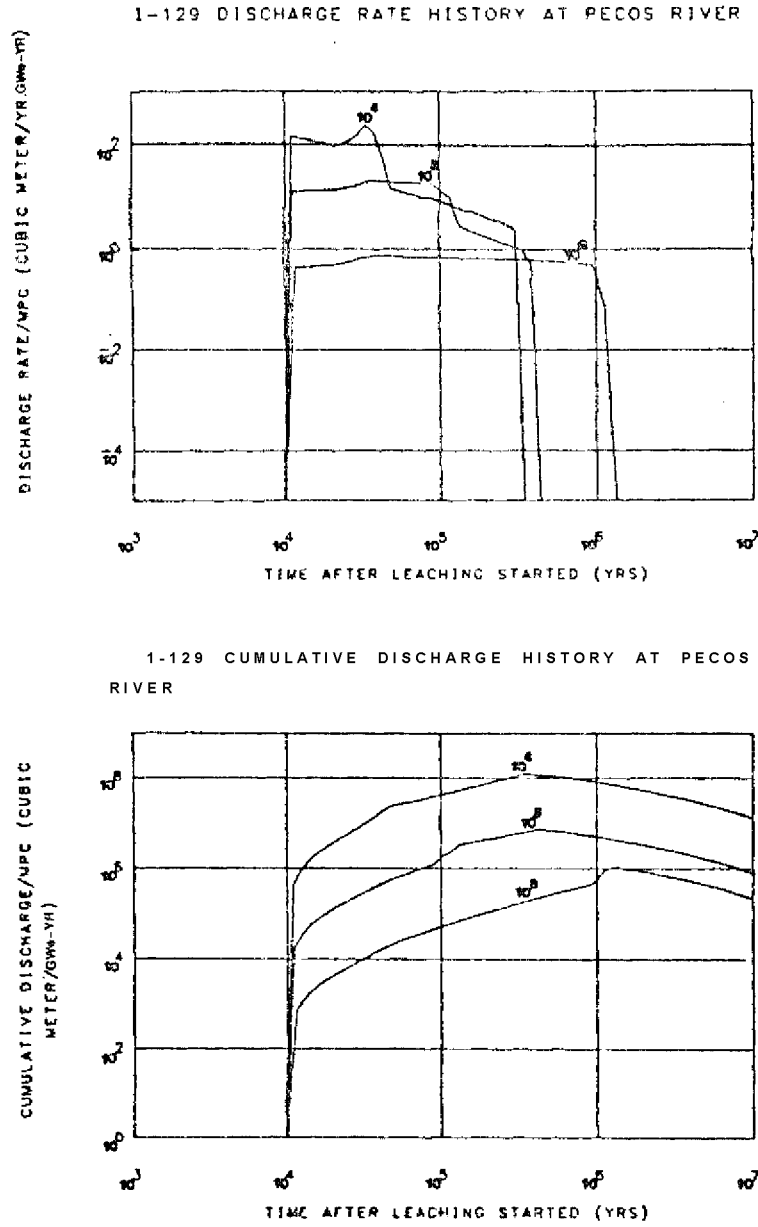


Figure 4.20 Ra-22.6 contaminated region in Rustler aquifer (raw data) after 10^6 and 10^7 years. Potentials are given in meters above MSL.



Fiaure 4.21 1-129 discharge rate/MPC (water dilution rate) and cumulative discharge/MPC (water dilution volume) at Pecos River discharging from Rustler aquifer (raw data) for leach times of 10^4 , 10^5 and 10^6 years

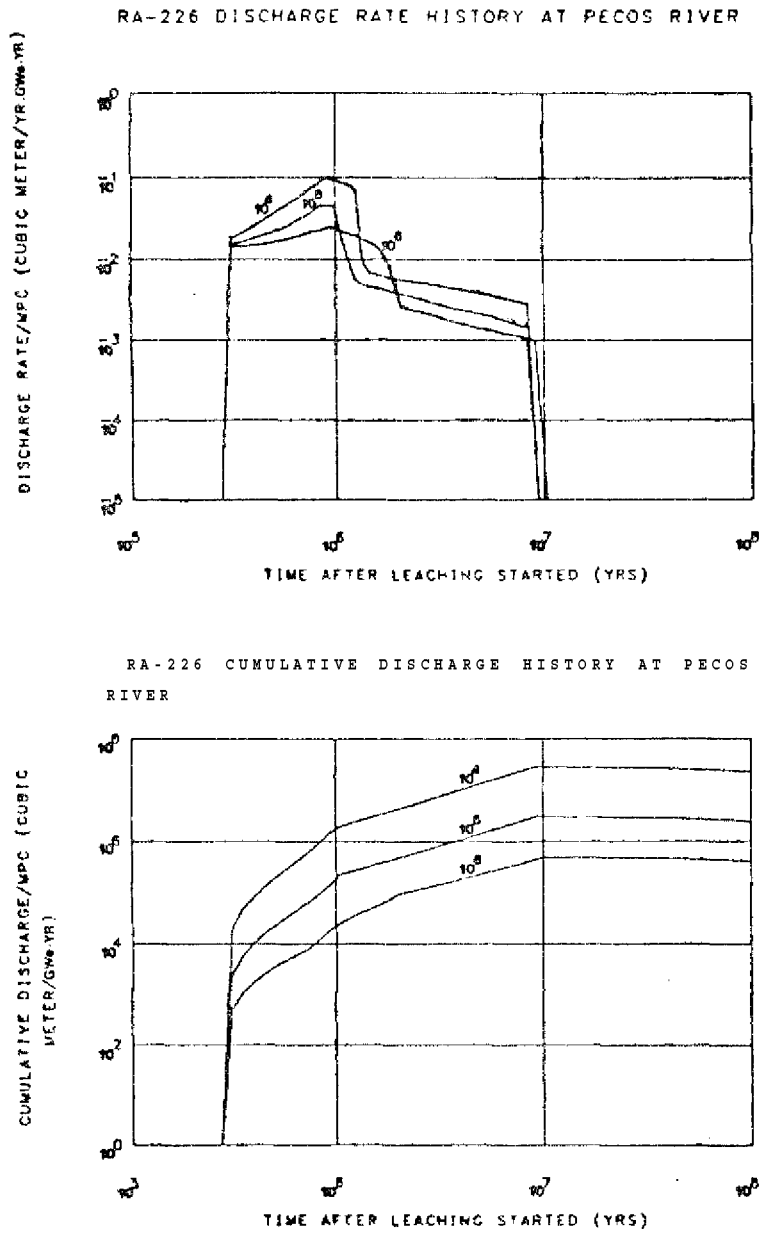


Figure 4.22 Ra-226 discharge rate/MPC (water dilution rate) and cumulative discharge/MPC (water dilution volume) at Pecos river discharging from Rustler aquifer (raw data) for leach times of 10⁴, 10⁵ and 10⁶ years

leach time of 10 years. One concludes that when Pecos River is flowing at its minimum capacity it is still larger by a factor of 1000. Taking into account the fact that the amount of waste considered in the calculations is the result of production of one Gw(e)yr by a LWR, the Pecos River minimum flow rate would be sufficient to dilute to MFC levels the contamination caused by the reprocessed high level waste of 330 LWR's operating during their 30 years lifetime at full capacity.

At the WIPP site the downward seepage of contaminated groundwater into the underlying Delaware Mountain Group aquifers will be very unlikely. This is because the temperature gradient caused by the decay heat in the waste packages will produce an upward driving force due to density gradients. In addition, even after sufficient time for the heat generation to be significantly reduced, the hydraulic potential in the Delaware aquifer, being larger than in the Rustler aquifer, will cause the flow through any connection between them to be upwards.

Even if the Delaware aquifer were to be contaminated, the potential hazard due to the discharge of radionuclides into the Capitan aquifer situated about 30 km to the north would be small because the water travel times in this aquifer are large. Nevertheless calculations were performed for this case based on calculated (D1) set of hydraulic heads.

Figure 4.23 shows the potentiometric surface in the

POTENTIOMETRIC SURFACE IN THE AQUIFER - DELAWARE AQUIFER

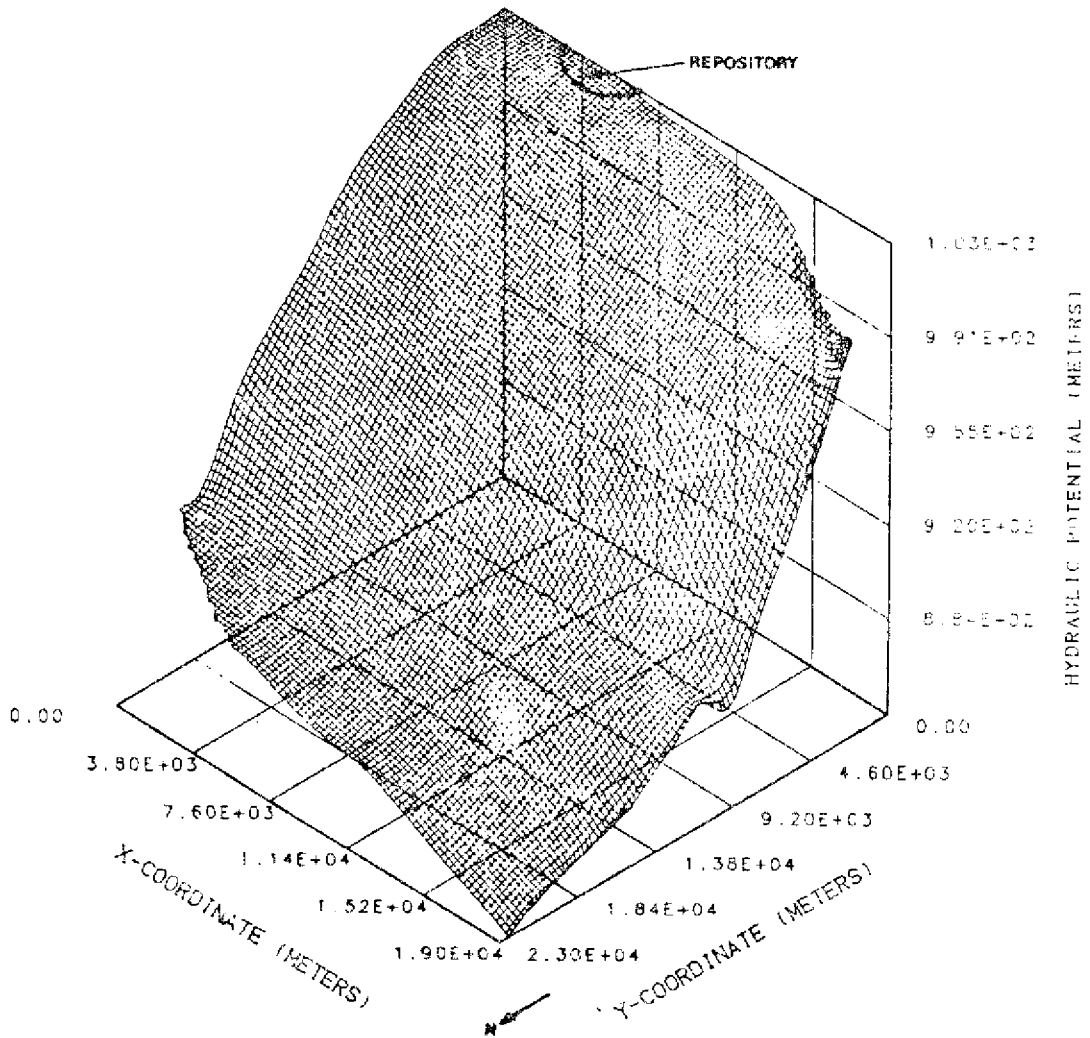


Figure 4.23 The Potentiometric surface in the Delaware Mountain Group Aquifer.

Delaware aquifer. The absence of irregularities like "valleys" and "hills" indicate that the streamlines will have no confluence or divergent tendencies but exhibit a rather regular pattern. Contrary to the Rustler aquifer, the Delaware aquifer flows northward discharging into Capitan aquifer. As it is shown in

6

Figure 4.24 it would take more than 10 years for 1-129 to reach Capitan aquifer.

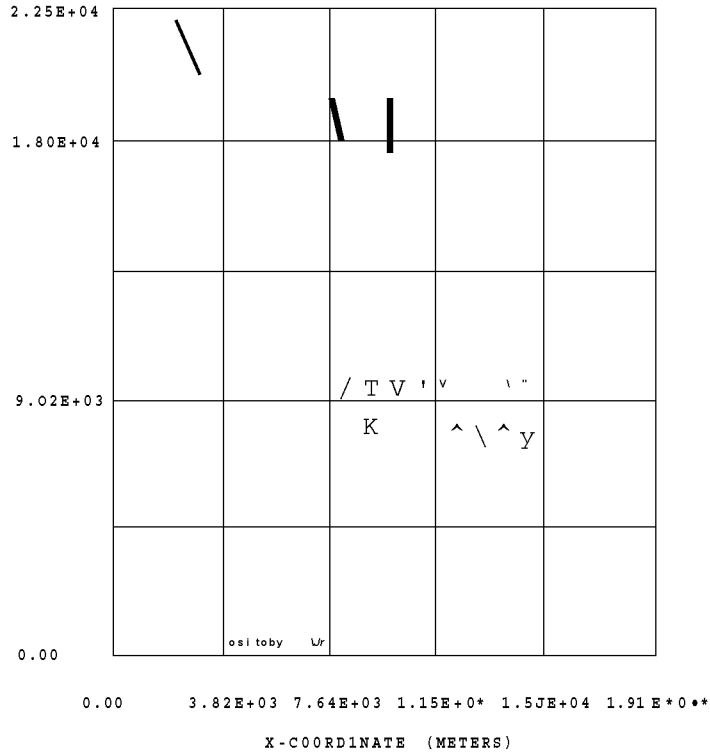
Besides the discharge into the Pecos River, there is another pathway to the biosphere that can be potentially hazardous to the public health. If a fresh-water-producing well is dug in the shadow region of the repository, deep enough to reach the Rustler aquifer, the water pumped might contain radioactive elements released from the repository.

3

A typical water producing well flow rate of about 350 m³/yr was assumed (M2). The calculated potentiometric surface in the Rustler aquifer was considered and the well location lies inside the shadow region. The well is located at the coordinates: x=15,400 meters and y=12,200 meters (see coordinate system in Figure 4.12 where the well location is defined by a "W").

After superimposing the existing natural hydraulic potential of Rustler aquifer to the potential due to the well (point sink in Eq.(4.3.9)) with above flow rate the resulting potential calculated by HYDRO shows no significant differences from the original Rustler aquifer potential. This is because the

1-129 CONTAMINATED REGION-DELAWARE AQUIFER
AFTER 1.00E+05YRS



1-129 CONTAMINATED REGION-DELAWARE AQUIFER
AFTER 1.00E+06YRS

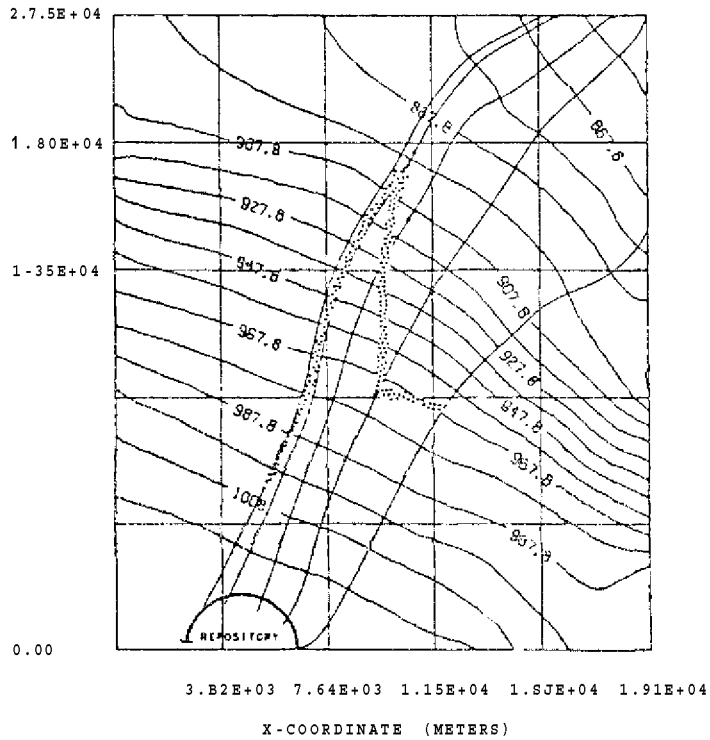
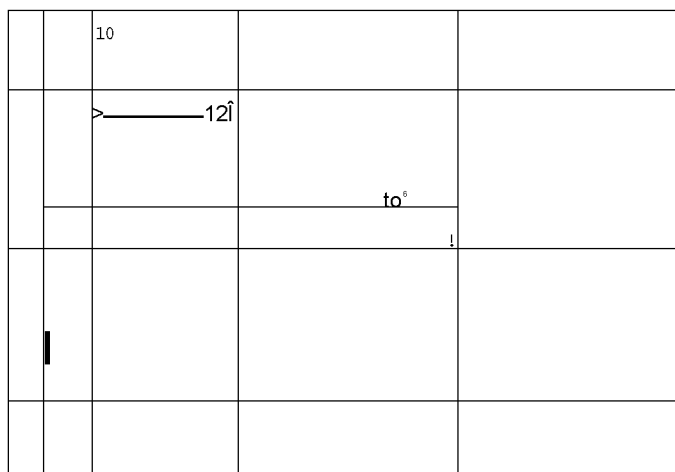


Figure 4 . 24 1-129 contaminated region in Dola'wr? *Vr in tain
'"•roup anui'Ter (calculated data) after 10-^ and 10* yrs.
Potentials are in meters above MSL.

well flow rate is small compared to the aquifer yield (by a factor of 1000). Therefore, one can use the hydrological calculation already done for the Rustler aquifer with the calculated set of potentiometric data. Figure 4.11 and Figure 4.12 thru Figure 4.15 are still valid, however, the well location is now part of the biosphere and the discharge rates, nuclide arrival times at the well are different from those quoted earlier.

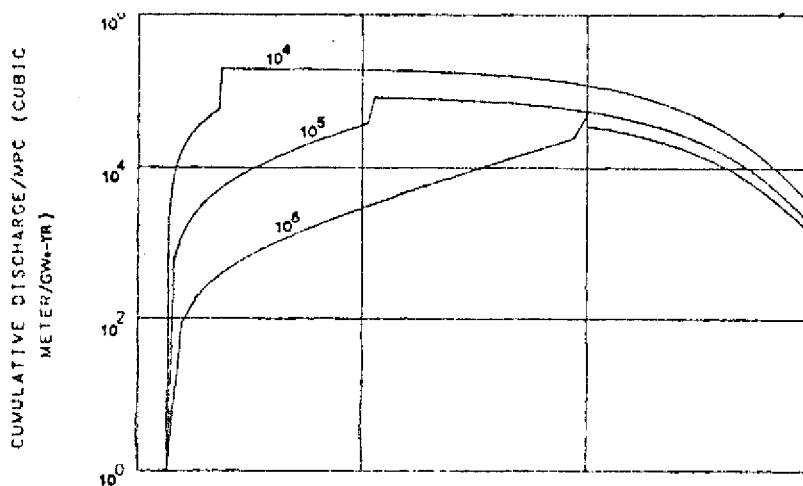
The water travel time to reach the well is 13,500 years, as compared with the 31,500 years to reach Pecos River. For this water travel time 1-129 and Ra-226 are still the most hazardous nuclides. Figure 4.24a and Figure 4.24b show their discharge rates and cumulative discharge in the well. The maximum water dilution rate for 1-129 is again almost three order of magnitude larger than that of Ra-226. For leach times of 10 years and 10 years 1-129 discharges earlier than Ra-226 and they discharge at different times because they have different retardation coefficient. Since the water arrival time to the well is of the order of 10^4 years and the unit retardation coefficient, the times of discharge for leach times larger than 10^4 will be equal to the leach times. If, however the retardation coefficient were not unity, then the time of discharge would be controlled either by the leach time or by the product of the water travel time to the well times the retardation coefficient, whichever is larger (see Eq. (4.3.5f)). The maximum 1-129 water dilution rate is about 10 m³/yr which 35 times smaller than the well flow rate of 350 m³/yr.

1-129 DISCHARGE RATE HISTORY - WELL



TIME AFTER LEACHING STARTED (YRS)

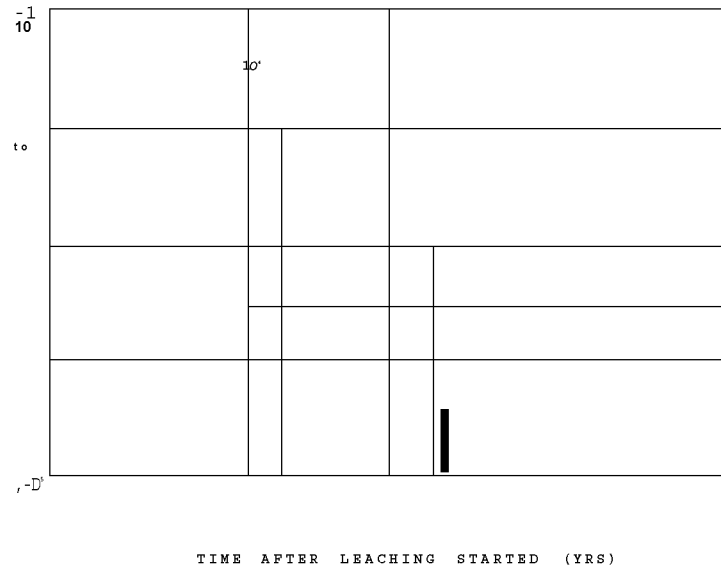
1-129 CUMULATIVE DISCHARGE HISTORY - WELL



TIME AFTER LEACHING STARTED (YRS)

Figure 4.24a 1-129 discharge rate/MPC (water dilution rate) and cumulative discharge/MPC (water dilution volume) at a well in Rustler aquifer shadow region (calculated data). Leach times values are: 10^4 , 10^5 and 10^6 years

RA-226 DISCHARGE RATE HISTORY - WELL



RA-226 CUMULATIVE DISCHARGE HISTORY - WELL

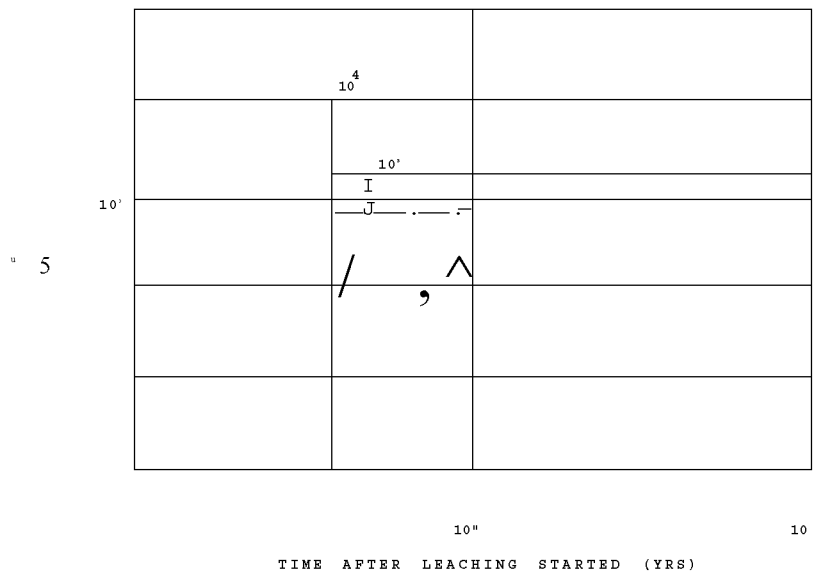


Figure 4.24b Ra-226 discharge rate/MPC (water dilution rate) and cumulative discharge/MPC (water dilution volume) at a well in Rustler aquifer shadow region (calculated data). Leach time values are: 10^4 , 10^5 and 10^6 years

Addendum to Section 4.6

Cole and Bond (C3), also studied the far field migration of radionuclides for the WIPP site. Their work is reviewed in this addendum.

The hydrological calculations in (C3) were performed by the computer program VTT (Variable Thickness Transient Flow, Si). This code solves numerically the governing equation for the groundwater conservation with inhomogeneous aquifer parameters values for the Darcy's flow. For the steady state problem, the model utilizes a finite difference formulation involving Newton's method and a direct Gaussian elimination procedure (see SI for a more detailed description). VTT uses the measured Rustler aquifer piezometric data (Figure 4.7) for the "model calibration" as described in Section 4.4.1. By assuming initial guesses for the aquifer hydraulic conductivity and the boundary conditions, the computer program VTT solves numerically Eq.(4.4.1). The resulting hydraulic head distribution is then compared to Figure 4.7 and by using some arbitrary weighting function to check the consistency between the solution obtained with the measured data new aquifer parameters and boundary conditions are deduced. These new values are used and a corrected solution for the hydraulic head is then derived. This procedure is repeated until an "acceptable" agreement is obtained between the calculated and measured hydraulic head.

One should note that this method does not guarantee uniqueness for the solution since there are infinitely many combinations of aquifer parameters and hydraulic head functions that satisfy Eq, (4.4.1), Therefore, the choice of a particular set of parameter values and the associated hydraulic head distribution by using model calibration is arbitrary, dictated only by the choice of the weighting functions. The resulting Rustler aquifer hydraulic conductivity and hydraulic head obtained by Cole and Bond in (C3) are shown in Figure A1 and Figure A2 respectively.

Figure A1 shows that the hydraulic conductivity distribution used in (C3) to characterize Rustler aquifer in the region between the repository site and the Malaga Bend is given by only three discrete values of 1, 4 and 32 ft/day. The method presented in Section 4.4 (and implemented in UCBNE21) was used for the Rustler aquifer with the calculated data, and a continuously varying hydraulic conductivity from 1 ft/day at the repository site up to about 65 ft/day close to the discharge location at the Malaga Bend was obtained.

The calculated hydraulic head for Rustler aquifer given in (C3) is shown in Figure A2. The shape of the potential lines as well as their corresponding values in feet above the MSL agree well with the calculated potentiometric data used in this work (Figure 4.8). The shape of the streamlines are also comparable to those obtained in the present work (Figure 4.12) with the

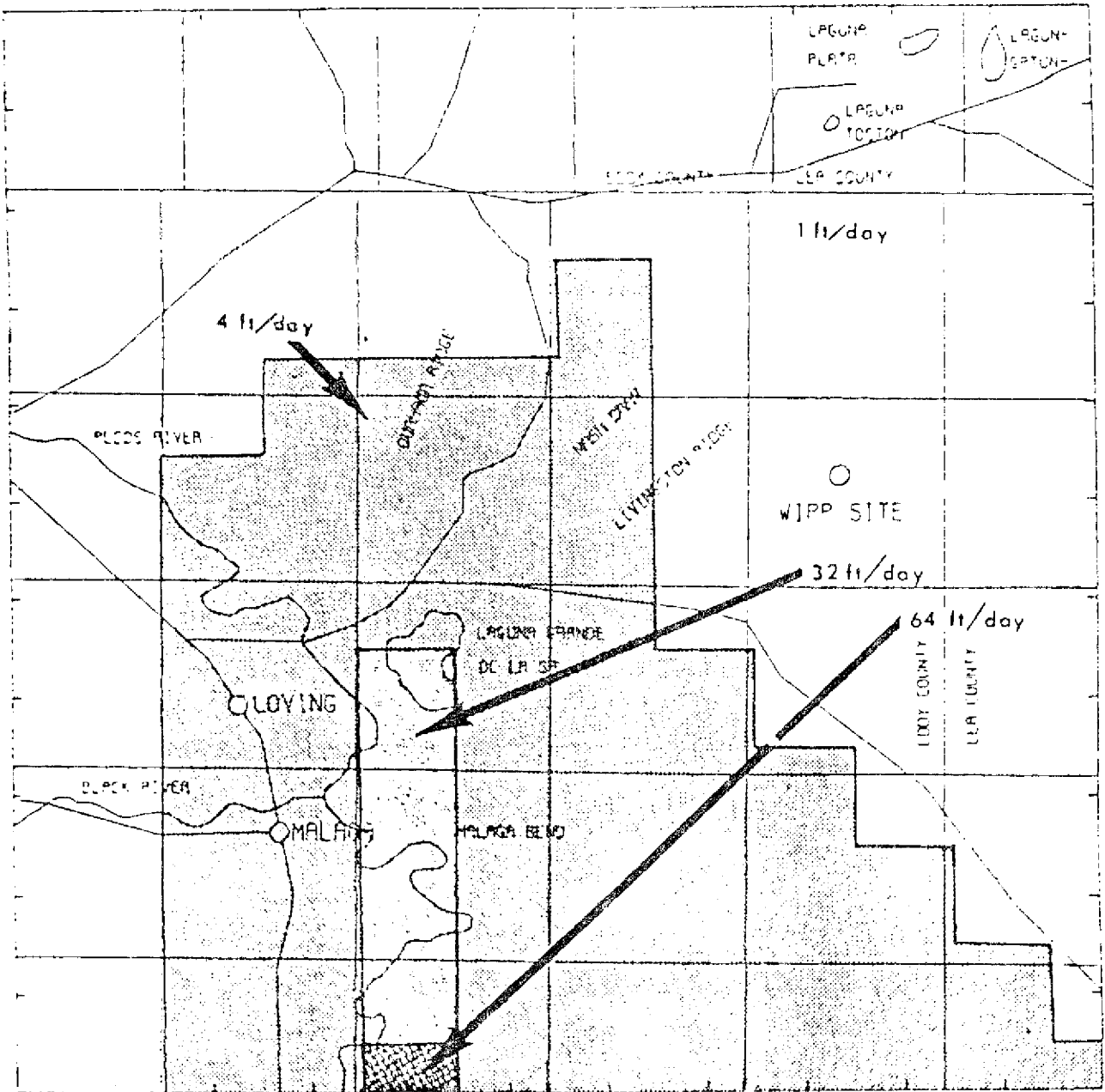


Figure A1 Hydraulic conductivity values used in C3.

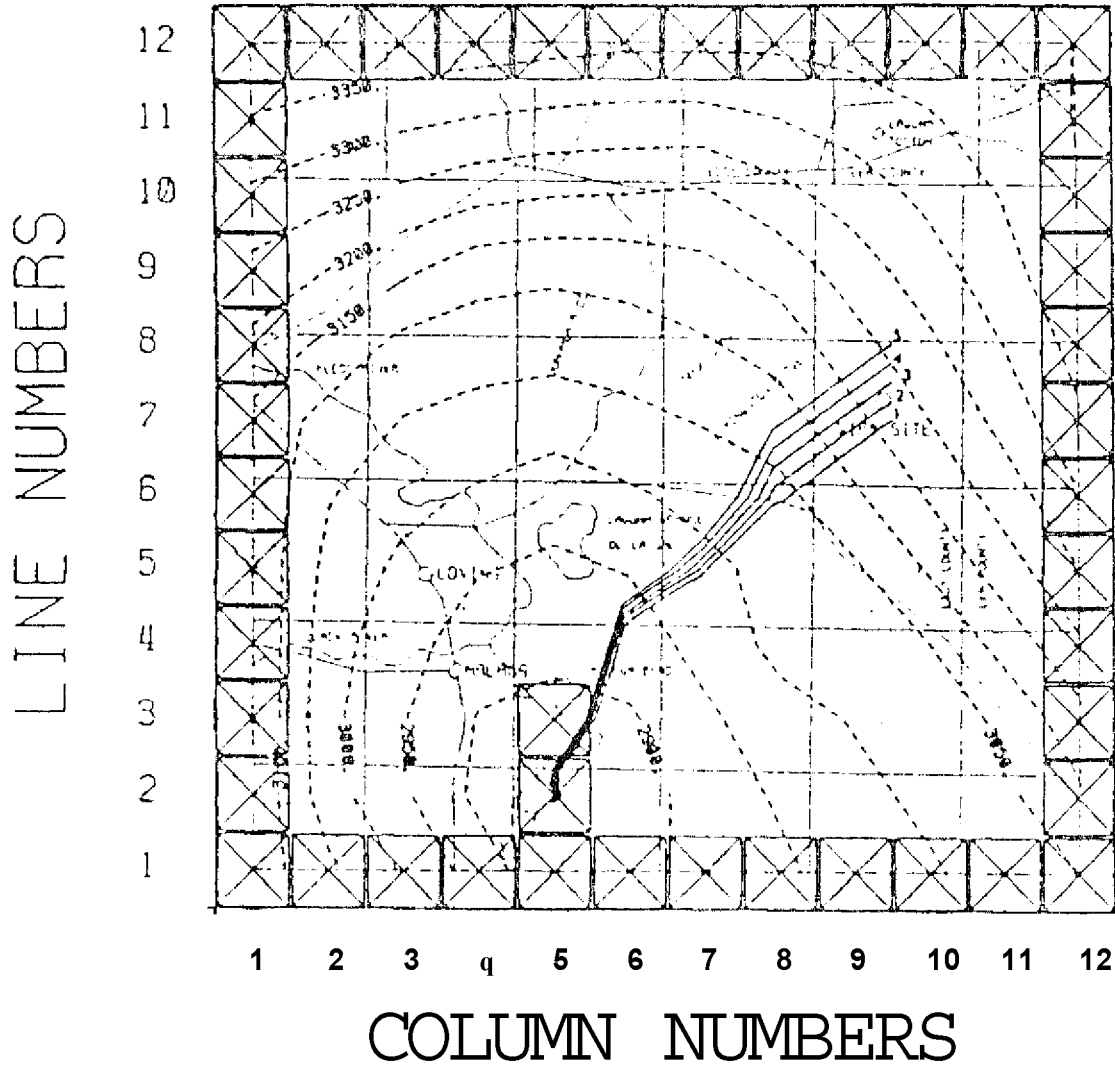


Figure A2 The nodal system used in C3 with the calculated hydraulic head distribution and the streamlines of the contaminated region.

A2 which are caused by discrete jumps in the hydraulic conductivity values used.

However, the most serious contention in our review concerns with the fact that the dimensional sealling used in (C3) is about two times smaller than the actual geographical scales used elsewhere for that region. It is stated in (C3) that the distance between two nodal points in Figure A2 is equivalent to 1.5 miles. Using this scaling factor, the distance between the repository site and Malaga Bend is 8 miles, according to Figure A2. On the other hand, data from (D1) indicates that the distance between those same points is 17 miles while data from (M1) and (R1) indicate 18 miles. Furthermore, from (B5) we have the confirmation that the distance is about 17 miles. Therefore, the scaling factor used in (C3) is smaller by a factor of approximately two. Although the values of hydraulic head are not affected by this error, the groundwater velocity (i.e. the gradient of the potential) as well as the distance to the biosphere are affected. Consequently, the water travel time to the biosphere is also affected. The resulting water travel times to reach the Malaga Bend calculated in (C3) by VTT and those obtained in this work calculated by HYDRO are shown in the Table A1 below for comparison.

Table A1 Comparison between water travel times to the Malaga Bend in Rustler aquifer obtained in (C3) and in this work.

Streamline no.	Water travel times (years)	
	Coles and Bond	This work
1	3.43E+3	2.23E+4
2	3.57E+3	3.15E+4
3	3.67E+3	4.65E+4
4	3.72E+3	4.24E+4
5	3.82E+3	4.11E+4

One can notice that the reduction by a factor of two in the dimensional scaling, with a corresponding increase by a factor of two in the local values of the groundwater velocity and in the total distance to the biosphere, caused the water travel time to be decreased by more than an order of magnitude. This difference in water travel time to the biosphere seriously affects the far-field migration of radionuclides since the arrival time of the first nuclide is greatly diminished and the concentration of a particular nuclide is increased.

Coles and Bond calculated the far-field migration of radionuclides in the WIPP site by using a simplified one-dimensional model. The average length of the five streamlines shown in Figure A2 was used as the equivalent one-dimensional path length and the corresponding average water travel time was

used. The results shown in (C3) also present 1-129 and Ra-226 as being the most hazardous nuclides migrating in the Rustler aquifer.

A quantitative comparison between the one-dimensional calculation carried out in (C3) with the error in the scaling factor and the two-dimensional calculation performed in this work has no important meaning. Nevertheless, the time when the maximum water dilution rate and the corresponding maximum water dilution rate for 1-129 and Ra-226 in Pecos River after discharging from Rustler aquifer obtained in (C3) and in this work are presented in Table A2 for comparisons. The time for beginning of leaching is 1000 years and the leach time is 150,000 years. The initial amount of each nuclide are those present in a LNR reprocessed waste.

Table A2 Comparison between 1-129 and Ra-226 maximum water dilution rates obtained by Coles and Bond and by this work.

	Time of maximum (yr)		Maximum water dilution rate (m Vyr)	
	Coles and Bond	This work	Coles and Bond	This work
1-129	8.70E+3	6.00E+4	1.00E+2	7.00E+1
Ra-226	1.00E+6	1.50E+6	6.10E+0	1.00E-1

In addition, one should also note that in (C3) it is assumed that none of the U-238 present in the spent fuel is lost to the reprocessed high level waste. However, about 0.5% of the U-238 is present in the HLW and is, as our calculation showed, the main source of Ra-226 10^6 years after the leaching started.

4.7 Modelling of the Far-Field Radionuclide Migration at the Site of the Basalt Waste Isolation Project (BWIP) in Hanford, Washington

4.7.1 Review and interpretation of existent hydrological data

Hydrological data used in this work were obtained primarily from the Rockwell International report: "Hydrologic Studies within the Columbia Plateau, Washington" (R2). That report presents an integration of the current knowledge of the Hanford site region hydrology. In this section we present a brief summary of the available information and the reader should refer to above reference for more detailed descriptions.

Among the hydrologic systems present in the Columbia River basalt formation the main studies are centered within the Pasco Basin located in south-central Washington State, particularly that portion of the basin within the Hanford Site (see Figure 4.25). A geological cross section of the Pasco Basin from southwest to northeast is shown in Figure 4,25a. This figure illustrates the structure and stratigraphy of the Hanford Site. Four major groups of flows can be distinguished: the Grande Ronde, the Wanapum, the Saddle Mountains Basalt and the Ringold formation.

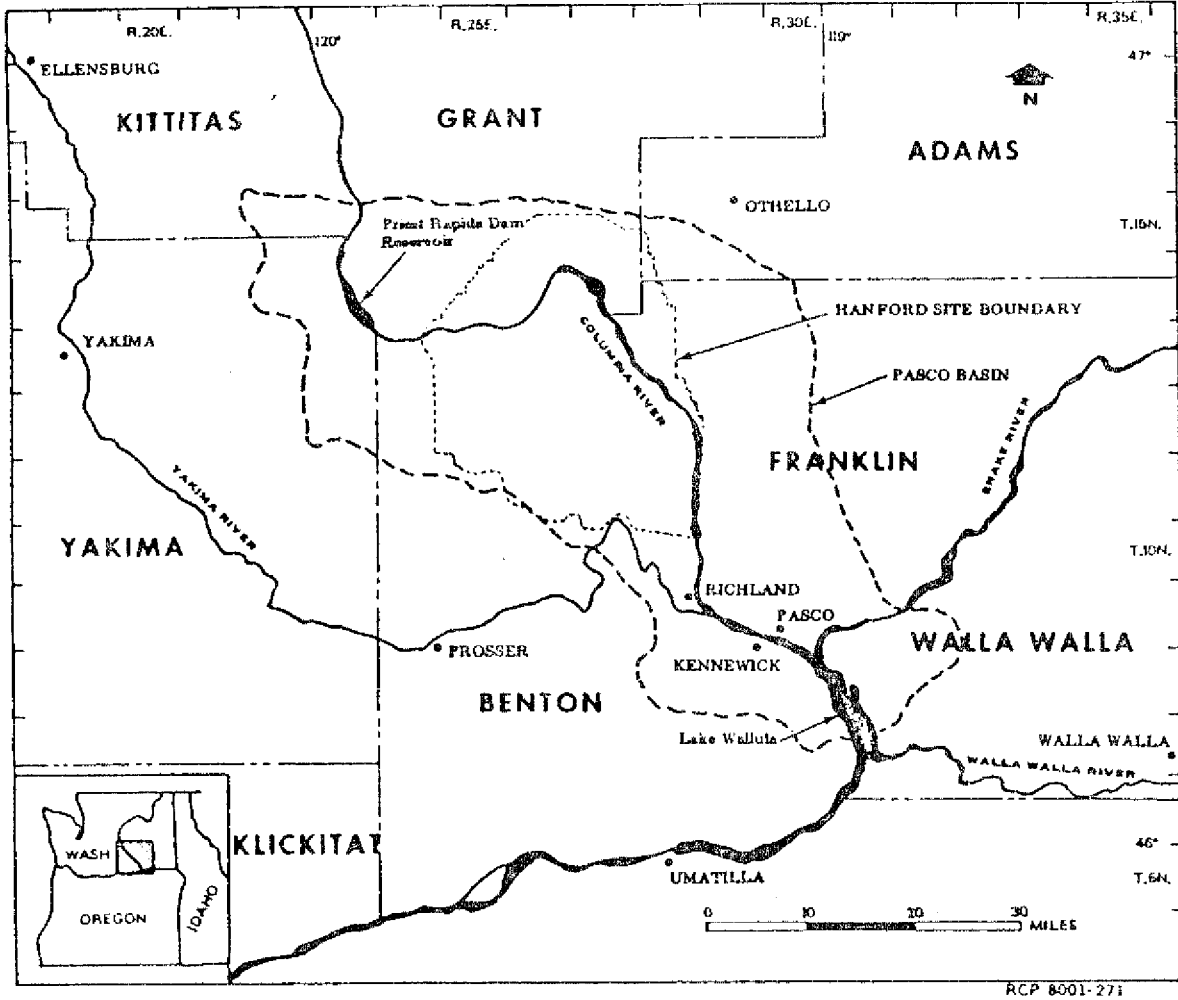


Figure 4.25 Hydrologic modelling region for the ÎT7IP site showing the Pasco Basin boundaries. (from R2)

RCP 8001-271

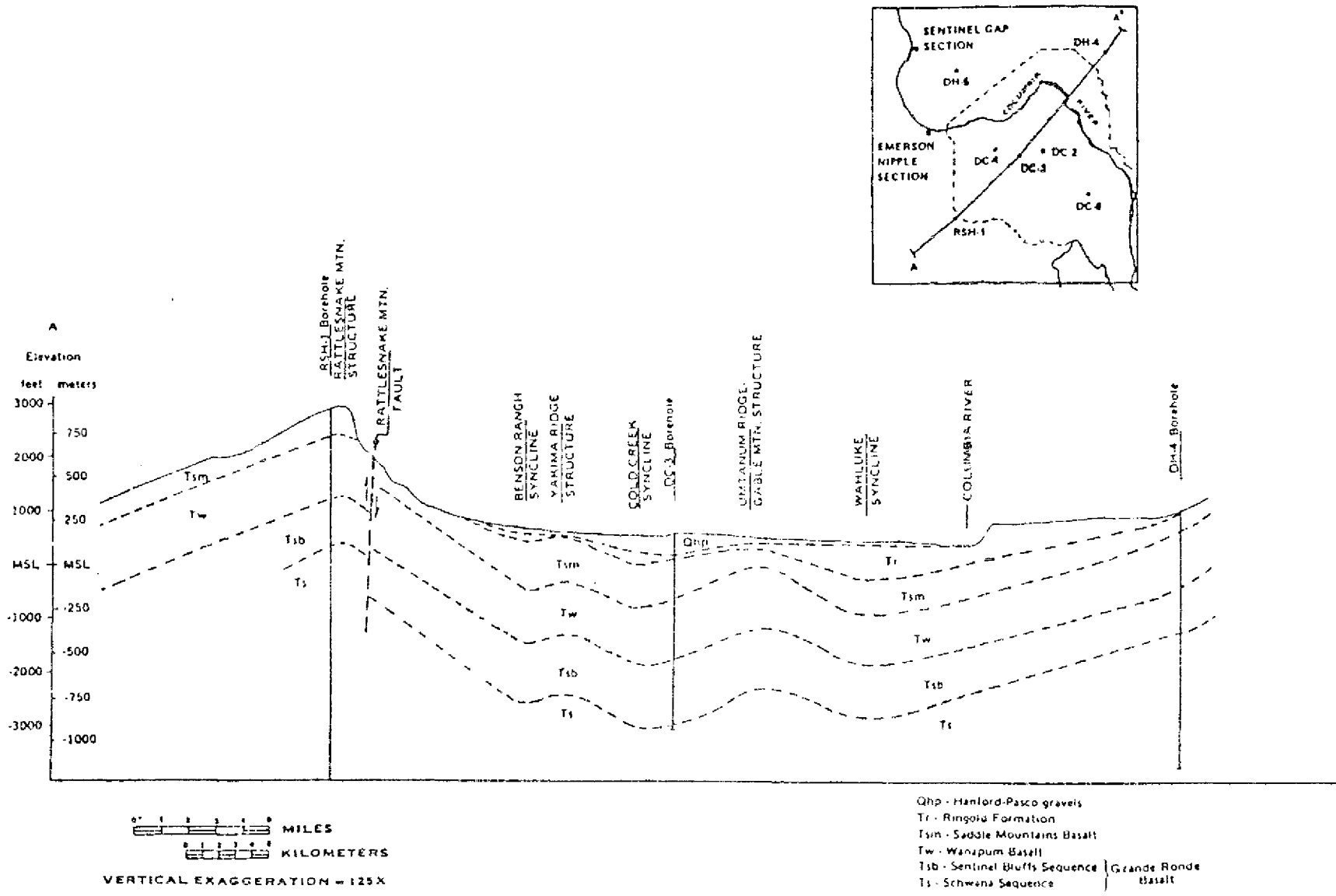


Figure 4.25a Geologic cross section of the Pasco Basin (R3).

Here we quote selected segments from (R2) on the description of the Pasco Basin with its flowing groups: "The Pasco Basin, an area of about 2,000 square miles contains one of the largest river systems in the continent, the Columbia River and its tributaries, the Snake and Yakima Rivers.

The water table is found principally in the Ringold Formation. The Ringold Formation is divided into three units: the upper, consisting of bedded fluvial silt and sand with some gravel; the middle, well sorted sand and gravel which are invariably cemented; and, the lower, primarily silt and clay with some interbedded sand and gravel. The reported hydraulic conductivity ranges from 20 to 600 feet per day for the middle unit, and 0.1 to 10 feet per day for the lower unit (R2). The unconfined aquifer attains a thickness of over 200 feet in portions of the basin with the base considered to be the top of the basalt or the thick, low permeable silt and clay of the lower unit of the Ringold formation. Discharge from the unconfined aquifer is primarily to the Columbia River, with lesser amounts to the Snake and Yakima rivers.

Within the Pasco Basin, the Columbia River Basalt Group (confined aquifers) consists of the Saddle Mountains, Wanapum, and Grande Ronde Basalts. The average total thickness of these basalts is about 5,000 feet. The confined aquifers present therein are associated with the more permeable interflow and interbedded zones and are generally located between confining

units composed of the dense, columnar portions of the basalt flows.

The Saddle Mountain Basalt and upper Wanapum Basalt receive recharge from precipitation and from stream runoff in the Rattlesnake Hills, Yakima ridge and the Saddle Mountains. The principal discharge area for aquifers within the Saddle Mountains and upper Wanapum Basalts is most probably to the Columbia River in the southeastern segment of the basin between the city of Richland, Washington and Wallula Gap. Groundwater flow beneath the Hanford Site is generally to the east and south.

Aquifers in the lower Wanapum and Grande Ronde Basalts receive minor or local recharge in the same areas as mentioned for the shallower basalts. Groundwater discharge is probably to the Columbia River, possibly in Lake Wallula, or further south in the Columbia George.

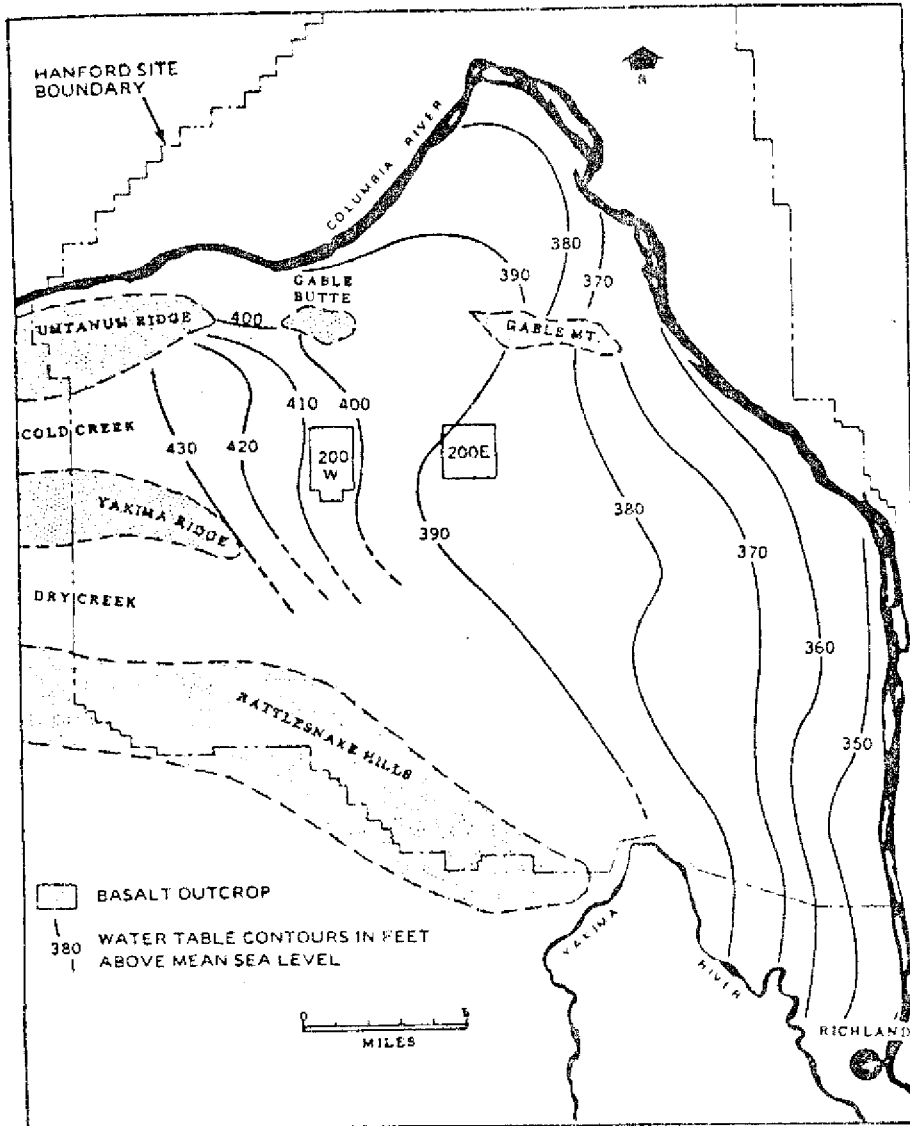
A generalized summary of the groundwater flow system in the Pasco Basin is presented. The unconfined aquifer is essentially a local system, with recharge and discharge contained within the basin. Aquifers in the Saddle Mountains Basalt and upper Wanapum Basalt principally receive recharge and discharge within the basin; although some inter-basin transfer takes place, the system is considered to be local. The lower Wanapum and the upper Grande Ronde Basalt aquifers are tentatively classified as intermediate. The lower Grande Ronde Basalt may be part of a

regional system. Recharge is from within the basin and from the surrounding plateau. Discharges areas have not been identified.

Columbia River flow rates at the aquifers discharge region depends on the electric production at the Priest Rapids Dam Reservoir located upstream. For the 60 year period of record maintained by the U.S. Geological Survey, the average discharge has been $3,250 \text{ m}^3/\text{sec}$ (120,400 cfs). The minimum recorded discharge of $111 \text{ m}^3/\text{sec}$ (4,120 cfs) occurred in 1932. In recent years peak flows during spring runoff have ranged from $4,320 \text{ m}^3/\text{sec}$ (160,000 cfs) to $14,850 \text{ m}^3/\text{sec}$ (550,000 cfs).

Figure 4.26 (obtained from R2) shows the estimated hydraulic potential map for the Ringold formation aquifers at the Hanford site. Beneath this unconfined aquifer lies the Saddle Mountains Group aquifers and an estimate of the potentiometric surface in this systems of aquifers is presented in Figure 4.27 (R2). The two groups of aquifers underlying Saddle Mountains Group, the Wanapum and Grande Ronde have insufficient piezometric data to construct a potentiometric surface for the region of the Hanford site.

At the Hanford site the exact location for the repository has not been defined yet. The proposed scenario to be assumed in assessing the performance of the repository considers an horizontal flow driven by the hydraulic potential gradient through the aquifer in which the repository is located. A crack



RCP 8001-286

Figure 4.26 Estimated 1944 water table map for the Hanford site (used as Ringold aquifer potentiometric data, from R2).

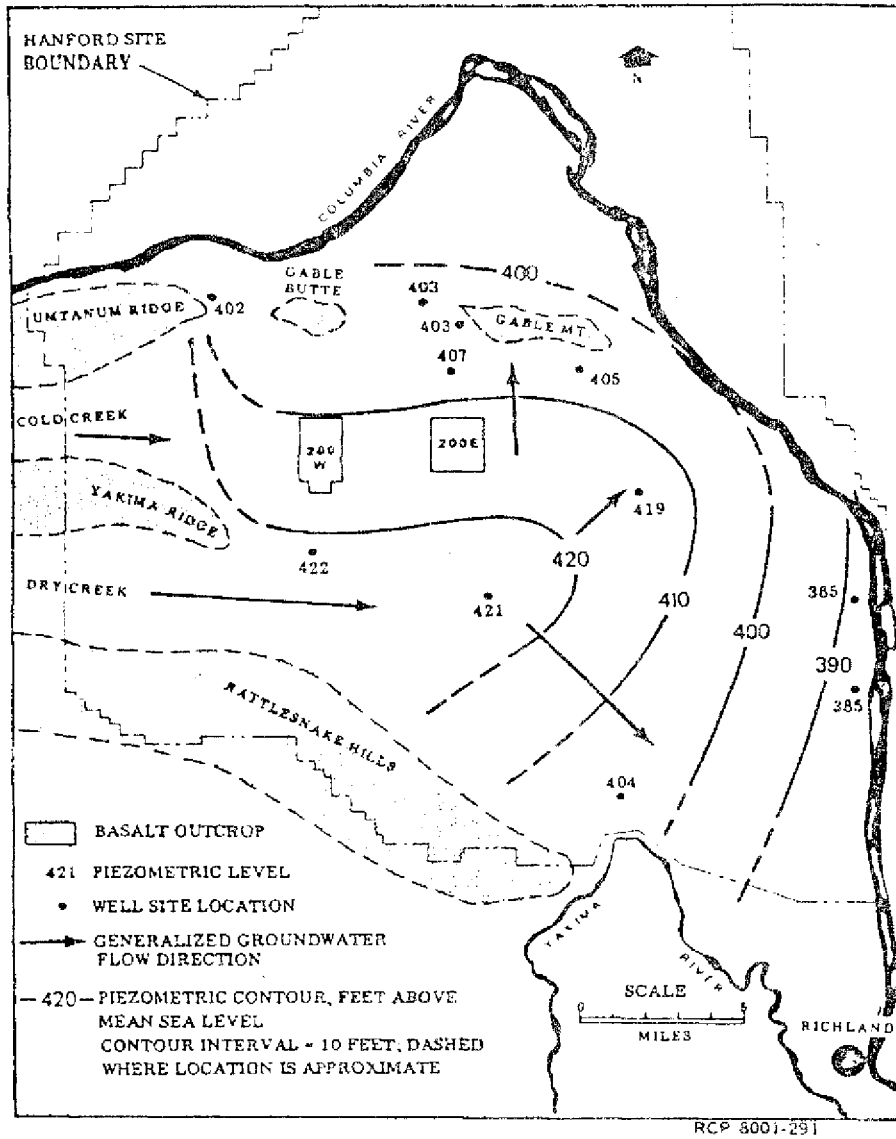


Figure 4.27 Potentiometric surface used for the Saddle Mountain Group aquifers, from R2.

is assumed to be formed at the repository site. Due to the temperature gradient caused by decay heat in addition to the natural vertical hydraulic potential gradient, groundwater from the horizontal flow is driven vertically upwards after passing through the repository. This contaminated upward flowing groundwater reaches eventually an overlying aquifer which carries the radionuclides until they discharge into the biosphere.

In this study however, a conservative assumption has been made. In any instance when radionuclides are leached out of the waste package into the groundwater they are instantly placed in the aquifer being studied. It is equivalent to say that the repository is located in the particular aquifer being analyzed. In other words, the time any radionuclide would spend in travelling vertically through the fracture is assumed negligible when compared to the time it spends in the aquifer until the discharge into the biosphere.

Therefore, the repository is placed either in the Ringold aquifer or in the Saddle Mountain Group aquifer. Due to lack of enough piezometric data, Wanapum and Grande Ronde aquifers will not be analyzed although they are possible pathways to the biosphere. Aquifer parameters values obtained from field data show that the hydraulic conductivity and porosity vary over a large range of values (R2,C6), making the choice of a representative value difficult. A summary of the hydrological data used in this work is presented in Table 4.5a (R2).

Table 4.5a Summary of hydrological data at the repository site (R2)

	Ringold aquifer	die Mountain aquifer
Thickness (m)	60	270
Hydraulic conductivity (m/yr)	A range from 10 to 105, used=500	3
Porosity	0.1	0.1

4.7.2 Determination of the contaminated regions and radionuclide discharge rates in the BWIP case

Similar calculations as were done for the WIPP site (Section 4.6.2) are repeated here for the BWIP site. Table 4.6 and Table 4.7 summarizes the nuclides parameters used in this case. These tables differ from the corresponding Table 4.2 and 4.3 for the WIPP site because the retardation coefficient of some nuclides are different for basalt formations. Table 4.6 presents the parameters used for the long lived fission products present in high level waste. Again as in the previous case 1-129 with its unit retardation coefficient and long half life requires the largest water travel time to be contained. Table 4.7 summarizes the parameters for the actinide chains present in reprocessed high level waste. Once more Ra-226 which activity is controlled by its precursor U-234 and U-238 is the most potentially hazardous actinide. Table 4.8 is a listing of the most hazardous nuclide in the BWIP site ranked according to the product 1^{\wedge} (see

Table 4.6 Long Lived Fission Products Parameters for BWIP site

Nuclide	a/ κ _i (yr)	(MPC). x (Ci/m ³)	c/ M. (Ci/GwYr)	10 ⁶ V _i (yr)	.001M _i /MPC (m ³ /GwYr)	
H-3	1.2E+1	1.0E+0	3.0E-3	1.9E+4	1.2E+2	6.3E+3
C-14	5.6E+3	1.0E+1	8.0E-4	1.3E+1	5.6E+3	1.6E+1
Se-79	6.5E+4	1.0E+0	3.0E-4	1.1E+1	6.5E+5	3.6E+1
Sr-90	2.8E+1	5.7E+3	3.0E-7	2.1E+6	4.9E-2	7.0E+8
Zr-93	9.5E+5	5.7E+2	8.0E-4	5.2E+1	1.6E+4	6.4E+1
Nb-93m	1.4E+1	1.0E+4	4.0E-4	5.0E+0	1.4E-2	1.2E+1
Tc-99	2.1E+5	1.0E+0	2.0E-4	3.9E+2	2.1E+6	1.9E+3
Ru-106	1.0E+0	1.0E+1	1.0E-5	1.1E+7	1.0E+0	1.1E+9
Cd-113ra	1.4E+1	1.0E+4	3.0E-5	1.3E+3	1.4E-2	4.5E+4
Sn-126	1.0E+5	5.7E+2	2.0E-5	1.5E+1	1.8E+3	7.4E+2
Sb-125	2.7E+1	1.0E+2	1.0E-4	2.1E+5	2.7E+0	2.1E+6
I-129	1.7E+7	1.0E+0	6.0E-8	1.0E+0	1.7E+8	1.7E+4
Cs-137	3.0E+1	5.7E+3	2.0E-5	2.9E+6	5.3E-2	1.5E+8
Cs-135	3.0E+6	5.7E+3	1.0E-4	7.8E+0	5.3E+3	7.8E+1
Ce-144	7.8E-1	1.2E+4	1.0E-5	2.1E+7	6.5E-4	2.1E+9
Pm-147	4.4E+0	2.5E+3	2.0E-4	2.6E+6	1.8E-2	1.3E+7
Sm-151	8.7E+1	2.5E+3	4.0E-4	3.4E+4	3.5E-1	8.5E+4
Eu-152	1.3E+1	2.5E+3	6.0E-5	3.3E+2	5.0E+3	5.5E+3
Eu-154	1.6E+1	2.5E+3	2.0E-5	1.9E+5	6.4E-2	9.4E+6
Eu-155	1.8E+0	2.5E+3	2.0E-4	1.7E+5	7.2E-3	8.7E+5

a/:From reference (R2), (B3).

b/:From 10CFR20,Appendix B and (P2).

c/:For reprocessed high level waste, LWR, 10 years decay, 0.5% U and Pu loss into the waste, (B2).

Table 4.7 Actinide Chains Parameters for The BWIP site

Nuclide	λ (yr)	K_1	$J?/(MPC)$	M_i^0 (Ci/GwYr)	$10T, /K.$ (yr)	$, 001M_i^0/W$ (m ³ /GwYr)
Ra-325	4.1E-2	2.8E+3	5.0E-7		7.5E+4	8.7E+5
Ra-226***	1.6E+3	2.8E+3	3.0E-8	-	4.4E+3	1.5E+3
Ra-226****	1.6E+3	2.8E+3	3.0E-8	-	7.9E+7	5.5E+1
Th-228	1.9E+0	5.7E+3	7.0E-6	-	1.2E+0	8.9E+4
Th-229	7.3E+3	5.7E+3	5.0E-7	-	7.5E+4	1.2E+4
Th-230***	8.0E+4	5.7E+3	2.0E-6	-	4.4E+3	3.2E-1
Th-230****	8.0E+4	5.7E+3	2.0E-6	-	7.9E+7	8.4E-3
U-233	1.6E+5	5.2E+2	3.0E-5	-	7.5E+4	2.0E+2
U-234	2.5E+5	5.2E+2	3.0E-5	1.2E+0*	4.4E+3	3.9E+1
U-235	7.1E+8	5.2E+2	3.0E-5	2.3E-3	1.2E+7	7.7E-2
U-238	4.5E+9	5.2E+2	4.0E-5	4.3E-2	7.9E+7	1.0E+0
Np-237	2.1E+6	2.8E+2	3.0E-6	1.5E+1**	7.5E+4	5.2E+3
Pu-238	3.6E+1	5.7E+3	5.0E-6	5.1E+2	1.5E-1	1.0E+5
Pu-239	2.4E+4	5.7E+3	5.0E-6	4.4E+1	4.2E+1	8.3E+3
Pu-240	6.6E+3	5.7E+3	5.0E-6	2.7E+2	1.2E+0	5.3E+4
Pu-241	1.3E+1	5.7E+3	2.0E-4	1.4E+4	3.1E+1	7.0E+4
Pu-242	3.9E+5	5.7E+3	5.0E-6	1.9E-1	6.6E+2	3.3E+1
Am-241	4.6E+2	1.0E+4	4.0E-6	4.9E+3	4.6E-1	1.2E+6
Am-242m	1.5E+2	1.0E+4	4.0E-6	1.2E+2	1.5E-1	2.9E+4
Am-243	7.9E+3	1.0E+4	4.0E-6	4.8E+2	7.9E+0	1.2E+5
Cm-242	4.5E-1	3.0E+3	2.0E-5	4.4E+5	1.5E-1	2.2E+7
Cm-243	3.2E+1	3.0E+3	5.0E-6	9.0E+1	1.0E-1	1.3E+4
Cm-244	1.8E+1	3.0E+3	7.0E-6	7.4E+4	5.9E-2	1.0E+7
Cm-245	9.3E+3	3.0E+3	4.0E-6	9.9E+0	3.1E+1	2.4E+3
Cm-246	5.5E+3	3.0E+3	4.0E-6	1.9E+0	1.8E+1	4.8E+2

•Includes the decay of Pu-218, Am-242n and Cm-242.

**Includes the decay of Pu-241 and Am-241.

***Based on the decay of U-234

****Based on the decay of U-238

_a/:From reference (R2), (B3).

h/:From 10CFR20, Appendix B and (P2).

c/:For reprocessed high level waste, LWR, 10 years decay, 0.5% U and Pu loss into the waste, (B2).

Am-242m is the metastable form of Am-242

Eq. (4.6.2)). As in the WIPP case, 1-129 and Ra-226 are the two first ranked nuclides.

Table 4.8 Potential Hazardous Nuclide Ranking for the BWIP site

Ranking	Nuclide	$10T / K(\text{yrs})$	$I. (\text{m yr})$
1	1-129	1.7E+8	7E+9
2	Ra-226	7.9E+7*	2E+8
3	Tc-99	2.1E+6	6E+7
4	Se-79	6.5E+5	3E+6
5	Th-230	3.4E+6*	1E+6
6	Np-237	7.5E+4	5E+5

*Ra-226 is assumed to be in secular equilibrium with U-238. Thus values of half-life and retardation coefficient for U-238 were used

Since piezometric data is at present available in sufficient quantity only for the Ringold aquifer and the Saddle Mountain Group aquifer, the hydrological calculations were restricted to these two groups of aquifers, although the Wanapum and Grande Ronde formations are also potential pathways to the biosphere.

Figure 4.28 is the three dimensional representation of the Potentiometric surface in the Ringold aquifer. Two distinct valleys in the surface indicate that the Ringold aquifer discharges into the Columbia River in two different locations. The projection of the river flow pattern on the Potentiometric

surface is also shown. Two arbitrary locations have been chosen for a sensitivity study. The first location denoted by "Repository 1" coincides with the present reprocessing plant where low level radioactive **waste has** been placed on the surface. The projection of this first location lies on one of the potentiometric valleys (see Figure 4.20). The contaminated streamlines converge and then flow eastward until they discharge into the Columbia River. The second location is 2 km away to the south from the "Repository 1". This second location was chosen between the two valleys as shown in Figure 4.28 so that one would not expect any confluence of the contaminated streamlines.

Figure 4.29 is the three-dimensional representation of the potentiometric surface in the Saddle Mountains aquifers. Contrary to the Ringold aquifer this aquifer presents a hill-shaped profile. This type of profile will tend to divide the streamlines. The divergence effect caused by this hill shaped surface is opposite to the confluence effect caused by the potentiometric valleys shown in Figure 4.28. Two different locations for the repository site are again considered: Repository 1 is located on the south, face of the hill and all the contaminated streamlines will flow southward; Repository 2 by its turn is located right on the ridge of the potentiometric hill. In this second case part of the streamlines will flow to the north and part will flow to the south. One should note that these repository locations do not coincide geographically with the two locations assumed for the Ringold formation calculations.

POTENTIOMETRIC SURFACE IN THE AQUIFER - RINGOLD AQUIFER

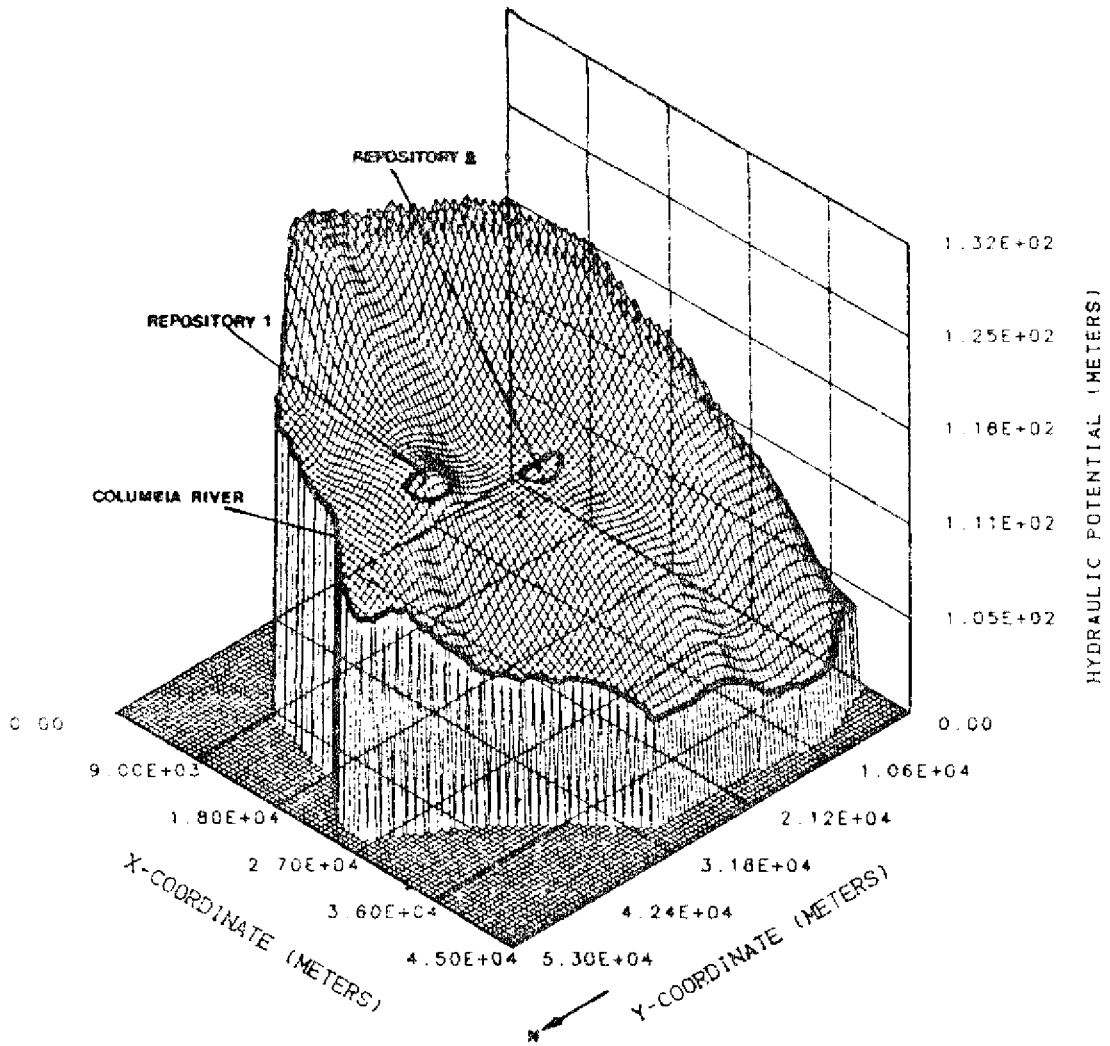


Figure 4.28 Potentiometric surface in Ringold aquifer with rejection of Columbia River onto the surface.

POTENTIOMETRIC SURFACE IN THE AQUIFER - SADDLE MOUNTAIN AQU,

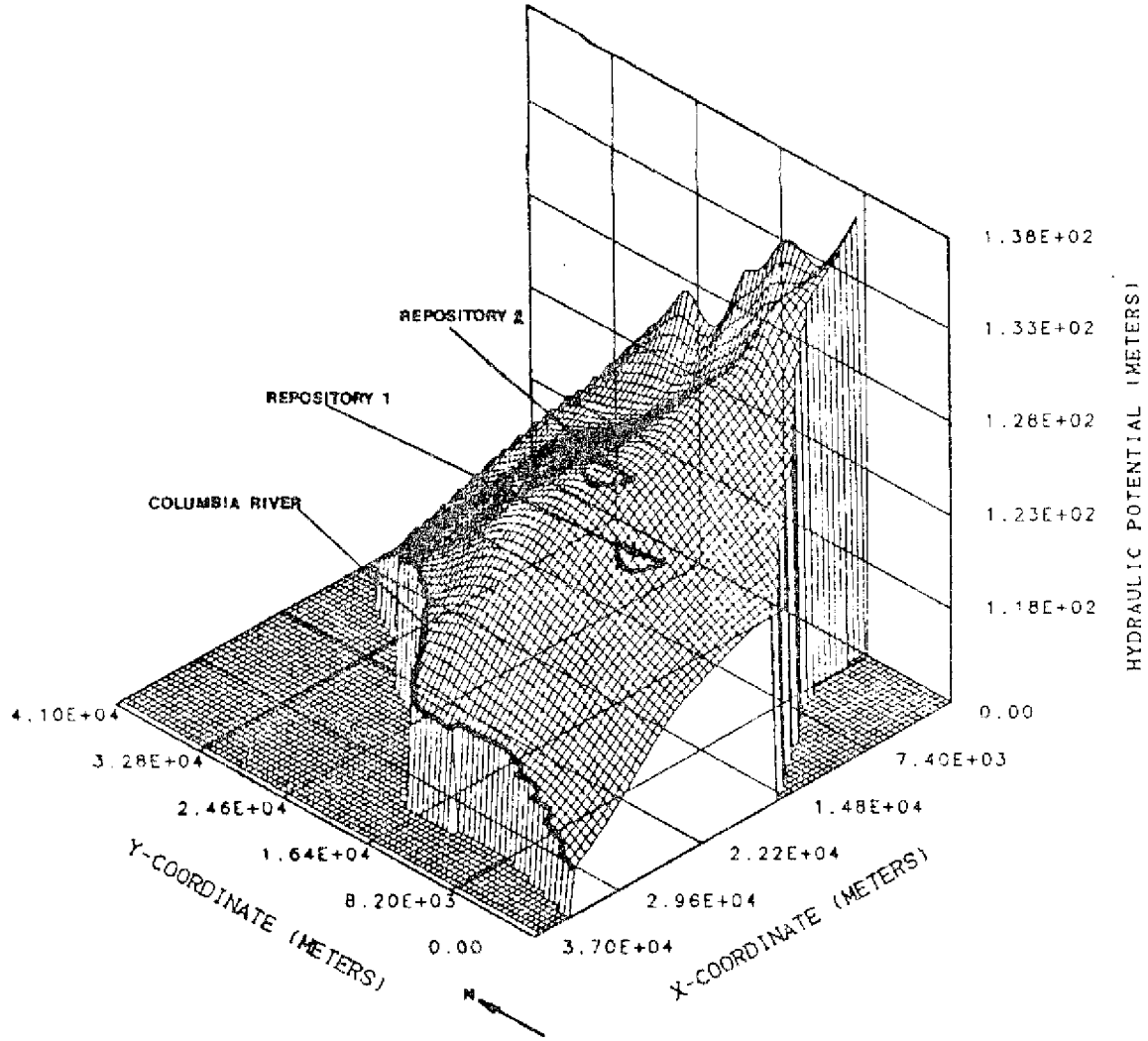


Figure 4.29 Potentiometric surface in Saddle Mountain Group aquifer with the projection of Columbia River onto the surface.

The shadow region in each of the calculations was characterized by five streamlines covering the entire shadow region. Table 4.9 contains a summary of the hydrological calculations results for the two aquifers considered in the BWTP site and it shows the water travel time for each streamline at the biosphere.

Table 4.9 Water Arrival Time (years) at the Biosphere for the BWIP site

Streamline no. a/	Water travel time (years)			
	Ringold repository-1	Ringold repository-2	Saddle repository-1	Saddle repository-2
1	2.67E+2	3.12E+4	1.24E+6	7.84E+6
2	2.93E+2	2.45E+4	1.41E+6	4.63E+6
3	1.95E+2	1.52E+5	9.15E+5	6.46E+6
4	3.41E+2	2.89E+4	1.36E+6	3.6 3E+6
5	5.31E+2	1.22E+4	5.62E+6	1.25E+6

_a/See Figures 4.30, 4.34, 4.38 and 4.41

For the Repository 1 the Ringold aquifer has very small water travel times to the biosphere. Early confluence of the streamlines near the repository causes the water velocity to be greatly increased, reducing the water travel time by orders of magnitude. If the repository were to be located at this position, in an accidental release of radionuclide from the waste into the aquifer, all radionuclides with $10T/K$ larger than 500

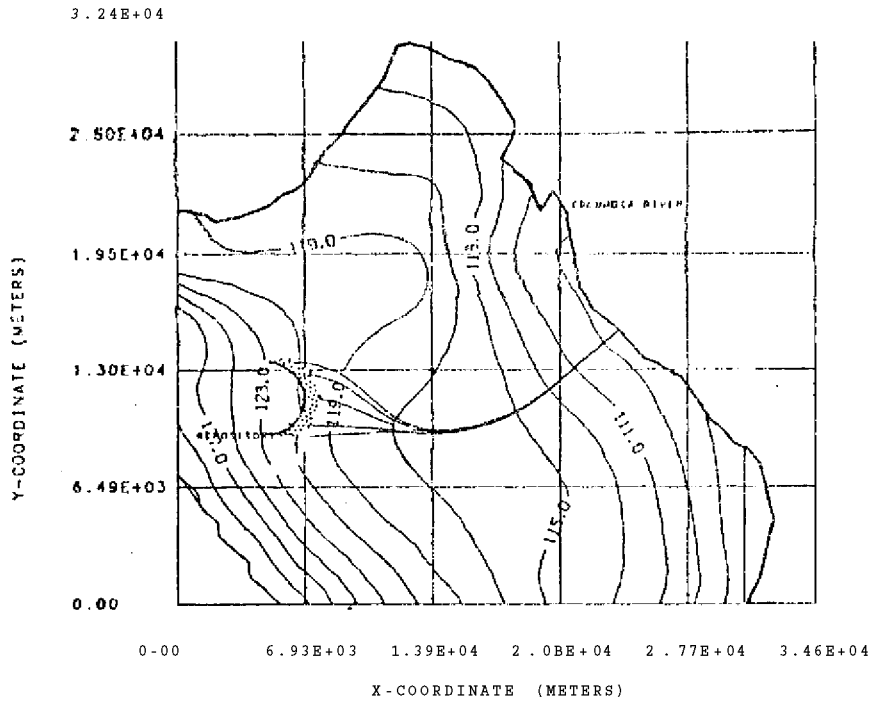
years would discharge into Columbia River. One can see from Table 4.6 and 4.7 that many nuclides should be important. On the other hand, by moving the repository to the second location (Repository 2) only 2 km to the south, the water travel time is increased by two orders of magnitude, reducing greatly the number of radionuclides that might be able to reach Columbia River.

Table 4.9 shows that the water travel times in the Saddle Mountains Group aquifers to reach the biosphere are larger than 10^6 years for any of the cases studied. 1-129 is the only nuclide that can have a significant discharge rate into the biosphere with such large water travel times.

The 1-129 and Ra-226 contaminated regions in the Ringold aquifer, Repository 1 are shown in Figure 4.30 and Figure 4.31 respectively. The confluence of streamlines takes place close to the repository, which increases the groundwater velocity and reduces the water travel time to the biosphere. It would take about 300 years for 1-129 and about 10 years for Ra-226 to start discharging into the river.

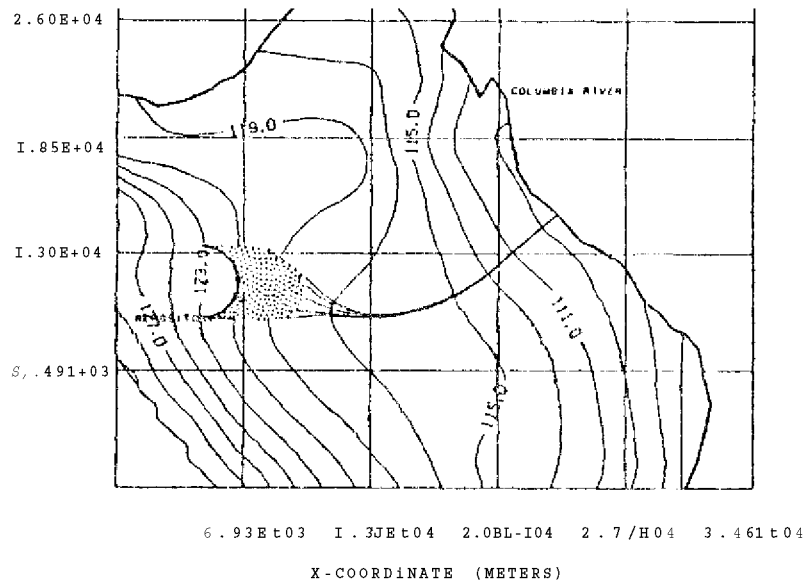
Figure 4.32 and Figure A.33 shows the discharge rate history of 1-129 and Ra-226 in the Columbia River through Ringold aquifer, Repository 1. Three leach times are considered: 10^4 , 10^5 and 10^6 years. For a leach time of 10^4 years, 1-129 dominates the water dilution rate until 10^4 years and after 10^4 years Ra-226 is the largest contributor although its water

1-129 CONTAMINATED REG10N-RINGOLD AQUIFER AFTER
5.00E+01 YRS



1-129 CONTAMINATED REGION-RINGOLD AQUIFER AFTER
2.00E+02 YRS

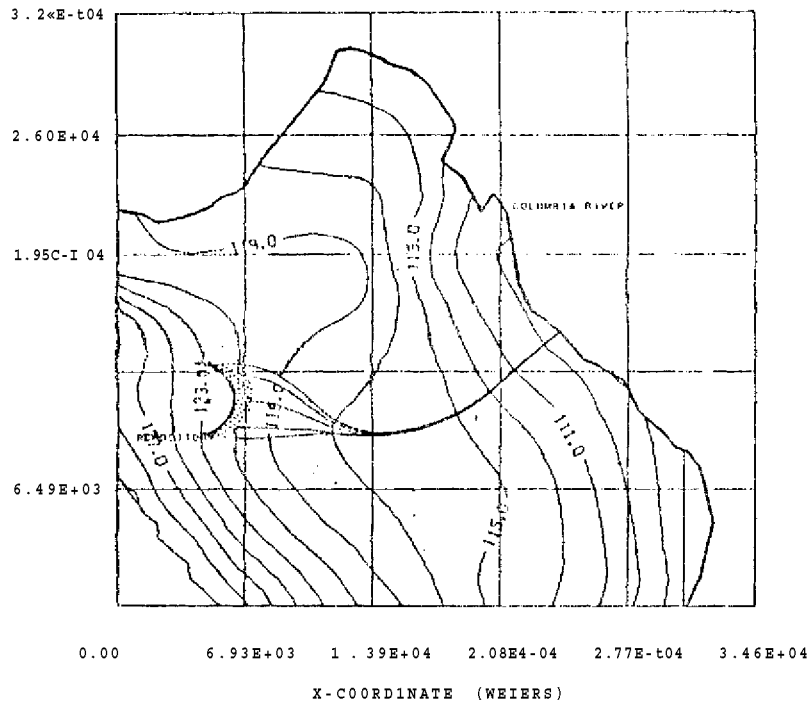
J. I4F<OI



nnre 4.30 1 — 129 cont a"! i n a'z or err 5. on \n ii" <~cl" n>
(rer>os.vtorv 1) ^ .ft^r °0 ?n/ 2T" " <>r\r<3.

T>PF i 1 1 Q 1 .Tn E- ^ 1" ^ PXP>*7P' **^.

RA-226 CONTAMINATED REGION-RINGOLD) AQUIFER AFTER 1.0QE+04YRS



RA-226 CONTAMINATED REGION-RINGOLD AQUIFER AFTER 1.00E+05YRS

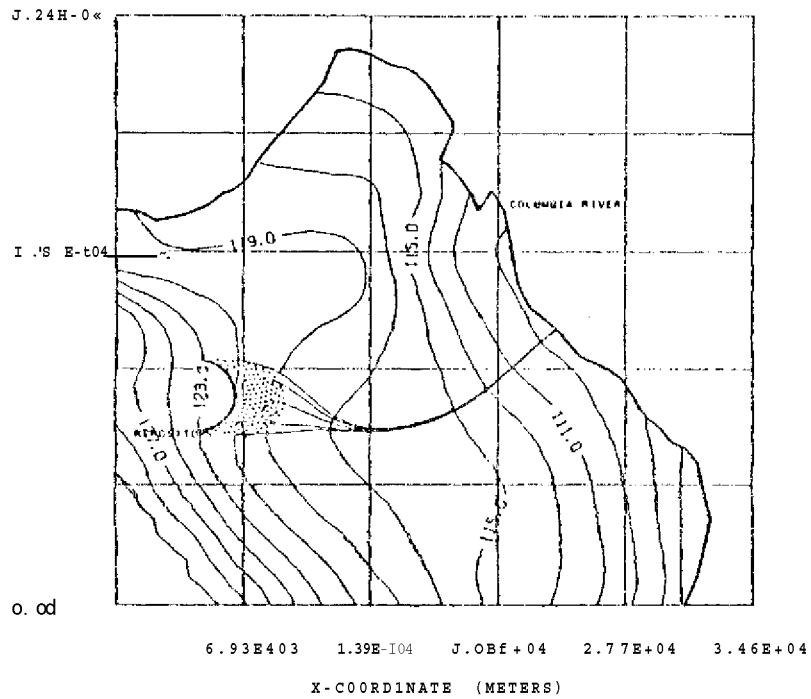


Figure 4.31 Ra-226 contaminated, region in Ringold aquifer (Repository 1) after 10* and 105 years. Potentials are in meters above M.S.L.

dilution rate is four orders of magnitude smaller than for 1-129. However, the maximum cumulative discharge of Ra-226 is one order of magnitude larger than the cumulative discharge of 1-129. This is because the total water dilution volume due to the decay of all U-238 present initially at the repository, producing Ra-226 nuclides is larger than the total water dilution rate due to the decay of all 1-129.

In the case of "Repository 2" for Ringold aquifer. Figure 4.34 and Figure 4.35 shows the contaminated region for 1-129 and Ra-226 at different times. Figure 4.36 and Figure 4.37 shows their discharge rate histories. For this second location the water travel times to the biosphere are larger by more than one order of magnitude and the nuclide arrival times are correspondingly larger. 1-129 takes longer than 10^4 years to reach the river while Ra-226 takes more than 10^7 years. The magnitude of the water dilution rates and water dilution volume for 1-129 and Ra-226 are not significantly changed when compared to the Repository 1 case. However, one must keep in mind that in the Repository 1 case, other nuclides besides 1-129 and Ra-226 (those with $10T^*/K_d$ larger than 500) can also discharge into the Columbia River because of the short water travel time to the biosphere. This can increase the total water dilution rate.

1-129 and Ra-226 contaminated regions in Saddle Mountains Group aquifers, "Repository 1" are shown in Figure 4.38 and Figure 4.39 respectively. As expected, the contaminated

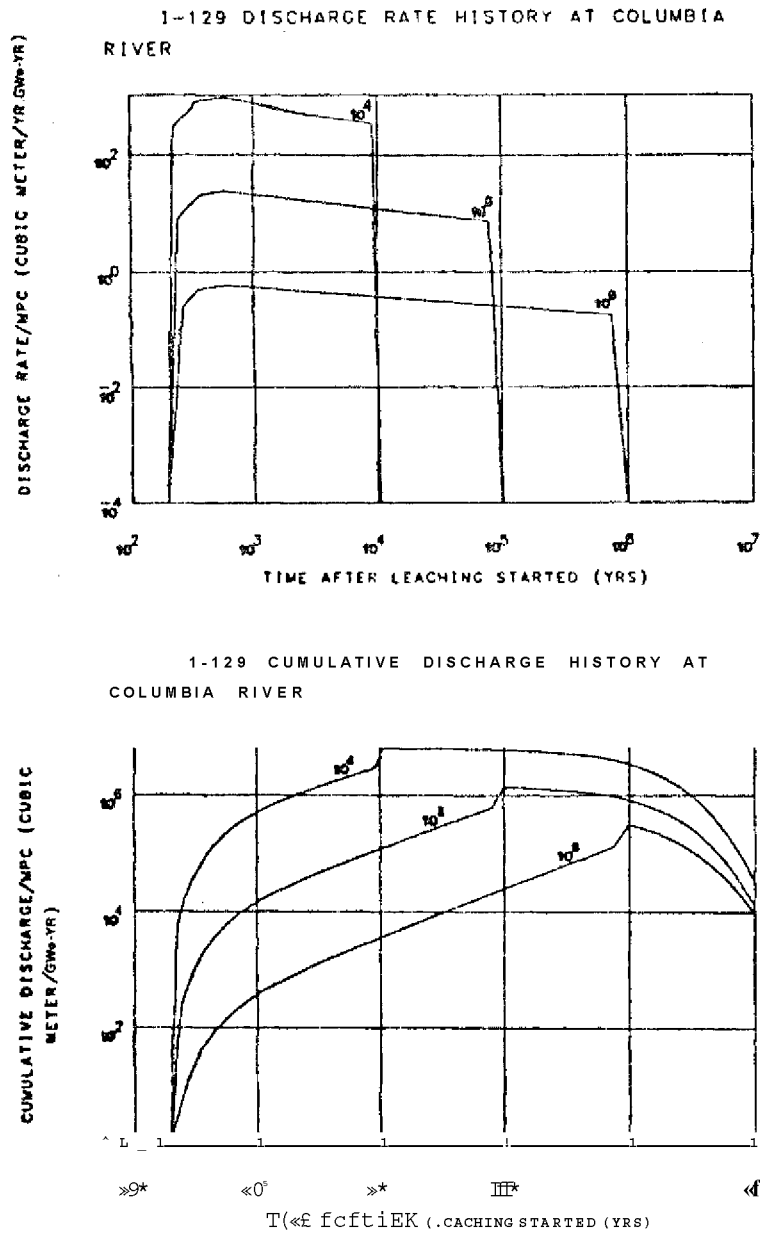


Figure 4.32 1-129 discharge rate/MPC (water dilution rate) and cumulative discharge/MPC (water dilution volume) at Columbia River discharging from Ringold aquifer (Repository 1) for leach times of 10^1 , 10^5 and 106 years.

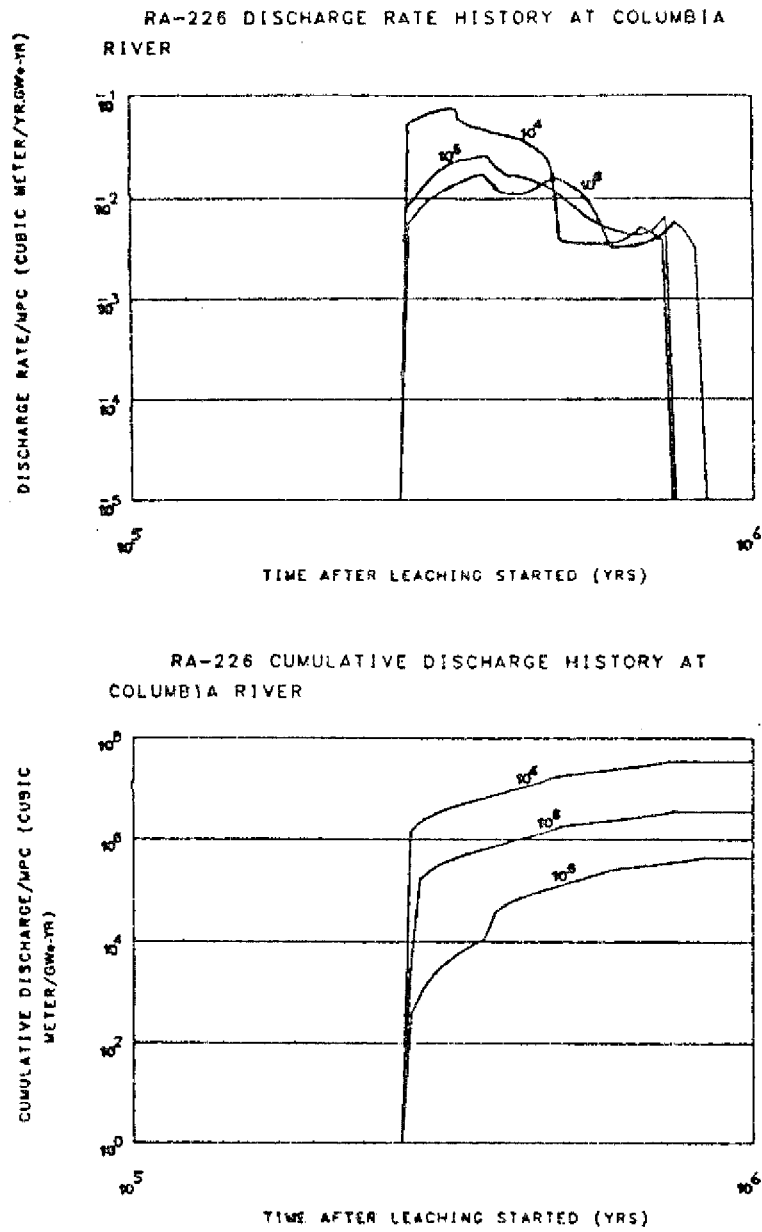
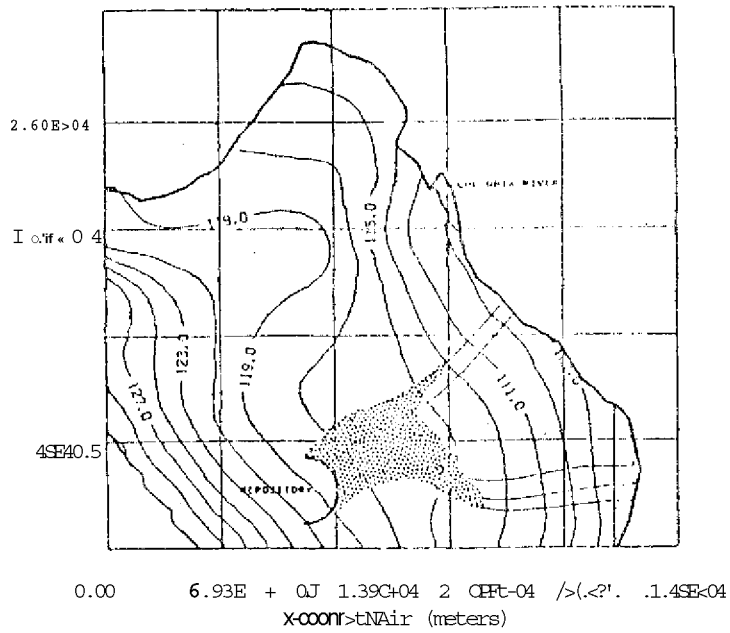


Figure 4.33 Ra-226 discharge rate/MPC (water dilution rate) and cumulative discharge/MPC (water dilution volume) at Columbia River discharging from Ringold aquifer (Repository 1) for leach times of 10^4 , 10^5 and 10^6 years

1-129 CONTAMINATED REGION-RINGOLD AQUIFER AFTER
1.00E+04 YRS



1-129 CONTAMINATED REGION-RINGOLD AQUIFER AFTER
1.00E+05 YRS

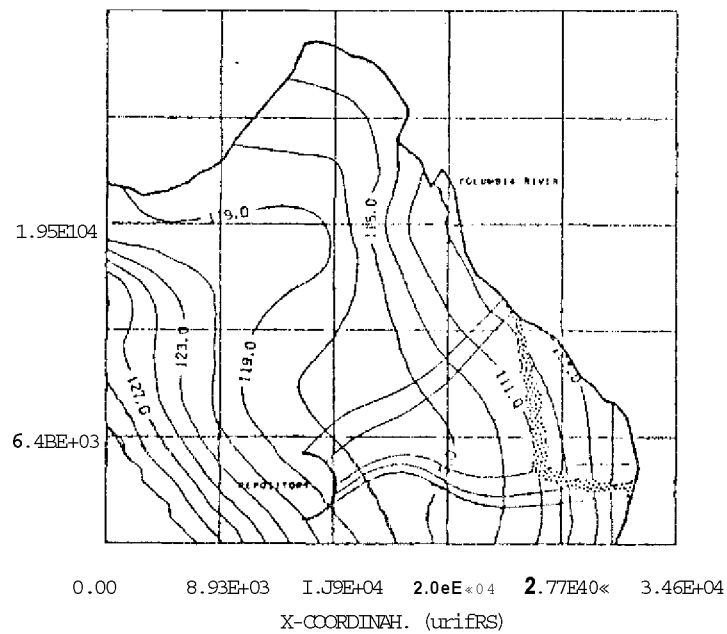
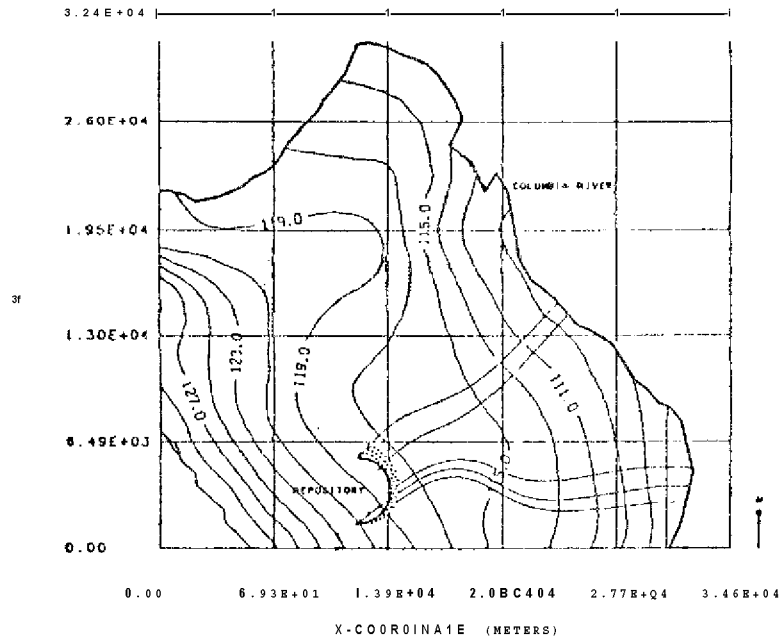


Figure 2.34 1-129 contaminated region in Ringold aquifer (Repository 2) after 10⁴ and 10⁵ years. Potentials are in meters above MPL.

RA-226 CONTAMINATED REGION-RINGOLD AQUIFER AFTER
1.00E+05YRS



RA-226 CONTAMINATED REGION-RINGOLD AQUIFER AFTER
1.00E+07YRS

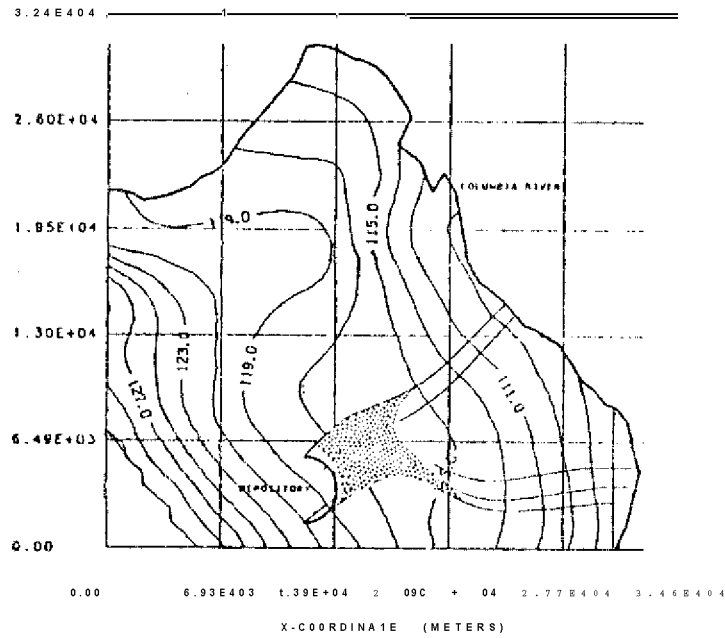


Figure A.35 Ra-22* contaminated region in Ringold (Repository 2) after 100,000 and 10,000,000 years. Potentials are in meters above T>L.

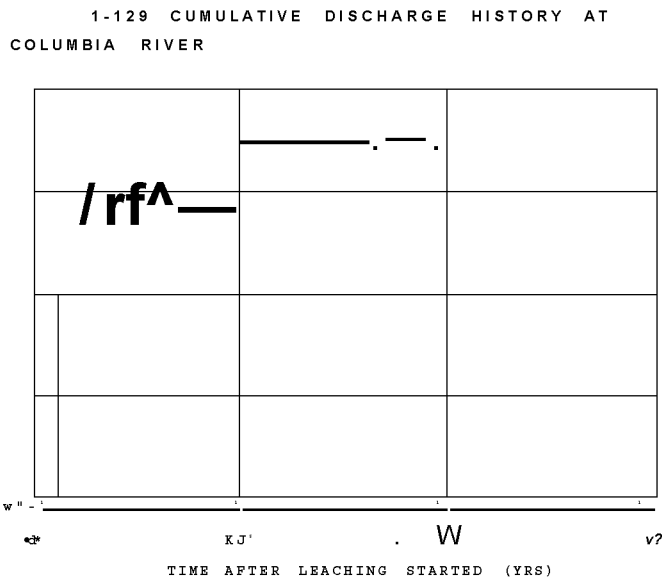
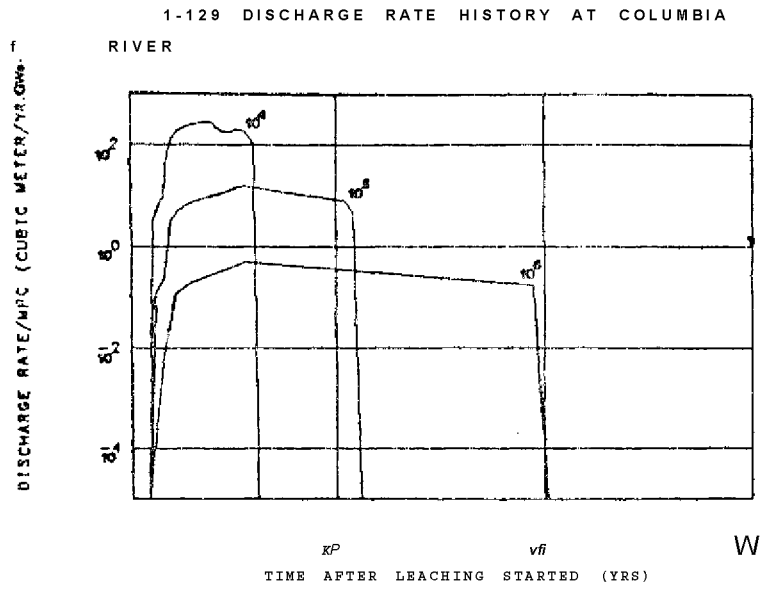


Figure 4.36 1-129 discharge rate/MPC (water dilution rate) and cumulative discharge/MPC (water dilution volume) at Columbia River discharging from Ringold aquifer (Repository 2) for leach times of 10^4 , 10^5 and 10^6 years

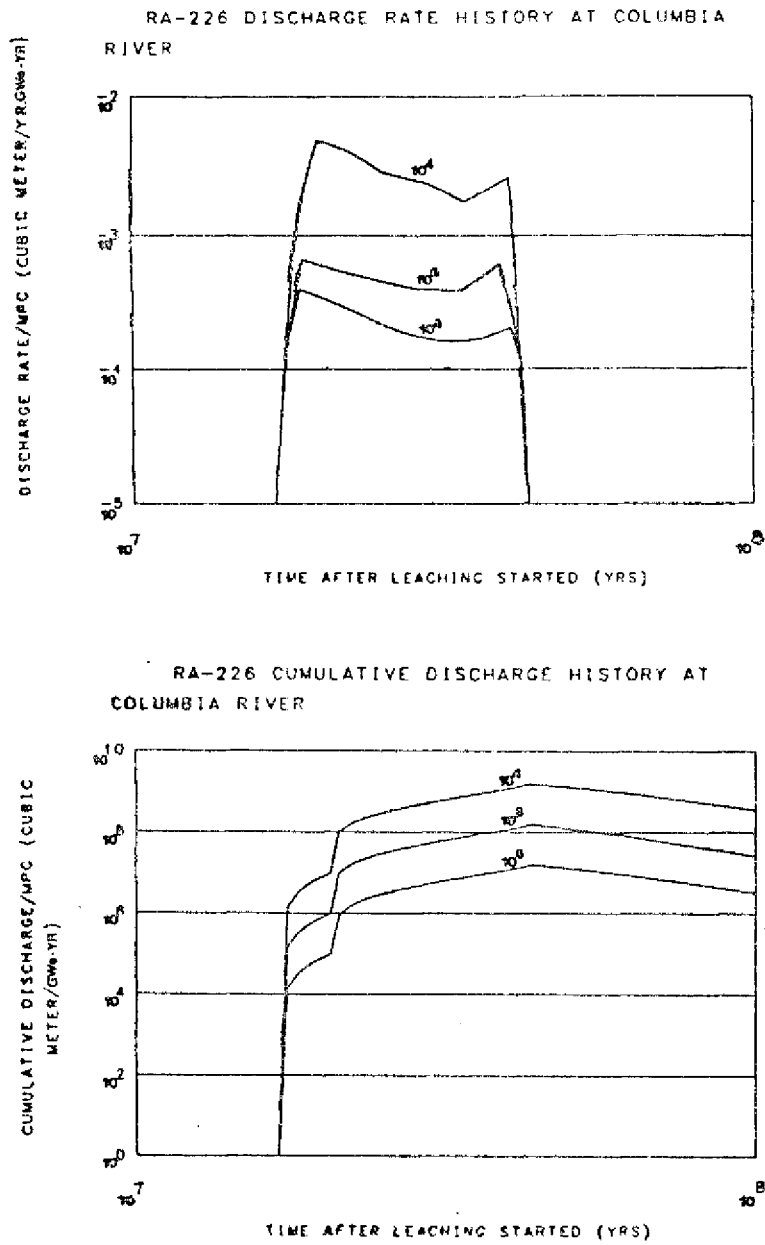


Figure 4.37 Ra-226 discharge rate/MPC (water dilution rate) and cumulative discharge/MPC (water dilution volume) at Columbia River discharging from Ringold aquifer (Repository 2) for leach times of 10', 105 and 106 years

streamlines neither confluence nor diverge strongly because the repository is located on the south face of the potentiometric surface. The streamlines develop rather uniformly towards the southeast reaching the Columbia River after about 10^6 years, (see Table 4.9). Ra-226 reaches the Columbia River along with its precursor TJ-238 after 10^7 years. 1-129 water dilution rate from the Saddle Mountain aquifer is shown in Figure 4.40.

The last case studied is the Saddle Mountain aquifer with the "Repository 2" location. This second location is on the ridge of the hill of the potentiometric surface. A peculiar behaviour is seen here. Part of the streamlines flow northward discharging into Columbia River and part of them flows southeastward also discharging into the same river, see Figure 4.41.

Although the water travel times at the biosphere for this second case are somewhat larger than those of the first repository (see Table 4.9), the important difference lies in the location of the discharge. In the Repository 1 case the location of discharge is a segment of about 10 km along Columbia River while for the Repository 2 the location of discharge spreads over a distance of about 35 km along the river. The contaminated regions for the Repository 2 are also larger than for Repository 1. Figure 4.41 and Figure 4.42 show the 1-129 and Ra-226 contaminated regions for this second repository location in Saddle Mountain aquifer. Figure 4.43 shows the 1-129 water

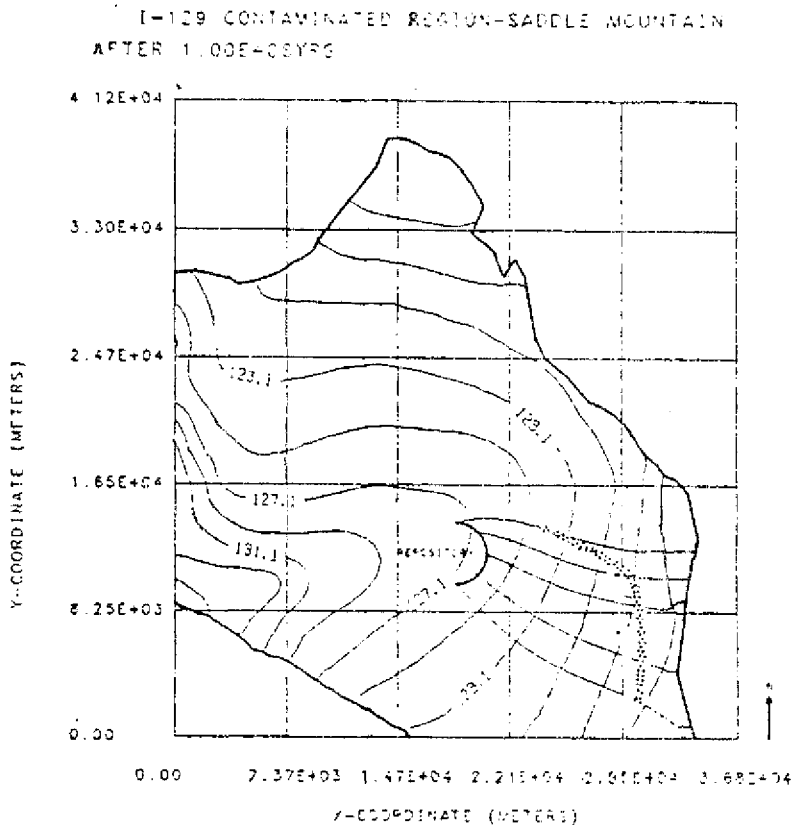
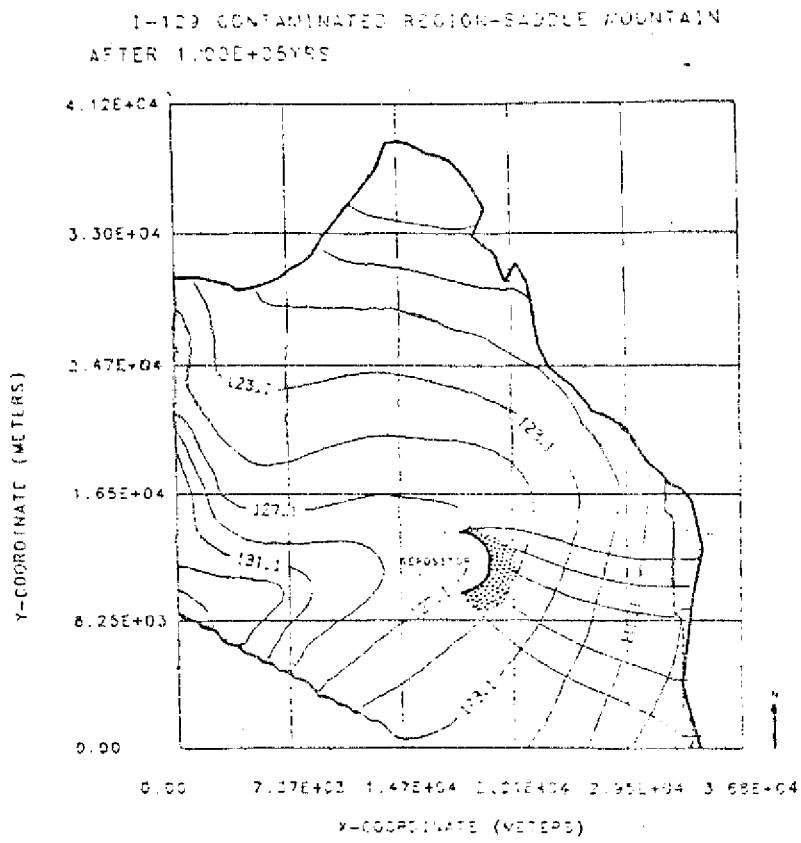


Figure 4.38 1-129 contaminated region in Saddle Mountain aquifer (Repository 1) after 10⁵ and 10⁶ years. Potentials are in meters above MSL.

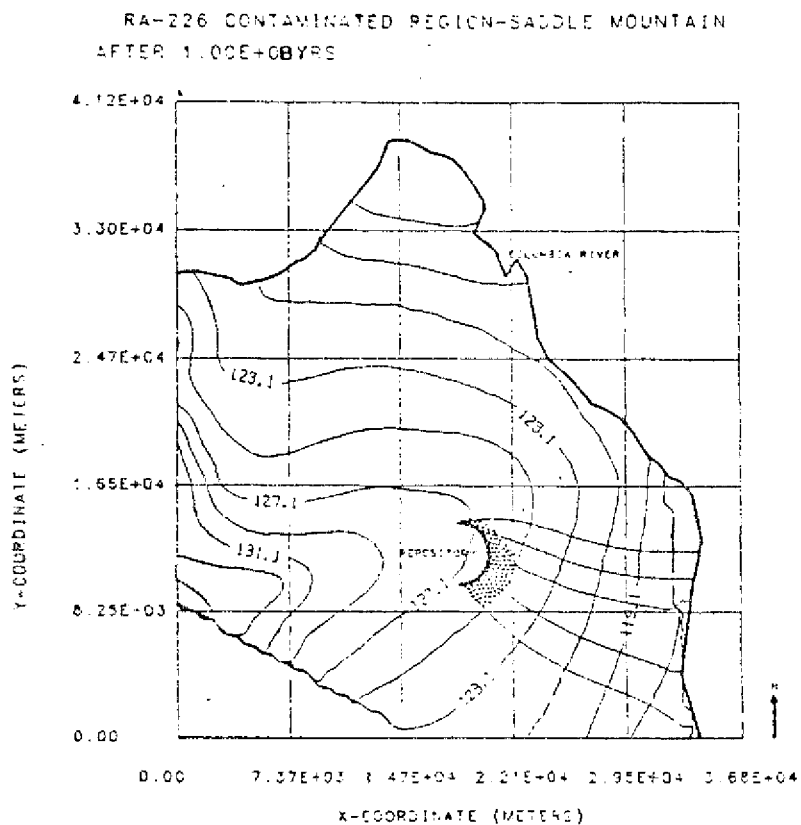
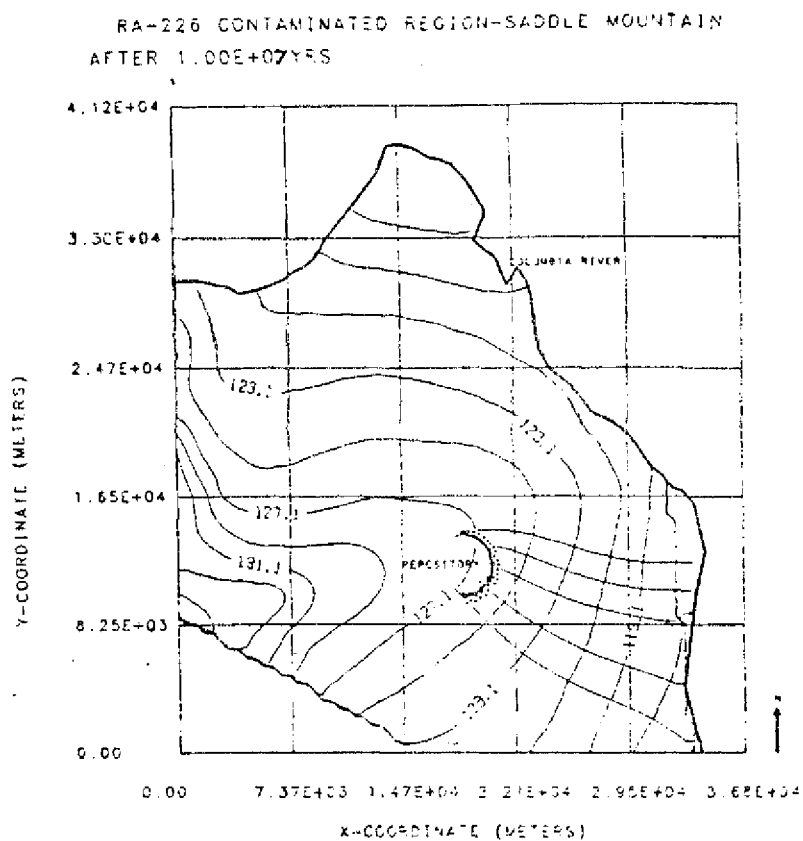
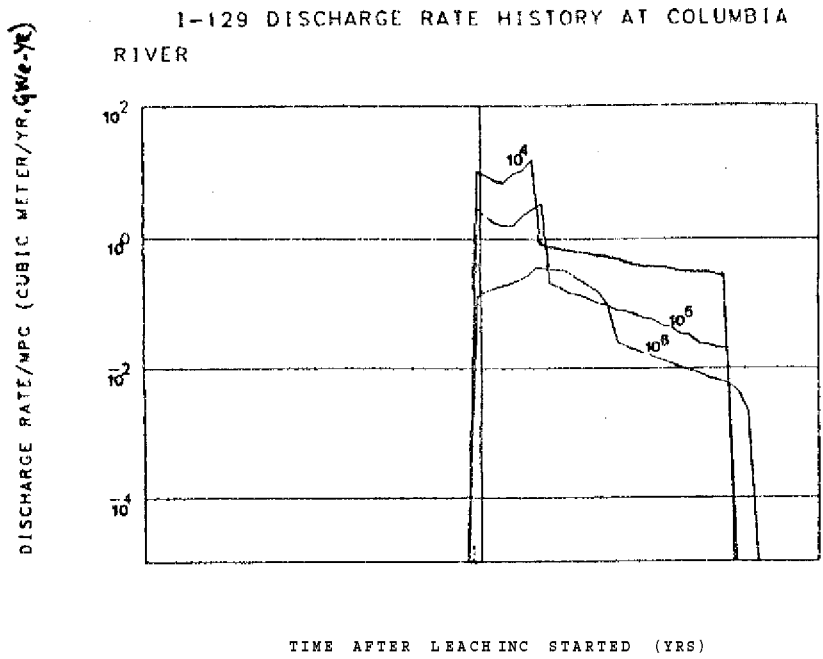


Figure 4.39 Ra-226 contaminated region in Saddle Mountain aquifer (Repository 1) after 10⁷ and 10⁸ years. Potentials are in meters above MSL.



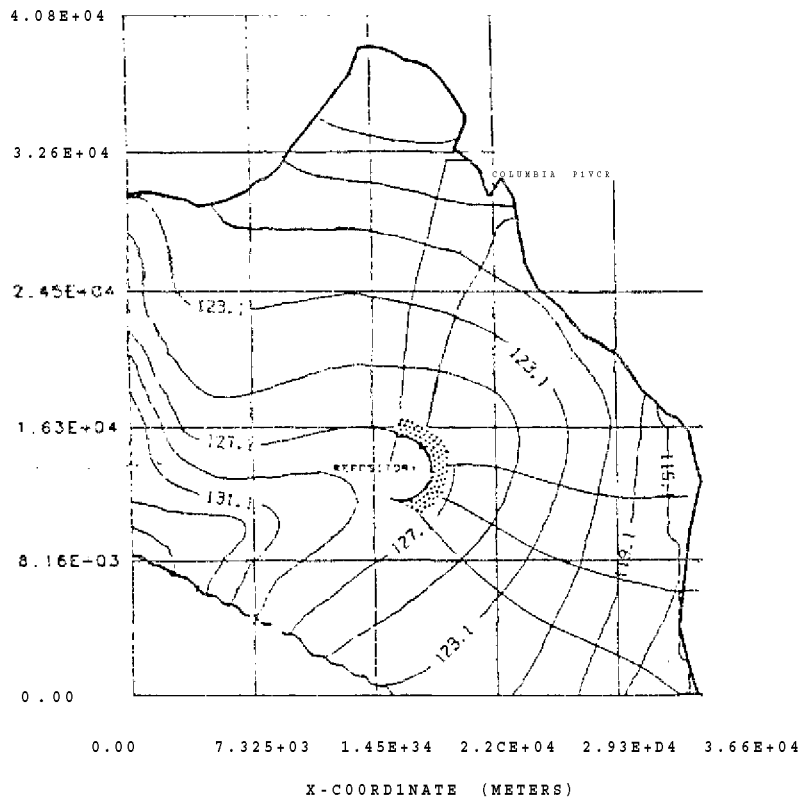
10<

10

TIME AFTER I. EACH INC STARTED (YRS)

Figure 4.40 1-129 discharge rate/MPC (water dilution rate) and cumulative discharge/MPC (water dilution volume) at Columbia River discharging from Saddle Mountain aquifer (Repository 1) for leach times of 10 , 10⁵ and 10⁶ years.

1-129 CONTAMINATED REGION-SADDLE MOUNTAIN
 AFTER 1.00E4-0 5YRS



CONTAMINATED REGION-SADDLE MOUNTAIN
 AFTER 1.00E+06 YRS

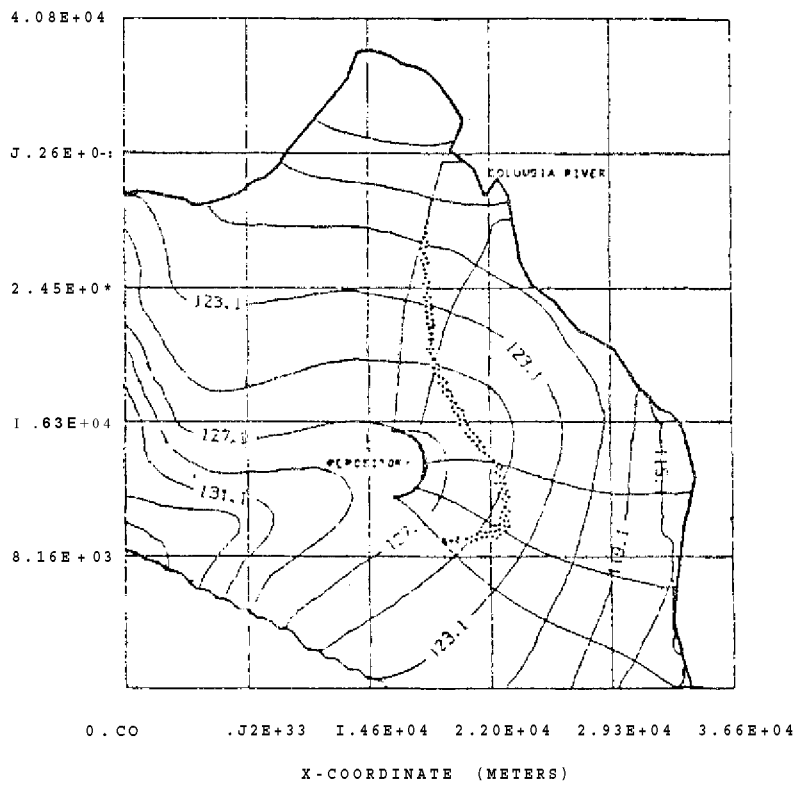
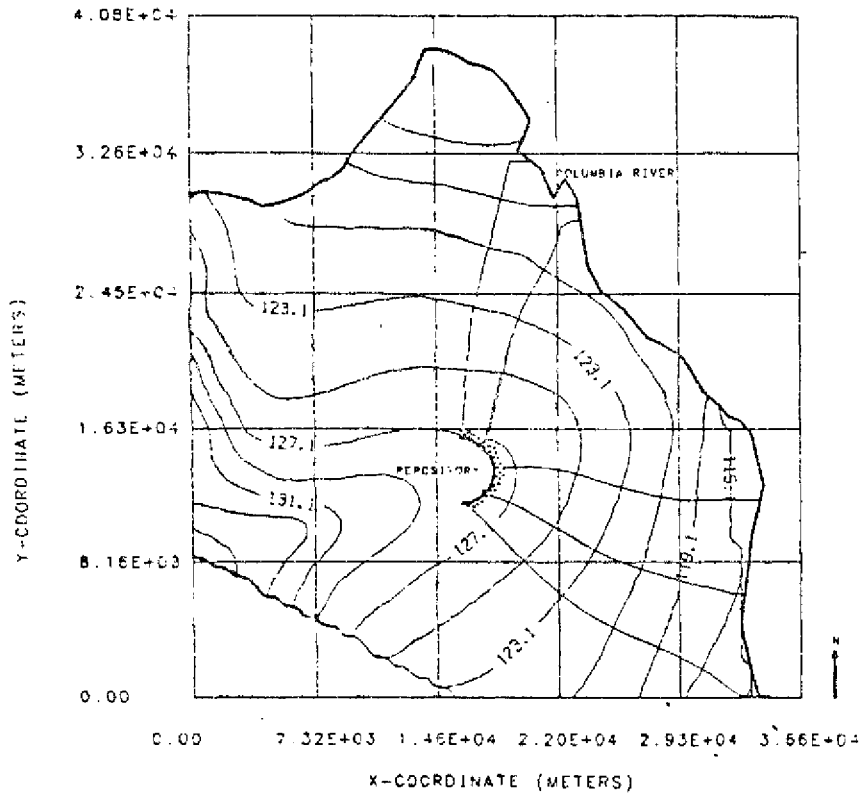


Figure 4.41 1-129 contaminated region in Saddle Mountain aquifer (Repository 2) after 5 and 10⁶ years. Potentials are in meters above MSL.



RA-226 CONTAMINATED REGION-SADDLE MOUNTAIN
AFTER 1.00E+01 YRS

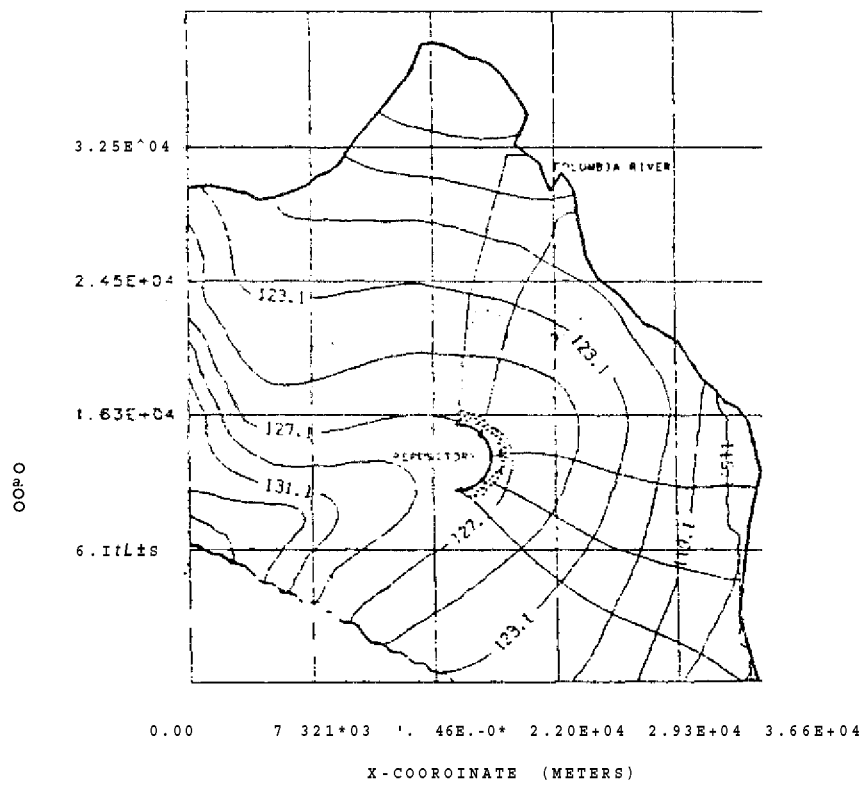


Figure 4.42 Ra-226 contaminated region in Paddle Mountain aquifer (Repository 2) after 10^0 and 10^7 years. Potentials are in meters above M.S.L.

1-129 DISCHARGE RATE HISTORY AT COLUMBIA
RIVER

TIME AFTER LEACHING STARTED (YRS)

1-129 CUMULATIVE DISCHARGE HISTORY AT
COLUMBIA RIVER

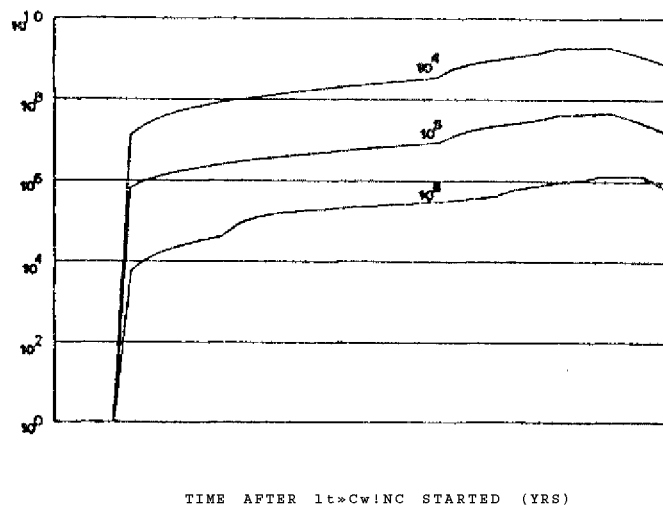


Figure 4.43 1-129 discharge rate/MPC (water dilution rate) and cumulative discharge/MPC (water dilution volume) at Columbia River discharging from Saddle Mountain aquifer (Repository 2) for leach times of 10^4 , 10^5 and 10^6 years.

dilution rate at Columbia River.

The following Table 4.10 shows the maximum total water dilution rate as defined in Eq. (4.4.22) for each of the four cases studied in the BWIP site .These values are contrasted against the recorded flow rates in the Columbia River.

Table 4.10 Maximum total water dilution rates and Columbia River flow rates

Columbia River flow rates:	Maximum:4.9E+11	(m /yr)
(60 years record)	Average :1.1E+11	
	Minimum:3.7E+09	
Ringold aquifer,"Repository 1"	1.0E+03
Ringold aquifer,"Repository 2"	•••••	•••••a•••••2•••••E*t*02
Saddle Mountain aquifer,"Repository 1".	1.5E+01
Saddle Mountain aquifer,"Repository 2".	1.5E+00

4.7.3 Effects of variations in the initial nuclide activities, in the time for beginning of leaching and in the nuclide MPC values

In this section we discuss how to extend the calculations to the disposal of unprocessed fuel instead of high level reprocessed waste. In addition, the effect of variation of the

delay time for beginning of leaching on the results obtained previously as well as the effects of changes in MPC values are discussed.

The extension of the calculation for spent fuel disposal.

The initial activities of each nuclide present at the time of burial were the result of reprocessing the spent fuel of a LWR after generating 1 Gw(e)yr of electricity with a load factor of 80%, thermal efficiency of 34% and a burnup of 30.4 Mwd/kg. These spent fuels are reprocessed after 150 days cooling period and 0.5% of the Pu and U are lost to the waste. The time lapsed between discharge and emplacement in the repository is assumed to be 10 years. To study the case of spent fuel disposal rather than reprocessed high level waste, the present analysis would still apply. Since only the initial activities of U and Pu are affected during the reprocessing one must multiply the Ra-226 discharge rates and cumulative discharge by 200 to account for the fact that 100% of the discharged U-233 will be initially in the waste instead of only 0.5%. This is possible because the nuclide arrival times to the biosphere are large enough so that only the decay of U-238 is important, if the nuclide arrival time at the biosphere were shorter than 10 years one must also consider the contribution of the Pu-238 decay. The hydrological calculations are of course not affected. The contaminated region as well as nuclide arrival times are also not affected.

The effects of the variation in the delay time for beginning of leaching on the calculations.

The value used throughout the calculations for the delay time in starting the leaching, to represent the durability of the waste package and, the engineered barriers was 1000 years. The first nuclide arrival times (Eg. (4.4.19)) of all nuclides present were such that only ^{129}I and ^{226}Ra (^{238}U), whose effective half lives are larger than 10 years, reach the biosphere. In view of this fact, increasing the delay time for beginning of leaching to up to 10 years will not change significantly the initial concentrations of these nuclides at the beginning of leaching. Therefore the results obtained for the concentrations and water dilution rates are not affected although the actual time for the nuclide to reach the biosphere is increased accordingly. If the set of retardation coefficients was such that other nuclides might also arrive at the biosphere (e.g. ^{242}Pu , ^{239}Pu , etc.) an increase in the delay time for beginning of leaching could affect the water dilution rates at the biosphere.

The effects of the variation of the nuclides MPC.

ICRP-30 (II) has recommended new biological uptake factors for some of the nuclides considered here. They can be translated into adjusted estimates of maximum permissible concentration (MPC^{\wedge}) for the purpose of calculating water dilution rates and water dilution volumes. The most significant changes affect ^{237}Np with a 200 times reduction in the MPC value and ^{226}Ra with a

60 times increase in MPC, (C4). These changes in MPC values does not invalidate the present results. Since the MPC are linear (inverse) multiplication factors, to convert the old water dilution rates and water dilution volumes into the new corrected values one would simply multiply the water dilution rates obtained in this work by the ratio of the new MPC divided by the old MPC. One can therefore extend the present calculation to include new values of MPC.

4.7.4 Summary and conclusion

Utilization of the present two-dimensional analytical solution to the radionuclide transport equation provided some qualitative informations about the migration of radionuclides through geologic media which the one-dimensional calculations lacked. These are the description of the two-dimensional contaminated region in the aquifer from the repository site to the discharge location at the biosphere at any time after the leaching started, and the determination of the location of discharge at the biosphere. Furthermore, by considering the aquifer as being two-dimensional should produce more realistic quantitative numerical results than one-dimensional calculations.

The calculations performed in Section 4.7 to assess the potential hazard to the public due the failure of the repository at the BWIP site have shown that the most potentially hazardous nuclides present in the waste are the I-129 and the Ra-226 (produced by the decay of U-238). In the event of an accident the contamination of the Columbia River does not exceed the allowed maximum permissible concentration for every nuclide present in the waste even when the river flow rate is assumed to be at its minimum recorded flow rate.

5. Literature References

B1. I. Briggs, "Machine Contouring Using Minimum Curvature", *Geophysics*, vol.39, no.1, February 1974.

B2. M. Benedict, T. H. Pigford, and H. W. Levi, "Nuclear Chemical Engineering", 2nd. Edition, McGraw Hill, N.Y., 1981.

B3. G. S. Barney and B. J. Wood, "Identification of Key Radionuclides in a Nuclear Waste Repository in Basalt", Rockwell International, RHO-BWI-ST-9, May 1980.

B4. H. C. Burkholder, M. O. Cloninger, D. A. Baker, and G. Jansen, "Incentives for Partitioning High Level Waste", *Nucl.Technol.*, 31, 202, 1976.

B5. B. Mann, Personal communication, November 1981.

C1. P. L. Chambre, "Classnotes for the course NE-255-Numerical Methods in Nuclear Engineering", University of California, Berkeley, 1979.

C2. D. G. Coles, D. J. Bradley, R. W. Mensing, and J. S. Schweiger, "Geochemical Studies of Sorption and Transport of Radionuclides in Rock Media", Lawrence Livermore Laboratory, NCD WP-79-147, 1979.

C3. C. R. Cole and F. W. Bond, "Comparison of Intera and

Wisap Consequence Model Application", Pacific Northwest Lab., PNL-3070, UC-70, January 1980.

C4. J. S. Choi and T. H. Pigford, "Water Dilution Volumes for High Level Wastes", Accepted for presentation at the ANS 1981 Winter Meeting, San Francisco.

C5. M. O. Cloninger, C. R. Cole and J. F. Washburn, "An Analysis on the Use of Engineered Barriers for Geologic Isolation of Spent Fuel in a Reference Salt Site Repository", Pacific Northwest Lab., PNL-3356, UC-70, December 1980.

C6. M. O. Cloninger and C. R. Cole, "A Reference Analysis on the Use of Engineered Barriers for Isolation of Spent Nuclear Fuel in Granite and Basalt", Pacific Northwest Lab., PNL-3530, UC-70, August 1981.

D1. U. S. Department of Energy, "Draft Environmental Impact Statement-Waste Isolation Pilot Plant", DOE/EIS-0026-D, April 1979.

D2. U. S. Department of Energy, "Draft Environmental Impact Statement-Management of Commercially Generated Radioactive Waste", DOE/EIS-0046-D, April 1979.

D3. G. Dahlquist and J. Wahlstrom, "Numerical Methods", Prentice Hall, New Jersey, 1974.

E1. Y. Emsellem and G. Marsily, "An Automatic Solution for the Inverse Problem", Water Resources Res., _7, pp.1264-1283, 1971.

F1. R. A. Freeze and J. A. Cherry, "Groundwater", Prentice Hall, New Jersey, 1979.

F2. E. O. Frind and G. F. Pinder, "Galerkin Solution of the Inverse Problem for Aquifer Transmissivity", Water Resources Res., _9, pp.1397-1410, October 1973.

F3. M. Foglia, F. Iwamoto, M. Harada, P. L. Chambre, and T. H. Pigford, "The Superposition Solution of the Transport of Radionuclide Chain Through Sorbing Media", ANS Transactions, 33, 394, 1979.

H1. M. Harada, P. L. Chambre, M. Foglia, K. Higashi, F. Iwamoto, D. Leung, T. H. Pigford, D. K. Ting, "Migration of Radionuclides Through Sorbing Media-Analytical Solutions I", Lawrence Berkeley Lab., LBL-10500, 1980.

H2. K. Higashi, "On the Migration of Three Member Decay Chain U-234-Th-230-Ra-226", Dept.Nuclear Eng., Univ.of Calif., Berkeley, Sept. 1978.

H3. M. D. Hill and P. D. Grimwood, "Preliminary Assessment of the Radiological Protection Aspects of Disposal of High Level

Waste in Geologic Formations", NRPB-R69, National Radiological Protection Board, Harwell, 1978.

H4. J. Hadermann, "Radionuclide Transport Through Heterogeneous Media", Nucl.Technol., 47, 312, 1980.

L1. D. H. Lester, G. Jansen, H. C. Burkholder, "Migration of Radionuclides through an Absorbing Media", AIChE Symp.Series, no.152, 71, 202, 1975.

L2. H. Lamb, "Hydrodynamics", Dover, New York, 1945.

✱

** L3. R. E. Love11, L. Duckstein, and C. C. Kisiel, "Use of Subjective Information in Estimation of Aquifer Parameters", Water Resources Res., J3, pp.680-690, 1972.

M1. J. W. Mercer and B. R. Orr, "Review and Analysis of Hydrogeology Conditions Near the Site of a Potential Nuclear Waste Repository, Eddy and Lea Counties, New Mexico", USGS Open File Report 77-123, February 1977.

M2. S. Marchetti, "Dose Consequence of Repository Failure and Leach Events for the Waste Isolation Pilot Plant", U.S. Department of Energy, WIPP, TME-3066, New Mexico, November 1980.

N1. R. W. Nelson and J. A. Schur, "A Preliminary Evaluation Capability for Some Two-Dimensional Groundwater Contamination

Problems", BCS Richland Inc. , BCSR-38, June 1978.

N2. R. W. Nelson, "In Place Determination of Permeability Distribution for Heterogeneous Porous Media through Analysis of Energy Dissipation", Soc. Petrol. Engrs. J., 8, pp.33-42, 1968.

N3. S. P. Neuman, "Calibration of Distributed Parameter Groundwater Flow Models Viewed as a Multiple Objective Decision Process Under Uncertainty", Water Resources Res., **J**), pp.1006-1021, 1973.

N4. R. W. Nelson, "Use of Geohydrologic Response Functions in the Assessment of Deep Nuclear Waste Repositories", Pacific Northwest Lab., PNL-3817, UC-70, May 1981.

PI. T. H. Pigford, P. L. Chambre, M. Albert, M. Foglia, M. Harada, F. Iwamoto, T. Kanki, D. Leung, S. Masuda, S. Muraoka, and D. K. Ting, "Migration of Radionuclides Through Sorbing Media-Analytical Solutions II", Lawrence Berkeley Lab., LBL-11616, 1980.

P3. T. H. Pigford et al., "Migration of Radionuclides Through Sorbing Media-Analytical Solutions III", Lawrence Berkeley Lab., 1981, to be published.

R1. J. K. Register, "Subsurface Hydrology of Strata Overlying the Salado Formation at the Waste Isolation Pilot Plant

Site, Eddy County, New Mexico", U.S. Department of Energy, WIPP Office, TME-3059, September 1980.

R2. Rockwell International Inc., "Hydrologic Studies Within the Columbia Plateau, Washington", Basalt Waste Isolation Project, RHO-BWI-ST-5, October 1979.

R3. Rockwell International, "Basalt Isolation Project-Presentation to the National Academy of Sciences", Richland, Wa., June 1981.

51. Science Applications Inc., "Tabulation of Waste Isolation Computer Models", Oak Ridge, ONWI-78, SAI/OR-749-2, December 1979.

52. Surface Gridding Library, "As Implemented at Lawrence Livermore Laboratory", Dynamics Graphics, Berkeley, November 1980.

53. B. Sagar, S. Yakowitz, and L. Duckstein, "A Direct Method for the Identification of the Parameters of Dynamic Nonhomogeneous Aquifers", Water Resources Res., 11, pp.563-570, 1975.

T1. D. K. Ting, P. L. Chambre, and T. H. Pigford, "Migration of Long Actinide Chains in Geologic Media", Transactions Amer.Nucl.Soc., 38, 1981.

Appendix A. Description of the computer code UCBNE25

UCBNE25 evaluates the analytical non-recursive solution to the one-dimensional transport equation without dispersion for the i -th member of a radioactive chain of arbitrary length.

A.1 Data input description. (See the program structure in Figure A.1).

Card 1: FORMAT (2I2)

Variable	Description
NCIIAIN (12)	Number of chains to be studied.
NGRAPH (12)	<0 produces a plot with the concentration history of every member of the chain for each set of parameter. >0 no plots are produced, only a printout. =0 produces a plot with the water dilution rate history of every member of the chain for each set of parameter.

Card 2: FORMAT(3(2F9.3,I2),F9.3,I2)

Variable	Description
Z0 (F9.3)	First value of path length (m) to be evaluated.
DELZ (F9.3)	Multiplying factor for the next MZ cases of path length to be evaluated.
MZ (12)	Number of different cases of path length to be

evaluated $Z=Z0x(DELZ)^n$; $n=1,2,\dots,MZ$.

VWO (F9.3) First value of water velocity to be used (m/yr).

DELVW (F9.3) Multiplying factor for the next MVW cases of water velocities to be evaluated.

MVW (12) Number of different cases of water velocities to be evaluated $VW=VW0x(DELVW)^m$; $m=1,2,\dots,MVW$.

TBLO (F9.3) First value of the time for beginning of leaching to be evaluated (years).

DELTBL (F9.3) Multiplying factor to obtain the next MTBL cases of time for beginning of leaching to be evaluated $TBL=TBL0x(DELTBL)^k$; $k=1,2,\dots,MTBL$.

DELLT (F9.3) Multiplying factor to get the next MLT cases of leach time. Each nuclide can have a different first case value for the leach time and these values are specified in the individual nuclide specification cards (see next cards).

MLT (12) Number of different cases of leach time LT to be evaluated $LT=LT0x(DELLT)^j$; $j=1,2,\dots,MLT$.

The next set of cards (Card 3 through Card 4+1) must be repeated for every chain being studied. In other words one need NCHAIN set of these cards.

Card 3: FORMAT(110,12)

Variable	Description
NTIME (110)	Number of time intervals that the contaminated time of each nuclide is to subdivided. The calculations will be performed for each time interval.

I (12) Number of members the chain has,

Card 4 to Card 4+1: FORMAT(12,A7,5F10.4), a total of I
cards

one for each member of this chain.

Variable	Description
NUMBER (12)	Hierarchy in the chain, NUMBER=1,2,... I
NNUCL (A7)	Nuclide name (e.g. TH-230).
THALF (F10.4)	Nuclide half life (years).
K (F10.4)	Nuclide retardation coefficient.
LT (F10.4)	Nuclide leach time (years).
C (F10.3)	Nuclide total activity at the time of burial (Ci).
TOX (F10.4)	Nuclide Maximum Permissible Concentration (Ci/m ³)

Figure A.1 Structure of the program UCBNE25.

```

Initialize

Read data input

Do every chain,NT=1,NCHAIN

Do every case of time for
beginning of leachinrr,
TBL=TBL0*(DELTBL)**N;N=1,..MTBL

Do every case of water velocity
VW=VW0*(DELVW)**J;J=1,..MVW

Do every case of leach time
LT=LT0*(DELLT)**K;K=1,..MLT

Do every case of path length
Z=Z0*(DELZ)**M;M=1,..MZ'

Do every nuc ide in the chain
NU=1,I

Determine the contaminated time
for every nuclide

Do every time interval
NT=a,NTTME I
      *      /

Evaluate the concentration and
the water dilution rate

Plot water dilution rate curves NGRAPH=0
Plot concentration curves NGRAPH<0
No graphs,just printouts NGRAPH>0

```

PIA. 368301, TING, D
'INPUT 62D0C 22.22.50 20 SEP 81 VIA CR04

265

.IDS
•USERPR
:OPY, INPUT/RR »OUTPUT/PR.
)I SPOSE,OUTPUT=PR,PA=IF.

PROGRAM UC3NE25
DANIEL K.S. TING
DECEMBER 1980
DEPARTMENT OF NUCLEAR ENGINEERING
UNIVERSITY OF CALIFORNIA »BERKELEY
BERKELEY, CA., 94720

** CONTROL CARDS LISTING **

t JOBCARD]
f PASSWORD]
*J SERPR
MNF4.
FETCHPS, ID0S, UL18, ULIBX,,
FETCHPS, GPAC8N7, GPAC, VA8^
LINK, F=LGO, F=GPAC, P=ULIB, X.
GRAPHIC, FN=FILM, FT=VA.
EXIT.
DUMP, 0.
GR'JMP.

** PROGRAM LISTING **

PROGRAM MAC1(INPLT,CUTPUT,TAPE5=INPUT,TAPE6=OUTPUT,FILMJ
C
C INITIALIZE THE PRCGPAM
C
ZOMMON/IGSZZZ/ZMCCE12C0)
DIMENSION XNAME(5C),YNAME(150),TNAME(150)
DOUBLE T10
DIMENSION NID0I,t»2(10J,W3(10»
DIMENSION OCTS.^SIVII0I.EII0I.Cd0I.TCXd0I,THALF(10I,B(10,10),
5.3ETA(10,10),DI(S,<;,S),A(10,10>,S(10),ST(III,NNUCL(101,TMAX(10),NUM
S3ER(10I,rfd(200»»,TIMEC200»
DOUBLE PRECISION K(10>,N(200),LT(10),NMAX(10)
DIMENSION TINLOGC2C0I,WCL0G1200)
DOUBLE PRECISION A,ADS,APRO,AT,B,BATEMAN,BETA,C,CMAX,C1,C2,C3,C4,C
\$5»DELLT,DELTA,DELTEL,DELVW,DELZ»Dt,DIFF,DM,DM AX,OS,01»02,03,04,05,
SD8,E,ERROR P,S,ST,S1,S2 »S3,T,TBL,TBL0,TDNAX,TEMP4,THALF,
\$TIME,TIMLQG,TMAS,TMAX,TMAZ,TMIN,TCX,T T,TTMAX,TI,T2,V.VIN,VM,VWO,WA
SLOG,WAPRtWO'tWCLCG,WMAX,W1,W2,W3,W6,X1,X2,X3,X4,Y,Z,ZO
DOUBLE PR1,PR2
DOUBLE EE,EEE,BB
DOUBLE EO,EE,EBCeCE,BOEC,s1M,s2M,s3M
C
C READ DATA INPLT
C
READ (5,201» NCHAIN,NGRAPH
201 FORMAT(2I2)
IEAD I5,105J Z0,0ELZtHZtVWO,OELVW,MVW,T8L0,DEL TBL,MTBL,DELLT,MLT
105 FORMAT(2F7.3,I2,2F9.3,I2,2F9.?,I2,F0.3,I2i

```

IF (NGRAPH.LE.C) CALL MCDESG ( I MODE , 6 , 0 . I
30 89 NC-1.NCHAIN
READ (5, 20 0) NTIKE,I
200 FORMAT I 110,12)
DO 99 N'J=1 , I
READ I 5> 106 J NUMBER (NL ) ,NNLJCL ( NU J ,THALF{NU) , K{NU) ,LT(NU) ,C(NU>,TOXt

E ( NU ) =ALOG (2. I/TFALF (NU)
106 FORMAT! 12,A7,5FI 0.A )
99 CONTINUE

EVALUATE B A T E K A N S FUNCTIONS
:ALL 8ATEMAN ( I , E , C , B )

EVALUATE EVERY CASE OF TIME FOR BEGINNING OF LEACHING

TBL=TBLO/CEL TBL
DO 61 ITBL = 1,MTBL
TBL = TBL *D E L T B L

EVALUATE ACTIVITIES AT THE BEGINNING CF LEACHING

DO 60 I 1*1, I
Y = 0.
DO 62 I I 1 = 1, I I
A6--EII 11 ) *TBL
62 Y = Y*B { 11, 111) *D E X F I W 6 )
60 C i I I 1 = Y * E ( I I M C i 1 l / E ( 1 J

REEVALUATE E A T E N A N S FUNCTION
:ALL BATEMAN ( I , E , C , B »

EVALUATE FOR EVERY CASE CF WATER VELOCITY

VW=V^O/DELVW
DO 63 IVW = 1 ,MVH
VW=VW*DELVW
DO 64 I J = 1,I
64 V I I J K V w / K I U S

EVALUATE THE BETA FUNCTIONS

DO 21 M 1 = 1, I
DO 22 J=1, I
IF!MI.F2.MJ) GO TC 22
IF{V(MJ) .EG.V(MI I 1 GO TO 59
BETA (MI , MJ ! M E I M ) * V I M J > - E ( M ) * V I M I ) ) / ( V ( M J ) - V ( M I I )
3 E T A ( M J , M I ) = B E T A { p I , H J )
50 TO 22
59 B E T A ( M J , M I 1 = 0 .
22 CONTINUE
21 CONTINUE

EVALUATE EVERY CASE OF LEACH TIME

DO 65 ILT = 1 , I
65 LH ILT »=LT ( I L T J / D E L L T
DO 66 I 3 = 1,ML T
DO 67 14=1,1
67 L H I 4 ) = L T ( 14 I * D E L L T

```



```

DO 38 K2 = 1. »NT!ME
T10=DLOG10 (TMIN} *CELTA*K3
TT=10. **T10

```

EVALUATE THE STEP FUNCTIONS

```

DO 39 K4 = 1, I
S(K4I=0.
ST ( K45 = C«
39 CONTINUE
DO 40 K5=1, I
IFIV(K5»*TT.GE.ZI St K5)=1.0D00
IFÍVU5JMTT-TI.GE.Z) ST ( K5J = 1. OD 00
40 CONTINUE
C1 = 0.
DO 51 12=1, II
ED= (- E1 12 »*(TT-Z/V( 11 I »)*OABS I S I I 1 » - ST ( II» >
CALL EXPO (ED.EE)
51 C1 = C1 + B (11, 12) * EE * Í S ( I 15 - s t í í 1 ) J
EB= (- E (UI * Z / V I I 1 M * DABS ( S ( I 1 » - ST U 1 ! )
CALL EXPO I E B . E E E I
C1 = C1 * E E E * 1 S ( I 1 S - ST ( I 1 ) I
C5 = 0.
IF ( 11 . EC . 1 » GO TO 71
WMAX = 0 .
00 521 L = 1, 11 - 1
DO 531 M = L, I 1
DS = S ( M Í - ST I N I
ADS ^ D A B S t 0 S )
DO 541 NR = L, I I
IFINR . EC . » * > GC TO 541
DO 551 J = I » L
W1 ( J ) = ( - BETA ( NR , M ) * UT - Z / V ( K n - E ( M ) « Z / V ( M ) l * S ( M )
- < 2 l J » = ( - T * ( E ( J l - 3 E T A ( NP , M » i - BETA ( NR , M i * { TT - Z / V ( M » l - E ( M i * Z / V ( M M * ST
# M )
W3 ( J ) = ( - E { J } * ( TT - Z / V ( M ) ) - E ( M ) * Z / V ( M ) I * A O S
1 F ( BETA ( NR , M l . EC . C . I W1 ( J 1 = 0 .
IF ( BETA ( NR , M ) . EC . C . ) V » 2 ( J I = 0 .
IF ( BETA ( NR , M ) . EQ . C . ) W3 ( J ) = 0 .
I F Í W1 ( J ) . GT . WMAX ) a NAX - W1 ( J I
I F ( W2 ( J ) . GT . WMAX ) V » P AX = W2 ( J )
551 I F ( W3 ( J ) . GT . WMAX I WMAX = W3 ( J »
541 CONTINUE
531 CONTINUE
521 CONTINUE
I F ( WMAX . GT . 60 C . I C I F F = V . MAX - 600 .
I F ( WMAX . LT . 60 C . > D I F F = 0 .
DO 52 NJ = 1, II - 1
C4 = 0 .
DO 53 NM = NJ, I I
C3 = 0 .
DO 54 NP = NJ, I 1
I F ( NR . EC . NN » GO TC 54
< i 2 " 0 &
DO 55 NK * 1 , NJ
PR1 = 1 . 0 D 0 0
DO 58 NC = NJ, I 1 - 1
58 PR1 = PR1 * E ( NCI * K ( NCI
PR2 = 1 . 0 D 0 0
DO 57 NC « NJ, I 1
I F ( NQ . EC NR ) GO TC 57
I F l NQ . EC NP » GC TC 57

```

```

PR2 = PR2ME(N3)*K(NC)*(K{NPJ-K(NMH*E(NM)*K(NM)*(MNC)-KINRN«-E(NR)
S*K(NRI*IK{KM1-K(NC)!
57 CONTINUE
X1=3(NJ,NKI*(K(NP)-K(NM))**(IJ-NJ-1I
X1=X1/(E(NK)*K(NR»-E(NKI*K(NM)-EINP)*K1NR) tE(NM|*K(NMJ|
X1=(X1+PR1»/PR2
S1=(-BETA(NR,N«I*UT-Z/V(NM)I-E(NV)*Z/V(NM))
S2=(-T*1E(NKI-3ET«(NPtNMII) fS1
S1=S1*S(N*»
S2=S2*ST(NP)
S3=(-E(KKi*TT-(E(K^})-E(NKII*(Z/\/(NM)1!
S3=S3*DABS(SIKM>-ST ihH))
51=S1-DIFF
52=S2-0 IFF
53=S3-0 IFF
CALL EXPO(51,X3)
IF(BETA(NR,NM).EC.C.) X3=0.
X3=X3*S(NM>
CALL EXPO(S2»X2J
IF(BETA(NR,NM1.EQ.C.»X2=0.
X2=X2*ST(NMJ)
CALL EXPO(S3,X4)
X4=X4*(S(NfI-S T C N sv ) >
C2=C2+X1*(X3-X2-X4)
55 CONTINUE
C3=C3+C2
54 CONTINUE
C4=C4+C3
53 CONTINUE
C5=C5*C4
52 CONTINUE
71 IF(II.EC.I>D I F F = C.

TEQ=(E(ii•m n / (E i u! *K{ ii n
IFEC5.GT.TEQ) GO TC «5 7
IFSDIFF.GT.6.0DC2» GO TO 97
M(K3)=C1+C5*DEXP(CIFF)
IF(NIK3 I.LT.O.» GC TO 97
TIME(K3)*TT
WD{K3}=MK3I*C(1I*EIII1)/(E(1I*TOX(11I*TI
146 IF(N(K31.GT.CPAX>T TMAX=TT
IF(N(K?) .GT.CMA>) CMAX=N(K3)
38 CONTINUE
30 TO 222
97 30 98 IX=K3,NTIME
Hi 1X1=0.
T10=DLOG1C(TMIN1+DELTA*IX
TT=10.**T10
TIME(IX)*TT
*D( IX)=1.0C-200
98 IF(IX.EG.1» GO TC 146
222 NMAX(m=CMAX*C(1)*E(11.MEm*TOX11i)*TI
TMAX(11I=T TMAX
WRITE(6,101*
101 FORMAT(IH1,5X,*NL"BEP*,2X,*NUCLIDE*,2X,*HALFLIFE(YR)?t,2X,*SORPTI
SON CONSTANT*,2X,*LEACH TIME(YRJ*,2X,^INITIAL ACTIVITY(CI)*,2X,
SPC(CI/M**3)*)
WRITE(6,10C)II,NNLCLI11»,THALF(IU,K(11»,LT(11»,C(11t,TOX(11>
100 =r)RMAT(7X,12,4X,A7,5X,IP03.2,9X,1PD8.2,10X,1PDF1.2.10X,1PL)8.2,12X,I
$PD3.2)
WRITE(6,102» z,v«,NMAX(II»,TMAX11I»
102 FORMAT(/,2X,*PATF LENGHT=#,1PD8.2,*(*)*,2X,*WATERVEL.=*,IPD8.2,
$MM/YR)«,2X,*MAX.hATER DIL.RATE=*,1PD8.2,*(M**3/GW*YR*»2i*,2X,*TIM

```

```

SE OF MAX,(YRJ**,1PD8-2 I
WRITEU,102)
103 FORMAT(//,8X,«TIME(YR)*,3X,*DIMENSIONLESS CONC.*,3X,*WATER OILUTI
SDN RATE {«**3/Gk*iR**2M)
00 80 NLCG=1,NTIKE
WCLQGLNLOGI=WD(M.CGJ
IF(NGRAPH.LT.OI hCLOG(NL CG)=N(NLG G)
IF(WCLOGINLOGI.LE.l.OD-3»WCLOGiN LOG!-•1.00-3
HCLOGINLOG»=ALOGIO(WCLOGINLOGIJ
80 TINLQG(NLOGi=CLCGlC!TSME(NLOGn
DO 56 K3=1,NTIME
WRITE(6,104ITIFE?K3)»NCK3I•VdDCK3!
104 FORMAT(8X,1P0B.2»6X,1P08.2,13X,1PD8.2)
56 CONTINUE

IF(NGRAPH.GT.C>GC TO 50
DRAW CURVES FDR EACH NUCLIDE

C
C
IFIWCLOGI1).GT0-3.) WCLOGl1J=-3.
CALL LINESG(Z«GDE,NTIME,TINLOG»WCLOGJ
50 CONTINUE
IF(NGRAPH.LE.OJCALLFRAME
68 CONTINUE
66 CONTINUE
63 CONTINUE
61 CONTINUE
89 CONTINUE
IF(NGRAPH.GT.O)GC TO 43
CALL EXITG(ZMQDE)
43 STOP
END
SUBROUTINE BATEMAMI»E,C»B)
DIMENSION EUOI,C(10»,B(10,10>
DOUBLE PRECISION E,C,E
DOUBLE TEMPI
DO 27 L1=1,I
DO 28 LJ=1,I
TEMP1=0.
DO 31 LM=1,LJ
TEMP2=1.
30 29 LR=LM,LI
TEMP2=TEMP2*(E(LP I
29 CONTINUE
TEMP3=1.
DO 30 LL=L1»LI
IF(LL.EC.LU GC 1C 30
TEMP3=TEMP3*(E(LL1-EILJI)
30 CONTINUE
TEMP1=TEMP1MC(LM)*E11J/(C(1>*E(LM)))*TEMP?/(E(LI)*TEMP3>
31 CONTINUE
B(LI,LJ)=TEMP1
28 CONTINUE
27 CONTINUE
RETURN
END
SUBROUTINE EXPOIX,Y)
DOUBLE X,Y
IF(X.LT.-6.002IGC TO 501
Y=DEXP(XI
30 TO 502
501 Y=0.ODCC
502 RETURN

```

Appendix B Description of the computer code UCBNE20.

B.1 Data input description.

1) 1st card: Initial system description:

VARIABLE	FORMAT	DESCRIPTION
NNUCL	12	total number of nuclides being considered
z_0	E12.4	first value of path length to be used (meters); $\{z_0 \geq 0\}$
T_0	E12.4	first value of leach time to be used (yrs); $\{T_0 \geq 0\}$
	E12.4	first value of water velocity to be used (m/yr); $(v_0 \geq 0)$
TBU	E12.4	first value of time for beginning of leach (yr); $(T_{b0} \geq 0)$

2) 2nd card: System parameters variation description

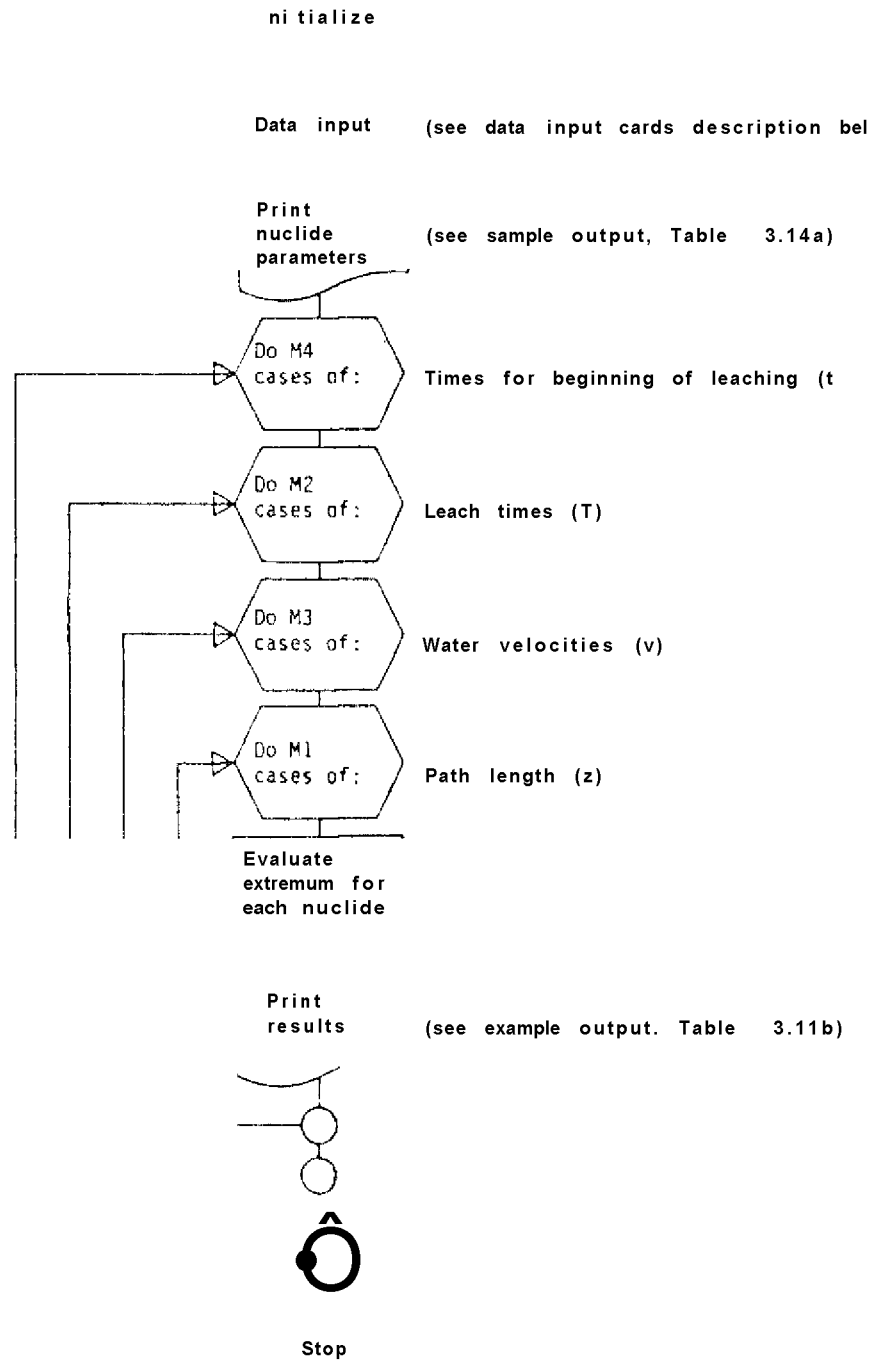
VARIABLE	FORMAT	DESCRIPTION
M1	12	total number of different path length cases to be evaluated $M1 = 1, 2 \dots$
DEL1	E10.4	multiplying factor for different path length cases: $z = z_0 \times (DEL1)^n$; $n = 1, 2 \dots M1$
M2	12	total number of different leach time cases to be evaluated $M2 = 1, 2 \dots$
DEL2	E10.4	multiplying factor for different leach time cases: $T = T_0 \times (DEL2)^n$; $n = 1, 2 \dots M2$
M3	12	total number of different water velocity cases to be evaluated, $M3 = 1, 2 \dots$
DEL3	E10.4	multiplying factor for different water velocity cases $vw = v_0 \times (DEL3)^n$; $n = 1, 2 \dots M3$
M4	12	total number of different time for beginning of leaching cases to be evaluated, $M4 = 1, 2, 3 \dots$
DEL4	E10.4	multiplying factor for different time for beginning of leaching cases $TBL = Tbl\# \times (DEL4)^n$; $n = 1, 2 \dots M4$

3) 3rd through (NNUCL_+ 2)th card: Nuclides description

It is required one card for each nuclide being considered, for a total of NNUCL cards. Each card has the following inputs:

<u>VARIABLE</u>	<u>FORMAT</u>	<u>DESCRIPTION</u>
NN	12	Nuclide identification number
NUCL	A6	Nuclide name (e.g., TH-229)
NH	12	Nuclide hierarchy: NH = 1 : if it is a first member of a chain NH = 2 : if it is a second member of a chain NH = 3 : if it is a third member of a chain NH = 4 : if it is in secular equilibrium with the nearest long lived precursor
NP1	12	NP1 = identification number of the 1st precursor if NH = 2 or 3. NP1 = identification number of the nearest long lived precursor if NH = 4. NP1 = 0 if NH = 1
NP2	12	If NH = 3, NP2 is the identification number of the 2nd precursor. NP2 = 0 otherwise
HFLV	E12.4	Nuclide half-life (yr)
^{SP}	E12.4	Nuclide sorption coefficient, $KD = 1 + LLZ_JL!$, J, <div style="text-align: right;">e S U</div>
TOX	E12.4	Nuclide maximum permissible concentration (MPC); (Ci/m ³)
C	E12.4	Initial activity at the time of emplacement, i.e., $t_0 = 0$, (Ci)

Figure B.1 Structure of the program UCBNE20.



FIA • 968301, TING.0
NPUT 620 CC 12.2°,04 12 SEF 51 VIA CP04
D=
FY, INFI'T/RR, OLTfUT/RR.
SFOSE, OUTFUT= FP .F<J=1*.

274

CGRAM UC BNE 20
MEL K.S. TING
F1L,196C
FARTHFNtCFNLCh. AR ENGINE. EF ING
IVfFSITY CF C*LIFCRNI£tEt*K£LEY
RKFLcY.CA., S4720

CCNTFCL CARDS LISTIFG **

CBCAR CI
ASSWORC1
SERPR
N4.
C.
IT.
KP,Q.
UHP.

FRCGFAH LISTING **

PFCGRAH HAX1 < I KFLT, CUT FLT, TAPE 5 = IN? UT, TAP EE =CITPLT)
DIMENSION f'CT FCC (100)
o IHLNSICN NLCL (1cC), NN (1cC), f£P1 (iCO, J'2 (1C?), Nh (1'JD), HFLV (1CC),
SVK (i00), C (10CMCX10Q), TMX (100), D*AX (100) JIFt. (100)
INTEGER S2 (3,3), S3 (3,3)
OIKN3ICNV (3), V2 (3), AL (3,3), EE (3,3), 7 (ICG), FRLCSF (ICC5, h (ICC)
REAL LACBCA (1Q0), KD (1S0KNNAX (100)

RFA C CATA INRJT

RLAD (5,200) NM'CL »Z0»T0»V0, TSLQ
200 FCF rAT (12,4112.4)
READ (5,42C) H1, DEL1»K2»OELt, ^3»DfiL3, '*'tDTL4
420 FCRMAT (12, C10.4, 1I, E10.4, I2, E10. «.,12, £10 •M
DC 2C1 = 1, NM'CL
READ (5,2 [1] NN (2) tM'CLCI), NF (I), NF1 (I >, NP2 (I), hFLV (I5, KC (I), TCX (I
n, c(i)
201 FCRMAT (12, Ac, 12, 2 12- 12.4 >
20 CCM3NLE
DC 10 I=1, NNUCL
LAKECA (I) = 0.693/HFLV (I)
E (I) = LAHECA (I >
10 AT (I) = LAMEDA (I) *XC (I)

EVALLATF THE ACTIVITIES AT EACH T I Mc F C R BEGINNING LEACHING

TEL = TBLC/CELU
DC 413 J413=1, M4
TEL = TBL*CEL4

KFITF. PROGRAM 7 IT Lt. , CASF FEING SOLVED AN C MCLICE FAF A EF. TEF< S

```

WRITE (6,2(4) TEL
>04 FCRHAT (1H1, /THE MCLICES F^RAHETERS AP.E LISTED E E L O W t , 5X , iT I H E FCC
$ EEGINMNG OF LEACHING IS t , 1X •i=>c a . 2 , IX , * ( YR ) * )
DC 414 I=1, NNUCL
IF (NH(I).EQ.3) GC TC k1s
GC TC 414
1(15 J1 = NF2(1)
J2=NP1(I)
AX=C(J1)*E(J2)»E(I)»('ZXF(-E(J1)*TBL)/((E(J2)-E(J1)M(? (I) -E(JD)) *
*E>P(-E<J2)*TBL) / ( ( £ (J1) -E (J2) ) * ( c (I) -r (JZ) ) ) (-F. (I >*TBL) / I (E (Ji
I)-E' (I))ME(J2)-£(!)))
AY=C(J2)»CC)*(EXF(-F(J2)«TEL)-E:XP(-;(I)'T5L))/ (E(J)-r(J2>)
AZ=C(I)*c>P(-£(I)*T?L)
C(I)=AX*A1+AZ
1F(C(I).LT.1. CE-2(o) C(I)=1.0E-2C0
414 CCM IMF
DC 416 1=1, NNUCL
IF (NH(I).EQ.2) GC TO 417
GC TC 416
417 J4 = NF1(1)
C(I)=C(I)*EXP(-E(I)*T?L)*C(J4)*E(I)*Vi X? <-E(J4)*TEL(-E(I)*T5L
S))/ (t(I)-E(J4))
IF(C(I).LT.1, OE-2CO) C(I)=1.0E-200
416 CCM3NUE
DC 18 1=1, NNUCL
IF(NH(I).EQ.1> GC TO M1?
GC TC 418
419 C(I)=C(I)*EXP<-E(I)*T3L)
IF(C(I).LT.1. OE-200) C(I)=1. OE-200
418 CCM INLF.
DC 462 I=-1, NNUCL
IF(NH(I).EQ.4) GC TO !!!
GC TC 462
461 J5 = NF1(I)
C(I)=C(J5)
IF(C(I).LT.1. (c. -2CO) C(I)>=1. GE-200
462 CCM2NUE
WRITE (6,205)
205 FCRMAT (//, fMJ*Efc; F*, 2X, * fLCLICC*, 2X, *HEM9FF*, 2X, *H.ALF-LIPE(YF) t, 2>
I, /SORPTION CONSTANTS/.2>, * HFC (CI/M*»3) * » 2/ , /INITIAL ACTIVITY
S(CI) * , 2>, /ATENL'ATICN FACTCR (1/Y~) /)
DC 30 1=1 .NNUCL
WRITE (6,2(6 >NN(I), NUCL(I), NH(I), HFLV(I), KO(I), TCX«I), C{I), A+(I)
206 FCRMAT (3X, I2, 4X, AfC, 5>, 12, ;X, 1FES.2, 9<, 1'EP.?, 10X, 1°C B.2, 13X, 1>- "Ee.2
f, 33X, 1FES.2)
30 CONTINUE
T=T0/DEL2
DC 411 J127=1, M2
T=T*CEL2
VK=V C/DEL3
DC 412 J27=1, *3
VW=VW*CEL3
Z=Z0/DELI
DC 650 J123=1, h1
Z=Z*CEL1
DC 11 1=1, NNUCL
11 VK(I)=VW/KD(I)

```

E VALLATE THE FXTRE HUH C F THE FIRST MCⁿEL^s

DC 4 C 1=1, NNUCL

```

GC TC 40
500 THAX ( I ) = Z / V < { I }
MFTHCD ( I ) = *E#
NKAX ( I ) = t > P ( - LAHECA ( I ) » TNAX ( I ) )
OPAX ( I ) = NNAX ( I ) « C ( I ) / ( T * TCX ( I ) )
TIHE ( I ) = T
40 CCHTIKLE

EVALUATE THE f XTFF HUH CF THE SECOND MEFBER

DC 50 I=i, NNUCL
IF (NH ( I ) .EC .2 > GC 10 6C0
GC tc 50
600 J=NP1 ( I >
CALL AFFOX2 ( I , Z , T thHAX , CHAX . THAX , TIi , N'1 . LAHECA , C , \ < K . TCX , fETHCC )
50 C C M INL'E

```

E VALLATE THE t XTRE HUH CF THE THIRD HE KEEP

```

DC 6 C 1 = 1 , NhUCL
IF (NH ( I ) .EQ .3 ) GC TO 11C&
gc tc 60
100 J1=NF2 ( I )
J2 = NP1 { 1 }
J3=I
V C1) =VK ( J 1J
V ( 2 ) =VK U 2 )
V ( 3 ) =VK ( J3 )
A1rLAMECA ( J 2 ) -LAHEDA ( J 3 )
A2 = LAHECA IJ3 ) -LAHECA ( J1 )
A3 = LAHECA ( J i ) -LAHECA ( J 2 )
0 = 1 . / ( V ( 1 ) * Ai » V < 2 ) * Af * V < 3 MA3 )
AL ( 1 , 3 ) = A2 / ( V ( 3 ) - V ( 1 ) )
A L ( 2 , 3 ) = A 1 / ( V ( 2 i - V ( 3 ) ) )
AL ( 1 . 2 > = A3 / ( V ( 1 ) - V ( 2 ) )
A L ( 3 , i ) = AL ( 1 , 3 )
AL ( 3 , 2 ) = AL ( 2 , 3 )
AL ( 2 , 1 ) = AL ( 1 t 2 )
EE ( 1 . 3 ) = ( LAHECA ( J1 ) * V ( 3 ) - LAr ' ECA ( J3 ) * V ( 1 ) ) / ( V ( 3 ) - V ( 1 ) )
BE ( 2 , 3 ) = ( LAH6CA ( J2 ) * V ( 3 ) - LAHeCA ( J3 ) » V ( 2 ) ) / ( V ( 3 ) - V ( 2 ) )
8E ( 1 , 2 ) = ( LAHB0A ( J1 ) * V ( 2 ) - LA ^ ECA ( J2 ) * V ( 1 ) ) / ( V ( 2 ) - V ( 1 ) )
BE ( 3 , 1 ) = EE ( 1 , 3 )
BE ( 2 , 1 ) = BE ( 1 , 2 )
BE ( 3 , 2 > = 8fc < 2 * 3 )

```

EVALUATE THE FLNCTICNS S2 (I , J) AND VZ (I)

```

IF ( V ( 1 ) , LT . V ( 25 ) GC TC ICE
IF ( V ( 2 ) .GT . V ( 3 ) ) GC TC 104
S2 ( 1 . 3 ) = 0
S2 ( 2 , 3 ) = -1
sc ( 1 , 2 ) = 1
IF ( V ( 1 ) .GT , V ( ? ) ) GC TO 1C 3
VZ ( 1 ) = V ( 2 )
VZ ( 2 ) = V ( 1 )
VZ ( 3 ) = V ( 3 )
NF=3
N ! > = !
NS = 2
S3 ( 1 . 3 ) = -1
S3 ( 2 , 3 ) = -1

```

```

GC TC IOS
VZ (1) = V (2)
VZ (2) = V (3)
VZ (3) = V (1)
NFr 1
Nh=2
KS=2
S3 (1,3)=1
S3 (2,3)=G
S2 (1i2)=1
GC TC 109
S2 (1»3)=1
S2 í2 ,3) -1
S2 (1 ,2>=0
VZ (1> = V (3)
VZ (2) = V (2 1
VZ (3) = V (1)
NF=1
Nt" = 2
NS=3
S3 (1 » 3) =1
S3 (2 , 3) = 0
S3 (1 , 2) = í
GC TC 103
IF (V (1) .LT .V(3) ) GC TC 10 6
52 (1 ,3) =1
32 52.3) =1
S2 (i .25=0
VZ (i) = V (3)
VZ (2) = V (1)
VZ (3) = V (2)
NF=2
Nf = 1
NS=3
53 (1 ,3) =0
S3 (2 ,3) =1
S3 (1 ,2) = -1
GC TC 108
52 (1 »3) = -1
S2 (2 ,3) = 0
S2 (1t2) = -1
IF (V (2) ,GT • V (3) ) CC TC 1C 7
VZ (1) = V (1)
VZ (2) = V (2)
VZ (3) = V (3)
NF=3
NF=2
NS=1
S3 (1 ,3) = -1
53 (2 ,3) = - J
S3 (1 ,2) s0
GC TC 108
VZ (1) = V (1)
VZ (2) = V (3)
VZ (3) = V (2)
NF=2
Nh=3
NS=1
S3 (1 ,3) s0
S3 (2 ,3) =1
S3 (1 .2) = -1
CALL APRO3 (I «Z.T.C.N^AV. rFAX.T'-IAX.TIVF» VZ.S3,S2.NF,Nr-,NS.AL.LAHE0

```

60 CCNTINLE

EVALUATE- THE CCSE FCF- THE KUCLICIS IN S E C U L A F EOUILIEFL I'

```

DC 7C I = 1, NNUCL
IF (NF < I >, EG .4 1 GC TC 1600
GC TC 70
300 J = NP1 (I)
RATIC = VK (J) / VK (I)
IF (NH (J) .E0.2 ) GC TC 1601
IF INHJ1 .EC3 ) GO TO 16C2
NAX (I) = NNAX (J) * C (J) * VK (I) / (C < I) * VK (J)
GC TC 1603
501 J2 = NF1 (J)
NNAX (I) = NHAX (J) * LAMEDA (J) * C < J2) / (O (I) * LAMGDA (J2) * KATIC)
GC TC 1603
602 J3 = NF2 (J)
NHAX (I) = NNAX (J) * LAMECA (J) * C (J3) / (C (I) * LAMEQA (J3) * FA7IC)
603 THAX (I) = THAY (J)
OHAX (I) = NNAX (I) * C (I) / (7 * TCX (I))
TIME (I) = TIME (J)
METHOD (I) = METHOC (J)
70 CCNTINLE
TCTAL = 0.
DC 90 I = 1, NNUCL
90 TCTAUTCTf LONAX (I)
DC 91 I = 1, NNUCL
91 FRDCSE (I) = (CMAX (I) / TOTAL) MOC.
WRITE (6, 2 (2))
202 FCRMAT (1H1 > 6X, tLEACHTIHE (Y -. ) t, 3X, * PAIHLENGHT (M) i, 3X, tWATE < ? V
SELCCITY 1f/YR) *)
WRITE (6, 2 (3)) T, Z, Vfc
203 FCRHAT (8X, 1PE12 .<t, 9X, 1PE12 . 4, EX, !Pt12.4)
WRITE (6, 2 17)
207 FCRMAT (1HQ > * NC < * t2X, * NUCL3CE * > 3X, < HEM3ER * t3X > < lST * > 3X, * 2NC#, 3X < * 7I
3 HE OF PEAK (YF) *, 3X, * HAXIHUNN / NC t, 3X, * KAT.0 I L. (M * 3 / CW * Yc * * 25 *, 3X
S * * CONTAN. TIHE (YR) *)
DC 80 I = 1, NNUCL
80 WRITE (6, 2 (9)) NN (I), NUCL (:), NH (I), N"1 (H, NP2 (I), THA > (I), HVAX (I), CMA >
< (I), TIHE (2))
209 FCRHAT (IX, I2, 3X, A6, 6 >, I2, 7X, I2, < X, I2, 7X, 1PE3.2, 9X, LPR * .2, 13y, 1FEe.
J2, 14X, IFF c. 2, 7X, CFF6.3, EX, z1)
650 CCNT INUt
412 CCNT INL'E
411 CONTINUE
413 CCNT I M F
STOP
ENC
SUBROUTINE APrtGXZn. Z. T. NHAX. CMAX. TMAX. TIHF. NPiiLAMenA. CIVK. TOX. N-
STFCD)
DINE NSICN Hf. THCC (100)
DIHENSICN TMAX (1GG), TIME (100), O^AX (13G), NP1 (10C), C (10C), V < (100), TC
$X (100)
REAL NH.AX (100), LAHECA (ICC)
METHCO (11 - tA*
A = LAHECA (I) / VK (I)
J = NP1 (I)
C1 = C (I) / LAMEDA (I)
C2 = C (JI / LAKBOA1J)
3 = LAHECA (J) / VK (J)
TC i v f T \ r r w * / t i i r n T O T O

```

```

If(A.GT.B) GO TC 7QC
THAX (I) = Z/VK(I)
NNAX (I) = (C1/C2+LAHECA(J)M*VK(I)/A3S(V<(J)-VK<I))) *EXr(-A*Z)
GC TC 701
7C0 B12=A85(LAMEDA(J5*VK(I)/<VK(I)-VK(J)))
Q1=ALCG((C1+C2*T*E12)t(C2*T*E12n
Q2=B-A
QQ=Q1/Q2
IF(Z.GE.QC) GC TC 711
THAX(IU2/VKCI)
NhAX(I)=(Ci/C2*LAh'ECMJ)*T*VK(I)/A9S(V<(J)-VK(I))) *EXt'(-A*Z)
GC TC 701
711 THAX(I) = Z/VK(J)
H2=0.
H2T=0.
IF(VK(I)*2/VK(J).C-E.Z> F2=1.
IF(VK(I)*(Z/VK(J)-T).GE.Z) H2T=1.
NhAX(I)=(C1/C2)*EXF(-LANECA(I)*Z/V<(I))'(H2-H2T)*T»E12*EX-(-LafECA
$(J)*2/VK(J))
GC TC 701
712 TT=2*Z/VK<1)
hNAX(I)=<C1/C2)*EXP(-LAHECA(I)*T>* (LAM3CA(J)/(LAMBCA(I)-LAhECA(J)
S))* (EXF(-LAMBDA(J))*TT-EXF(-LAM3DA(I))*TT)
THAX(I)=TT
701 DHAX(I)=NHAX(I)*LAHEDA(I)*C(J)/(T*TOX(I)*LAMECA(J))
IF(C(D/TCX(I)).LT.0.1) GC TC 625
IF(VK(I)KLT.VMJ) GO TC 627
IF(Z/VK(JJ-Z/VKC).GT.T) GC TC 626
TIHE(I)=T
GC TC 625
625 TIHT(I) = Z/VK(J) - Z/VKC)
GC TC 625
627 T1HE(I) = Z/VK(I) - Z/VK(J) * T
GC TC 625
628 TIHE(I)SAES(Z/VK(I) - Z/VK(J))
625 RETURN
ENC
SLEROUTINE APFCX3(I,Z,T.C.NHAX.O MAX,THAX, TIHE,VZ,S3»S2,NF,NH,NS,AL
J,LAMEDA,C,V,VK,TC>,E£,J1,J2,J3,ME-TH0D)
DIHE NSICN METHCC(IOG)
DINENSICN AL(3,3),C(1C0),V(3),VK(1GG),TOX(1G0),tf;{3,3>
DIHFHSICN TIM1(1CC),C"AX(1CG),TMAX(1CQ),V7(3>
REAL NHAX(100),LAHBCA(100)
IMEGfCR S3(3,3),S2(3,3)
A23(Z,T)=-AL(2,3)*Z-BF(2,3)»T
A13(Z,T)=-AL(1,3)*Z-3E(1,3)*T
A12(Z,T)=-AL(1,2)*Z~er<1,2)*T
B1=C(J2)*LAH8CA(J1)/(C(J1)*LAHBOA(J2))
3=LAH8CA(J2)»T*3i*V(3)/(V(2)-V(3))
A=IAHBCA(J2)*T*V(3)*D*LAMEDA(J1>
METHCD(I)=*A<
W1=8*BE(2,3)/(A*(EE(NH,NF)-BE(NF,NS)))
W2=B'BL(2,3)/(A*(Ft(NM,NS)-EF(NF,NS)M

EXTREHUN IN REGION 1

TL=Z/VZ(3)
TR=Z/VZ(2)
X2=Z*(AL(HH,NF)-AL(NF,NS))
X3=EE(NH,NFJ-BE(NF,NS)
IF(VK(J1).EQ.VZ(3)) GC TC 33C
r f M / / i 4 \ tr r 11"7 * . . . 1-r- f f -t-i*

```

XH=i.o-e/β

~~F~~ = ~~XK~~*EFUM»NF>/Efc (NF.NS)
(X4.LT.C») GCTC 312

X1=ALGG (X4)

TT= (X1-X2 1/X3

~~IF~~ (W1.GE.1.3) GOTC 332

IF (TT.LE.TP) GO TC 333

T1rZ/V2 (2)

GC TC 334

IF (TT.GE.TL) GO TC 335

T1=Z/VZ (2)

GC TC 334

T1=TT

GC TC 334

T1=Z/VZ (3)

GC TC 334

XH=A / (A-e)

X4=Xh*EE (NH,NF) /EE (NF,NS)

IF (X4.LT.0.) GC TC 312

X1=ALOG (X4)

TT= (X1-X2)/X3

IF (W1.LE.-1.0) GCTC 336

IF (TT.LE.TP) GO TC 337

T1=Z/VZ (2)

GC TC 334

IF (TT.GE.TL) GO TC 33«.

T1=Z/VZ (2 S

GC TC 334

T1=TT

GC TC 33U

T1 = 2/y2 (5 3

GC TC 331.

Xh=1.0

X4=Xf*eL(Nf,NF) /E6 (NF.NS)

IF (Xi..LT.C.) GO TC 312

X1=ALGG (Xi.)

~~TT~~ = ~~(X1-X2)~~ 1/X3

IF (TT.LE.TR) GC TC 311

T1=Z/VZ (2)

GC TC 334

IF (TT.GL.TL) GC TC 333

T1=Z/VZ í2)

GC TC 334

~~T1=TT~~

~~X2 3A23(Z,T)A5S3(B)~~

X13=A13 (Z.'1) *IA9f (S3<1,3))

X12=A12 (Z,71) *IAES (S3 (1,2))

CCNC1= (E-A) *EXP (X23) *S3 (2 i3) 4A»f.XP (XI 3) * S3 (1,3) - A*EXP (XI 2 5*S3 (1,2)

EXTREMLM IN FEGICN 2

TL=Z/VZ (2)

TR=Z/VZ (1)

Y2=Z • (AL (KM,NS) -AL (NF,NS))

Y3=BE (Nh,NS) -9E (KF•NS)

IF (VK(J1) .EC.VZ (3)) GC TC 3~C

IF (VK(J1) »EG.VZ (2)) GC TC 341

Yf=1.C

Y4=Yf*EL (NM»NS) /Er (NF,NS)

IF {Y4 • LT «C.) GO TC 411

~~Y1 = A11OGv(Yfc) vx~~

```

IF (T7.IF.TF.) GC TC 342
411 T2= Z/VZ (2 )
GC TC 3*3
342 IF(TT.GE.TL) GC TC 34^
T2=Z/VZ (2 )
GC TC 343
344 T2=TT
GC TC 343
341 YN' = A/(A -9 )
Y4=YN**6E ( NM ,N S) /EE (N'FiNS )
IF (YU.LT .0.5 GC TC 411
Y1=ALCG<Y4)
TT= ( Y1-Y2 )/Y3
IF (W2 .LE. -1.0 ) GC TO 345
IF (TT.LE.TR) GO TC 346
T2= Z/VZ (2 )
GC TC 343
346 IF (TT.GE.TL) GO TC 347
T2=Z/VZ (2 )
GC TC 343
347 T2=TT
GC TC 343
345 T2=Z/VZ (1 1
GC TC 343
340 YH = 1 ,0- E/A
Y4=YN*B6 (KM,N S) /EE (N F , NS )
IF (Y4.LT.C.) GC TC 411
Y1=A LOG (Y4)
TT= (Y1-V2 J/Y3
IF (W2.GF . 1. 0) GC TC 35 Q
IF (TT.LE.TK) GC TC 351
T2 = Z/VZ (2 !
GC TC 343
351 IF (TT.GE.TL) GO 352
T2= Z/VZ (2 )
GC TC 343
352 T2= TT
GC TC 343
350 T2=Z/VZ (1 )
343 Y23=A23 (Z ,125 *I AES (S 2(2 ,3 İ )
Y13= A13 (7 ,T2) *IAE5 (S 2 (1 ,3 ) )
Y12=A12 (Z ,T2>MAES (S2 (: ,2)>
CCNC2=(E-A)*E>P(Y23>*S2(2,3) *A*EXP(Y13))»32(1,3) -A»EXP(Y12)*£2(1,2)
IF(CCNC1.GT.COKC-2> GO TC 473
CCNC=CONC 2
TN=T 2
GC TC 483
«73 CCNC=CC NC1
TN=T1
,e 3 T3=Z/VK (I )
IF (VK (I) .£Q.V2(3) )GO TC 491
U23=A23 (Z ,T3i*IAES (S2(2,3))
U13=A13(Z»T3) *IAES (S2(1 .3))
U12=A12 (7 ,T3) *IAES (S2(1,2))
XN=(E-A)»EYP (J2 3) *S2(2,3)+A*EXP(U13)*S2(1,3) -A*LXP(ü12)''S2 ( 1 ,2)
GC TC 492
»91 U23=A23 (Z ,T3) *IAES (S3(2,3))
U13= A13 (Z ,T3) -IAES (S3 (1 ,3 ) )
U12=A12 (Z ,T3) *IAES (S3 (1 ,2))
XM= (E-A) *EXF(L23) *S3 (2,3) *A*EX^p(Ui3)*?3 (1 ,3) -A X P (L12) *S3 (1,2)
»92 CCSC3=(C(J3)»LAFECA(JÍ)/(C(J1)*LAK5DA(J3)))»EXF(-LAR'ECA(I)*T2^X»'
IF(CCNC.GT.CO NC3) GC TC 490

```

```
NrAX (I) =CCNC3
ThAX (I) =T 3
GC TC 1500
490 NhAX (I) =CCKC
THAX (I) =T •
500 DHAX (I) =Nr -AX (I) *LAHeDA (I) «C (J1) > / (T *LA "9DA (Ji) 'TCXII)
IF (C (IJ/TCX (I) .LT .CCI) GC TC 523
IF (VK (I) .EG .VZ (1) ) GC TC 525
IF (VK (I) .fC .VZ (2 > ) GO TC 527
IF (Z/VK (I UT.GT.Z /VZ (1) ) GC TC 526
TIHE <I) =2/VZ (i) -7/VK (I)
GC TC 405
526 Tiff (I) =T
GC TC 40e
527 IF (Z/VK (I HT .CT .2 /VZ (1) ) GC TC 525
TIHE (I) =2/VZ (1) -Z/VZ (3)
GC TC 406
525 TIHE II> =2/VK (I) -Z/VZ (3) »T
GC TC 406
528 TIHE (I) =Z/VZ (1) -Z/VZ (3)
4Q8 RETURN
FKD
```

Appendix C. Description of the computer program UCRNE21

C.1 Subprogram HYDRO data input description

Subprogram HYDRO determines the streamlines of the contaminated region and evaluates the hydraulic conductivity and the water travel time along these streamlines for a two-dimensional groundwater flow. Hydraulic head distribution can be input either by analytical expressions or by measured field data.

Card 1: FORMAT(5F10.3).

Variable	Description
XMIN (F10.3)	Minimum abscissa of the region of interest (m).
XMAX (F10.3)	Maximum abscissa of the region of interest (m).
YMIN (F10.3)	Minimum ordinate of the region of interest (m).
YMAX (F10.3)	Maximum ordinate of the region of interest (m).
DEL (F10.3)	Grid size in the x-direction and y-direction (m)

Card 2: FORMAT(5F10.3,110).

Variable	Description
XREP (F10.3)	Abscissa of the center of the repository arc (m).
YREP (F10.3)	Ordinate of the center of the repository arc (m)
RAD (F10.3)	Radius of the repository arc (m).
TETAI (F10.3)	Initial angle of the repository arc (radians) zero is the positive x axis, it is positive counterclockwise.

TETAF (F10.3) Final angle **of** the repository arc (radians). Same orientation as for TETAI.

NTETA (110) Number of streamlines to be considered on the **repository arc.**

Card 3: FORMAT(110,5F10.3). This card is required even if no point sinks or sources are being considered.

Variable	Description
NW (110)	Number of point sinks or point sources. NW=0 if no point sinks or sources are being considered.
VINFI (F10.3)	Horizontal uniform flow velocity (m/yr). VINFI=0 if no uniform horizontal flow exist.
EPSILON (F10.3)	Constant aquifer porosity.
THICK (F10.3)	Thickness of the aquifer near the point sinks and sources.
COND (F10.3)	Hydraulic conductivity (m/yr) for the point sinks and point sources system.
CONREP (F10.3)	Hydraulic conductivity at the repository site.

Card 4: FORMAT(3F10.3), one. card for each point sink/source. If NW=0, no cards 4 are required.

Variable	Description
XP (F10.3)	Abcissa of the point sink/source (m).
YP (F10.3)	Ordinate of the point sink/source (m).
QS (F10.3)	Flow rate of the point sink or source (m/yr).

Card 5: FORMAT(5F10.3), this card input the field

piezometric data, it is required at least 8 of these cards. It is not necessary to specify the number of these cards being input.

Variable	Description
XWORK (F10.35)	Abcissa of the data location (m).
YWORK (F10.3)	Ordinate of the data location (m).
CONDX (F10.3)	Reserved for future use.
CONDY (F10.3)	Reserved for future use.
POT (F10.3)	Aquifer potential at the data point (meters above the mean sea level).

Comment: If no field data is being used, no cards 5 are required,

MA.368301, TING, 0
MPUT 6200C 23.01.13 20 SEP 81 VIA CR04

286

5=
SERPR
?Y, INPUT/RR.OUTPUT/RR.
5POSE, CJTPUT=PR, PA=1F.
DGRAM UC8NE21 SUBPROGRAM HYDRO
M I EL K.S. TING
GUST 1981
PAPTMENT OF NUCLEAR ENGINEERING
IVERSITY OF CALIFCPNIA, BERKELEY
RKELEY, CA., 54720

CONTROL CARDS LISTING **

OBCARD]
ASSW3RD]
SERPR
F4.
THLIB.
TCHPS, SDL, ULIXjUL IB.
NK»F=LGQ, P=ULI X, X•
• TAPE, TAPE11 = /TING/MAC2/EX PER IE, 3 748 2.
IT.
MP, 0.
UMP.

PF-D3RAM LISTING **

PROGRAMMAC2 (INPUT, OUTPUT, TAPE5^INPUT, TAPE 6 = OUTPUT, TAPE11, FILM I
LEVEL 2, XSTR, YSTR, TSTP, POTEN, PSTR
: QMMON/DUMMY/XSTR{50, 100 t, YSTR(50, 100 », TSTR!50, 1 CO I, POTEN(1 00, 100»
S, PSTR150, ICO)
LEVEL 2, C, XP, YT, NV, VINFI
3DMM3N/SIG/O1100), XP(1001, YTI 100) ,NW, VINFI
LEVEL ?, CCNDX, CCNCY, EPS, POT
CCMMIN/HYDRO/CONDX(200) , CONDY(200 I, EPS(200) , PCT(200)
LEVEL 2, DPX, DPY, XGRID, YGRID, NX, NY» D P H I
20MM3N/0P/DPX{ICC, 10GJ, DPY(100, 100) , XGRID(100 I, YGRID(100) , NX, NY, DP
SHI(100, 100 I
LEVEL2, OX, CY
30MMIN/DE/DXC 10 0, 100 8 rDY1100, 100)
0 1 MENS IGN Y{3), WCPKI21), IWOPK{10!
3IMENSICN ARRWCRK(ICO, 100 J
3 I MENS ICN XBDARR(IOC) , YBDARR{100)
3DMMON/DOT /XWORK(200) , YWORK(200) , DATWOP.K{200) , I WKARP(10000»
DIMENSION YP{3», PY(3)
EXTERNAL F, DP C T
* * * }EAD DATA INPUT *****!*****
RELERR-1.CE-6
ASSERR = 1. OE-5
NTAPE = I 1
READ(5, IOC) XMIN, >MAX, YMIN, YMAX, DEL
100 CRM4T(5F10.3)
MX = INT ((XMAX- XMIN)/DELM)
1 F I A MOD (I XMAX-XMIN) .DELUGT.O. > NX = NX O
XMAX = XMIN*CEL >MNX- 1 I

```

\JY=INTUY*AX-YMIIU/DEL + T)
IF ( AMODI (YM4X-YMIN) , DEL ) . GT . C • ) NY=NY *• I
YMAX=YMINtDEL+ (NY- 1 »
READ! 5, ICI) XREP, YREP, RAO, TETA I, T°TAF, NTETA
01 FORMAT (5F10.3, I1Cî
READ (5, 132) N»», VINFI, EPSILON, THICK, CCND, CONREP
02 FORMAT (I10.5F10.2 )
IF (NW.LE.O I GO TC 10
30 11 J- 1, NW
READ (5, 103 S XP (J) , YT (J) , CS
.03 FORMAT (3F10.3 •
11 3 ( J ) - QS / ( EPSI LCMTHICK*6.2R32 )
10 WRITE (NTAPE, 112 I XFIN, XMAX, YMÎH, Ax, DLL, NX, NY» NTETA
.12 FORMAT (IX, 5E9.2, 3 15 »
NDATA=C
14 IF (EOF {5} aNE» 0 » ) GO TC 13
NDATA=NCATA+1
READ (5, 107 I XWORK {NCATAJ, YWORK (N' OATA) , CONDX (NDATA) , CONDY (NDATA I , POT
$ (NDATA (
i 07 FORMAT !5F10.3 »
GO TO 14
13 0 EL X = DE LY = DEL
NDATA=NDATA-1
: ALL BGNGPD
J JX = NX
XM = XMIN
XX = XMAX
J JY = NY
YM = YMIN
YX = YMAX
; ALL SETGRCi J JX, X R«, XX, J JY, YM, YX)
EVALUATES POTENTIAL FINCTION FOR A DISTRIBUTION OF SOURCES AND SINKS
DO 50 JX=i, J JX
XGRID1JX) XM*OELX* (JX-1)
PX=XGRIC (JX)
DO 51 JY=1, J JY
YGR I D ( J YÎYP+DELY' UJY-1)
PY ( 1 I=YGPIC (JY)
SUM=0.
IF (NW.LE.C) GG TC 25
DO 52 JS=1, NW
PAR=SQRT ((XGRIC (JXJ-XP (JS> ) **2» (YGRIO (JY» -YT (JS) ) **2)
IF (PAR.LE.O C) GO TC 52
SUM = SUM<• C ( JS »*ALCG (PAR »
52 CONTINUE
25 ³UTEN ( JX, JY) = -Vlnfl *XGRID ( JX) -SU'4
POTEN ( JX, JY » ^ PCTEMJX, JY1 * EPSILON / COND
IF (Nw.LE.C) GC TC 54
CALL F (PX, FY, YP)
DX (JX, JY» = -1. / YPÎ 2)
DY (JX, JY) = -YP (1) / YP (2 I
3X (JX, JY1=DX (JX, JY) *EPSILON/COND
DY ( JX, JY) =CY (JX, J\ ) *EPSILON/COND
GO TO 51
54 DX (JX t JY i = C.
DY (JX, JY) =C.
51 CONTINUE
50 CONTINUE
IF (NDAT i.LE.O ! GC TO 26
30 24 ICATA=1, NCATA
24 DATWORKÎ ICATA1 -PCTt ICATA)
1ALLCLCGPdt XWORK, VWORK, DATWORK, NDATA, ARRWORK, 100, 100, IWKAPP, 1 0000)

```

```

:ALL CLCBNC(XrFORK ,YWORK ,CATWORK ,NDATA ,i ,100 ,XBDARR ,YBDARR ,INMBND»
CALLCLCPLMXBDAPP ,YBDARR ,INMBND ,1 , -999999 . , APPWQRK ,100 ,100 >
IALL DERI V (APRWORK)
I ALL DERI 2 (ARRWCPK ,DPH I ,XGRID ,YGRID , N X ,NY)
GO TO 53
26 DC 27 JX=i ,JJX
DO 28 JY=1 ,JJY
ARRWORK (JX ,JY>=0 .
DPH I (JX ,JY)=0 .
DPX (JX ,JY »-0 .
DPY (JX ,JY)=0 .
28 CONTINUE
27 CONTINUE
53 DC 69 MX=1 ,NX
DO 61 MY-1 ,NY
POTEN (MX ,MYI=APRVCRK (MX ,MY)+PnTEN (Mx ,VY)
DPX (MX ,MY J=DPX (MX ,HY)+DXIKX ,MY>
DPY (MX ,MY »^DPY (VX ,VY) •DY (MX ,MY)
61 CONTINUE
69 CONTINUE
3ELTA= (TETA F-TETA I) / (NTETA-1)
DD 55 LX=1 ,NX
DO 56 LY=1 ,NY
WRITE (NTAPE ,111) FCTEN (LX ,LY)
11 FORMAT (1X ,E13 .5)
56 CONTINUE
55 CONTINUE
WRITE (6 ,12?1
.22 FORMAT (IH1 , * * * * PCTENTIAL FUNCTION MATRIX (METERS ABOVE MEAN SEA
SLEVEL I * * * * I
CALL WRITER (PCTEN ,NX ,NY ,XGRID ,YGR!D»
WRITE (6 ,123)
.22 FORMAT (1hi , * * * * < POTENTIAL GRADIENT IN THE X DIRECTION * * * *
CALL WRITER (DPX ,NX ,NY ,XGR ID ,YGRID )
WRITE (6 ,124 )
.24 FORMAT (1H1 , * * * * POTENTIAL GRADIENT IN THE Y DIRECTION * * * * >
CALL WRITER (OPY ,NX ,NY ,XGRID ,YGRID !
DETERMINATION OF TFE SHADOW REGION
DO 33 NT=1 ,NT ETA
IETA=TETA I+<NT-1MDELTA
XR=XREP»RAD*CCS (TETA >
yR=YREP*-RAD*S IN IT ETA j
NINI=0
DO 34 NS=1 ,NX
IF (XGRICINSJ .LT .XP) GO TO 34
NINI =NS
GO TO 70
34 CONTINUE
70 IF (NINI .EC .1 ) GC TC 71
IF (NINI ,FC .O » N I N I=NX
x=XR
Y ( I )=YR
Y ( 2 )=ALCG (CCNREP )
Y(3 >=0 .
DO 72 IN=1 , N I N I- 1
XOP=XGR IDIMN1 -1 >-DEL* ( 1N-1 )
IFLAG=1
NEQ- 3
CALL RKF (DFOT ,NEC ,Y ,X ,XOP ,RELERR , ABSE PR , IF LAG ,WORK ,IWORK}
XSTR (NT ,N I N I- IM=*CP
YSTR (NT ,NIM-IN)=V ( 1 )
PSTR (NT ,NIM-IN1 =EXP (Y (2M

```

```

XTRINT , NIM - I M y ( 3 i
=XOP
IF (Y(3)» .LT. 0. > TSTP (NT , NINI - INi = 0.
IF (Y(1) .GT.« YMAX) GC TO 73
IF (Yd) .LT. YMIN) GC TO 74
GO TO 72
75 YSTRINT , NIM - IN > OMAX
rSTP (NT , NIM - IN) = C.
30 TO 72
74 YSTR (NT , NIM - IN) = tVIN
TSTR (NT , NiM - ÎN » = C
72 CONTINUE
DD 44 IX = 1 , NIM - 1
KX - NINI - LX
IF (KX.FC. I) GC TO 44
DS = TSTR (NT , KX » - TSTR (NT , KX - 1 I
IF (DS.GE. 0. I GC TC 45
3D TO 44
45 DO 43 MX = 1 , KX
XSTRINT , MX) = XSTRIM , KX)
YSTP (NT , MX) = YSTR (NT , KX >
PSTR (NT , MXI = PSTR (NT » KX !
TSTR (NT , MX » = TSTR (NT , KX >
43 CONTINUE
GO TO 71
44 XCONTINUE
71 X=XR
Y(1) = YR
Y í 2) = ALCG (CCNREP )
Y(3 > = 0.
DO 75 ÎN = NINI , NX
XCP = XGPID (NINI) « -CEL * ( IN - NINI J
IFLAG = 1
MEQ = 3
CALL RKFIDPCT , NEC , Y , X , XOP , RELERR , ABSERR , IF LAG , WORK , I WORK »
XSTRINT , IN í - XCP
YSTR (NT , INi = Y(11
PSTR (NT , IN) = EXPLY (2) )
TSTR (NT , IN) - Y(3 I
IF (Y(3) .LT. 0. ) TSTR (NT , IN) = 0.
IF (Y(1 » .GT. YMAX1 CC TO 76
IF (Y(1) • IT • YMIN) GC TO 77
GO TO 75
75 YSTRINT , IM - YM . AX
TSTR (NT , IN) = 0.
GO TO 75
77 YSTR ÎNT , ÎM = Y * IK
TSTR (NT , IN 5 = 0.
X = XOP
75 CONTINUE
DO 41 LX = NINI , i X
i F (LX . EC . MNI i GO TO 41
DS = TSTR (NT , LXI - T ! 1 P (NT , LX - 1)
IFIDS . LE . O . » GC TC 42
30 TO 41
42 3D 46 MX = LX , NX
XSTRINT , MXi = XSTR (NT , LX I
YSTR (NT , MX) = YSTR (NT , LX)
PSTR (NT , MX ! = PSTR (NT , LX )
TSTP (NT , MX) - TSTR (NT , LX)
46 CONTINUE
GO TO 33

```

41 CONTINUE
33 CONTINUE

290

```
OC 62 N1=1tNTETA
TE TA= TE TA I +CELTA* (M-1 )
ANGLE=(TETA*180. 1/3.14 16
KRITE(6,108) M, ANGLE
.08 =DRMAT(1H1,11X,*STREAMLINE NO.*,I4,3X,*ANGLE IN REPOSITORY IS*,F10
S.3,* DEGREES* I
rfrRITE(6,125)
.25 CRMAT(IX,*NX*,5X,*X-(VETFRS > *,5X,*Y-{METFPSI * ,5X,*TRAVEL TIME (YR
il*,3X,<CQKDUCTi\|1TY (M/YR1*I
DO 65 N2=1»NX
WRIT E (NTA»E,1 16 > XSTP (N 1,N2 » .VSTRI NI ,N21 , î'S TR( NI , N2 >
.16 FORMAT(IX»3E13.5 I
WRITE(6,110) N2,XSTR(N1.N2) « YSTR(M,N?» ,ISTR(NI ,N21,PSTR(NI,N2 >
.10 FORMAT(IX,14,3X,4(1PE13.6,3X>>
65 CONTINUE
62 CONTINUE
CALL ENCGRC
STOP
END
SUBROUTINE DERIV(M
```

THIS VERSION OF CERIV EVALUATES THE PARTIAL DERIVATIVES USING A
CENTRAL DIFFERENCE APPROXIMATION AWAY FROM THE BOUNDARY

```
LEVEL 2,DP>,0PY,XGRID , YGPID,NX,NY,DPHI
COMMON/OP/DPX{10C,1CC» ,DPY(100,100» ,XGRID?100J ,YGR10(100t ,NX,NY,DP
$3I(100,100!
DIMENSION MICO,ICO)
DELX=(XGRIC(NXi-XCFID(1»!/{NX-D
DELY=(>GRIC(NY)-YGFIC(1)))/(NY-1)
DO 10 LX=1,NX
30 20 LY=1,NY
M2=LX+1
M1=LX-1
M2^LY+1
N1=LY~1
3=2.*DELX
IFILX.EC.1) M1=LX
IF(LX.EC.Î) D=DELX
IFILX.EC.NXI M?"LX
IF(LX.EC.NXI C=DELX
IF(LY.EC.1» N1=LY
ÎF(LY.EC.NY) N2=LY
IF(LY.EC.1) D=DELX
IF{LY.EC.NY) C=DFLY
DPX(LX,LY)=(A(M2,LY)-A(M1,LY))/D
DPY(LX,LY)=(A(LX,N2)-A(LX,N1))/D
20 CONTINUE
10 CONTINUE
RETURN
END
SUBROUTINE DER12(« ,DPH!,XGRID,YGR!D»NX,NYI
LEVEL 2,DPHI,XGRIC,YGRID,NX,NY
DIMENSION A(1C0,1C0),XGRID(100),YGRID(100),DPHI(100,1001
DELX=(XGRIC(NX)-XGFIC(1i)/(NX-1>
OELY--(YGRID(NY)-YGFID(1)) / ÎNY-I)
DO 10 LX=1,NX
DC 20 LY=1,NY
M2-LX+1
```

H1»LX-1
N2=LY«-1

291

```
IFUX.EQ.1J M1=LX
IF(LX.EC.NX» M2=LX
IF(LY.EC.1)N1=LY
IFUY.EC.NYI N2=LY
PXMMM2,LY>-2.*MLX,LY)4&(M1,LY)/(3ELX**2.I
PY=(A(LX,N2)-?.*A(LX,LY)+A(LX,N1>)/(DELY**2.)
3PH1(LX,LYi=PX*PY
20 CONTINUE
10 CONTINUE
RETURN
END
SUBROUTINE DPCTt X,Y,YP)
LEVEL 2,DPX,DPY,XGRIC,YGRI 0.NX,NY, O^HI
COMMJN/OP/CPX(100,100),DPY(100,100),XGRID(100),YGRID(100),NX,NY,DP
SHI(100,100)
DIMENSION Y(3>,YP(3)
NS=NX
DO 10 IX=1,NX
IF(XGRID1 IX).GE.X) NS=IX
IF(XGRIC(IX).GE.X) GO TO 40
10 CONTINUE
40 NG=NY
DO 20 IY=1,NY
IF(YGRIC(IY».GE.Y(1>i NG^IY
IF(YGRIC(IY).GE.Y(1)I GO TO 30
20 CONTINUE
30 IF(NG.EC.1I GC TC 50
A=DPY(NS,NG)-CFY(\S,NG-?.)
3=(Y(11-YGRID(NC-1))/(YGRID(NGI-YGRID(NG-1)I
DPDY=A*8+CPYf NS,NG-1!
C=DPX(NS,NG)-CPX(NS,NG-1)
DPDX=C*E*DPX(NS,NG-1>
GO TQ 6C
50 DPDY=DPY(NS,NGI
DPDX=DPX(NS,NG>
60 IF(DPDX.EC.O.) DPDX=1.OF-290
rPl1)=DPDY/DPDX
YP(2»=-CPHI(NS,NC1/DPDX
IF(Y(2).GT.730.) GC TO 77
VX=DPDX*FXF(Y(2)}
77 IFt Y(2»>.GT.73C.) vX=I.OE-290
IF(VX.EC.C.) VX=1.0E-290
YP(3)=-1./VX
RETURN
END
SUBROUTINE WRITER(A,NX,NY,B,C>
LEVEL 2,A,B,C,NX,hY
DIMENSION M100.100I,B(100),C(100)
ARG=NX/11.
SIPAGE=IM(ARG)
IF(AMOC(FLCAT(NX»,11.).GT.O.)NPAGE=NPAGE+1
DO 10 NP=i,NPAGE
IF(NP.EC.1)WRITE16,100)(B(I),I=1,MINO(11,NX))
100 FORMAT(2X,/,IX,*>(METERJ*,2X,11(IPEIO.3,1Xa(
LFIN INP-1)*11+10
IF(N'').GT.1)WRITE(6,102)(B(I),1=(NP-1)*11,MINO(LFIN,NXU
102 -ORMAT(1H1,*X(ME7ERi*,3X,11(1PE10.3,1XM
WRITE(6,1C3)
103 FORMAT(IX,*Y(METER I t)
```

```

DO 20 LINE=1,NY
IF(HP,GTO 1) GC TC 2C
rWRITE(6,101) C(LINE), (MJ,LINE), J=1,M!NO('1,NXI)
GO TO 20
30 1 F í NP.EC.NPAGEUP HE (6,101)C(LINE \ , (A!J,LINE), J=(NP-1)*11,NXI
IF(N?.LT.NPAGEIWRITE(fc,101>C(LlNEI, (A(J,LINEf,J=(NP-li*11, (NP-ii*i
$1+10)
101 FORMAT (IX, 12(1PE10.3, 1X))
20 CONTINUE
10 CONTINUE
RETURN
END
SUBROUTINE F{ X,Y,YP)
LEVEL 2,C,XP,YT,Nh,VINFI
CUMM3N/SIG/C(10C»,XP(1COL,YTt100i,NW,VINFI
DIMENSION Y(3),YP13)
SUM1=0.
SUM2=0.
DO 10 J«1,NV»
A=(X-XP(J»I**2.KY(1)-YT(J))**2.
IF{A.EQ.O.) GC TC 10
SUM1 = SUM1HQ(J) * (X-XP(J)) /A
SUM2=SUV2+ (Q{JI * (Y(II-YT(JiII/A
10 CONTINUE
DX=-VINFI-SUM1
DY=- SUM2
YP{1) =DY/CX
YPC2j=-1./CX
RETURN
END

```

C.2 Subprogram PLOTMAC data input description

Subprogram PLOTMAC evaluates the concentration of the i -th member of a radioactive chain of arbitrary length along the streamlines of the contaminated region of the two-dimensional groundwater flow.

Card 1: FORMAT(2A10,F10.3)

Variable	Description
HOLL1 (A10)	Hollerith to be displayed in the graph.
HOLL2 (A10)	continuation of HOLL1.
POTPLOT (F10.3)	If less or equal to zero no graphs are generated only a printout. Otherwise a plot is produced.

Card 2: FORMAT(5F10.3,110,F10.3)

Variable	Description
XREP (F10.3)	Abcissa of the center of the repository arc (m).
YREP (F10.3)	Ordinate of the center of the repository arc (m).
RAD (F10.3)	Radius of the repository arc (m).
TETAI (F10.3)	Initial angle of the repository arc. Zero is the positive x axis (radians), positive counterclock.
TETAF (F10.3)	Final angle of the repository arc (radians).
NTETA (110)	Number of streamlines to be considered on the repository line. The streamlines are equally spaced.
ANGNO (F10.3)	Angle between the north direction and the positive x axis.

Card 3: FORMAT(4I5,2F10.3). PLOTMAC allows the user to zoom in a region inside the original region of interest defined in HYDRO_i producing an amplified view of a given part of the region of interest.

Variable	Description
NXPLMX (15)	Maximum grid number in x-direction to be shown in the plot.
NXPLMN (15)	Minimum grid number in x-direction to be shown in the plot.
NYPLMX (15)	Maximum grid number in y-direction to be shown in the plot.
NYPLMN (15)	Minimum grid number in y-direction to be shown in the plot.
SUMAX (F10.3)	Maximum value of the potential function (m) .
SUMIN (F10.3)	Minimum value of the potential function (m).

Card 4: FORMAT(1I10,4F10.3). This card is equal to card 3 in HYDRO, see section C.1.

Card 5:FORMAT(3F10.3). These cards are equal to cards 4 in HYDRO, see section C.1.

Card 6: FORMAT(2(I10,2F10.3))

Variable	Description
NMEMBER (I10)	Number of members in the chain.
TLEACH (F10.3)	Leach time (years).

TBEGIN (F10.3) Delay time for beginning of leaching (years).

NTIME (I10) Number of different time values after the leaching for which calculations are to be done.

TIMEO (F10.3) The first value of time to be used (years).

DTIME (F10.3) Multiplying factor for the NTIME cases of times to be evaluated: $TIME = TIMEO * (DTIME)^{**K}; K=1, ..NTIME$

Card 7 to Card (7+NMEMBER): FORMAT(A7,5F10.3), one of these cards are required for each member of the chain, the cards must be ordered as the chain is.

Variable	Description
NNUCL (A7)	Nuclide name (e.g. Ra-226).
THALF (F10.3)	Nuclide half life (years).
K (F10.3)	Nuclide retardation coefficient.
C (F10.3)	Nuclide total activity at the time of burial (yr).
RCG (F10.3)	3
GRAP (F10.3)	Maximum Permissible Concentration (Ci/m). If GRAP is larger than zero a plot for this nuclide is produced, otherwise only the print-out of this nuclide concentration is generated.

Card 8+NMEMBER: FORMAT(2F10.3), these cards describe the biosphere by given a number of coordinates, any number of cards is acceptable. If biosphere is not to be shown in the plots no card is included in this section.

Variable	Description
XBIO (F10.3)	Abcissa of the biosphere coordinate (m) .
YBIO (F10.3)	Ordinate of the biosphere coordinate (m).

Comment: The coordinates must be sequentially input.

IA.368301,TING,0
PUT 62J0C 23.27.27 2C SEP 81 VIA CR04

296

IERPR
'Y, ISIPUT/RR, OUTPUT/RR.
-POSE, OUTPUT = PR, PA = .\F.

)GRAM UCBNE21 SUBPROGRAM PLOTMAC
JIEL K. S. TING
iUST 1981
'APTMENT OF NUCLEAR ENGINEERING
! VERSITY OF CALIFCPNIA, BERKELEY
IKELEY.CA., 94720

CONTROL CARDS LISTING **

DBCARD1
ASS»I3RD]
SERPR
' 4 .
rCHPS, IDDS, ULIB, ULI8X.
rCHPS, GPACBN7, GPAC, VAEN.
TTAPE, TAPE11=/TING/MAC2/PUSTLE3,3 74 03 .
NK, F=LGO, F=GPAC, P=ULIB, X.
APHIC, FN=FILM, FT=VA»
IT.
1P.0.
JMP.

PP03 RAM LISTING **

```
PROGRAM PLCTMAC ( INPUT, OUTPUT, TAPE5- INPUT, TAPE6-OUTPUT, TAPEU, FILMI
COMMON/IG SZZZ/ZMCCE( 200)
DOUBLE SRPMX, SPPMN, TIE
DIMENSION XBIC(2C0), YBIO(200)
JIMENSICN VEXI1), VEY11), PLOT(40)
DIMENSION ABST(20!), BACT(20I), ABSM(20!, 3ACM(20i, ABSL(20i, BACH2Ot
DIMENSION XWELL(2C), YWELL(20), S(20)
DIMENSION MAX(40), 7fiX(20>
DIMENSION ZHAX(20i, ZMIN(20!, DIFFEUOO>
DIMENSION NN.UCK 2C), GRAP(20)
COMMON/AN AME/XKAMEf 50?, YNAME{5J!, TNAME(100 J, ZNAME(50)
LEVEL 2, E, K, C, RCG, TvMEMBER, TLE&CH, TBF.G IN
DOUBLE THALF, K(20), E(2C), C12C)
COMM, DN/CONC/N*EMBEF, TLEACH, TBEG IN, E, K, C, RCG(208
LEVEL 2.XSTR, YSTR, TSTR
COMMON/STREAM/XSTR(50, 100), YSTR(50, 1CO), TSTR(50, 100)
LEVEL 2, POTEN
COMMON/CUMMY/PCTEN(100, 100)
DIMENS IGN XWORK(2C0 I, YWORK(200I, DATWORK(?OOI, ARRWORK(100, 100I
SJTAPE=11
READ(5, 100) HCLL1, HOLL2, POTPLOT
100 FORMAT(2A10, F10.3)
READ(5, 120IXREP, YFEP, RAD, TETA I, TETA F, NTETA, ANGNO
120 FORMAT(5F10.3, I10, F10.3)
READ(5, 130 1 NXPLNX, NXPLMN, NYPLMX, NYPLMN, SUMAX, SUM IN
120 FORMAT(4I5, 2F10.3)
```

```

LIO FORMAT ( 110, 4F10.3 »
  IFINW.LE.C» GC TC 56
  DO 57 J=1 »NW
  READI5, 121 » XWELLÎ J i , YwELL(J) , QS
121 FORMAT î 3F10» 3 )
  57 J(J I=QS/(EPSILON*ThlCK*6.2822 >
  563 EADI51105 >NUMBER, TLEACH, TBEGIN»NTIMEF, TIMEO, DTIME
105 FORMATI2( I 10, 2F10.3 ) )
  30 12 1=1, NMËV8EP
  READI5, 106 JNNUCL( I « » THALFiK( I ) , C i I ) , RCG( I I , GPAP( I )
106 FORMAT « A7, 5F10.3 I
  12 E( i ) =DL CG( 2. DOO I /TFALF
  READ(NT APE, 112) Xv IN, XMAX, YMIN, YMAX, 0EL»NX, NY, NTETA
112 FORMAT(IX, 5E9* 2, 3 If)
  DO 10 LX=1, NX
  DO 11 LY = I » NY
  READÎNTAPF., 111 ) PCTEN I LX, LY )
111 FORMAT(IX, E13.5 »
  11 CONTINUE
  10 CONTINUE
  DO 15 N1=1, NTETA
  DO 16 N2= 1 ,NX
  READ(NTAPE, 116t XSTR(N1, N21, Y5TR(N1, N2i, TSTR(N1, N2>
116 FORMAT(1X, 3E13.5 )
  16 CONTINUE
  15 CONTINUE
  SIDATA = C
  14 I F(EOF(5 J.NE.O. ) GC TO 17
  SIDATA-NCATA+1
  READ(5, 1021 XBIOUCATA) , YBIC(NDATA)
102 FORMAT I2F10.3»
  30 TO 14
  17 XV.AX = XMINMNXF LMX - 1J*DEL
  XMIN=XMINf (NXPLMN-1»*DEL
  XMAX^ XV AX-XMIN
  XREP = XP EP-XMIN
  XTRANS = XM IN
  XMIN=0 .
  YMAX = YMINKNYPLMX - 1 ) *DEL
  YMIN=YMIN+ (NYPLMN- 1 > *DEL
  YMAX=YMAX-YMIN
  YREP = YREP- YMIN
  VTRANS=YMIN
  YMIN=0 .
  NDAT A=NC ATA- 1
  3D 20 JX--NXPLMN, NXPLMX
  DD 21 JY=NYPL*N, NYFLMX
  MX-JX-NXPLMN*1
  MY=JY-NVP tMN*1
  POTEN(MX, MYI=POTEN(JX, JY»
21 CONTINUE
20 CONTINUE
  DC 22 MET A=1, NTETA
  DO 23 IX=KXPLMN, NXPLMX
  MX =IX-NXPLMN*1
  XSTR(META, MX1)=XSTR(META, IX»-XTRANS
  rSTR(META, MX)=Yslf(META, IXI-YTRANS
  TSTR(META, MX)=TSTP(META, IXJ
23 CONTINUE
22 CONTINUE
  NIX=NXPLMX-NXPLMN•1
  NiY=NYPLVX-NYPLMN*1

```

```

DTA=(TETA F-TETA I 1/INTE TA- 1 )
I F (A3SIXREP-XMIN» . CT . ABS (XREP- XMAXM KD' -1
1FIA3SIXREP-XMIN1 . LE . ABS (XREP-XMAXII KD= 1
I FUXMAX-XMINJ . GT . (YMAX-YMIN)I GO TO 43
A3=80 .
A2=A4=2C .
A1=( (XMAX-XMIN) * ( «3-A4 ) ) / (YMAX-YMIN J•A2
GO TO 44
42 41=80 .
A2=A4=20 .
A3= ( tYMAX-YMN» * ( ai -A2 ) ) / lX*AX - XMIN) »AA
44 DIVX=(XVAX-XMIN) / 5 .
DIVY=(YMAX-YMIN» / 5 .
AN=( 3 . 1416*ANGNC) // 80 .
AA=A1 *3 .
VEX(1 I -AA+5,, *CCS (ANJ
VEY11)=20 . . 5 . *5INFAM)
DIF=TETA F-TETA I
ANG1~ITETA I*18C . ) / 2 . 1416
3ANG=(DIF*180 . 1 / 3 . 1416
••••'DRAW POTENTIAL LINES AND STREAMLINES OF THE SHADOW REGION
CALL MODESG(ZMCOE,6,CI
TIME=TIMEC/DTIME
DO 13 ITT-1,NTIME
TIME=TIME*CTIME
DO 41 LU=1»NMEMB5R
SRPMX=-1 . OD+300
SRPM , =1 . 0C+ ?00
DO 31 JU=1,LU
SRPMX"DMAX1 (SRPMXtK{JU}J
SRP*N=DMINKSRFMN, K (JU ) )
21 CONTINUE
ZMAXt LU)= TIME/SFF^N
TIE=(TIME-TLEACH)/SPPMX
ZMINTLUI=DPAX1 (O . CCO, TIFi
WRITEI 6, 103) NNLCL (LU) , ZMAX (LU) , ZMIN ( LUI
103 FORMAT (IX, 47, 2 (1PES . 2, 3X) (
41 CONTINUE
DO 29 NU= I ,NMEM8EP
^RITE (6, 104) NNUCL (NU)
104 FORMAT !IX, A7)
IF (GRAP (NL) . LE . O . > GO TO 29
CALL SU8JEG (ZMODE, XMIN, YMIN, XMAX, YMAXI
CALL OBJCTC1ZMCDE, «2, A4, A1 , A3)
CALL SETSMG (ZMQDE, 45, 1 . 5 J
CALL GR1DG (ZMDDE, CIVX, DIVY, C, Oi
CALL LA3ELG (ZMOD6, C, DIVX, 0, -9 . 2)
CALL LA3ELG (ZMODE, I, DIVY, 0, -9 . 2)
ENCODE { 50, 1CO0, XNAME I
000 FORMAT (* X-COORDINATE (METERS}*)
ENCODE ! 50, 1001, YN4ME I
001 FORMAT t * Y-CCRDINATE (METERS) * >
ENCODE ( 10C . 10C3, T\JAME) NNUCL (NMEMBER) , HCL L \, HOLL 2, TIME
003 FORMAT (A7, * CONTAMINATED REGION- *, A10, A10, *4FTER*, 1PE9, 2, *YPS
CALL TITLZSIZMCDE, 1 . 1 . 1 . 0)
CALL TITLZSIZMODE, 1, 2, 1 . E1
CALL TITLEG (ZMOOE, 50, XNAME, 50, YNAME, 100, TNAME i
CALLSETSMG (ZMCDE, 45, 1 . 0)
DO 45 NT=1, NTETA
DC 46 MX=-1, NX
XWORK (MX) =XSTR (NT ,MX)
46 YWORK (MX) =YSTR (NT ,MX I

```

```

45 CALL LINESG(ZMQBE»NX»XV*ORK,Y*ORK)
DO 47 JJ=1,NX
DC 48 NN~1,NY
ARRWORK1JJ,NN>=PC TEN(JJ,NN)
48 CONTINUE
47 CONTINUE
XO=A2/1C0.
Y0=A4/1C0.
CALL CCNZSIZMCDE,I,8,XO)
CALL CCNZS(ZMQDE,1,9,Y0)
CALL CCNZSIZMCDE,1.18.1>
CALL CCNZSIZMCDE,1,17,1)
CALLCCNRECIARRtOCRK,100,NX,NY,SUMAX.SUMIN»-10.,-1,-1,0)
***** DRAW REPOSITORY.BIGSPHERE AND NORTH DIRECTION *****
CALL SETS*G(ZMCDE,185,1.0J
CALL CIRARG(ZMODE,XREP,YREP,RAO,ANG1,DANG»
IF(INDATA.GT.O)CALL LINESG5 ZHODE,NCATA,X310,YR10)
CALL SETS*G(ZMODE,14,3.0)
CALL VEC2XYIZMCCE,AA,20.,4.,ANGNO,0.,0.,11
IVAL'JE=IHN
CALL SETSMGtZMODE,189,0.51
CALL SETSVG(ZMCDE,84,IVALUEI
CALL POINTGtZMGDE,1,VEX,VFY)
CALL SETS^GIZMODE,14,0.)
IF(NW.LE.O) GC TC 59
CALL SETSMGIZMODE,189,0.4)
DO 55 NWELL=1,NW
DC 54 1=1,F
ANGU=(1-1)*45.*3.1416)/180.
ANGULO=(1-1)*45.
1DMX=AMAXI((YMAX-tMN),JXMAX-XMIN)
RADIUS=RDMX/30.
SENGHT=C.8*RACILS
AX=RADIL'S*CCSS ANGL)
AY=RADILS*SINT ANGL)
XARR=XWELL(NWELL1-XTRANS
YARR=YWELL(NWELL1-YTRANS
IF(Q(NWELLI.LT.C.) XARR=XAPR+AX
IF(0(NWELL»LT.C.) YARR=YARP*AY
IF(CMNWELLI.LT.C.) ANGLLC=(I«-3)*45.
CALL VEC2XYIZMCDE,XARP,YARR,SENGHT,ANGUI0,0.,0.,1»
54 CONTINUE
55 CONTINUE
59 CALL SETSMG(ZMCDE,189,Q.5>
IF(POTPLOT.LE.O,t GO TC 83
CALL SFTSMG(ZH00E,45,1.0)
CALL SETSMGIZMCDE,50,0.i
83 :)D 24 NSTR=1*NTETA
DIMIN=•1.0E+300
DO 30 LX=1,NX
DIFFE(LX)=ABS(TSTF(NSTR,IX)-ZMIN(NU)1
DIMIN=AMIN1(0IMIN,DIFFE(LX)I
20 CONTINUE
DO 51 LX=1,NX
51 IF(DIFFECLX1.EO.DININ» KX=LX
IF(TSTP(NSTR,KX).EC.O.) GO TO 18
ABSTINSTR)=XSTR(NSTR,KX)
8ACT(NSTR«=YSTR(NSTR»KX»
GO TO 15
18 TETA=TETA1+(NSTR-1)*(TETAf-TETA1)/(NTETA-1)
A3SUNSTRi«XREP*RAC*CCS(TETAJ
3ACT(NSTR)=YREP>RSC*SIN(TETA)

```

```

19 WRITE16 ,131» NSTR,ABST(NSTR»»BACT(NSTR»
.31 FORMAT(1X,*TRAILING*,2X,I4,3X,2.PE9»2,3X,1PE9.2! 300
24 CONTINUE
I VALUE=1H*
CALL SETSMG(ZMODE,84,IVALUE»
CALL SETSMG(ZMODE,45,1.0!
IT(GRAPLNUI.GT.O.(CALL PCINTG(ZMODE,NTETA,ABST,BACTI
00 35 J5=1,NTETA
WRITE(6,106) J5
L08 FORMAT(1X,I4,3X,5I1PE9.2,3X)
WRITE(6,147)
147 FORMAT(2X,*NX*,3X,*X-IMETERI*,3X,*Y-(METERbx,*SIGMA(YR»*,3X,*N
$/N0*,3X,*QILUTICN RATE(CUBIC METER/YEAR I*)
TAX(J5)=-1.0E+300
00 36 J6=1,NX
Z-TSIR(J5,J6>
CALL MACKNU,Z,TIME,A,BS
XWORM J6>-E
WRITE(6,105)J6,XS1RIJ5,J6),YSTR(J5,J6),TSTP(J5,J6),A,B
109 FORMAT(1X,I4,3X,5I1PE9.2,3X)
36 CONTINUE
DO 38 LX=1,NX
28 TAX(J5)=AMAX1{TAX(J5J,XWOPK(LX))
DO 53 LX^1,NX
53 IF(TAX(J5),EQ»XWOPK(LX)) KX=LX
ABSM(J5 J=XSTR(J5,KX1
BACM(J5)-YSTR(J5,KX)
IF(ABSM(J5J.E2«AeST(J5J» GO TO 26
GO TO 26
26 IF(BACM{J5}.NE.RACT(J5)) GO TO 28
ABSM(J5J=XSTR(J5,KX+KO>
BACM(J5YSTR(J5,KX*KD!
28 WRITE(6,133I J5,ABSM(J5),BACM(J5)
125 FORMAT(1X,*MAXIMU»*,2X,I4,3X,1PE9.2,3X,1PE5.2i
35 CONTINUE
DO 33 J3=1,NTETA
3IMIN=*UOE«-300
DO 34 LX"1,NX
DIFFE(LX>=ABS(TSTP(J3,LXJ-ZMAX{NUI>
DIMIN=AMIN1(DIMIN,CIFFE(LXM
34 CONTINUE
DO 52 LX=1,NX
52 IF(DIFFE(LX».ECO WIM KX" LX
A3SL(J3 J=XSTR(J3,KX)
BACL(J3)=YSTR(J2,KX1
riRITE(6,1»2I J3,ABSLIJ3»,BACL(J3)
132 FOPMAT(1X,*LEADING*,2X,I4.3X,1PE9.2,3X,1PE9.2)
32 CONTINUE
I VALUE-- 1H*
IF(GRAP(NU».GT.O.»CALL PCINTG(ZMODE,NTETA,ABSL,BACLI
CALL FRAME
29 CONTINUE
13 CONTINUE
CALL EXITG(ZMCDE»
STOP
END
SUBROUTINE MAC1111,Z,TT,P,W)
DIMENSION TCX(20)
COMMON/D/B,BETA
LEVEL 2,1,T,TeL,E,K,C,TOX
LEVEL 2,B,BETA
CCMMON/CONC/I,T,TEL,E,K,C,TOX

```

```

DOUBLE  E(2C)»K(2C),C120i»B120»201»BETA(20,201
DOUBLE  S1TS2»S3
DOUBLE  C1»C2»C3»C4,C5,X1»X2,X3,X4,PR1»PR2
DOUBLE  E3»EC»EE»EEE
DIMENSION  W1(20),wZI 20 ),W3(20>
DIMENSION  S(20),SU20),V(20)
CALL  BATEMAN(I,E,C,B)
DO 60  11=1,1
Y=0.
DC 62  111=1,II
rV6*-E(III)»*T3L
Y=Y+B(II,1U i*EXPIK61
C(II 1=Y*E1IÎ)*C11)/fî.î )
CALL  BATEMAN(I,E,C,B)
VW=1.
DO 64  IJ=1,I
• \/(1J}=V»/K(IJS
DO 21  Mi=i,i
DO 22  MJ=I,I
IF(MI.ECJ.MJ>GC TC 22
IFIVÍMJUEC.VÍMI II GC TO 59
3BETA(MI,MJ1ME(MII*\/(MJ>-E(MJ>+\MMI1»/(V(MJ)-V(MIN
BETAIMJ,MII=BETÄ(MI,FJ)
GO TO 22
) BETAIMJ,MI)=0.
i CONTINUE
CONTINUE
DO 39  K4=1,I
S(K4)=0.
ST(K4)»=0.
! CONTINUE
DO 40  K5=1,I
IFfV(K5i*TT.GE.ZI S(K5i~1.
IF(V(K5)*(TT-T).CE.ZI ST(K51=1.0
I CONTINUE
C1=0.
DO 51  12=1,11
ED=(-E(12>* (TT-Z/V(II)» ABS(S(I1)»-STfI1)»
CALL  EXPO!EO,EEI
C1=C1+B(I1,I)»*EE*(S(i1)-STUin
EB=(-Etili*Z/V(I1II*ABS(S(I1i-ST(11i)»
CALL  EXPct EE,EEE)
C1=C1*EEE*(S(I1)-ST(I1>J
C5=0.
IF(II.ECU GO TC 71
WMAX=0.
DO 521  L»1,11-1
DO 531  f. = L,11
Ds-SIMI-SKHI
ADS=ABS(DS J
DO 541  NR=L,I 1
IFINR.ECMI GC TC 541
DO 551  J=1,L
W1(J)=(-BETA(NR,w|*(TT~Z/V(M))-E(MI*Z/V(M))>*S(Mi
^2(J1=(-T*(E(J1-BETA(NR,Mi)-BETA(NR,"),t*(TT-Z/V/(M)»>-E(Mi*Z/N/(M)»)*ST
s i M)
W3(J)=(-E(JI*(TT-Z/V(M)-E(M)*Z/V(M)|)*ADS
IF(BETA(NR,Mi.EQ.C.» w1(J) - 0.
IF(BETA(NP,MJ.EC.C.IW2SJ = 0.
IF(BETA(NR,M|.ECC.>K3(J) = 0.
IF IW1ÍJI.GT.WNAXJ nMAX=W1 JI
IF(W2(J)».GT.WMAX) WMAX=H2 Ji

```

```

51 IF (W3( J1.GT.WAX » hMAX=W3(J>
41 CONTINUE
.31 CONTINUE
21 CONTINUE
  IF(WMAX.GT.600.) CIFF=WMAX-600.
  IFIWMAX.LT.600.) CIFF=0.
  DO 52 NJ- 11 U-1
  C4=0.
  DO 53 NM=NJ,I 1
  C3=0.
  DO 54 NR = NJ 11 1
  IF(NR.EC.KF) GO TC 54
  C2=0.
  DO 55 NK=1,NJ
  PR1=1.DOO
  DO 53 NQ=NJ,I 1-1
58 PR1=PR1*E(NCf*K(NC.
  ?R2=1.DOO
  DO 57 Nc = NJ »I 1
  IF(NO.EC.NR> GO TC 57
  IFtNQ.EC.NH» C-C TC 57
  PR2=PR2*1EtNQ» *K(NC)*(KtNR)-K(NM)>t-E(NH)*K(NM)*(K(NQ)-K(NR))+E(NR)
  $*K(NRJ*(K(NM,-K(NC))»
57 CONTINUE
  X1=B(NJ,NK)*(K(NP)-K(NM,,** (I1-NJ-1)
  X1=X1/(E(NK1*K(NR1-E(NK,*K(NM1-E(NRi*K(NP»*E{NM1*K(NMI.
  X1=(X1*PR1J/PR2
  S1=t-BET4(NR»NMI*tTT-Z/V(NM)S-E(NM)*Z/V(NMI!
  S2=rJ-T*(E(NK>-8ETMNP,NM>>)*S1
  S1=S1*S(NM)
  S2=S2*SY(Nf I
  S3M-EtMa*TT-(E(NM,-E1NKN*{Z/V(NM)))
  S3=S3*ABS(SINKJ-ST(NMI))
  S1=S1-DIFF
  S2=S2-DIFF
  S3=S3-DIFF
  CALL EXP0(S1,X3)
  IFtBETA1NRtNMI.EC.C.J X3=0.
  X3=X3*S(NM»
  CALL EXP0(S2,X2J
  IF(BETA(NR»NMI.EC.C.> X2=0.
  X2=X2*ST(NHi
  CALL EXP0(S3,X4)
  X4=X4*(SINK»-ST(N*))
  C2=C2+XI*(X3-XZ-X4>
55 CONTINUE
  C3=C3*C2
54 CONTINUE
  C4=C4+C3
53 CONTINUE
  C5=C5+C4
52 CONTINUE
71 IFUL.EC.11 DIFF-C.
  TEC=(E(1»*K(\JI/(E(II)*K(111)
  IFIC5.GT.TEC1 GO TC 97
  IF(DIFF.GT.600.. GO TO 97
  P=C1+C5*EXP(DIFF i
  IF(P.LT.O.I P=0.
  ,V=P*C(11*E(II»/(E(1>*TOX(11>*T)
  GO TO 58
97 P=0.
  W=0.

```

98 RETURN

303

```
END
SUBROUTINE B4TEMAM I,E , C,B)
LEVEL 2,E,C,B, I
DIMENSION E(20,, C(2G), B120, 20J
DOUBLE C,E,TEMPI,E
DO 27 L1 = 1, I
DO 28 LJ=1, I
TEMP1=0.
DO 31 LM'1, LJ
TEMPZ-1.
DO 29 LR=LM, L I
TEMP2=TEMP2»E(LR )
```

29 CONTINUE

```
TEMP3=1.
DO 30 LL=LM, L I
IFILL.EC.LJ» GC TC 20
TEMP3~TEMP3*1EILLJ-E(LJ> )
```

3D CONTINUE

```
TEMP1=TEMP1*(C( If* »*E(1»/(C(1I*E(LM)M*TEMP2/(E(LI)»TEMP3)
```

31 CONTINUE

```
3(LI, LJ1=TEMP1
```

28 CONTINUE

27 CONTINUE

```
RETURN
END
```

```
SUBROUTINE EXPOLX , Y )
DOUBLE X, Y
IF(X.LT.-6.0D2 > GC TO 501
Y=DEXP(X )
GO TO 502
```

501 Y=0.0D00

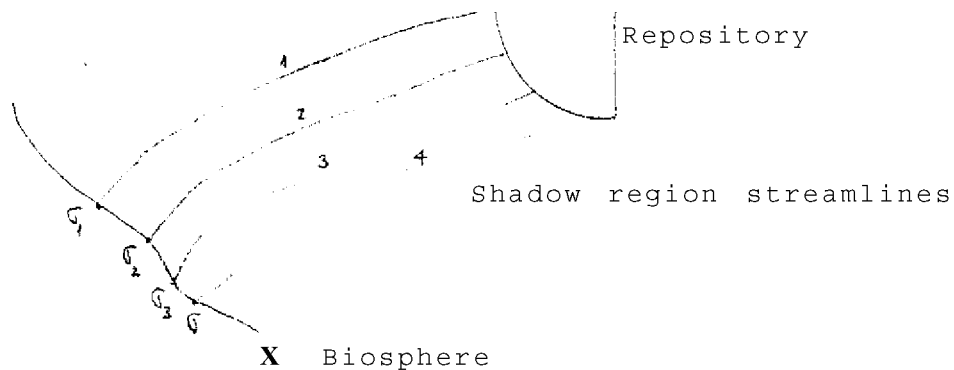
502 RETURN

```
END
```

C.3 Subprogram DCHARGE data input description

Subprogram DCHARGE evaluates the discharge rate, the water dilution rate rate, the cumulative discharge and the water dilution volume at the biosphere for a i -th member of a radioactive chain of arbitrary length migrating in groundwater through a two-dimensional geologic media.

The subprogram DCHARGE is entirely independent of the PLOTMAC program. It is related to HYDRO subprogram only by the water travel time at the biosphere which must be read out of the HYDRO printout. Another set of data that must be obtained from the HYDRO print outs are the volumetric flow rates between the streamlines of the shadow region. Suppose the system studied can be represented by the following sketch



The values of $o(1), o(2), \dots, o(NTETA)$ as well as $Qd), Q(2), \dots, Q(NTETA)$ can be obtained from HYDRO. The fractional volumetric flow rate is defined as

$$RQ(J) = Q(J) / \sum_{D} Q(D), J=1,2,\dots,NTETA \quad (C.3.1)$$

Once the hydrology is defined by HYDRO, DCHARGE can evaluate the water dilution rate and the water dilution volume Eq. (4.2.26) and Eq. (4.2.27) respectively for any radionuclide chain at any point inside the shadow region. The particular location where the calculations are to be performed is not characterized by a coordinate pair but rather by the correspondent water travel time value at that point.

Card 1: FORMAT(110,2(F10.3,I10))

Variable	Description
NTETA (110)	Number of contaminated streamlines to be considered. It is not necessarily the same as in HYDRO. (NTETA must equal or larger than two).
TBLO (F10.3)	First value of delay time for beginning of leaching to be used (years).
DELI (F10.3)	Multiplying factor for the next NTBL cases of time for beginning of leaching to be evaluated.
NTBL (110)	Number of different cases of time for beginning of leaching (TBL) to be evaluated. TBL=TBL0x(DEL1) ;k=1,2,___NTBL.
TO (F10.3)	First value of leach time to be used (years).
DEL2 (710.3)	Multiplying factor for the next NT cases of leach time to be evaluated.
NT (110)	Number of different cases of leach time (T) to be evaluated :T=T0x (DEL2) ^j ;j=1,2,...NT.

Card 2 through Card 2+NTETA: FORMAT(2F10.3). NTETA of these cards are required, one for each streamline describing the shadow region.

Variable	Description
SIGMA (F10.3)	Value of the water travel time at the location where this streamline intercepts the biosphere (years).
RQ (F10.3)	Fractional volumetric flow rate as defined in Eq. (C.3.1) for this streamline.

Card 3+NTETA: FORMAT(3I5)

Variable	Description
NTIME (15)	Number of time intervals that the contamination time of a radionuclide at the biosphere is to be divided. NTIME does not affect the accuracy but to produce a smooth plot it is recommended that NTIME be equal to 20 or larger.
NMEMBER (15)	Number of members in the radioactive chain.
KS (15)	Number of intervals that the biosphere curve is to be subdivided between two consecutive streamlines. The accuracy of the calculations is very sensitive to this number. If leach time is small compared to the arrival time of the nuclide this number should be increased. A first try is KS=50.

Card 4+NTETA through Card 4+NTETA+NMEMBER:

FORMAT(A7,5F10.3). One of these cards is required for each member of the chain. The cards must be ordered in the same way the chain is.

Variable	Description
NNUCL (A7)	Nuclide name (e.g. RA-226).
THALF (F10.3)	Nuclide half life (years).
K (F10.3)	Nuclide retardation coefficient.
C (F10.3)	Nuclide total activity at the time of burial (Ci)
RCG (F10.3)	3
CALC (F10.3)	Nuclide maximum permissible concentration (Ci/m) If CALC <0 the program does not calculate for this nuclide although uses its parameters for its daughters calculations.If CAL0 0 the program prints and plots the results for this nuclide.

Figure C.I Structure of the subprogram DCHARGE.

```

Initialize

Read data input

Do every case of time for
for beginning of leaching
TBL=TBL0*(DELI)**K;K=1,..NTBL.

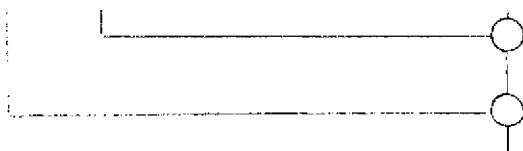
Do every case of leach time
T=T0*(DEL2)**J;J=1,..NT.

Do every member of the chain
I=1,2,..NMEMBER.

If CALC > 0 evaluate the water
dilution rate (Eq.4.4.20) and
water dilution volume (Eq.4.4.21).

If CALC >0 plot and print the
results for this nuclide:the water
dilution rate and the water dilution
volume. I

```



IA. 868301, TINGt 0

INPUT 6200C 13.23.39 10 SEP 81 VIA CR02

309

) =

'Y, INPUT /R.R, OUTPUT/RR.

5POSE, 0JTPUT=PR, PA*1F.

) CRAM UCBNE21 (SUBPROGRAM OCHARGE)

*4IEL K.S. TING

PARTMENT OF NUCLEAR ENGINEERING

[UNIVERSITY OF CALIFORNIA, BERKELEY

KELE ^, CA., 94720

CONTROL CARDS LISTING **

0BCARC1

ASSWOFD)

SERPR.

F<., L*0.

THLIB.

TCHFS, IDOS, ULIB, ULIBX.

TCHFS, GPACBN7, GPAC, VA3N.

NK, F=LGO, F=GFAC, P=ULIB, X.

APHIC»FN*FILM, FT=VA.

IT.

MP, 0.

JMP.

PROGRAM LISTING

```
PROGRAM OCHARGE (INPUT • OUT PUT , TAP£5= INPUT , TAP£6*0 UT PUT , FILM1
COMMON/IGSZZZ/ZMCDE(201)
COMMON/CONC/NKEHEER, T, T3L, E, K, C, RCG( 20 )
DIMENSION X(2Q), H(2Q)
DIMENSION NKUCL(20), CALC(20)
DOUBLE TMAX, TMIN
00U3LE ZMIN, ZMAX
DOU3LE THALF, K(20), E(2C), C(20), SRFMX, SRPMN, SMAX, SMIN
DIMENSION XNAME(70J, YNAHE(70) » TNAHE(15G>
DIMENSION ZMIN(20>, ZKAX(20), SIGMA(2L), RQ<20)
DIMENSION PLCTES<1GQI, 1IMEPC1C0)
DIMENSION RATE(5*100) tTOTAL(5*100) «TIKE(51100)
DIMENSION RN(180Q).TOXRATE(5,10t).TOXTOTA(5.1QCI
READ(5,100! NTETA, TBLC, DELI, NTBL, TO, OEL2, NT
100 FORMAT (I10•2(2F10.31110>>
DO 22 ITETA=1, NTETA
READ(5,1011 SIGfA(ITETAJ, RQ(ITETA)
101 FORMAT (2F10.3)
22 CONTINUE
READ(5,102) NTIhf»NMEMBER, KS
102 FORMAT (315)
DO 10 1=1, NMEMBER
READ(5,103) NNUCL(I), THALF»K(I), C(I), RCG(I), CAL3 CI)
1C3 FORMAT (A7,5F10.3)
10 E(I) =DLOG(2.D00)/THALF
READ(5,107) HOL1.HCL2
107 FORi AT (2A8)
TBL = T3L0/DEL1
```

```

DO IODO IT BL=i»NTBL
TBL= TBL* CEL1
DO 11 NUC=i f NMEKBER
IF (CALC iNUC) .LE.O.) GO TO 11
TMAXs-1.00*300
TMIN*1.00*300
TsTO/DEL 2
DO 1QÜ1 IT=i,NT
T=r»0EL2
SRPIXs-1.0*300
SRPMN= 1.0*300
DC 12 JU=1, KUC
SRPMX=DMAXi (SRPMX,K (JU>i
12 SRPMN= DMIN1 (SRPKN,K (JU) )
00 13 NS TR=1,NTETA
2MAX (NSTR)x SIGMA (NSTR)*3RPMX*T
13 ZMIM(NSTR) = SIGMA (NSTR) *3RPMN
SMAX D*300
SMIM =1.D*300
00 14 NS TRs1 ,NTETA
SHAXsDMA XI (SMAX,Z*AX (NSTR) )
SKIN=DMIM (SMINTZKIN iNSTR) )
14 CONTINUE
00 17 NSTR = 1,NTETA
17 X(NS TR) = FLOAT (KS*NSTR)
00 18 NS TR=1,NTETA
00 19 NS=1, KS
NN=KS*NS TR • (NS-1)
RN(NN) =RQ (NSTR) /KS
19 CONTINUE
16 CONTINUE
CALL POLINT (NTETA, X, SIGMA, Hi
DELT A= (DLOGi0LSMA » -DLOG1 C(SMIN)) / (NTIME-1)
DO 15 IT IMEs1,NTIME
AXPA sDLOG10 (SMIM*(ITIME-1 >*DELTA
TlMi (IT, ITIME)*10. ••AXPA
TT=TIME (ITtITIME)
TGTALOT ,ITIME)=Q.
RATE (IT, ITIME) =0.
DO 20 NSTR=KS,NTETA*KS
XX=FLOAT (NSTR)
CALL POLYVL (0, XX,Z,YP,NTETA,X,H, WORK , 1ERR)
CALL MACKNUC,Z,TT,SMIN,P,W)
RATE (IT,IT Ihe)=RATE (IT,ITIME) *P»C(1) *RN(NSTR) /T
TOTAL (IT,ITIMt) =TOTAL (IT, ITIML > *W»C(1) »RN(NSTR) /T
20 CONTINUE
TOXRATE (IT, ITIME I=RATE (IT, ITIME) /RCG (NUC)
TOXTOTA íIT,ITIME) =TOTAL (IT,ITIME) /RCG (NUC)
15 CONTINUE
WRITE (6,104) NNUCL(NUC),T 8L,T
LC4 FORMAI 11H1 ,5X, *NUCLIDE - 11A7 , 3X, * DELAY TIME (YRS) =*,1Pt 8.2,3X,*L
tEAC-( TIME (YRS) =*,1PE8.2)
WRITE í6,105)
LC5 FCRMAT í//,1X,jcTIME (Yt) í , 2X, * DISCHARGL RATE (CI/YRGWYR) *, 2X, íCUMUL
SATIVE OI SCHARGE (CI/GWYR) *, 2X, /RATE/MPC (M3/YRGWYR) t, 2X, tCUMULATIi
SE/MPC (M3/GWYR) t)
00 16 IT IME=1, NTIME '
WRITE (6, 106) TIHE íIT, ITIME) , RATE (IT, ITIME) ,TOTAL {IT, III ME í ,TOXRATE
KIT, ITIME) ,TCXTCTA (IT,ITIME)
1C6 FORMAI (IX,1PE8.2,12X,1PE8.2,20X,1PE6.2,20X,1PE8.2,¿0X,1 PE 8.2)
16 CONTINUE
TMAX=DMAXi (SMAX,TMAX)

```

```

T H I N=D M I M ( S M I N , T M N )
1  CONTINUE
CALL  MODESG ( Z M O O E , 6 , 0 )
RATE M X s - 1 . O E + 3 0 0
RATE M N ' i « . Q E * 3 0 0
TOTAL M X = - 1 . C E + 3 0 0
TOTAL M N * i . Q E * 3 0 0
DO 1 0 0 3  I T « 1 , N T
0 0 2 3  I T I M E = 1 » N T I F E
I F ( T O X R A T E ( I T , I T I M E ) K L T . 1 . G E . < . > T O X * A T E C I T I T I M E I = 1 .
I F ( T O X T O T A ( I T • » I T Z M E i » L F . 1 • 0 » T O X T O T A ( I T , I T I M E » « 1 . 0
T I M E ( I T , I T I M E ) s A L O G 1 0 ( T I M E ( I T , I T X W E ) >
R A T E M X B A M A X I ( R A T E M X , T O X R A T E ( I T , I T I M E ) I
R A T E M N = A M I N K R A T E M N , T O X R A T E ( I T . I T I M E > )
T O T A L M X = A M A X 1 ( T O T A L M X , T O X T O T A ( I T , I T I M E ) )
T O T A L M N = A M I N 1 ( T C T A L M N , T O X T O T A ( I T , I T I M E ) )
T O X * A T E < I T , I T I M E U A L O G 1 0 ( T O X R A T E ( I T , I T I M E ) )
T O X T O T A ( I T , I T I M E ) = A L O G i G ( T O X T O T A ( I T , I T I M E ) )
2 3  CONTINUE
0 3  CONTINUE
X M A X = F L O A T ( I O I N T ( D L O G 1 0 ( T M A X ) ) ) * 1 . 0
X H I N = F L O A T ( I O I N T ( D L O 6 1 C ( T M I N ) ) )
O I V X s 1 . 0
D I V Y s 1 . 0
A s A L O G 1 0 ( R A T E M N )
Y M I N s F L O A T ( I N T ( A ) )
I F ( A • L E • 0 . ) Y M I N = F L O A T ( I N T ( A ) ) - 1 .
B s A L O G 1 0 ( R A T E M X )
Y M A X s F L O A T ( I N T ( 8 ) ) * 1 .
I F ( 3 . L E . 0 . ) Y M A X = F L O A T ( I N T ( B ) )
I F ( A B S ( Y M A X - Y M I N ) . G E . & . ) O I V Y = 2 , 0
    P L O T   T H E   C I S C H A R G E   R A T E
C A L .   S U B J E G   « Z M C D E , X M I N , Y M I N , X M A X , Y M A X )
C A L L O B J C I G < 2 M G Q E , 3 0 , , 2 0 . , 9 0 • , 6 0 , )
C A L L   S E T S M G ( Z M C C E , 4 5 , 1 . 5 )
C A L L   G R I O G ( Z M O O E , C I V X , D I V Y , 0 , 0 )
C A L L   L A B E L G ( Z M O O E , 0 , 0 I V X , 0 , 3 )
C A L L   L A B E L G ( Z M O O E , 1 , D I V Y , 0 , 3 )
E N C O D E ( 5 0 , 2 0 C 0 , X N A M E )
0 0  F O R M A T ( 1 0 X , / T I M E   A F T E R   L E A C H I N G   S T A R T E D   ( Y R S ) * )
E N C O D E ( 7 0 , 2 0 0 1 , Y N A M E )
0 1  F O R M A T ( 2 X , I T   D I S C H A R G E   R A T E / M P C   ( C U B I C   M L T E R / Y R ) / )
E N C O D E ( 1 5 0 , 2 0 C 2 , T N A M E )   N N U C L ( N U C ) , H 0 L 1 , H 0 L 2
0 2  F O R M A T ( A 7 , *   C I S C H A R G E   R A T E   H I S T O R Y   A T / . 2 A 8 )
C A L L   T I T L Z S ( Z M O O E , 1 , 1 , 1 . )
C A L L   T I T L Z S ( Z M O D E , 1 , 2 , 1 . 8 1 )
C A L L   T I T L E G ( Z M O D E , 5 0 , X N A M E , 5 0 , Y N A M E , 1 5 U , T N A M E )
0 0 1 0 0 4   I T s 1 t M T
T O X R A T E ( I T » 1 ) = Y M N
T O X * A T E ( I T , N T I M E ) = Y M I N
0 0 1 0 0 5   I T I M E = 1 , N T I M E
T I M E P ( I T I M E ) = T I H E ( I T , I T I M E )
0 5  P L O T E R ( I T I M E ) = T O X R A T E ( I T , I T I M E )
C A L L   L I N E S G ( Z M C D E , N T I M C , T I M E P , P L O T E R )
I C  C O N T I N U E
    P L O T   T H E   C U H M U L A T I V E   D I S C H A R G E
C A L L   F R A M E
D I V Y = 1 . 0
W N A X s F L O A T ( I N T ( A L O G 1 0 ( T O T A L M X ) > ) + 1 . 0
W M I N = F L O A T ( I N T ( A L O G 1 0 ( T O T A L M N ) I )
I F ( ( W M A X - W M I N ) . G E . 6 . )   D I V Y = 2 . 0
C A L L   S U 3 J E 6 ( Z M O O E , X M I N . W M I N , X M A X , W M A X )

```

```

CALL 06JCTG(ZMOCE,30.,20.,90.,60.i
CALL SETSMG (ZMOCE,45,1.5)
CALL GRIDG(ZMOOE,CIVX,ûIVY,û,G)
CALL LA6ELG(ZMODE,û,OIVX,0,3)
CALL LABELG(ZMCDE»1»DIVY»0,3)
ENCOOL (70,2003,YNAME)
03 FORMAT it CUMULATIVE 01SCHARGE/MPC CCUBIC METER) *)
ENCOOE(150,2004,TNAME) NNUCL(NUC),HOL1,HOL2
04 FGRMAT (A7,* CUMULATIVE 01SCHARGE US TORY AT/ ,2A8)
CALL TITLZS(ZMOOE,1,1,1.)
CALL TITLZS (ZMOOE,1,2,1.8)
CALL TII LEG(ZMODE,50,XNAME,50,YNAME,15û,TNAMEJ
OO 1006 IT-i.NF
OO 1007 ITIME=i,MIME
TIMEP(ITIME)=TUE(IT,ITIME)
107 PLOTTER(ITIME)=TCXTOTA(II,ITIME)
CALL LINESG(ZMOCE,NTIME.,TIMEP,PLOTTER)
OELTA1*(XMAX-TIME(IT»NTIME))/(NTI»E-1)
DO 1500 ITIME=1»NTIME
TIMEP(ITIME)=TIME(IT»NTIME)*(ITIME-1)*OELTA1
AXP=10.»*TIMEP(ITIME)
PLOTTER(ITIME)=TOXTOTA(IT,NTIME)»EXP(-E(NUC)*AXP)
;CC CONTINUE
CALL LINESG(ZMCCE,NTIME,TIMEP,FLCTER)
106 CONTINUE
CALL FRAMe.
11 CONTINUE
JOC CONTINUE
STOP
END
SUBROUTINE MAC1(I1,Z,TT,TA,P,W)
DIMENSIONIGK TOX(20I
CC.-MON/L>/B,8ETA
COMMUN /CONC/I,T,TBL,E,K,C,TOX
OOUBLE E(20),K(20),C(2û),6(20,20),BETA(20,20)
CûUBLE A1,A2,A3,Y1,Y2,Y3,D1,Q2,D3,D4,P1,P2,P3,P4
OOUBLE S1,S2,S3
OOUBLE EZ,EY,TA,EW,EF
DOUBLE AF,AZ
DOUBLE C1,Ci,C3,C4,C5,X1,X2,X3,Xt.,PR1,PR2
DOUBLE EB,cD,EE,EEE
DIMENSION hi(20),W2(2û»,W3(20)
DIMENSION S<2C),ST(20),V(20)
CALL BATEMAN(I1,E,C,8*
OC 60 11=1,11
Y*0.
OO bZ 111=1,11
X6=-E(III)*T8L
62 Y=YfB(II.HX)*EXP(H6>
60 C(II)=Y'£(II;j*C(i)/EC11
CALL BATEMAN(I1,E,C,B)
VH=1.
OO Q*, IJ=1,I1
6-, V(IJ)=VW/K(IJ)
OC 21 MI=1,11
OO 22 MJ=1,I1
IF(MI.EQ.MJ) GC TO 22
IF(V(MJ).EQ»V(MI)) 60 Tû 59
BETA(MI,MJ)s(E(MI)'V(MJ)-E(MJ)*V(MI))/(V(MJ>-V(MI))
BETA(MJ,HI)=BETA(MI,MJ)
GO TO 22
59 BETA(MJ,MI)=0.

```

```

22 CONTINUE
21 CONTINUE
DO 39 Ki.=1,I 1
S(K4)= 0.
ST(K4)=0 •
39 CONTINUE
00 <tQ K5si, I1
IF(V K 5) *TT>GL.Z) S (K5)=1.
IF(V (K5J * tTT-TJ .GE.Z) ST (K5) *1•0
40 CCNTINUE
P1=û .
Ci=Q .
ÛC 51 12*1,11
£0= (-E (121 * 4TT-Z/1? (I11) I* ÂBSISîîîî-ST (ID)
CALL EXPO(ECEE)
IF(TT.GE.K(I1)>Z) GO TO 30
EF=£Z=0.000
GO TO 31
30 IF(TT.GE.(K(ID*Z*T>) GO TO 32
IF(TA,LE.K(I1)>Z) GO TO 33
EF=-E(I2 1*(TA-Z/V(11) I
EZ=-E(I2 )*(TT-Z/V(ID)
GO TO 31
33 EF=0•
EZ=-E(I2 )MTT-Z/V(ID)
GO TO 31
32 IF(TA.GT.K(ID*2) GO TO 34
EF=2 .
EZ=-E(12)*(TT*T)
GO TO 31
31. IF(TA.GT,(K(ID>Z*T) GO TO 35
EF=-E(12 >*(TA-Z/Vd1M
EZ=-E(12 )•CTT+T)
GO TO 31
35 EF=£Z=0.
31 CALL EXPü(EF,EY)
CALL EXPO(EZ,EH)
P1*P1*B(II.12)•(EY-EM)/£(12)
51 C1=C1<-8(I1.I2)*EE>(S(I1)-ST(ID)
EB=(-c(II)*Z/V(ID)*A35(SUD-ST(ID)
CALL EXPO(EB,EEE)
C1<C1>EEE*(S(ID-ST(ID)
C5=0•
P5=0.
IFC11.EQ.11 GO TO 71
KMAXxc .
00 5 21 Ls1,11-1
00 5 31 H=L,11
DS=S(M)-ST(M)
ACS=ABS(OS)
OC 541 NR=L,11
IF(NR,EC<M) GO TO 541
CO 551 J=1,L
H1(J)=(-BETA(NR,WMTT-Z/V(M))-L(M)*Z/V(M))>S(M)
H2(J)=(-T>(E(J)-8ETA(),K))-BETA(NR,M)>(TT-Z/V(M))-E(M)>Z/VIM)>*ST
S(M)
K3(J)=(-E(J)*(TT-Z/V(M))-E(M)>Z/V(M))>ADS
IF(3ETA(NR,M).EQ.O.) H1(J)xQ.
IF(BETA(NR,M).ECO.) H2(J)=0,
IF(8ETA(NR,»/).EQ.O.) W3(J)xO.
IF(W1(J).GT.HMAX) WMAX=W1(J)
IF(W2(J).GT.WMAX) WMAX=W2(J)

```

```

51 IF {H3 ( J ) .GT.WMAX) HMAX=H3 (JS
1.1 CONTINUE
31 CONTINUE
21 CONTINUE
IF < WMAX.GT.600.) DIFF=WMAX-OC0.
IF (WMAX.LT.600.) OIFFSÛ.
OC 52 NJ=1,11-1
C4=Q •
Pi»=0 •
00 53 NM=NJ, I1
C3=0 .
P3=0.
DO 5 k NR=NJ, U
IF (NR.EQ.NM) GO TO 5%
02=0 .
P2=0«
DO 55 NK=1, NJ
PR1r 1. DO 0
00 58 NQ=NJ, I1-1
58 PR1=PR1*E(NQ) *K(NQ)
PR2=1. DOC
00 57 NQ=NJ, I1
IF(NQ.EQ.NR) GO TO 57
IF(NQ.EQ.NM) GO TO 57
PR2=PR2ME(NQ) »K(NQ) • (K(NR)-K(NM)) •E(NM) »K(NM) »(K(NQ)-K(NR)) > *E(NR >
$»K(NR) » (K(NM)-K(NQ))
57 CONTINUE
X1=3 (NJ, NK) * (K(NR)-K(NM)) »»(I1-NJ-1i
X1=X1/ ÍE(NK) *K(NR)-E(NK) *K(NM)-E(NR) »K(NR)+E(NM) *K(NM))
X1=(X1*PR1)/PR2
S1=(-BETA(NR,NM) * (TT-Z/V(NM)) -E(NM) »Z/V(NM))
Ai= Í-BEIA(NR,NM) «CTA-Z/V(NM)) -E(NM) *Z/V(NM))
IF(TA.LT.K(NM) »ZI A1=-E(NM) *Z *K(NH)
S2=(-T*(E(NK)-BETA(NR,NM))) *S1
A2=(-TME(NK)-BETA(NR,NM)) ) +A1
IFdA.LT.(K(NM)*Z*T) -Ü2=-T*E(NK)-E(NM) »Z*K(NM)
51=S1*S(NM)
52=S2*ST(NM Î
S3=(-E(NK) *TT-(E(NM)-E(NK)) *(Z/V(NM)))
A3=(-E(NK) • ÎA-iE(NM)-E(NK)) »(Z/V(NM))
IF(TT.GL.K(NM)*¿) GO TO 8 C
AF=A Z=0-
GO TO 81
80 IF(TT.Gt «(K(NM) *Z*T) | &0 TO 82
IF(TA.LE.K(I1)*2) 60 TO 83
AF=A 3
AZ=53
GO TO 81
83 AF=-E(NM) * Z*K(NM Î
A7=53
GO TO 81
82 IF(TA.GT «K(NM) *Z) GO TO 84
AF=-E(NM) * Z*K(NM)
AZ=-E(NK) * T-E(Nh) »*Z*K(NM)
GO TO 81
84 IF(TA.GT.(K(NM) *Z+T) ) GO TO 85
AF=A 3
AZ=-E(NK) *T-E(NM) *Z*K(NM)
GO TO 81
85 AF=AZ=0.
81 AF=AF-01FF.
AZ=A Z-DIFF

```

```

At = A1 - DIFF
S2 = S2 - DIFF
A2 = A2 - OIFF
S3 = S3 - DIFF
CALL EXPC(S1, X3)
CALL EXP0(A1, Y3)
IF(3ETA(NR, NM).EQ.f1.) X3 = 0.
IF(BETA(NR, NM) •EQ.O.) Y3 = 0,
X3 = X3 * S(KM)
O3 = (Y3 - X3) * (K(NR) - K(NMI)) * S(NM) / (t(NM) • <(NR) - E(NR I) » <(NM))
CALL EXP0(S2, X2)
CALL EXP0(A2, Y2)
IF(3ETA{NR »NH).EQ.O.) X2 = 0.
IF(BETA(f\R»NM).EQ.O.) Y2 = 0.
X2 = X2 * ST(NM)
D2 = (Y2 - X2) * (K(NR) - K(NM)) • ST(NM) / (E(NM) » K(NR) « E(NR) * K(NM))
CALL EXPO(S3, X<.)
CALL EXPO(AF, Yi)
CALL EXPO(AZ, Di)
Qk = (Y1 - 01) / E(NK)
X<i = X< * (S(NM) - ST(NM))
C2 = C2 * X1 * (X3 - X2 - X4)
P2 = P2 «- X1 * (O3 - O2 - D<»)
55 CONTINUE
C3 = C3 * C2
P3 = P3 * P2
5k COM INUL
Ck = Ok * -CZ
Pk = Pk * P3
53 CONTINUE
C5 = C5 * C4
P5 = P5 «- P4
52 CONTINUE
71 IF(I1.EQ.1) DIFF=0.
TEQ = (t(1) » K(1)) / (E(I1) * K(I1))
IF(C5.GT.TEQ) GO TO 97
IF(P5.GT.TEQ) GO TO 97
IF(OIFF.GT.6CL.) GO TO 97
P = C1 * C5 * EXP(DIFF)
W = P1 * P5 * EXP(DIFF)
IF(P.LT.0.) P = 0.
IF(*<.L.T.0.) H=0.
GO TO 98
97 P=0.
W=0.
98 RETURN
END
SUBROUTINE BATE f.AN(11f «C «B)
DIMENSION E(2C), C(20), 8(20, 20)
DOUBLE C, E, TEMPI, B
DO 27 LI=1, I
DO 28 LJ=1, I
TEMP1=0.
DO 31 LM «1, LJ
TEMP2=1.
DC 29 LR=LM, LI
TEMP2=TEMP2 » E(LR)
29 CONTINUE
TEMP3 * 1.
00 30 LL * LM, LI

```

```

IF(LL.EQ.LJ) GO TO 30
TEMP3=TEMP3*IE<LL>-E(LJ)>
30 CONTINUE
TEMP1=TEMP1+IC(LM)*E(11/<C(1)>E(LM)>>•TEMP2/IE(LI)>>TEMP3)
31 CONTINUE
B(LI,LJ)STEMP1
28 CONTINUE
27 CONTINUE
RETURN
END
SUBROUTINE EXPO(X,Y>
DOUBLE X,Y
IF(X.LT.-6.002) GO TO 501
Y=DEXP(X)
GO TO 502
01 Y=0.0Df10
02 RETURN
END

```

C.4 Subprogram POT3D data input description

Subprogram POT3D produces a three dimensional plot of the hydraulic head distribution used in the subprogram HYDRO.

Card 1: FORMAT(2A10,2F10.3)

Variable	Description
H0LL1 (A10)	Hollerith to be displayed in the graph legend.
H0LL2 (A10)	Continuation of H0LL1.
SUMIN (F10.3)	Minimum value of the potential function (in) , see HYDRO printout.
SUMAX (F10.3)	Maximum value of the potential function (m) , see HYDRO printout.

[A.6683 01 ,TING, 0

UT 620 0C 13.31.31 10 SEP 81 VIA CR02

318

E

r, INPUT /RR» CUTPUT/RR.

POSE,0J TPUT=PR,PA«1F.

GRAM UC8NE21 (SUBPROGRAM POT 3D)

IEL K.S, TING

ARTMENT OF NUCLEAR ENGINEERING

VEFSITY OF CALIFORNIA,BERKELEY

KELE t.CA. ,94720

CONTROL CARDS LISTING

BCARC1

SSHCRD]

ERPR

4.

CMPS, IDOS, ULIB, ULIEX.

CHPS, GPAC8N7. GPAC, VA8N.

TAPE, TAPE 11 = /TING/J/AC2/RUSTLE 3, 37483.

K, F=LG3, F=GFAC, P=ULI8, X.

PHIC, FN=FILM, FTsVA.

T.

P.O.

MP.

PROGRAM LISTING **

```
PROGRAM POT 3D(INPUT,OUTPUT,TAPE5 = INPUT, TAPE6 = OUT PUT,TAPE11, FILM)
COMMON/IGSZ22/ZMCOE(2 00)
DIMENSION VEX (1) , V£Y (1) , PLOT U0)
COMMON/ANAME/XNAME(50) ,YNA ME(5 C) » TNA ML(10 0) ,ZNAME(5 0)
DIME NS ION XWORK (100) » YMORK(10 0)» ARRWORK (10 0, 10 0)
READ(5,100) HOLL1,HOLL2,SUMIN.SUMAX
CO FORMAT (2A10 , 2F10 » 3)
MAPE=11
READ (NTAPE,112)XMIN,XMAX, YMIN, YMA>,DEL,NX, NY,NTETA
12 FORMAT (IX,5E9.2,315)
00 10 LX=1,NX
DO 11 LY=i,NY
READ (NTAPE,111) ARRWORK (LX,LY)
11 FORMAT (1X,E13.5)
11 CONTINUE
10 CONTINUE
IF ({ XMAX-XMIN) .GT. (YMAX-YMIN) > GO TO 43
A3=30.
A2=A4=20 .
A1= ( (XMAX-XMIN) * (A3-A4) ) / ( YMA X-YMIN) *A2
GO TO 44
43 A1 = 30.
A2 = Ah= 2C .
A3= ( (YMA X- YMIN >• (A1-A2I) ) / ( XMAX-XMIN) *A<.
4h DIVX= (XMAX-XMIN) /5.
CIVY= (YMAX-YMIN) /5.
DIVZ= (SUMAX-SUM1N) /5.
rat! m nn P^a t rnrF .A . n i
```

```

CALL BEGIN3 (PLOT)
PLOT (1 UXMIN
PLOT (2 )= XMAX
PLOT (3 )= THIN
PLOT (< > ) = YMAX
PLOT (5 USUMIN
PLOT (6 ) = SUHAX
PLOT <7 ) = 9Q .
PLOT (3 1 * 1 .
PLOT (19) << 1 .
PLOT (26) = 2 * 6
PLOT (27) = i o 0
CALL SU6U3D (ZMODE , PLOT I
CALL OBJCTG (ZMOCE , A2 , A< . , Ai , A3 >
CALL GRI 03 0 (ZMGCE , PLOT , QI \ , X , DIVY , DIVZ)
CALL SETSMG (ZMG0E , 45 , 1 . 2)
CALL LABL3D (ZMODE . PLOT , 1 , 01 VX , 2 , 9 . 2)
CALL LA8L3D (ZMODE , PLOT , 2 , DIVY , 2 » 9 . 2)
CALL LA8L30 (ZMC0E , PLOT , 3 , 0 IVZ , 2 , 9 . 2)
ENCODE (5 0 , 100C , XNAME)
JOG FORMAT (* X-COORDINATE (METERS) t)
ENCDOE (5 0 . 1001 . YNAME)
301 FORMAT It Y-COORCINATE (METERS)?)
ENCODE (5 0 . 1Q04 . ZNAME)
304 FCRMAT It HYDRAULIC POTENTIAL (METERS) / )
ENCODE ( 100 , 1006 . TNAME ) HOLLI , HOLL 2
306 FORMAT It POTENTIAL SURFACE IN THE AQUIFER - * , A1G , A1C)
CALL TITL3D (ZMODE , PLOT , 50 , XNAME , 50 , YNAME , 50 , ZNAME , 100 , TNAME)
00 54 K1 = 1 , NX
XWORMK1 } = XMIN * (K1 - 1) * OEL
54 CONTINUE
DO 55 K2 = 1 , NY
YWORK (K2 ) = YMIN - KK2 - 1) * OEL
55 CONTINUE
CALL SURFCE (ZMOCE , PLOT , XWORK , YKORK , ARRWORK , 10 0 , NX , NY , Q)
CALL EXITG (ZMODE)
STOP
END

```

Appendix D-Derivation of The Contamination Time Interval and the Contaminated Region for the Second and Third Member Nuclides when $N_0 \neq 0$.

D.1-Determination of the contamination time interval θ , for the second member when $N_0 \neq 0$ (Table 3.7).

The solution for the concentration of the second member is expressed by Eq.3.4.8. The contamination time interval is defined as the time interval in which the concentration is non zero at a fixed position. The first term on the right hand side of Eq.3.4.3 is non zero in the time interval $(z/v_2 + T - z/v_1 \geq T)$ because the function $S(v_2 t - v_2 (t - T))$ is non zero in this interval. Likewise, the second term is non zero in the interval $(z/v_1 - z/v_2)$ if $v_1 < v_2$ or $(z/v_1 - z/v_2)$ if $v_1 > v_2$. When the two terms are added the resultant concentration is non zero in the superposition of the above time intervals when each individual term is non zero. The different configurations resulting from the superposition are shown in the following diagrams

$$N_2 = 0 \qquad \qquad \qquad = 0 \qquad \qquad \qquad e_2 = z/v_2 + T - z/v_1$$

$$v_2 \qquad \qquad \qquad z/v_1 - \qquad \qquad \qquad z/v_2 + T$$

When $v_1 < v_2$ two possibilities arise

$$z/v_2 + T < z/v_1 : \qquad N_2 = 0 \qquad \qquad \qquad m = n$$

$$\qquad \qquad \qquad z/v_1 \qquad \qquad \qquad z/v_2 + T \qquad \qquad \qquad z/v_1 \qquad \qquad \qquad z/v_2$$

$$N_0 = 0$$

$$z/v_1 + T > z/v_2$$

$$z/v_1 \quad z/v_2 \quad z/v_1 + T$$

Above results are summarized in Table 3.7.

D.2-Determination of the contaminated region R_0 for the second member when $N_0 = 0$ (Table 3.7).

The contaminated region is defined as the region in which the concentration is non zero at a fixed time t . The first term in Eq. 3.4.8 is non zero at a fixed time t in the region defined by $(v_2 t - v_2(t-T) = v_2 T)$ because the function $S(v_2 t; v_2(t-T))$ is non zero in this region. The second term is non zero in the region $(v_1 t - v_1 t)$ if $v_1 > v_2$ or $(v_2 t - v_1 t)$ if $v_2 > v_1$, because the function $S(v_1 t; v_2 t)$ is non zero in this intervals. By adding the two terms, the resultant concentration will be non zero in the superimposed region of the two individual non zero regions. The different possibilities are shown in the following diagrams

$$N_0 = 0$$

$$v_2 > v_1$$

$$v_2(t-T) \quad v_1 t \quad v_2 t$$

$$R^0 = v_1 t - v_2(t-T)$$

When $v_2 < v_1$ two different possibilities arise

$$N_0 = 0$$

$$v_2(t-T) > v_1 t$$

$$v_2 t \quad v_1(t-T) \quad v_1 t$$

$$R^0 = v_2 t - v_1 t$$

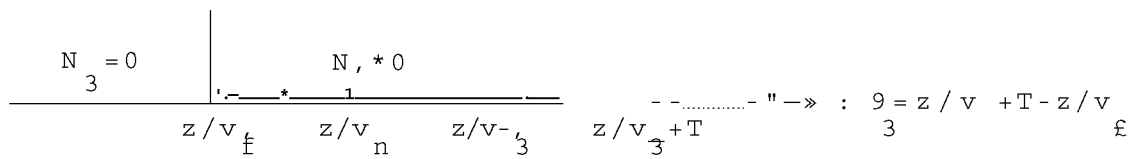
$$v_2(t - T) \quad N_2=0 \quad v_1 t \quad v_2 t \quad N_2=0 \quad R_2 = v_2 T$$

These results are summarized in Table 3.7.

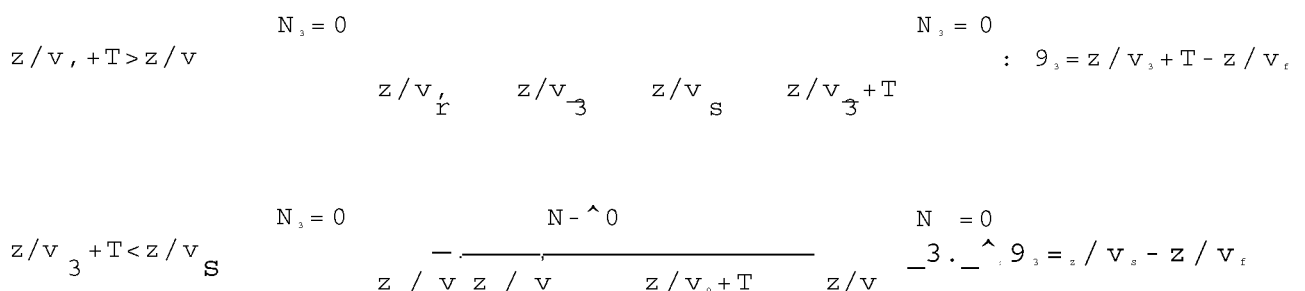
D.3-Determination of the contamination time interval for the third member when $N_2 \neq 0$ (Table 3.10).

The solution for the concentration of the third member is expressed by Eq. 3.5.15. One can distinguish two terms: the first term which represents the contribution of the third member nuclides initially present at the repository and the second term (bracketed term) which represents the contribution from the decay of the precursors. At a fixed position, the first term is non zero in the time interval $(z/v^+ - z/v_- = T)$ because the function $S(v_1 t; v_2(t-T))$ is non zero in this interval. The second term is non zero in the time interval $(z/v_s - z/v_f)$ where v_s is the slowest nuclide velocity and v_f is the fastest nuclide velocity. This is because at least two of the functions $S(v_i t; v_j t)$ are non zero in this interval (see Table 3.8). When the two terms are added, the resultant concentration will be non zero in the superimposed interval of the individual non zero time domains. The following diagrams show the different possibilities for the contamination time interval depending on the relative magnitude of the nuclide velocities.

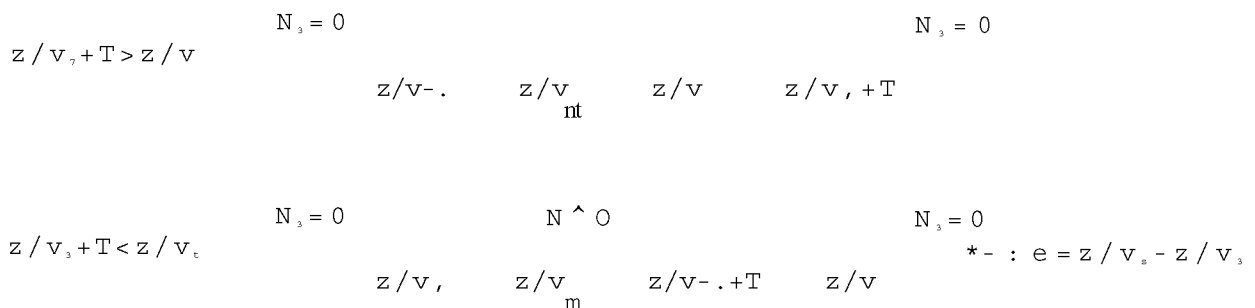
1) -When the third member is the slowest nuclide, i.e. $v = v_1$
 (case 1: $v_1 > v_2 > v_3$ and case 6: $v_2 > v_1 > v_3$ in Table 3.3)



2) -When the third member has the intermediate velocity, i.e.
 $v_3 = v_m$ (case 3: $v_1 > v_3 > v_2$ and case 4: $v_2 > v_3 > v_1$ in Table 3.5)



3) -When the third member is the fastest nuclide, i.e. $v = v_3$
 (case 2: $v_3 > v_2 > v_1$ and case 5: $v_3 > v_1 > v_2$ in Table 3.8)

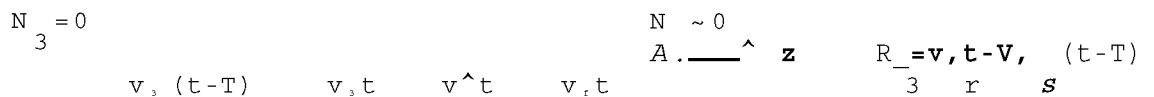


Above results are summarized in Table 3.10.

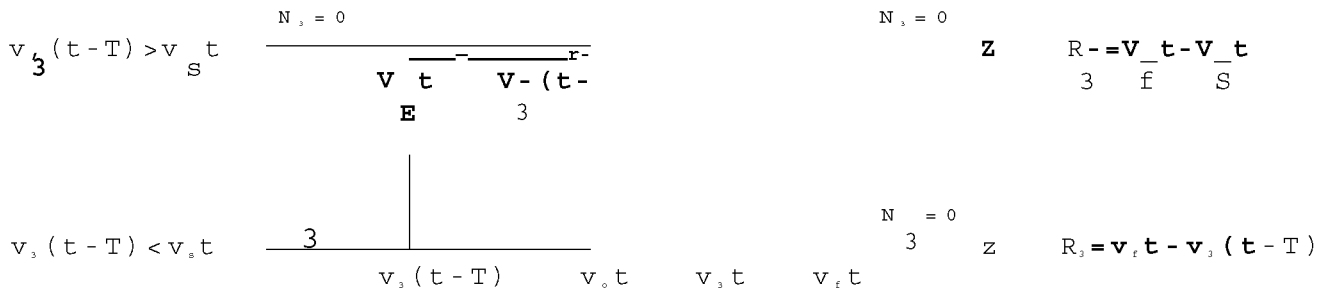
D.4-Determination of the contaminated region R, for the third member when $N^{\wedge}v_0$ (Table 3.10) .

Let us consider again the concentration distribution for the third member, as being the superposition of two terms as discussed in D.3. At a fixed time, the first term is non zero in the region defined by $(v_3 t - v(t-T) = v^{\wedge}T)$ because the function $S(v^{\wedge}t; v_3(t-T))$ is non zero in this region. The second term is non zero at a fixed time in the region $(v_1 t - v_2 t)$ where, again, v_1 stands for the slowest nuclide velocity and v_2 stands for the fastest nuclide velocity. This is because at least two of the functions $S(v^{\wedge}t; v_i t)$ are non zero in this region (see Table 3.8). When the two terms are added, the resultant concentration will be non zero in the region of the superposition of the two individual non zero concentration regions of each individual term. The following diagrams show the different possibilities for the contaminated region depending on the relative magnitudes of the nuclide velocities.

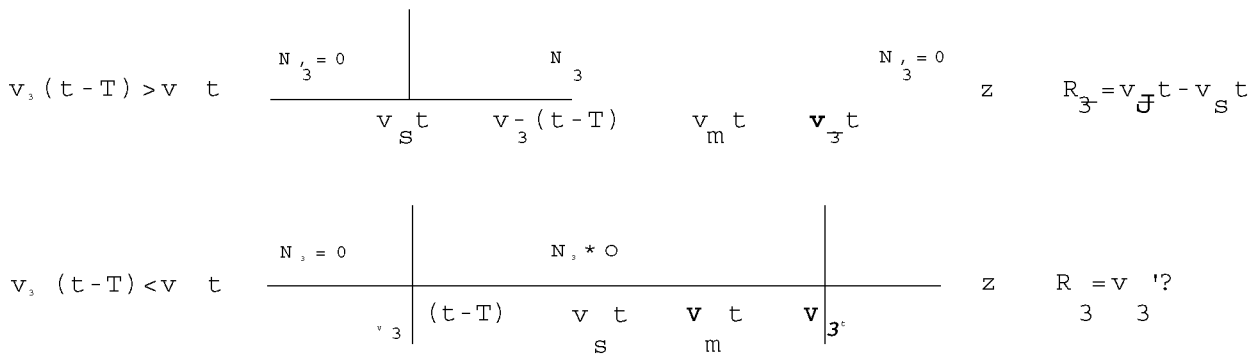
1) - When the third member is the slowest nuclide, i.e. $v_3 = v_1$ (case 1: $v_1 > v_2 > v_3$ and case 6: $v_2 > v_1 > v_3$ in Table 3.3)



2) - When the third member has the intermediate velocity, i.e. $v_3 = v_2$ (case 3: $v^{\wedge} > v_3 > v_1$ and case 4: $v_3 > v_2 > v^{\wedge}$ in Table 3.8)



3)-When the third member is the fastest nuclide, i.e. $v_3 > v_f$
 (case 2: $v_3 > v_s$ and case 5: $v_3 > v_m$ in Table 3.8)



Above results are summarized in Table 3.10.



M17067